COMPARATIVE RADIOLOGICAL ANATOMY OF HUMAN, PORCINE AND OVINE VERTEBRAE

Dr Timothy Ariyanayagam

Thesis submitted to the University of East Anglia

for the degree of

Doctor of Medicine (MD)

At the Faculty of Medicine and Health Sciences Graduate School

June 2019

ABSTRACT

Osteoporotic vertebral fractures represent an important health burden in the Western world, in particular given the aging population demographics of most Western countries. At present, the treatment options for osteoporotic vertebral fractures are limited, and often conservative, relying on medical pain management. Transpedicular spinal interventional techniques such as vertebroplasty and kyphoplasty offer a minimally invasive treatment option for osteoporotic vertebral fractures. However, there has been recent controversy regarding the efficacy of vertebroplasty for pain relief. Although these percutaneous techniques continue to be used and developed, there is no consensus on the pre-clinical testing of new instruments and cements. Human cadaveric vertebrae are expensive and of limited availability, and animal vertebrae offer a more easily accessible alternative, but there is no agreement within the literature as to which species best approximates the human.

This thesis explores the currently available evidence comparing human and animal vertebrae, and performs comparison studies assessing basic morphometric measurements, bone texture, and statistical shape analysis, to decide upon the best animal model for the use in assessing novel transpedicular instruments and vertebral bone cements. The findings would also apply to developments in surgical transpedicular screws.

The morphometry showed that sheep are generally closer to humans in the thoracic spine, whereas pigs are closer in the lumbar spine. Bone texture analysis demonstrated no significant differences in trabecular thickness between humans and either sheep or pigs. Statistical shape analysis corroborated the findings of basic morphometry. Taking the findings in combination, I would suggest that for the purposes of transpedicular techniques, the sheep is a closer model to the human in the thoracic spine, and the pig is closer in the lumbar spine.

CONTENTS

LIST OF FIGURES

7. Total anteroposterior length

8. Right pedicle height

9. Right pedicle width

10. Left pedicle height

11. Left pedicle width

LIST OF TABLES

4. Transverse process width

5. Spinal canal width

6. Spinal canal length

7. Total anteroposterior length

D. Shapiro Wilk test for human, pig, and sheep CT measurement data distribution

1. T1

2. T2

3. T3

4. T4

5. T5

6. T6

7. T7

8. T8

9. T9

10. T10

11. T11

12. T12

13. T13

14. T14

15. L1

16. L2

17. L3

18. L4

19. L5

20. L6

E. Tables showing comparisons between human, pig and sheep CT vertebral measurements

1. Vertebral body height

2. Vertebral body width

3. Vertebral body length

4. Transverse process width

5. Spinal canal width

6.   Spinal canal length

7.   Total anteroposterior length

8.   Right pedicle width

9.   Right pedicle height

10.   Left pedicle width

11.   Left pedicle height

F. Tables showing comparisons between human male and female CT vertebral measurements

1.   Vertebral body height

2.   Vertebral body width

3.   Vertebral body length

4.   Transverse process width

5.   Spinal canal width

6.   Spinal canal length

7.   Total anteroposterior length

8.   Right pedicle width

9.   Right pedicle height

10.   Left pedicle width

11.   Left pedicle height

G. Tables showing comparisons between human old and young CT vertebral measurements

1.   Vertebral body height

2.   Vertebral body width

3.   Vertebral body length

4.   Transverse process width

5.   Spinal canal width

6.   Spinal canal length

7.   Total anteroposterior length

8.   Right pedicle width

9.   Right pedicle height

10.   Left pedicle width

11.   Left pedicle height

ACKNOWLEDGEMENTS

I would like to thank everyone involved with my MD thesis, in particular:

- My primary supervisor, Professor Andoni Toms, whose infinite patience in the face of my eternal struggles with deadlines never ceased to amaze, whose constant support was instrumental throughout my entire MD, and without whose advice and encouragement, I would never have embarked on this journey.

- My clinical radiology consultant colleague Professor Tom Turmezei, who provided the idea for performing statistical shape analysis and supervised Chapter 5, and whose technical expertise and multiple MatLab scripts which were vital. Additionally, for his patience and understanding with a non-mathematician attempting to slowly comprehend novel concepts.

- My secondary supervisor, Professor Iain MacNamara, who has been supportive through the entire process

- Dr Frederick Barber, my radiology trainee colleague who provided valuable assistance as a second reviewer for Chapter 2

- The Norwich Medical School Department of Anatomy, who kindly allowed me to use their dissection lab, as well as providing me with training in vertebral dissection techniques

I would also like to thank my friends and family for their understanding, encouragement and moral support!

THESIS OUTLINE

The main aim of this thesis is to decide upon the best animal model for assessing transpedicular vertebral instruments and cement. The thesis comprises an introductory chapter, a systematic review, three studies, and a summary chapter.

Chapter 1

Introduction to the background topics of osteoporosis, vertebroplasty, bone texture and statistical shape analysis.

Chapter 2

Systematic review of the available evidence comparing animal and human vertebrae

Chapter 3

A study comparing basic morphometrics of pig, sheep, and human thoracolumbar vertebrae

Chapter 4

A study comparing bone texture analyses of pig, sheep, and human L1 vertebrae

Chapter 5

A study using statistical shape analysis to compare statistical shape models of pig, sheep, and human L1 vertebrae

Chapter 6

A summary of the findings and conclusions drawn from the studies within the thesis, putting these into the context of the background literature

CHAPTER 1: INTRODUCTION

1.1 SPINAL OSTEOPOROSIS

1.1.1 HISTORY

The term osteoporosis is derived from the Greek "osteon" relating to bone, and "poros" meaning passage or pore. It was first used by Jean Georges Chretien Frederic Martin Lobstein (1777–1835), a French pathologist and surgeon, who noted that the bones of some patients appeared more porous than others (1). Earlier work in the mid-18th Century by the Scottish surgeon John Hunter (1728-1793) had already demonstrated that the process of bone growth and repair involved a remodelling process (2), and this was later expounded upon by German orthopaedic surgeon Julius Wolff (3).

However, initially no connection was made between these two processes and osteoporosis was considered to be of idiopathic aetiology until the early 20th Century. After reading research on the connection between ovarian function and calcium metabolism in pigeons, US endocrinologist Fuller Albright (1900-1969) noted that many of his osteoporosis patients were post-menopausal, and that treating them with oestrogen therapy resulted in improved bone mineralisation (4, 5). Newer research suggests that the causes and contributory mechanisms are probably even more complex than simply being due to an oestrogen deficient state (6).

The modern definition of osteoporosis stems from that proposed by Albright himself: decreased bone mass due to insufficient bone matrix production by osteoblasts (4, 7, 8). This results in increased bone fragility. Bone mineral density (BMD) is assessed using Dual Energy X-ray Absorptiometry (DEXA). The standard reference site is the neck of the femur.

Osteoporosis may be diagnosed when bone density is more than 2.5 standard deviations below the mean value for young adult, which is known as the T-score (9).

1.1.2 EPIDEMIOLOGY

Osteoporosis represents a significant health burden in the Western world, with grave consequences for morbidity and mortality. The incidence of osteoporosis in 2010 in the 27 European Union countries (EU27) was estimated as 5,500,000 men and 22,100,000 women. There was an estimated incidence of osteoporotic vertebral fractures of 273 per 100,000 in the UK in 2010. 42,809 deaths in the EU27 were considered directly attributable to an osteoporotic fracture (i.e. other co-morbidities and contributory factors had been excluded). In 2010 the total cost of osteoporosis to the UK (including fracture costs and pharmacological interventions) was estimated at €5,408,000,000 (10).

1.1.3 BONE ANATOMY AND PHYSIOLOGY

To understand the pathophysiology of osteoporosis, it is useful to consider the normal physiological process of bone mineralisation.

Bones are divided into four main categories based on their shape and size: long bones, short bones, flat bones, and irregular bones (in which category vertebrae are considered). The different categories of bone have different ratios of cortical vs cancellous/trabecular bone, and vertebrae tend to have a ratio of 25:75 cortical to cancellous bone (11).

Cortical bone is the dense, hard bony tissue that forms bone cortex. Cancellous (also known as trabecular) bone is the bone tissue of the medulla, consisting of a network of trabeculae which run through the marrow tissue.

The basic histological units of bone are osteons. These are cylindrical structures of peripheral lamellar bone which is itself calcium hydroxyapatite reinforced by a type I collagen matrix, with a central fluid-filled lumen containing blood vessels. In cortical bone, these are called Haversian systems, and are in general laid parallel to the long axis of the bone (12, 13). In cancellous bone, these are known as trabeculae or trabecular packets, and align according to mechanical stress (13, 14). The mechanical properties of cortical and cancellous bone suggest that they respond to stress as though they are different materials (15). Their mechanical response also varies to differing degrees depending on the particular bone being analysed, with less heterogeneity seen in cortical bone (13).

The two principle cells of bone are osteoblasts and osteoclasts. Osteocytes are derived from mature osteoblasts within bone lacunae.

Osteoblasts are the cells of bone formation, arising from pluripotent mesenchymal progenitor cells. Mature osteoblasts produce much of the extracellular matrix proteins and also regulate the deposition of calcium hydroxyapatite crystals (16). Osteoblasts also play a regulatory role in the differentiation of osteoclasts via Wnt5a-Ror2 signalling thus increasing RANK expression and osteoclastogenesis (17).

The bone matrix is predominantly mineralised; bone is approximately 50-70% mineral content. Calcium hydroxyapatite $[Ca_{10}(PO_4)_6(OH)_2]$ is the main inorganic component, crystallising under cellular control (18).

Osteoclasts are the cells of bone resorption. They arise from mononuclear precursor cells of the monocyte-macrophage lineage. Their differentiation, maturation and activation are primarily under the control of osteoblastic and marrow stromal cell cytokine production (19). Once activated, osteoclasts secrete hydrogen ions to dissolve the mineralised calcium

hydroxyapatite component of bone (11). Osteoclasts in long, short and irregular bones also secrete the cathepsin K enzyme which breaks down the collagenous component of bone matrix (11, 20). Osteoclasts found in flat bones secrete the matrix metalloprotease (MMP) enzyme (21).

Osteocytes develop from mature osteoblasts, and play a mechanosensory role in regulating bone remodelling via foot processes within bone canaliculi which detect fluid flow in response to mechanical stress (22). Osteocyte apoptosis has been shown to be associated with osteoclastic activity (23). It is interesting to note that osteocyte apoptosis is inhibited by oestrogen, bisphosphonates and calcitonin (24, 25).

1.1.4 BONE GROWTH

Bone growth encompasses several processes: longitudinal growth, radial growth, modelling and remodelling. Longitudinal growth occurs at the physes where there is chondral proliferation with subsequent mineralisation. Modelling results in changes to bone shape in response to stresses such as mechanical force. Remodelling is the process of constant bone renewal, which removes old, damaged bone tissue to help maintain strength (11). This also plays a role in calcium and phosphate homeostasis.

Remodelling is considered to consist of four phases: activation, resorption, reversal, and formation (11). Much remodelling occurs in a random manner, but there is also evidence to suggest that it may be targeted to areas that require repair, perhaps related to disruption of osteocyte systems or osteocyte apoptosis (23). Remodelling is performed by a temporary arrangement of osteoclasts and osteoblasts known as the "basic multicellular unit".

Activation involves the recruitment, activation and differentiation of osteoclastic precursor cells (26).

Resorption occurs as described earlier, with acid secretion by mature osteoclasts increased by parathyroid hormone (PTH) and prostaglandin E_2 (PGE$_2$), and decreased by calcitonin (26). The lytic enzymes and acids are secreted into a sealed area, and form a cavity known as Howship's resorption lacune (27).

Once resorption is complete and before bone formation can be initiated, the residual proteinaceous matrix is removed by a phagocytic cell of probable osteoblastic origin, also known as the "reversal cell" (27).

Finally, osteoblast precursors migrate into the lacune and mature, and form new bone. The biochemical or biomechanical controls over the transition between resorption and formation are not well understood. Proposed mechanisms include osteoclast derived coupling factors such as sphingosine 1-phosphate, mechanical strain and PTH, or possibly a combination of these. The termination of bone formation is also poorly understood (27).

1.1.5 PATHOPHYSIOLOGY OF OSTEOPOROSIS

The pathophysiology of osteoporosis is complex and multifactorial, with many contributory factors: endocrine, age-related, genetic, immunological, mineral homeostasis, and iatrogenic, to name a few.

The underlying process by which osteoporosis develops is the inadequate production of bone matrix by osteoblasts, and is therefore related to bone remodelling. Osteoclastic activity plays a role in the development of bone fragility but it is the insufficiency of osteoblastic activity which is key to osteoporosis; there are physiological states of increased osteoclastic activity which do not result in bone fragility, such as the pubertal growth spurt,

fracture repair, and the remodelling of bone in response to the application of increased forces (28, 29).

1.1.6 THE ROLE OF SEX HORMONES

Oestrogen deficiency has long been held to be a key contributing factor to the development of osteoporosis, ever since Albright's observations in the 1930s. Subsequent studies have supported his assertions that oestrogen therapy may reverse the effects of osteoporosis (30-32), and that cessation of oestrogen therapy results in BMD loss at the same rate as un-treated control groups (33). Additional supportive evidence comes from the fact that women experience two phases of BMD loss. The initial rapid loss phase immediately post-menopause/oophorectomy and lasts for about a decade (34). After a certain level of cancellous bone loss, biomechanical bone homeostasis acts to limit the rate of demineralisation (35), and there is a slower, steady BMD decline.

Men, who generally do not undergo a relatively abrupt loss of sex hormones, experience a single steady phase of BMD loss, which is essentially the same as the slower phase seen in women (34). In men, both testosterone and oestradiol are thought to have a BMD protective effect (36, 37); the role of testosterone is not as clearly defined as oestrogen in women, and is complicated by the fact that the testes produce oestradiol, that circulating testosterone may be converted to oestrogen in peripheral tissues, and that osteoblasts and osteoclasts in men display oestrogen receptors (38, 39).

It is also unclear if the age-related decline in testosterone levels is of significance, with some evidence showing correlation between BMD and testosterone levels (40), but other studies have not demonstrated this (41). Furthermore, there is some evidence that there is a stronger association between low oestrogen levels than low testosterone levels, in men with primary osteoporosis (42, 43).

On a cellular level, osteoclast and osteoblast apoptosis is inhibited by oestrogen (24, 25). Oestrogen also decreases RANKL expression by osteoblasts, which in turn decreases the activation of osteoclasts (19).

The weight of evidence is therefore strongly suggestive of a key role of sex hormone deficiency, in particular oestrogen, in the development of osteoporosis.

1.1.7 THE ROLE OF AGING

Although sex hormones are clearly of importance, there is much evidence that other factors must also contribute to the disease state. Some studies demonstrate that BMD loss begins as early as the third decade of life, well before the menopause (44, 45). Age may affect BMD through a variety of mechanisms, including decreased bone cell responsiveness to external influences, decreased numbers of osteoblast and osteoclast precursors, and through decreased muscle strength causing a relative "disuse" of bones resulting in remodelling to decrease mass (46).

Aging is also related to cumulative oxidative stress from a lifetime of generating reactive oxygen species (ROS). Oxidative stress has been shown to decrease BMD (47), and a possible mechanism for this is via osteoclastogenesis (48).

Aside from its contribution to loss of BMD, aging also has other effects on bone fragility. These include the deterioration of type I collagen (49). Aging can of course also be said to contribute to other factors such as hormonal deficiency, as the menopause is a consequence of aging.

1.1.8 THE ROLE OF MINERAL HOMEOSTASIS

Disorders of calcium and phosphate homeostasis are more associated with osteomalacia than osteoporosis. Theoretically PTH and 1,25-dihydroxyvitamin D [1,25(OH)$_2$D] may have a role in bone remodelling. With aging and/or renal failure, there is decreased hydroxylation of 25-hydroxyvitamin D to 1,25-dihydroxyvitamin D. There may also be contribution to this by the loss of extra-skeletal effects of oestrogen on calcium metabolism (50). This results in decreased calcium absorption from the gastrointestinal tract. The resultant increase in PTH, secondary hyperparathyroidism, increases bone remodelling by stimulating acid secretion by osteoclasts (26, 51).

Trace minerals such as copper, manganese, magnesium and zinc are involved in bone metabolism, and their deficiency may play a role in the development of osteoporosis (52). Magnesium, copper and zinc levels have been shown to be decreased in osteoporotic patients (53, 54). However, there is also some conflicting evidence that other than zinc, levels of these trace minerals does not correlate with BMD (55).

1.1.9 THE GENETICS OF OSTEOPOROSIS

There is an established evidence base suggesting a degree of heritability of BMD, from family and twin studies, with segregation analysis strongly suggesting a polygenic component (56-58). Regarding BMD loss, studies have demonstrated heritability at the wrist and spine, but interestingly not at the femoral neck (59-61).

Several genes have been shown to have a significant association with osteoporosis. A full discussion of these is beyond the scope of this introductory segment. Some examples with particular relevance to the spine or other contributory factors already discussed, include:

- DCDC5 and DCDC1 (62), which may be associated with lumbar spine BMD, though their role in bone metabolism is uncertain.
- ESR1 (62, 63).

- FOXC2 and FOXL1 (62); both play a part in bone metabolism, and have an association with spinal BMD.

Other genes with less established evidence have also been investigated. Of note, COL1A1 which encodes the collagen type I alpha chain, has contradictory evidence, though a series of meta-analyses evaluating the Sp1 polymorphism suggest that there is a link with fracture risk and BMD (64, 65).

1.1.10 GLUCOCORTICOID INDUCED OSTEOPOROSIS

Glucocorticoids are widely used medications in a variety of inflammatory conditions, often as a last resort in difficult to manage cases. They are known to have a broad range of side effects, one of which is osteoporosis.

The pathogenesis of glucocorticoid-induced osteoporosis is multifactorial. Glucocorticoids have an inhibitory effect on osteoblast function (66), and induce osteoblast and osteocyte apoptosis (67, 68). They may also have an anti-apoptotic effect on osteoclasts, as suggested by a study on mice (68). However, a human study using serum and urinary indices of osteoclast activity showed no significant difference between a low-dose glucocorticoid group and a placebo group for two of the three osteoclast activity markers (69).

In addition to direct effects on bone cells, glucocorticoids suppress endogenous sex hormone synthesis, and also inhibit calcium absorption in the gut. Although no secondary elevated PTH levels are seen in patients on low to moderate dose oral glucocorticoids, there may be an increased sensitivity of bone tissue to PTH (70).

1.1.11 OSTEOPOROTIC VERTEBRAL COMPRESSION FRACTURES

As described above, osteoporotic bones have impaired bone mineralisation, which results in increased bone fragility. This results in an increased susceptibility to fractures, which are termed either osteoporotic fractures, or fragility fractures. These fractures differ from those which occur in normal, healthy bones, and occur following either minimal or indiscernible trauma, such as a fracture of the neck of the femur after falling from standing height (71).

Osteoporotic fractures most commonly occur in the femoral neck, and the thoracolumbar spine. The socioeconomic cost of osteoporotic fractures is discussed in Section 1.1.2.

Osteoporotic vertebral fractures result in the collapse of the anterior vertebral body. According to the AO (*Arbeitsgemeinschaft für Osteosynthesefragen)* Spine foundation international classification of spinal fracture morphologies, this pattern is termed a compression fracture, due to the presumed direction of the forces that result in pathological loss of vertebral height (72).

1.1.12 MANAGEMENT OF OSTEOPOROTIC VERTEBRAL COMPRESSION FRACTURES

Given the morbidity, mortality risk and cost of osteoporotic vertebral fractures, it is perhaps surprising that the treatment options are currently poorly defined with no consistency between guidelines from different medical bodies (73).

In clinical practice, the first line management is often with conservative medical management with pharmaceutical analgesia and with or without bed rest, spinal immobilisation, or physiotherapy (74).

The principle of surgical management of osteoporotic vertebral fractures is foremost to preserve biomechanical stability (75). Techniques include long segment posterior stabilisation or anterior reconstruction. Surgical management involves both intraoperative risk such as direct nerve damage and blood loss, and anaesthetic risk which is higher in the elderly population due to higher incidence of comorbidities and decreased physiological reserve. Post-operative complications include risk of venous thrombosis and pulmonary embolism, iatrogenic spinal canal narrowing and neural compromise, infection, and failure of the procedure due to poor osteoporotic bone quality.

Due to these increased risks, surgical management is usually reserved for those cases with compromised spinal stability who require urgent stabilisation to prevent nerve damage (75).

Minimally invasive percutaneous cement augmentation techniques are an alternative to optimised conservative management, and often an adjunct to surgical treatment. These techniques include vertebroplasty which involves the injection of bone cement into the fractured vertebral body via transpedicular needles, and kyphoplasty which involves first using an inflatable balloon to create a cavity before injecting cement. Vertebroplasty is the main technique considered in this thesis and discussed in further detail below, but many of the same principles apply to kyphoplasty, and indeed, the evidence in section 1.2 of this chapter suggests that both techniques have similar efficacy, though may differ in ideal patient selection.

1.1.13 SUMMARY

Osteoporosis is a complex contributor to bone fragility in the older population, with an increased risk of fractures. The significant morbidity/mortality and economic burden have made it an important topic of research. A great many factors participate in the development

of osteoporosis, but the two most important are perhaps age-related changes and oestrogen deficiency.

Given that oestrogen therapy/hormone replacement therapy has its own not insignificant risks (including breast cancer (76), ovarian cancer (77), endometrial cancer (78), deep venous thrombosis (79)), the "golden bullet" for osteoporosis prevention may lie at the cellular or genetic level.

Until then, we must consider osteoporosis as an inevitable consequence of longer modern lifespans, and look to effective treatments, which may include vertebroplasty as discussed in section 1.2 of this chapter.

1.2 VERTEBROPLASTY

1.2.1 DEFINITION

Percutaneous vertebroplasty (PVP) is the minimally invasive percutaneous cement augmentation of vertebrae under fluoroscopic or CT guidance.

1.2.2 HISTORY

Fluoroscopically guided vertebroplasty was first performed in France in 1984, by Deramond and Galibert (80), a French radiologist and neurosurgeon. The authors rather boldly and successfully pioneered this technique for the treatment of an aggressive cervical spine haemangioma. This, and the subsequent procedures by the same team, were reported in an initial series published in 1987. One year after this, Bascoulergue et al. published the use of vertebroplasty in the treatment of osteoporotic vertebral compression fractures (VCF) (81) .

The technique was popularised in Europe, and it was not until almost a decade later that it was introduced in the USA (82). It is currently a widely used procedure, though controversy exists regarding its efficacy, which is discussed below.

1.2.3 TECHNIQUE

1.2.3.1 INDICATIONS AND CONTRAINDICATIONS

The main indications for PVP are osteoporotic vertebral compression fracture   (82-84) or metastatic vertebral compression fracture,(85) which are refractory to optimal medical therapy and either unsuitable for or not necessitating open surgical repair. There is also

evidence to support prophylactic vertebroplasty in adjacent vertebral levels to prevent subsequent fractures (86, 87).

Absolute contraindications are active infection or an unstable fracture/posterior element involvement. Relative contraindications are coagulopathy, epidural metastatic extension, osteoblastic metastases, spinal cord or nerve root compromise.

1.2.3.2   PATIENT SELECTION

There have been several recent studies which call into question the efficacy of vertebroplasty (88-91), suggesting that it is no more effective than a sham procedure involving the insertion of needles without any cement injection. The conflicting evidence is discussed in more detail in Section 1.2.4. Given this controversy, it is important to select appropriate patients given that vertebroplasty is not without risk. The complications are outlined in Section 1.2.3.5.. It is crucial to establish that the VCF is in fact the source of the patient's pain, and that the injury is acute (ideally within 6 weeks from onset) (92, 93).

The first stage in patient selection is careful clinical evaluation. At our centre, this is usually performed in a joint clinic between musculoskeletal interventional radiologist and orthopaedic spinal surgeon. A detailed history can help to date the fracture with onset of pain, though this is not always straightforward. Clinical examination should demonstrate point tenderness at the level of, or one level below (which would represent the spinous process of the involved vertebra), the fracture. In patients with multilevel fractures, clinical examination can be complicated.

Pre-procedure imaging also plays a key role in patient selection. Plain radiographs are often the first line imaging modality. While they are useful in identifying patients with fractures, it is not possible to reliably age a fracture based on plain radiographic findings, unless a

previous radiograph pre-dating the fracture is available. Therefore, patient selection usually includes spinal MRI with a fat-saturated fluid sensitive sequence. This can demonstrate marrow oedema or granulation tissue, which is associated with acute injuries. CT may also be performed to assess cortical breaches where these are not well demonstrated on MRI.

1.2.3.3   RADIOLOGICAL GUIDANCE

Vertebroplasty is usually performed under fluoroscopic guidance, which is required for needle placement and for continuous screening during cement injection to assess for cement leak.

Gangi et al. have described the use of a combination of CT and fluoroscopy (94, 95). However, to my knowledge, the use of combined CT and fluoroscopic guidance has not been shown to be superior to fluoroscopy alone.

Others have described the use of CT-guidance alone (96, 97). There have not been any studies directly comparing the cement leakage rates of continuous fluoroscopic screening vs CT. Comparison using leakage rates in the established literature based on fluoroscopy is difficult, especially as this may in fact underestimate cement leakage due to greater difficulty visualising smaller volumes of leaking cement under fluoroscopic examination (98).

However, the usefulness of fluoroscopic screening during cement injection is the provision of real-time feedback, which allows the termination of cement injection as soon as leakage is identified. Until there is robust evidence to suggest the superiority of either fluoroscopy, CT, or a combination of the two, it is likely that selection of imaging modality will depend on a balance between operator preference, availability and time-dependence.

1.2.3.4   PROCEDURE:

Informed consent should be obtained where possible.

The procedure is performed under sterile conditions. The patient is ideally positioned prone, with arms either flexed to 180° or abducted to shoulder height. Initial screening is performed to confirm the appropriate levels for intervention, and to mark skin entry sites.

At our treatment centre, we administer local anaesthesia (bupivacaine 0.25%, up to 10mL) with 21G spinal needles, to the subcutaneous soft tissues down to the periosteum of the pedicles. This is performed under fluoroscopic guidance. The spinal needles may be removed at this point or left in to help guide the angulation of the bone cannula.

Small skin incisions are made at the desired skin entry sites, and a bone cannula and trocar are inserted to the pedicle. This is advanced through the pedicle under continuous AP screening using an orthopaedic mallet. Care is taken to avoid breaching the medial pedicle wall which could result in dural sac injury and cement leakage into the spinal canal.

Alternative approaches may be used. In the thoracic spine, a parapedicular approach can be taken between the lateral pedicle wall and the rib head. In the lumbar spine, a posterolateral approach may be used (99).

Once past the posterior vertebral wall, the bone cannula and trocar are advanced to approximately halfway along the AP length of the vertebra under lateral fluoroscopic guidance. They are ideally positioned such that once the cement delivery device is introduced, it may be positioned at the anteroinferior aspect of the vertebral body.

At this stage, it is our usual practice to take a bone marrow biopsy to exclude occult malignancy. After this, we ream the marrow beyond the bone cannula to allow ease of cement deliver device placement. The delivery device is advanced to the anteroinferior aspect of the vertebral body under lateral fluoroscopic guidance. Cement delivery may be performed either via unipedicular or bipedicular approach..

There are a variety of cements available for vertebroplasty. We currently use either polymethylmethacrylate cement (PMMA) or Cortoss™. Cement is injected under constant fluoroscopic screening to assess for leakage. There is limited evidence to suggest an optimal volume of cement to be injected. One study suggests that there is no association between injected PMMA volume and subsequent fracture, and therefore the authors recommend that as much cement as possible be injected (100). A subsequent study suggests that cementing 24% volume of the vertebral would provide optimum pain relief (101).

Once cement injection is completed, time is allowed for the cement to set to avoid tracking posteriorly as the bone cannulae are withdrawn. For this reason, the bone cannulae are withdrawn under lateral fluoroscopic screening to assess for posterior cement tracking.

Figure 1.1 shows selected images from a fluoroscopically guided vertebroplasty demonstrating needle placement and cement injection.
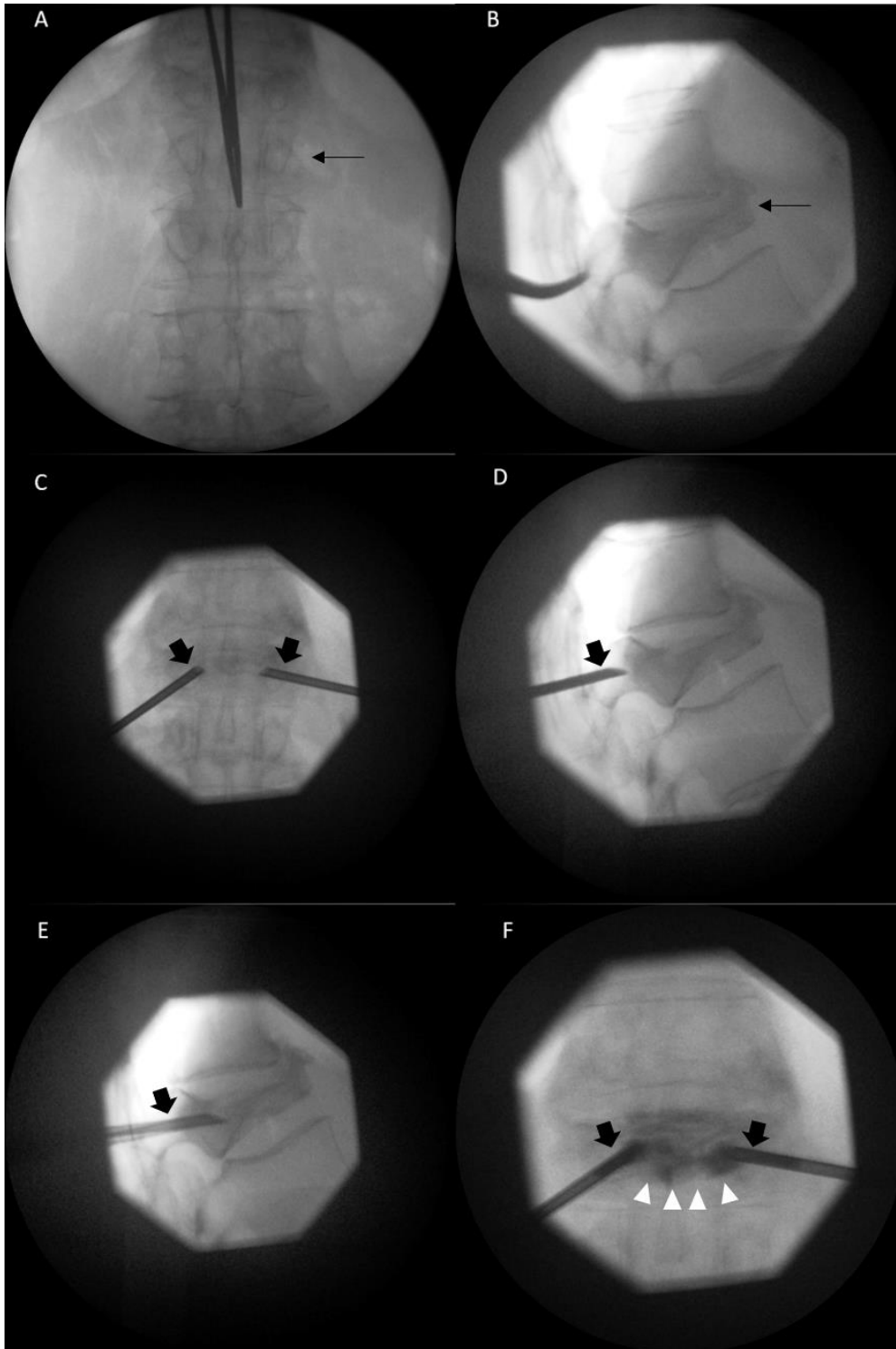
Figure 1.1 – Selected fluoroscopy images from a fluoroscopy guided percutaneous vertebroplasty on a L1 osteoporotic wedge fracture. *A and B show anteroposterior (AP) and lateral views of the fracture at the L1 level, indicated by narrow black arrows. C and D show the introduction of the transpedicular needles in AP and lateral views indicated by broad black arrows. D shows the transpedicular cannulae within the pedicles, and E shows the cannulae having been advanced into the vertebral body. F shows injection of radiopaque bone cement indicated by white arrowheads.*

The patient may be moved into a supine position for anaesthetic recovery. They will remain

flat for at least one hour, in order to allow the cement to fully set. The patient is admitted to

a surgical ward for overnight observation and reviewed the following day with a view to early discharge.

Clinical follow-up is useful, providing feedback to the operator and the referring clinicians. It is also an opportunity for the patient to discuss any ongoing concerns, and to assess for any subsequent VCFs in adjacent vertebral levels. At my centre, follow-up is undertaken by the referring spinal surgeon in outpatient clinic.

1.2.3.5   COMPLICATIONS

The most important complications that may occur following PVP relate to leakage of cement. If there is cement leakage into paraspinal veins, this can result in cement pulmonary embolism (102). Hodler et al. found that small to moderate volumes of cement leakage (defined by the authors to be cement leakage of a length up to the height of the vertebral body) were not associated with significant effect on clinical outcome (103).

Cement leak into intervertebral foramina or the spinal canal can result in neurological deficit (104). Other complications are rare, and include infection, rib or pedicle fractures, and soft tissue haematomata. The literature suggests that there is an overall complication rate of 1% – 2% in PVP performed for osteoporotic VCFs (99).

1.2.4 EVIDENCE FOR VERTEBROPLASTY

Since the introduction of vertebroplasty, there have been several studies assessing the efficacy of the procedure. However, there remains a dearth of large, prospective, randomised controlled trials. The few that have been performed focus on pain relief, and there is little in the way of strong evidence for functional improvement following vertebroplasty. The situation is further complicated by the fact that most of the available literature is based on the use of a single cement (PMMA). Table 1.1 shows the demographics of selected studies.

Study	Study Type	Number	Fracture type	Cement	Primary Endpoint Measure	Final Follow-up Length
Jensen et al. 1997 (105)	Prospective case series	47	Osteoporotic	PMMA	VAS	Immediate post-operative
Cortet et al. 1999 (106)	Prospective case series	20	Osteoporotic	PMMA	VAS, McGill-Melzack score	6 months
Cyteval et al. 1999 (107)	Prospective case series	23	Osteoporotic	PMMA	Huskisson pain scale	6 months
Barr et al. 2000 (108)	Retrospective	84	Osteoporotic (70) Malignant (13) Haemangioma (1)	PMMA	VAS	
Grados et al. 2000 (109)	Retrospective	34	Osteoporotic	PMMA	VAS	12 - 84 months (mean 48 months)
McGraw et al. 2002 (110)	Prospective case series	156	Osteoporotic	PMMA	VAS	6 - 44 months (mean 21.5 months)
Perez-Higueras et al. 2002 (111)	Prospective case series	12 initial levels + 4 new VCFs	Osteoporotic	PMMA	VAS, McGill	60 - 71 months (mean 65 months)
McKiernan et al. 2004 (112)	Prospective case series	66	Osteoporotic		Osteoporosis QoL Questionnaire	6 months
Kobayashi et al. 2005 (113)	Prospective case series	250	Osteoporotic	PMMA	VAS, mobilisation of previously immobile patients	4 - 25 months (mean 15.3 months)
Voormolen et al. 2007 (114)	Prospective open-label case-control	18 PVP / 16 OMT	Osteoporotic	PMMA	VAS, QUALEFFO, RMDQ	14 days
Buchbinder et al. 2009 (89)	Prospective double-blinded RCT	38 PVP / 36 Sham	Osteoporotic	PMMA	Pain score, QUALEFFO, RMDQ	6 months
Kallmes et al. 2009 (91)	Prospective double-blinded RCT	68 PVP / 63 Sham	Osteoporotic	PMMA	RMDQ, Pain score	3 months
Klazen et al. 2010 (92)	Prospective open-label case-control	101 PVP / 101 OMT	Osteoporotic	PMMA	VAS	1 year
Clark et al. 2017 (115)	Prospective double-blinded RCT	61 PVP / 59 Sham	Osteoporotic	PMMA	NRS pain score	6 months
Firanescu et al. 2018 (90)	Prospective double-blinded RCT	91 PVP/ 89 Sham	Osteoporotic	PMMA	VAS	1 month & 12 months
Buchbinder et al. 2017 (88)	Cochrane Review	1020 across 7 studies	Osteoporotic	PMMA	VAS, NRS	1 month - 12 months

Table 1.1 – Demographics of selected studies assessing the efficacy of vertebroplasty. VAS = visual analogue scale. NRS = numeric rating scale. QUALEFFO = quality of life questionnaire of the European Foundation for Osteoporosis. RMDQ = Roland Morris disability questionnaire

In 1997, a prospective study by Jensen et al. showed significant improvement in pain scores in the immediate post-operative period (82). A prospective study in 1999 by Cortet et al. showed significant improvement in pain scores over 6 month post-operative follow-up (106).

Another prospective study in 1999 by Cyteval et al. also showed significant improvement in pain scores at the immediate and 6-month post-operative periods (116). Barr et al. performed a retrospective review of 84 levels over a 3-year period, looking at both osteoporotic and malignant VCFs (117). They showed significant improvement in pain relief in 95% of the osteoporotic VCF group, but only 50% of the malignant VCF group. It should be noted that the malignant VCF group suffered from low numbers, with only 8 vertebral levels performed. Grados et al. carried out a retrospective review of patients with varying length of follow-up, up to 84 months (mean 48 months), and showed significant improvement in pain scores (109). In 2002, McGraw et al. performed a prospective case series with a larger number of vertebral levels performed (n = 156), and similarly showed immediate and continued pain relief (110). That same year, Perez-Higuera et al. published a prospective case series with long-term follow-up of at least 5 years; the results indicated that PVP could provide sustained pain relief (111). McKiernan et al. showed significant improvement in quality of life following PVP, immediately and up to 6 months (112). As already demonstrated by these studies, Kobayashi et al. demonstrated significant pain relief following PVP, but importantly showed that 81.7% of immobilised patients were mobile at 24 hour follow-up (118).

These studies showed early promise for the efficacy of vertebroplasty as a therapeutic option for both osteoporotic and metastatic VCFs but suffered from a lack of control groups. The 2007 VERTOS study attempted to address this particular limitation, by comparing 18 PVP patients with 16 treated with optimal medical therapy (114). The authors looked at osteoporotic VCFs between 6 weeks and 6 months old, and found that at day 1 and day 14 post-operatively, the PVP cohort had better Visual Analogue Score (VAS) and used less analgesia. However, the study was limited by low numbers. The follow-up period was also short as, after 14 days, 14 of the optimal medical therapy cohort requested PVP.

In August 2009 two double-blinded RCTs comparing PVP with a sham procedure were published in the New England Journal of Medicine. In contrast with the available evidence, both of these studies showed no significant difference between PVP and placebo in terms of pain relief of QoL scores (119, 120).

The sham procedures for these studies were well designed, and these two trials represented the highest level of evidence available for the evaluation of PVP.

Buchbinder et al. (89) performed the same steps as for the PVP cohort, including the same local anaesthesia and skin incisions, and inserted a 13G needle "to rest on the lamina". At this point, the sharp stylet was replaced with a blunt one which was tapped. PMMA was prepared in the operating room. This was done to create the sounds and smells as if PVP was being performed.

Kallmes et al. (91) similarly gave local anaesthesia to both cohorts but did not place the PVP needle in their sham procedure. Instead, they applied pressure to the patient's back to simulate the sensation of PVP. They also prepared PMMA to recreate the smell of PVP.

The results of these studies garnered much controversy, perhaps not least because they flew in the face of not only the weight of lower tier evidence already available, but also the anecdotal experience of clinicians around the world. There followed several editorial articles attempting to rebut these studies (121, 122). As the authors pointed out in a follow-up response article, uncontrolled and open studies are at risk of over-estimating treatment benefit for a variety of reasons, including the "favourable natural history of vertebral fractures" (i.e. the pain tends to improve over time regardless of treatment), placebo effect, and volunteer bias, to name a few (123).

Although both studies were robustly designed, there are several limitations in their execution which are not simply "spurious reasons to dismiss our results", as Buchbinder and

Kallmes claimed in the above response. The key limitations to both studies relate to their patient selection. Both studies suffered from low patient numbers, as enrolment into an operative RCT is a difficult process.

Both selected patients with back pain due to fractures of no more than 1 year duration. However, 1 year is a long duration given the natural history of vertebral fracture pain. This is well beyond the length of time that most clinicians would describe as an acute fracture, which would extend up to 6 weeks (124). The average duration of pain in the Buchbinder trial was 9.5 weeks, and in the Kallmes trial was 18 weeks.

Only 25 patients included by Buchbinder et al. (89) had fractures of less than 6 weeks duration. Kallmes et al. (91) did not specify how many had fractures less than 6 weeks duration in their initial study, but in the previously mentioned response article they noted that 20% of their patients had fractures of less than 6 weeks duration (they do not specify whether this is 20% of their total population, or 20% of their PVP cohort; the difference could be of importance when considering possible subgroup analyses). Subgroup analysis by Buchbinder et al. did not find any significant difference in outcome between those with fractures less than 6 weeks and greater than 6 weeks of age, though the authors admit in their subsequent response article that these subgroup analyses were underpowered. However, they also state that since the overall effect of vertebroplasty in both studies was close to zero, it is unlikely that any particular subgroup would show significant benefit (123).

Buchbinder et al. used the presence of marrow oedema as proof of the acute nature of a fracture (125). Kallmes et al. (91) only performed MRI in cases where they felt that fracture age was uncertain (itself raising possible questions regarding their patient selection), and again used marrow oedema as a defining characteristic. In the context of fractures, bone marrow oedema is generally held to represent a combination of trabecular microfractures with associated haemorrhage and oedema (126, 127). However, as far as I am aware, there is no evidence available to suggest that the persistence of marrow oedema without the

presence of a fracture cleft is due to an unhealed fracture. In fact, clinical experience would suggest that the appearance of marrow oedema may persist beyond the presence of an unhealed fracture. Previous work on post-traumatic bone marrow oedema without fractures in the knee suggests that the appearances of marrow oedema can take 2 – 4 months to resolve (128).

This is an area in which further study is clearly warranted, but certainly Buchbinder and Kallmes' claims that the mere presence of high T2 marrow signal is diagnostic of an acute injury cannot be validated at present.

Following these two RCTs, the open-label RCT VERTOS II study was published, again comparing PVP and OMT (92). The inclusion criteria specified only patients with back pain of less than 6 weeks duration. The authors showed significantly improved reduction in VAS in the PVP cohort compared with the OMT cohort. However, the study was unblinded, and therefore at greater susceptibility to bias than the prior double-blinded RCTs.

In 2017, a third double-blinded placebo-controlled RCT was performed by Clark et al (93). The sham procedure performed by the authors was similar to that used by Kallmes et al. (91). The authors specified strict inclusion criteria, in particular only accepting patients with pain of less than 6 weeks duration. They demonstrated that PVP was significantly better than placebo for pain reduction.

Kallmes and Buchbinder responded with an editorial article in the British Medical Journal (BMJ) highlighting limitations with this study (129). In particular, they raise concerns about the sham procedure. The fact that Clark et al. (115) used an odourless cement is a reasonable point of contention. However, their claims regarding the lack of deep needle placement meaning the sham procedure was not as effective as their own previous studies, is not valid; certainly, the fact that Clark et al. (115) inserted needles at all made their sham procedure perhaps more robust than Kallmes et al. (91).

Another potential limitation of the VAPOUR trial is the conflicting results between numeric rating scale (NRS) pain score and visual analogue scale (VAS). Additionally, there was no significant difference between the two groups in terms of analgesic use. These findings raise questions about whether the authors have overstated the benefits of vertebroplasty.

In 2018, VERTOS IV trial (130) was published. This was the largest sham-procedure controlled trial to date, with 91 patients in the vertebroplasty group and 89 in the sham group. The authors found that no significant differences in pain reduction between the groups at either 1 month or 12 months post-procedure. Initially, to address some of the criticisms of earlier trials regarding the inclusion of patients with older fractures, the authors excluded patients with a history of >6 weeks of focal pain at the level of the fracture. However, due to difficulty with recruitment, they relaxed this criterion to include patients with up to 9 weeks of pain, 6 months after starting recruitment.

In 2017, Buchbinder et al. published a comprehensive Cochrane systematic review, which has been updated in 2018 (131). This initially included preliminary results from the VERTOS IV trial, and was updated to account for the full published results. The review concluded that overall, the weight of the evidence suggested that there was no benefit to vertebroplasty compared to sham procedure. The authors noted that although many of the studies comparing vertebroplasty with optimal medical therapy did show benefits, these studies were considered as high risk of bias due to a lack of any blinding of either authors or participants.

However, the limitations of the individual sham-controlled trials once again applies to this review, in that patient selection may have been inappropriate. The review is of great use to clinicians in that it consolidates and evaluates the evidence suggesting that for fractures older than 6 weeks, vertebroplasty provides no significant improvement in pain relief over a sham procedure.

The benefits of the sham procedure are considered unlikely to be due to the injection of local anaesthetic, which would not continue to be efficacious after several months. It is more likely that it provided some short term relief, and that the pain relief in both groups was predominantly due to the natural history of fracture healing.

The results of the review were indeed contentious. Indeed, the authors of the VERTOS IV trial themselves noted that they continue to offer vertebroplasty to a select group of patients. Based on results from Clarke et al. (93), it is possible that vertebroplasty may still be an effective treatment for hospital inpatients with osteoporotic fractures less than 6 weeks old, with severe pain (VAS >7).

The limitations of available evidence and the conflicting results have generated much heated argument, with apparent partisan battle-lines drawn. Undoubtedly authors and clinicians on both sides of the debate have much at stake, and with each new trial, there follows a flurry of editorials attempting to discredit any findings contrary to a particular group's beliefs. Selecting patients for these studies remains difficult, not only in terms of recruiting adequate numbers of patients, but also on determining fracture age. Patients may have multiple fracture events at the same vertebra, and this can make aging fractures particularly challenging. This same issue would apply to clinicians selecting patients for a vertebroplasty procedure.

In the UK, vertebroplasty continues to be used in carefully selected clinical scenarios at certain spinal centres, albeit without NICE guidance since 2009. Although most operators have good anecdotal experience (93, 130), the conflicting literature is a cause for concern, especially given the potential for harm with an operative procedure. It is this author's belief that the only claim that can be made with any certainty is that it is of great importance that more studies be performed, in order to ensure that patients receive the best care.

1.3 CADAVERIC MODELS FOR SPINAL INTERVENTIONS

1.3.1 BACKGROUND

Spinal procedures such as vertebroplasty are continuously evolving, with new cements and techniques such as Cortoss™ cement (132), or unipedicular injection which involves placing one needle via one pedicle rather than two needles through both pedicles (133). One of the difficulties in developing tools in this area is pre-clinical phase testing.

Human or animal cadaveric models represent a potential method for testing new devices and cements. Animal models would seem particularly useful given their wide availability and low cost. However, there is little consensus in the literature about which animal model should be used for transpedicular techniques such as vertebroplasty, if indeed any are appropriate.

1.3.2 HUMAN CADAVERIC MODELS

The role of human cadavers in the medical sciences dates back to ancient history, with records suggesting that ancient Greek physicians performed cadaveric dissection, for several centuries, to further their understanding of human anatomy and disease processes.

Following a period of history during which cadaveric dissection was considered blasphemous by the Church in Europe, there was a revival of the practice in 14th century Italy. Since then, human cadavers have been widely used primarily in an educational role in medical schools, but also for teaching purposes such as for surgical skills training (134).

Human cadavers have also played a role in research by providing biomechanical information

regarding various tissues, as well as models for certain diseases. Early work on using cadavers to model response to injury was performed in Germany in the mid-19th century. Further cadaveric work on injuries led to improved safety developments in the motor and aviation industries (135).

There are advantages to cadaveric models compared to animal models or computer simulations, in particular the fact that they exactly represent human anatomy. There are also limitations to the use of cadavers. Of particular relevance is the fact that cadavers lack muscle tone and pre-injury voluntary muscle contraction, which play an important role in the biomechanics of an injury (136, 137). Attempts to simulate muscle tone with external hardware or cadaveric preparation have not been successful. Additionally, there are physiological responses to injury such as haemorrhage and inflammatory responses that will also be lacking in a cadaveric model (135).

The forces applied to a cadaveric spinal block will also differ from those seen within live humans with what have been termed "follower loads" *in vivo* which depend on muscular and ligamentous attachments and result in almost pure axial compression of each spinal segment (138).

1.3.3 ANIMAL CADAVERIC MODELS

Animal models represent a cheaper and more widely available alternative to human cadaveric vertebrae. However, there is little consensus as to which animal species is most appropriate for use as a model of the human vertebra when considering percutaneous transpedicular spinal procedures. This is discussed in more detail in Chapter 2, a systematic review of the evidence for various animal models.

Animal models of disease, both live and cadaveric, are well established in the literature

throughout medical sciences. There is such vast variation in the animal kingdom, even between relatively closely related species, that it is not sufficient to simply test one's hypothesis on any animal and hope that results are applicable to humans. In 1929, the Danish physiologist August Krogh suggested that for any particular problem, there may be a particular animal or group of animals that will be appropriate for testing (139).

In the field of musculoskeletal research, a set of guidelines has been suggested following a 2007 forum discussion between musculoskeletal researchers, veterinarians, ethicists and legal experts. Much of the guidance discusses the ethical considerations when performing experiments on animals, but their guidelines include consideration of "Potentially confounding variables (genetic background, seasonal, hormonal, size, histological, and biomechanical differences)" (140).

The first issue is the selection of an appropriate non-primate species. Pigs, sheep and calves are often considered as reasonable analogues for human spines, due to size and anatomical similarity. Of these animals, pigs are generally held to be the closest approximation to humans in terms of vertebral dimensions (141, 142). The comparisons available the literature have focused on basic morphological measurements, such as vertebral body height, width and length, and pedicle height and width. These measures are discussed in more detail in Chapter 3, which describes a study comparing the morphometry of human, pig and sheep vertebrae.

Although the physiology and anatomy of quadrupeds must differ from humans, the literature suggests that in fact axial loading forces are predominant in quadrupeds, just as in humans (141). There are also similarities in the paraspinal musculature. Figure 1.2 shows the paraspinal muscles of the lumbar spine in humans, pigs and sheep.
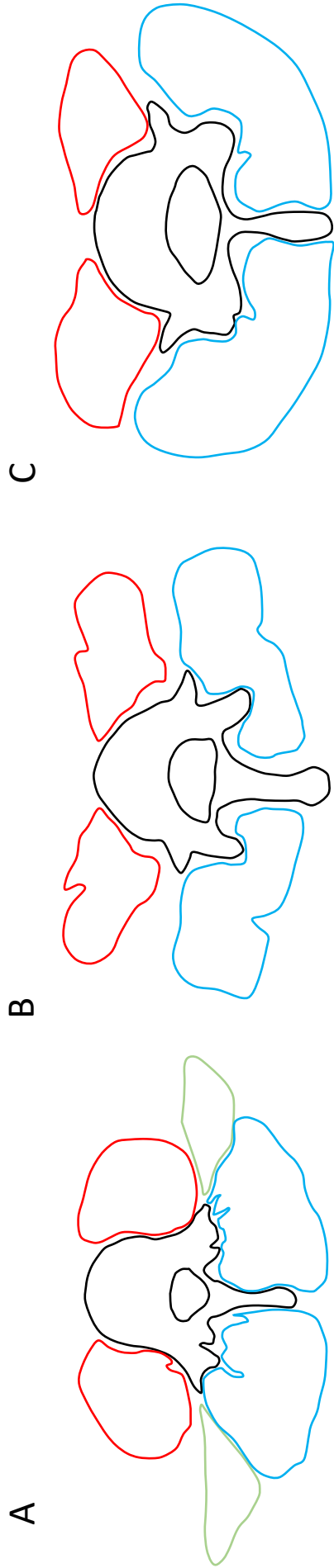
Figure 1.2: Diagram of the paraspinal muscles of A - humans, B - pigs, and C - sheep. The diagram shows an axial slice through the level of the L4 vertebra. The psoas muscle is outlined in red, and the erector spinae muscle group is outlined in blue. The human spine has an additional bilateral muscle, the quadratus lumborum, which is outlined in green

There are inevitably differences in physiological loading and anatomical variation between pigs and humans. Quadrupeds in general have higher axial loading and therefore greater bone mineral density, which must be taken into consideration.

Furthermore, the selection of species may depend upon the specific tests required, as discussed in the narrative systematic review of the relevant literature.

Additionally, the age of the specimen will be of relevance. Slaughtered sheep and pigs tend to be younger than the relevant human population, and therefore differences in bone mineral density and presumably also cement spread characteristics, will also be compounded.

1.4 BONE TEXTURE

The external morphometry of the vertebrae is one factor to consider when contemplating a model for examining percutaneous transpedicular techniques. The internal microarchitecture may also be of importance, particularly in the context of bone cement injection. The pattern of cement spread and loading mechanics could be expected to vary depending on the internal trabecular arrangement, as discussed below. Using texture analysis on vertebrae offers a non-destructive method to compare the trabecular microarchitecture between species.

1.4.1 BONE ANATOMY

In clinical, radiological, and anatomical terms, a "bone" is conventionally defined as an organ of the skeletal system. As discussed earlier, bones are divided into four main

categories based on their shape and size: long bones, short bones, flat bones, and irregular bones (in which category vertebrae are considered) (11).

Somewhat confusingly, "bone" as a term is also used to describe several components found within the "bone" as an organ. The usage of "bone" as a term may refer to either bone matrix excluding osteoid tissue, bone matrix including osteoid tissue, or bone matrix including marrow and other soft tissues (143) . In order to conform to the convention of terminology for bone histomorphometry proposed by Parfitt et al. in 1987 (143), I will use the term bone to refer to bone matrix including osteoid tissue.

This bone matrix includes cortical bone, and cancellous (trabecular) bone. Medullary tissue contains a network of trabecular bone which runs through the soft tissues of the marrow. This is of relevance to intramedullary cement injections as the spread of cement and resulting cement-trabecula interface is likely related to load transfer, as the interface is the site of the majority of microarchitectural cracks on stressing (144).

Computerised modelling suggests that the partially interdigitated interface of cement and trabeculae is the predominant site of loading. The partially interdigitated interface refers to the areas where the cement has not fully spread through the gaps in the trabecular architecture, i.e. there is some interdigitation but there also remains a broad bone to cement interface. This differs from the fully interdigitated interface, where the cement has spread through the inter-trabecular spaces to form a branching pattern of spread. As most load transfer occurs at the partially interdigitated interface and relatively little load transfer occurs at the fully interdigitated interface, it is suggested that the partially interdigitated interface is more important for mechanical strength (145). Other computerised modelling studies suggest that the majority of stress shielding may occur in this fully interdigitated region (146).

When considering an animal model for use in testing vertebral cements, the trabecular architecture may therefore be of relevance.

1.4.2 BONE TEXTURE ANALYSIS

Texture Analysis (TA) is a method by which the internal microarchitecture of the bone may be assessed. The first use of imaging to analyse trabecular architecture documented in the literature was described in 1971 (147). The authors developed a system for assessment of trabecular architecture using plain radiographs.

In 1973, Haralick (148) developed computable greyscale textural features using photo-micrographs of sandstone, and panchromatic aerial photographs and satellite imagery of land-use categories (148). With the subsequent development of Computerised Tomography (CT) as a clinical imaging modality, these methods began to be used for the CT analysis of trabecular architecture (149).

CT texture analysis assesses the same structures as conventional histomorphometry and therefore terminology follows the histomorphometric convention established by Parfitt et al. in 1987 (143).

BV	Bone Volume
TV	Tissue/Total Volume
BV/TV	Apparent bone fraction
Tb.Th	Apparent Trabecular Thickness
Tb.Sp	Apparent Trabecular Separation
Tb.N	Trabecular Number

Table 1.2 – Texture Analysis terminology and abbreviations

The statistical model analysis of textural features is divided into first-order and second-order statistics based on the work of Haralick (148, 150). First-order statistics refer to pixel grey

level intensity, with no information on spatial arrangement, and include mean intensity, thresholds, entropy, and skewness and kurtosis of pixel density histogram. The features included in Table 1.2 are all derived from first-order statistics. The BV/TV represents the proportion of the volume that is bone matrix by taking the number of bone pixels divided by the total number of pixels. Tb.Th gives a measure of the thickness of trabeculae as defined by the greatest diameter of any given trabecula, and Tb.Sp the thickness of marrow spaces between trabeculae as the greatest diameter of any given space.

These are useful information when considering cement injection and spread, given the properties of the cement/bone interface and loading as discussed above.

Second-order statistics contain spatial information. These include run-length matrix, second-order entropy, homogeneity, dissimilarity, and correlation. For example, a run-length matrix $p(i,j)$ is defined as the number of runs with pixels of a grey level i and run length j (151) and is of particular use when assessing coarseness.

Although micro-CT is the preferred method of image acquisition (152), it is only viable for cadaveric specimens due to the extremely long acquisition times which can take up to several hours. Faster scan times are possible, but even these scans can take several minutes for a small volume acquisition, though this may vary depending on the scanner. Scan times in the order of 5 - 15 minutes can be achieved by using larger voxel sizes with lower resolution as a trade-off (153). However these scans may not provide any significant benefit over clinical high resolution CT when assessing smaller structures. To my knowledge, no work has been performed to assess this. Standard high resolution CT images have proven sufficient for performing TA (154).

1.5 STATISTICAL SHAPE ANALYSIS

Basic morphometric measurements are not the only method of comparing the external shape of vertebrae. Statistical Shape Analysis (SSA) is a field which provides methods of comparing the morphologies of objects. Of specific interest to this study are the use of similarity transformations, thin plate spline (TPS) deformations, full generalised Procrustes analysis (GPA) and principal component analysis (PCA) to create a statistical shape model (SSM). A statistical shape model is a deformable object which represents the shape variation of an object around a mean object shape.

The full description of the mathematics involved in these processes as well as SSA in general, is beyond the scope of this thesis. For a more detailed discussion, the reader is referred to *Statistical Shape Analysis 2nd Edition* (155). A simple description is provided below.

1.5.1 TERMINOLOGY IN SHAPE ANALYSIS

When considering shape analysis, I will use several definitions proposed by Kendall (156). Shape is therein defined as "*all the geometric information that remains when location, scale, and rotational effects are removed from an object*". Shape is therefore invariant to Euclidean transformations.

Landmarks are points that are assigned to the surface of an object. Kendall defined them as "*a point of correspondence on each object that matches between and within populations*". They are valuable when attempting to align complex shapes, as they provide fixed, corresponding points to assist in the alignment process. Landmarks may be subdivided into three groups (155). A scientific landmark (also termed an anatomical landmark) is "*a point assigned by an expert that corresponds between objects in some scientifically meaningful*

way". Mathematical landmarks are "*points located on an object according to some mathematical or geometrical property of the figure*". Pseudo-landmarks are "*constructed points on an object, located either around the outline or in between scientific or mathematical landmarks*".

Semilandmarks are defined by Gunz et al. (157) as a set of points used to represent curved surfaces that cannot be quantified with landmarks. These are of use in complex shapes with curved surfaces, such as vertebrae.

I will also use Dryden and Mardia's definitions of labels, configuration, configuration space, configuration matrix, and centroid size (155).

A label is defined as "*a name or number associated with a landmark, and identifies which pairs of landmarks correspond when comparing two objects.*" Thus when a landmark is associated with a label, it is called a labelled landmark.

A configuration is the full set of landmarks of an object.

Centroid size is the definition used for the size of an object by many authors, including Kendall (156), Bookstein (158), and Dryden & Mardia (155). The centroid size S(X) is "*the square root of the sum of squared Euclidean distances from each landmark to the centroid*", and the centroid $(\overline{X})$ is the mean of the coordinate values.

The centroid allowed me to use a computable equivalent of the centre of gravity around which to calculate vector deviations, and to align shape models.

1.5.2 HISTORY OF SHAPE ANALYSIS

Shape analysis has been performed by a variety of methods in biological fields throughout history. Galileo first noted that bones in larger animals are not simply just larger than the equivalent bones in smaller animals but differed in shape due to the different mechanical strains they would undergo (159). Formal shape analysis has traditionally been performed by a method which has come to be termed multivariate morphometrics (160, 161). It involves the placement of landmarks on the shape, and then performing multivariate analyses on the distances and angles between these landmarks on the shapes being compared. Early examples of such work include comparisons of skull shape between racial groups (162). These techniques are non-geometric, and the datum used is distance or angle between coordinates, rather than the coordinates themselves. This is similar in principle to the basic morphometry measurements used in much of the background literature comparing animal and human vertebrae – these studies use isolated distance measurements.

Geometrical shape analysis offers an alternative approach to shape analysis. This differs from multivariate morphometrics in that it considers the entirety of the shapes themselves, rather than using derived quantities such as distances or angles between landmarks. An early example of this technique was used by Thompson (163). He placed Cartesian grids on a shape such as a hand-drawn human skull. This grid was then deformed to fit a hand-drawn animal skull such as a chimpanzee, with each segment of the grid corresponding to the same part of the animal skull as the human. Figure 1.3 provides an example from Thompson's work of grids being used to deform crab carapaces from one species to another.

Fig. 142. Carapaces of various crabs. (a) *Geryon*; (b) *Corystes*; (c) *Scyramathia*;
(d) *Paralomis*; (e) *Lupa*; (f) *Chorinus*.
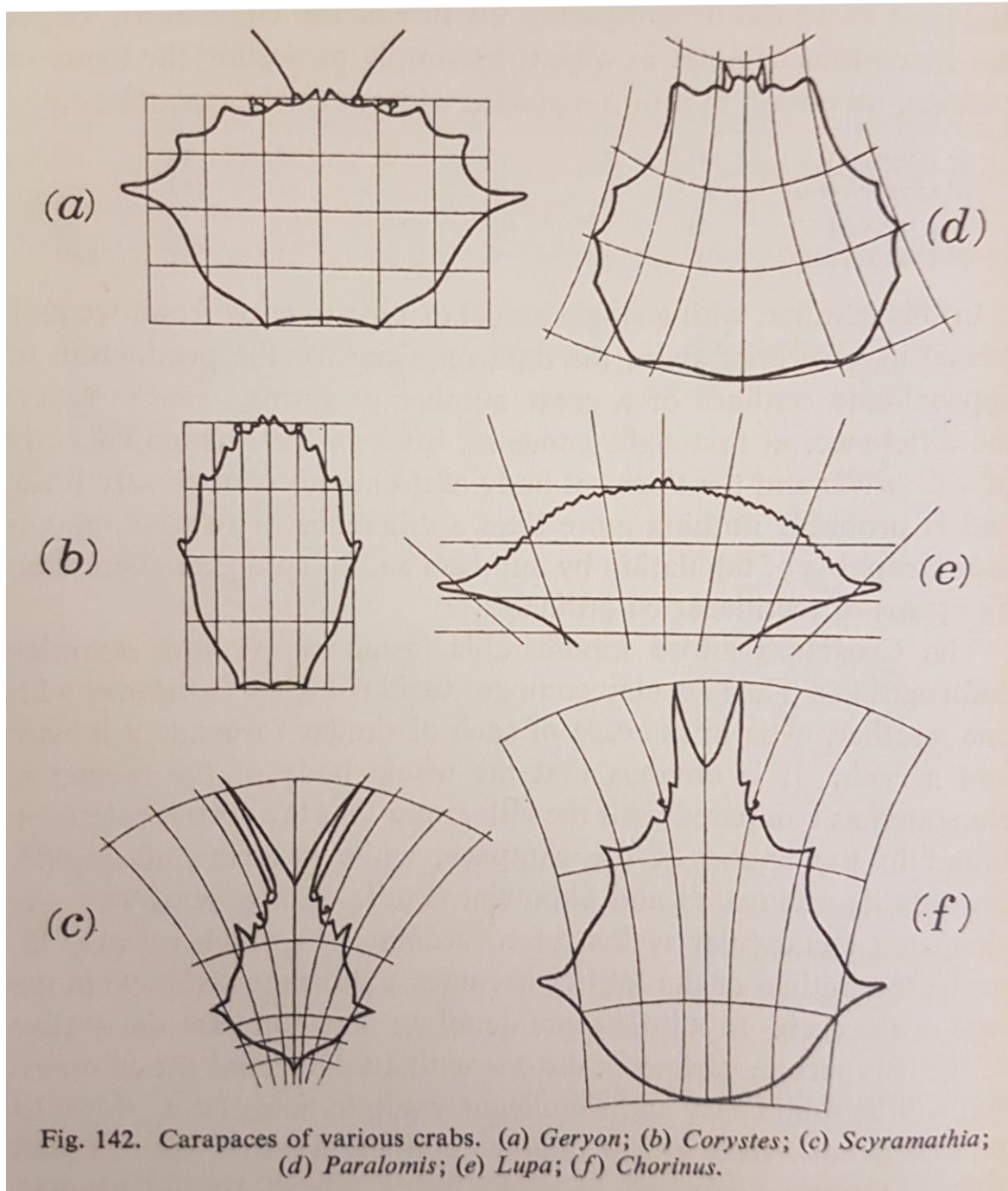
Figure 1.3 – Cartesian grids deformed between the carapaces of different crab species, taken from Thompson's *On Growth and Form (1917).* (a) shows the Geyron species with a Cartesian grid overlaid. (b) - (f) show various deformations of the Cartesian grid changing the shape of the Geyron species to the shape of Corystes, Scrymathia, Parolomis, Lup, and Chorinus species.

Thompson's technique was highly subjective, and his early hand-drawn images were not particularly accurate (164), however the concept was established. The field of geometric shape analysis was furthered in the late '70s with work by Kendall (156) and Bookstein (158).

With the advent and rapid development of computer hardware and software, methods of transformation were explored further. Kass et al. (165) developed an active contour model which they named a "snake". The snake allowed accurate identification of edges, lines and contours. Cootes et al. subsequently developed "smart snakes" (166, 167). These active shape models were similar to the snakes of Kass et al., but provided more robustness as they allowed for greater control of the possible deformations using training sets, such that deformations were only possible if characteristic to the objects being represented.

1.5.3   AFFINE AND SIMILARITY TRANSFORMATIONS

Affine transformations are linear functions that preserve parallel lines and planes between shapes, and are the simplest possible size and shape change to match two objects. Figure 1.4 shows an example of an affine deformation from Thompson's 1917 *On Growth and Form* (163), where a square grid placed over the outline of a fish species is transformed into a parallelogram grid over a second fish species.

Fig. 146. *Argyropelecus olfersi.*   Fig. 147. *Sternoptyx diaphana.*
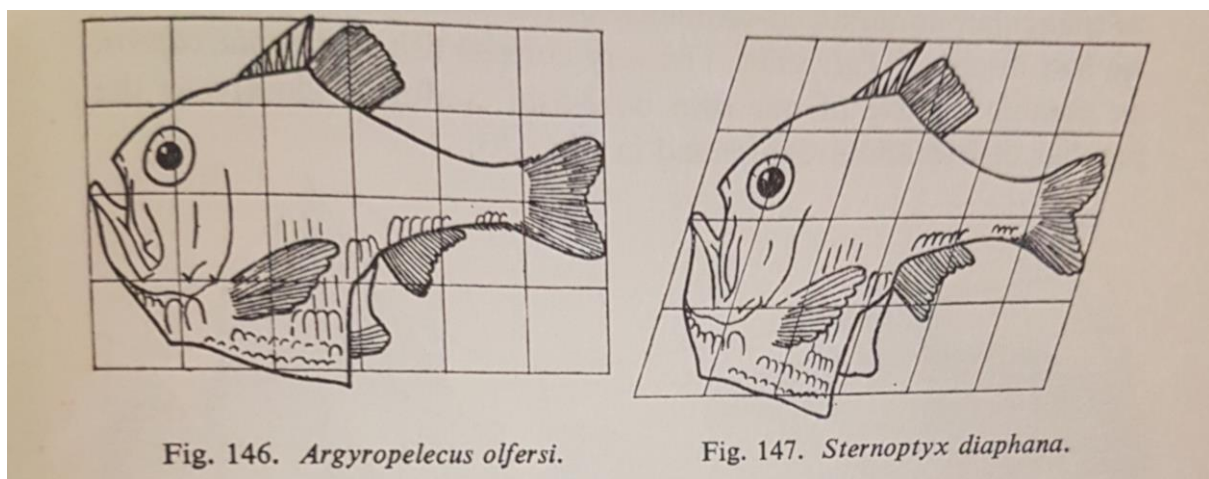
Figure 1.4 – From Thompson's *On Growth and Form (1917)*, deformation of the shape of one the Argyopelecus olfersi fish to the Sternoptyx diaphana, by using an affine transformation, from a square grid to a parallelogram grid.

A similarity transformation is a function that manipulates a Euclidean shape while preserving all the angles and ratios of distances, by translating, rotating, isotropic scaling, and reflecting. We can therefore see that this will preserve shape, as shape is independent of these parameters. From Dryden and Mardia (155), the Euclidean similarity transformations of a matrix of coordinates *X* are a set including scale, rotation matrix, and a translation factor.

Using the centroid coordinates to perform initial alignment removes translation. A similarity transformation can then be applied to match one shape to another, removing rotation and scaling.

1.5.4 THIN PLATE SPLINES

A thin plate spline (TPS) is an interpolation function that may be used as a method of deformation to fit a shape onto another while minimising bending energy. It is essentially a mathematical model application of Thompson's transformation grids. The initial application of TPS was limited to two-dimensional shapes but has subsequently been described for three dimensional shapes (168).

The TPS deformation relies on the use of homologous landmarks between two objects. The function interpolates the space between landmarks in a manner that minimises the bending energy. In more technical terms, it minimises the integral of the squared second derivatives of the interpolation.

The name "thin-plate spline" comes from the analogy of mechanical bending and is apt; the basis function is related to the equation of a uniformly thin metal plate being deformed from flat to bent (169).

TPS deformations may be used with semilandmarks, which is of relevance to the study in Chapter 5. As vertebrae are complex objects with multiple curved surfaces, semilandmarks are of use in creating shape models in this study.

1.5.5 PROCRUSTES ANALYSIS

The general Procrustes analysis (GPA) provides a method for aligning objects and generating a mean shape. It is a sum-of-least-squares technique which matches shape configurations with similarity transformations. A least-squares matching procedure was used in the literature at least as far back as by Boas (170), when describing a technique for skull morphology assessment. However, the term "Procrustes analysis" was first used by Hurley and Cattell (171) while defining a technique to test hypotheses by assessing the matches between factor patterns from a given set of data and from a hypothesis.

Procrustes was a mythological Greek blacksmith and bandit, also known as Damastes. He was a son of Poseidon who would invite travellers to spend the night in an iron bed, into which no-one ever fit exactly. He would stretch those who were too small by hitting them with his hammer and would amputate the "excess" from those who were too tall. He died when the hero Theseus captured him and fitted him to his own bed. The concept of "deforming" a shape to fit another shape is central to Procrustes analyses.

There are several variants of Procrustes analysis. I consider here the full general Procrustes analysis (Full GPA), as this is most relevant to the study in Chapter 5. The term "full" here refers to translation, rotation and scale transformations, compared to the partial GPA which only requires translation and rotation (172).

From *Statistical Shape Analysis 2nd Edition* (155), the full GPA method is defined as "*translating, rescaling and rotating the configurations relative to each other so as to minimize a total sum of squares*".

In essence, the full GPA performs a similarity transformation between objects to minimise the sum of squared differences between the vertex points of each object.

The Procrustes analysis thus provides a set of points of minimised sum of squared distances between the points of each sample object and the object to which they are being compared. The full proofs for this method may be found in detail in Chapter 7 of *Statistical Shape Analysis 2nd Edition* (155).

Once GPA has been performed, principal component analysis may be used to create a mean shape and statistical shape model which describes variation from the mean shape.

1.5.6 PRINCIPAL COMPONENT ANALYSIS

Principal component analysis (PCA) may be used to describe the variability of shape of the examined objects. It is a useful tool for reducing the number of dimensions of multi-dimensional data; although up to three dimensions may be represented with a straightforward plot, this is difficult with higher dimensionality. As the name suggests, PCA allows the user to identify the "principal component", or the component with the most significant relationship between data. Other components may also be assessed or ignored if not significant.

PCA was first described by Karl Pearson in 1901 (173), then subsequently further developed and so named by Harold Hotelling in 1933 and 1936 (174, 175). Cootes et al. (166) and Kent et al. (176) developed PCA for data from Procrustes analysis.

PCA is performed by subtracting the mean of each dataset from each datum point and creating a covariance matrix for the mean-adjusted data. Whereas standard deviation can only be applied to each dimension of multidimensional data independently, covariance is a measure of how two dimensions vary from the mean with respect to eachother. With datasets containing more than one dimension, multiple covariance calculations can be performed. The covariance matrix contains all possible covariance values between all the dimensions of a dataset.

The eigenvectors and their corresponding eigenvalues are then calculated. An eigenvector is a vector that upon the application of linear transformation, changes only by a scalar factor, i.e. if the transformed vector is a scalar multiple of the original vector, then it is an eigenvector. Each eigenvector has a corresponding eigenvalue, which is the scalar multiplication factor of that eigenvector upon linear transformation.

The direction of the eigenvectors shows patterns in the data, and all eigenvectors are orthogonal to each other. An example of this might be to consider 2-dimensional data on a data plot. One eigenvector might form line of best fit along the plotted data points, and a second orthogonal eigenvector might show variance of that data around the line of best fit.

The eigenvector with the largest corresponding eigenvalue is the "principal component". In the example above, this would be the eigenvector describing the line of best fit. The principal component is the most significant relationship between the data dimensions. For multidimensional data, there may be several components, aside from the principal component, that describe significant variation. Using this method, only components with sufficiently large eigenvalues as to be of interest can be assessed, while others with smaller values can be ignored with relatively little loss in information value.

The components with sufficiently large eigenvalues to be included will therefore show the most important deviations from the mean shape. These component deviations from the mean shape can be combined with the mean shape generated by GPA to produce shape modes, which are models demonstrating the variation produced by each component.

1.6 AIM OF THE THESIS

The primary aim of this thesis is to address the current shortage of evidence around selecting an animal species to model human vertebrae for use in early phase testing of new vertebroplasty cements and instruments, as well as for the purposes of training operators.

As discussed in the thesis outline, this will first involve a systematic review of the currently available literature comparing animal and human vertebrae. The following chapters will describe studies comparing pig, sheep and human vertebrae in terms of morphometrics, bone texture analysis, and statistical shape analysis.

The purpose of these studies will be to decide on which species, pig or sheep, is a closer approximation of human vertebrae in evaluating new vertebral cement materials, transpedicular needles, and for training new operators in vertebroplasty techniques.

CHAPTER 2:
SYSTEMATIC REVIEW OF ANIMAL MODELS
FOR SPINAL PROCEDURES

2.1 INTRODUCTION

Percutaneous transpedicular cement augmentation techniques aim to treat vertebral fractures with the injection of bone cement via needles, avoiding the need for open spinal surgery. These techniques, such as vertebroplasty and kyphoplasty, offer therapies for patients with osteoporotic spinal fractures. Three sham-controlled trials have suggested limited efficacy of vertebroplasty compared to placebo (119, 120, 130), which conflicted with anecdotal clinical experience and other trials including another sham-controlled trial (93).

Given the inconsistencies in the literature, further research into this area is important to ensure optimal treatment for patients. As well as clinical trials, there continues to be development and refinement of the techniques. These include investigations into a variety of bone cement options (117, 132, 177, 178).

Since early phase testing often cannot be performed on live humans, researchers require alternatives. Human cadaveric studies have a long history of use in medical research. Human cadaveric spines are not without their drawbacks, such as the effects of death and cadaveric preparation and preservation on the elasticity of tissues, the lack of active circulation or an

inflammatory response, to name but a few. Because they are similar in dimensions and morphology to the intended target of clinical research, they are in many ways the ideal substitute for live human subjects. Unfortunately, they represent a high cost and constrained resource, which often results in low sample sizes in cadaveric studies.

Animal models have therefore been used as alternatives. An animal model must be developed to mimic the particular aspects of the human pathology or anatomy that is to be tested. This could mean that different animals are preferred for different procedures.

In spinal surgical research, various animals, both live and cadaveric, have been used. Work has been done using nonhuman primates, which might seem a logical choice given superficial anatomical similarities to humans, in particular when bearing in mind size and gait (179). The cadaveric spines of large quadrupeds have also been used, in particular cows, sheep and pigs (180-182). These have previously been used on the basis of superficial similarity in size and shape. While studies have been done comparing various anatomical aspects of animal and human vertebrae, the evidence base has several important limitations. For example, most studies compare only a single animal with humans, and the lack of uniformity of certain measurements or even method of measurement, means that while a particular study may provide valuable information about the similarities and differences between one species and humans, it is difficult to compare the results with another study.

A systematic review of the literature by Sheng et al. in 2010 (183) identified 7 articles comparing human and animal vertebrae, including pigs, cows, sheep, deer and baboons. Since this review, new studies have been performed.

This narrative systematic review aims to collate the available studies looking at comparison between pig, sheep, cow and human spines, to assess whether any conclusions may be drawn in particular regarding the most appropriate animal model for use in testing percutaneous transpedicular cement augmentation techniques. I also aim to discuss the limitations of the available evidence and propose a framework for further studies.

2.2 METHODS

The OVID engine was used to search Embase and Medline databases. Search terms used were: human, animal, spine, verteb*, sheep, ovine, pig, porcine, cow, bovine. The search was limited to English language studies between 1974 and 2018.

Studies were included if they looked at sheep, pigs, cows, deer, goats and contained anatomical comparisons of the thoracic or lumbar spine between the animal and humans. I did not include nonhuman primates or dogs as these are less commonly used in research and are less widely available in the UK for research purposes. Studies only assessing intervertebral discs or biomechanical properties such as range of motion were also excluded, since these parameters were not relevant to my current aim.

47 search results were returned. After excluding duplicates, the remaining results were reviewed by two authors for their relevance according to the criteria detailed above, and 30 studies were excluded, giving a final total of 9 studies selected for review (142, 184-191). (Figure 2.1)
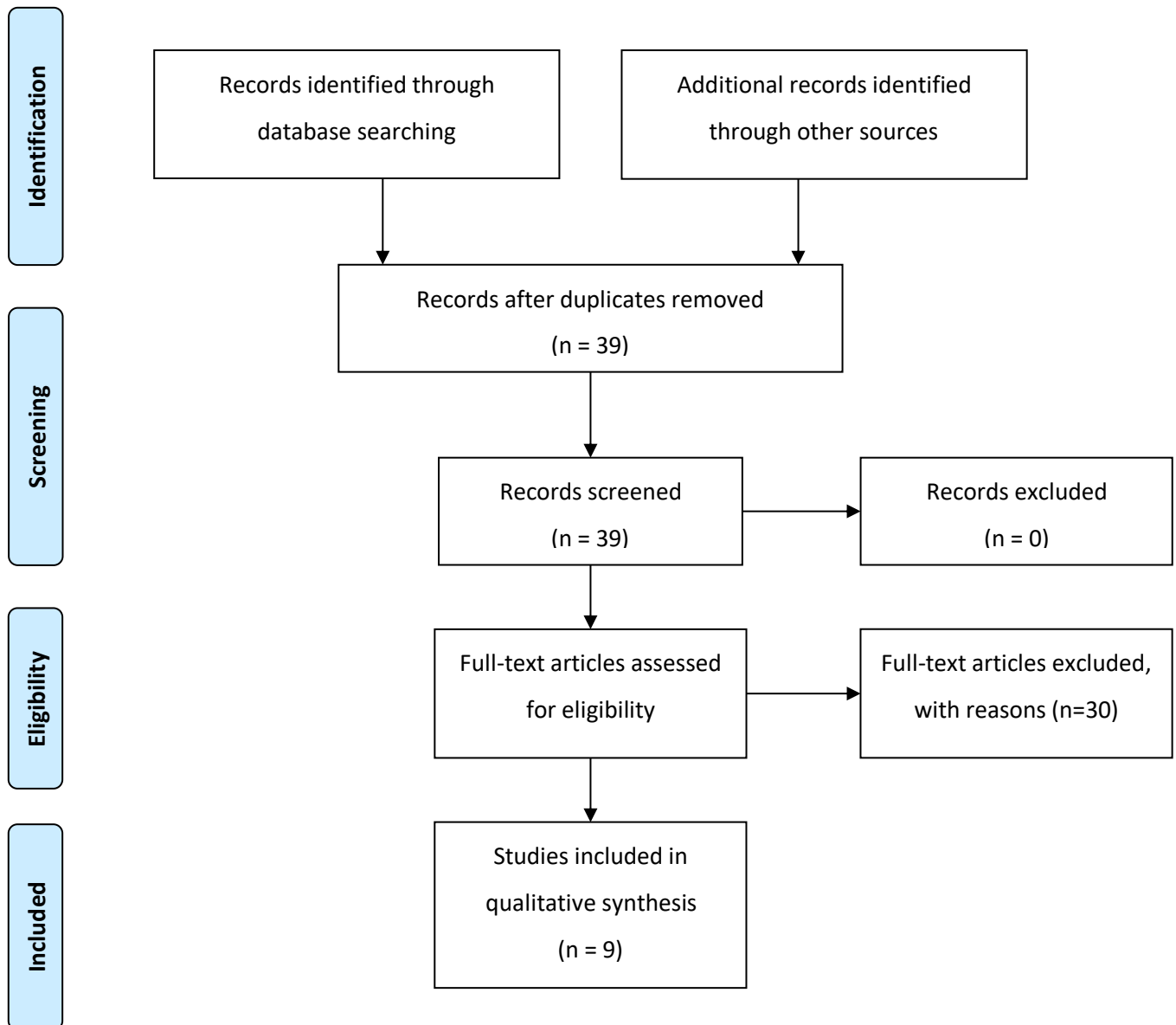
Figure 2.1 – Systematic review flow diagram showing the identification, screening, eligibility assessment of OVID search results from the Medline and Embase databases. Record screening and eligibility assessment was performed by two authors.

The results were taken from the included studies and combined for assessment. I also assessed the methodological rigour and validity of the conclusions of the studies.

I include within the results comparative human data from Panjabi et al., the most commonly cited human measurement study within the reviewed literature (192, 193).

2.3 RESULTS

Of the ten papers selected for review, three compared more than one species with humans. There was a total of one paper on cows, four on pigs, three on sheep, one on goats and one on deer. Commonly assessed parameters throughout most of these studies include: total length (TL), intertransverse length (IL) vertebral body width (VBW), vertebral body length (VBL), vertebral body height (VBH), spinal canal height (SCH), spinal canal depth (SCD), pedicle width (PW), pedicle height (PH), and pedicle angle (PA) (Figure 2.2). Where relevant, I include additional measurements that are not contained in all studies.
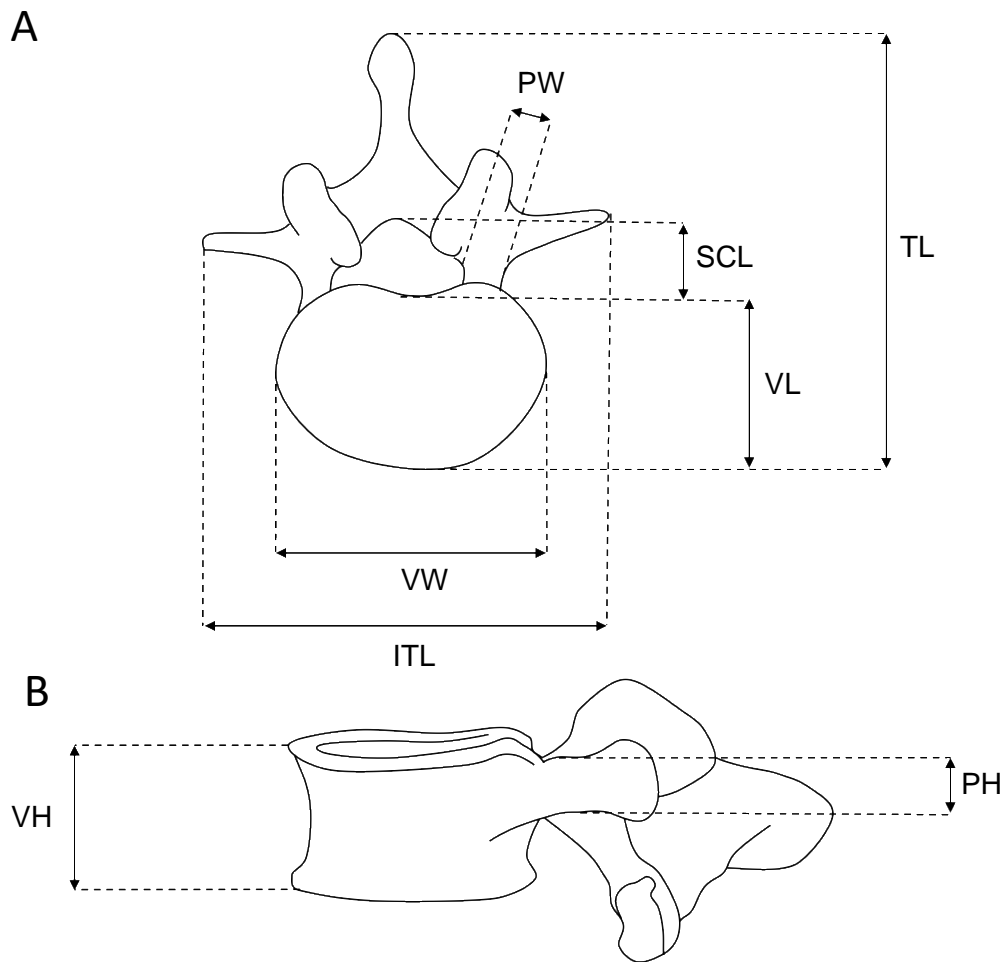
Figure 2.2 Diagram of a human lumbar vertebra showing the measurements of vertebral structures performed in the studies included in the systematic review A- superior view of the human lumbar vertebra. B – lateral view of the human vertebra. VH = vertebral body height; VW = vertebral body width; VL = vertebral body length; TL = total anteroposterior length, SCL = spinal canal length, PW = pedicle width, PH = pedicle height

The demographics of the included studies is shown in Table 2.1. Figures 2.3 – 2.9 compare the most commonly measured features relevant to vertebroplasty, wherever raw data were provided.

Table 2.2 shows selected comparison data from Yingling et al (185). These data are presented separately as the authors compared pig cervical vertebrae with human lumbar vertebrae.

Authors	Year	Species	Anatomical Segment	Animal Specimen	Number of animal spines	Human Specimen	Number of human spines	Measurement tools
Cotterill et al (184)	1986	Cow	Thoracic - T6&T12, Lumbar - L3	Fresh cadaveric 6-8 weeks old calves	10	Embalmed cadavers	10	Hand-held micrometer
Yingling et al (185)	1999	Pig	Cervical - C2-C7, compared with human lumbar	Pig cadaveric, otherwise unspecified.	3	Measurements from established literature	n/a	Hand-held calliper
Bozkus et al (186)	2005	Pig	Thoracic Spine (T1 - T16)	fresh cadaveric 6-month-old swine, mean weight 30 kg	10	Embalmed cadavers	10	Hand-held micrometer, Radiological - plain radiograph
Dath et al (187)	2007	Pig	Lumbar Spine (L1-L6)	fresh cadaveric 18 - 24-month-old swine, weight 60 - 80 kg	6	Measurements from established literature	n/a	Hand-held digital calliper
Busscher et al (142)	2010	Pig	Whole Spine (C3 - L6)	fresh cadaveric 4-month-old swine, mean weight 40 kg	6	Embalmed cadavers	6	Radiological - CT
Wilke et al (188)	1997	Sheep	Whole Spine	fresh cadaveric 3 - 4-year-old sheep, mean weight 72 kg	5	Measurements from established literature	n/a	Hand-held micrometer
Mageed et al (189)	2013	Sheep	Thoracolumbar (T2-L6)	Live 2-year-old sheep, mean weight 62 kg	5	Measurements from established literature	n/a	Radiological - CT
Kumar et al (190)	2000	Deer	Whole spine	Fresh cadaveric age 20 - 27-month deer, weight 46 - 52 kg	6	Measurements from established literature	n/a	Hand-held micrometer
McLain et al (191)	2004	Farm Pig	L4	Fresh cadaveric, 55 - 65 kg	10	Embalmed cadavers	7	Hand-held digital calliper
		Mature Yucatan Micropig	L4	Fresh cadaveric	5			
		Dairy Goat	L4	Fresh cadaveric, 35 - 40 kg	10			
		Sheep	L4	Fresh cadaveric, 45 - 50 kg				

Table 2.1 – Demographics of studies included in the systematic review, for cow, sheep, humans, deer and pig vertebrae
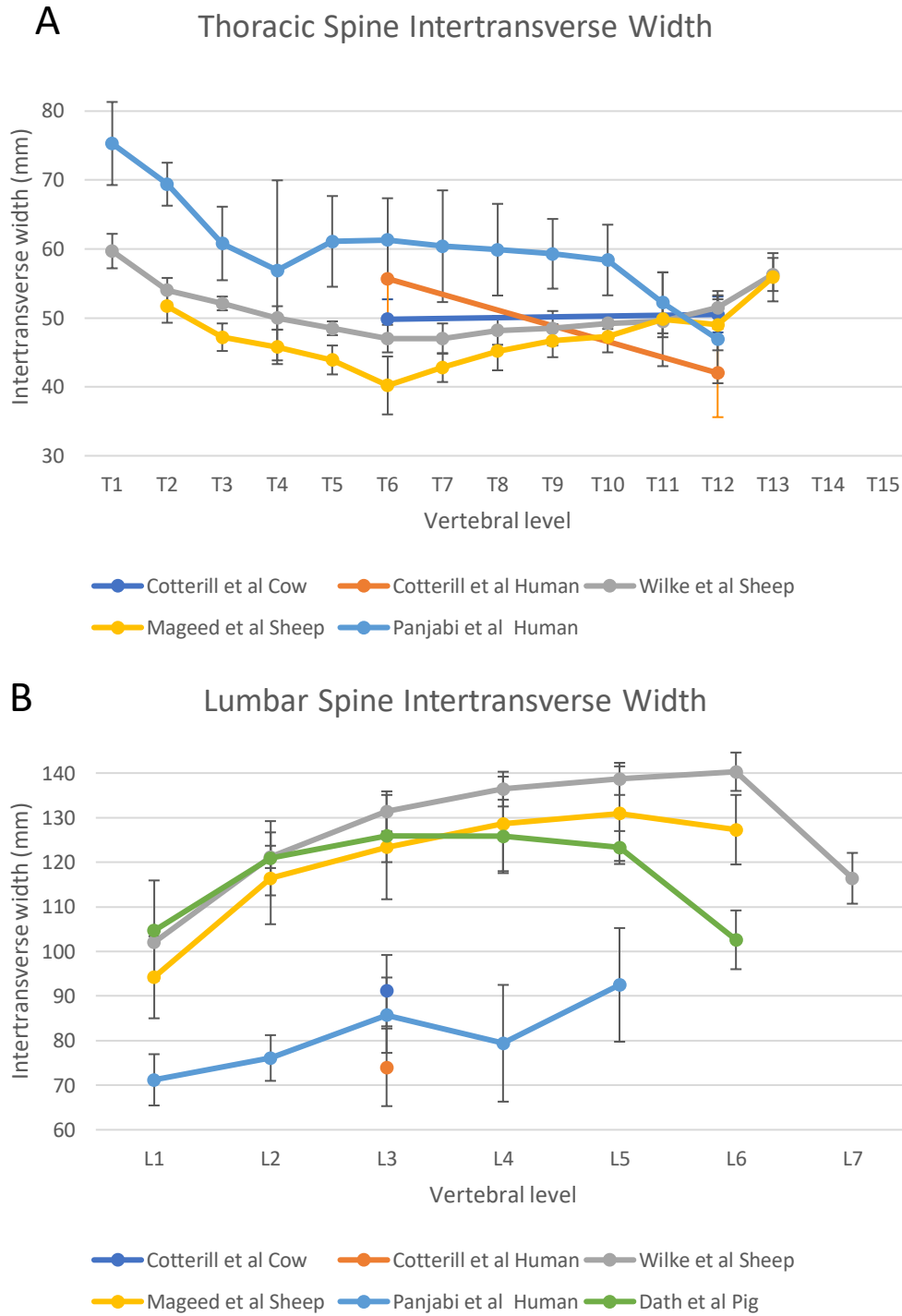
Figure 2.3 – Scatter plot of mean intertransverse process widths (mm) and standard error bars, taken from the studies included from the database search for cow, sheep, humans, deer and pig vertebrae. A – Thoracic spine intertransverse width. B – Lumbar spine intertransverse width.

A — Thoracic Anterior Vertebral Body Height

B — Lumbar Anterior Vertebral Body Height
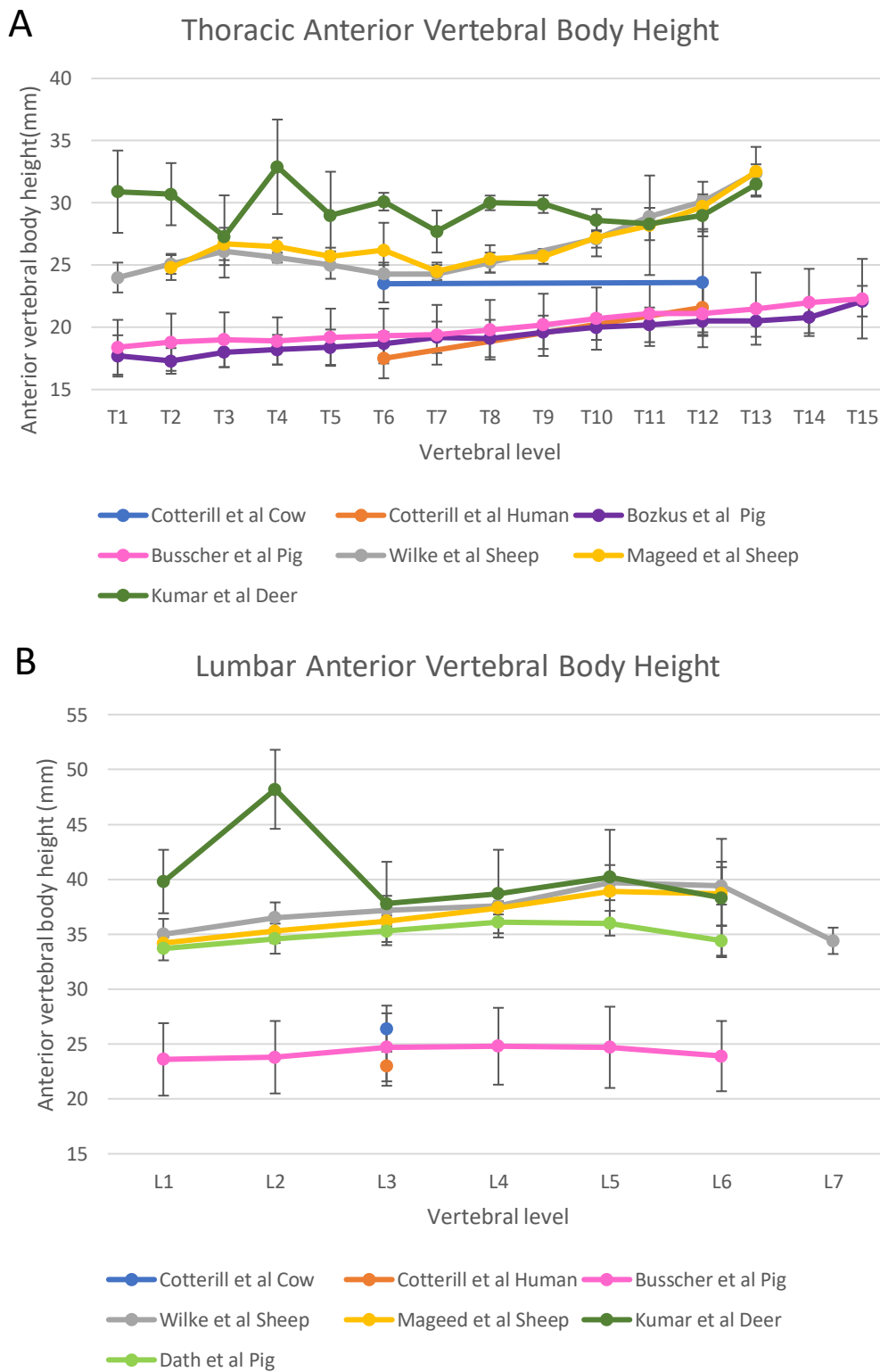
Figure 2.4 – Scatter plot of mean anterior vertebral body height (mm) and standard error bars, taken from the studies included from the database search for cow, sheep, humans, deer and pig vertebrae. A – Thoracic spine vertebral body height. B – Lumbar spine vertebral body height.
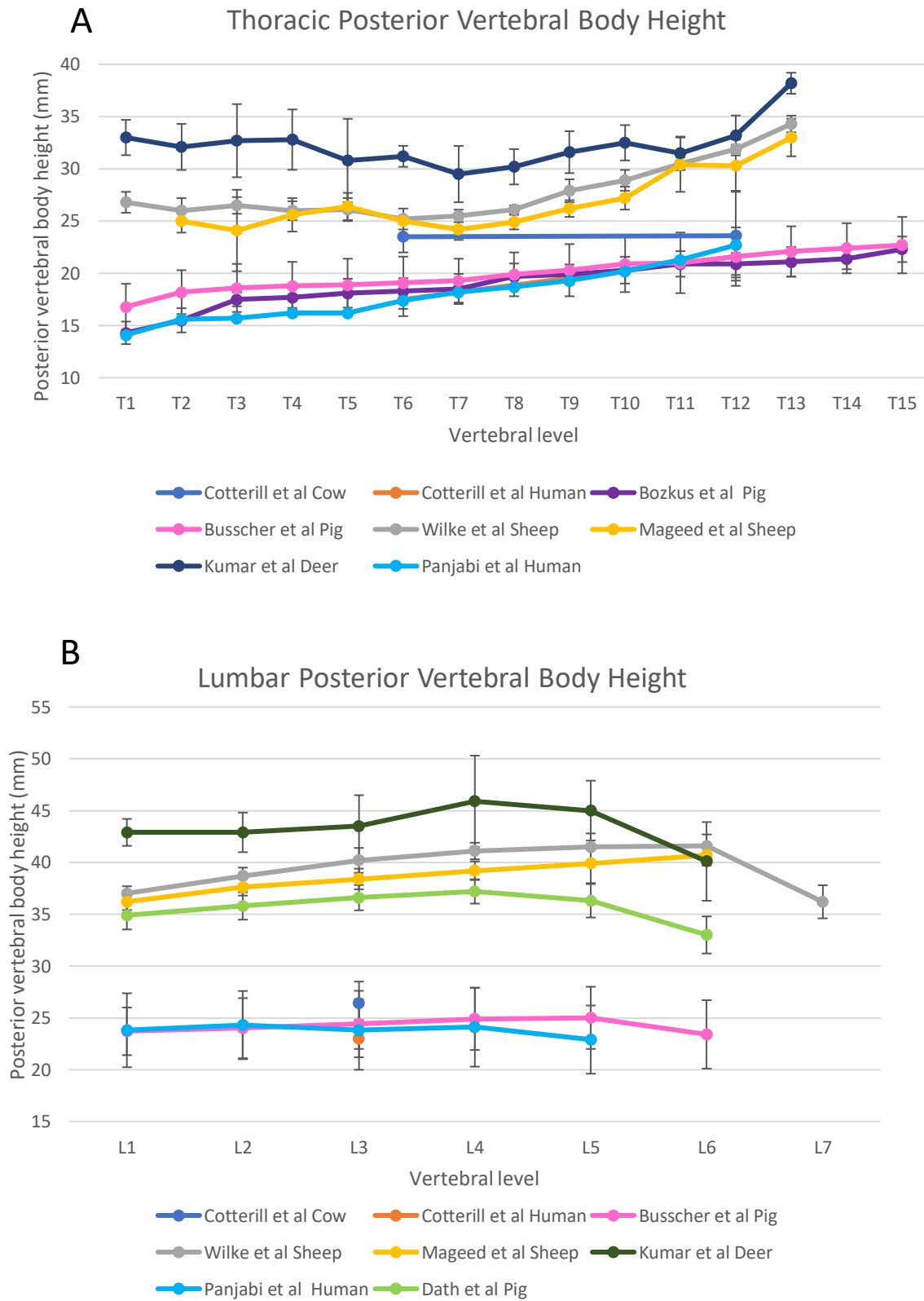
Figure 2.5 – Scatter plot of mean posterior vertebral body height (mm) and standard error bars, taken from the studies included from the database search for cow, sheep, humans, deer and pig vertebrae. A – Thoracic spine vertebral body height. B – Lumbar spine vertebral body height.

A

Thoracic Vertebral Body Width

B

Lumbar Vertebral Body Width
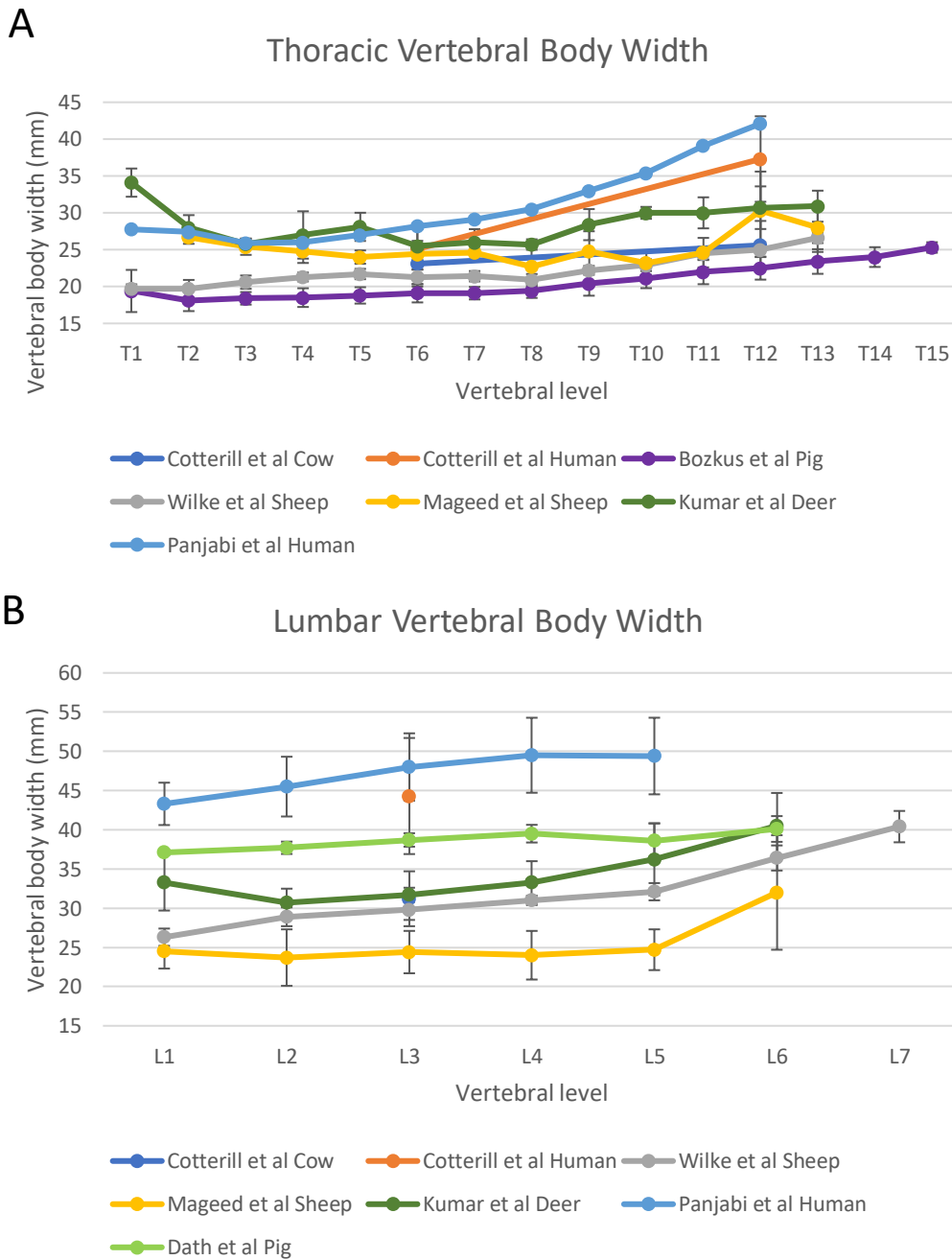
Figure 2.6 – Scatter plot of mean posterior vertebral body width (mm) and standard error bars, taken from the studies included from the database search for cow, sheep, humans, deer and pig vertebrae. A – Thoracic spine vertebral body width. B – Lumbar spine vertebral body width.

A — Thoracic Vertebral Body Length

B — Lumbar Vertebral Body Length
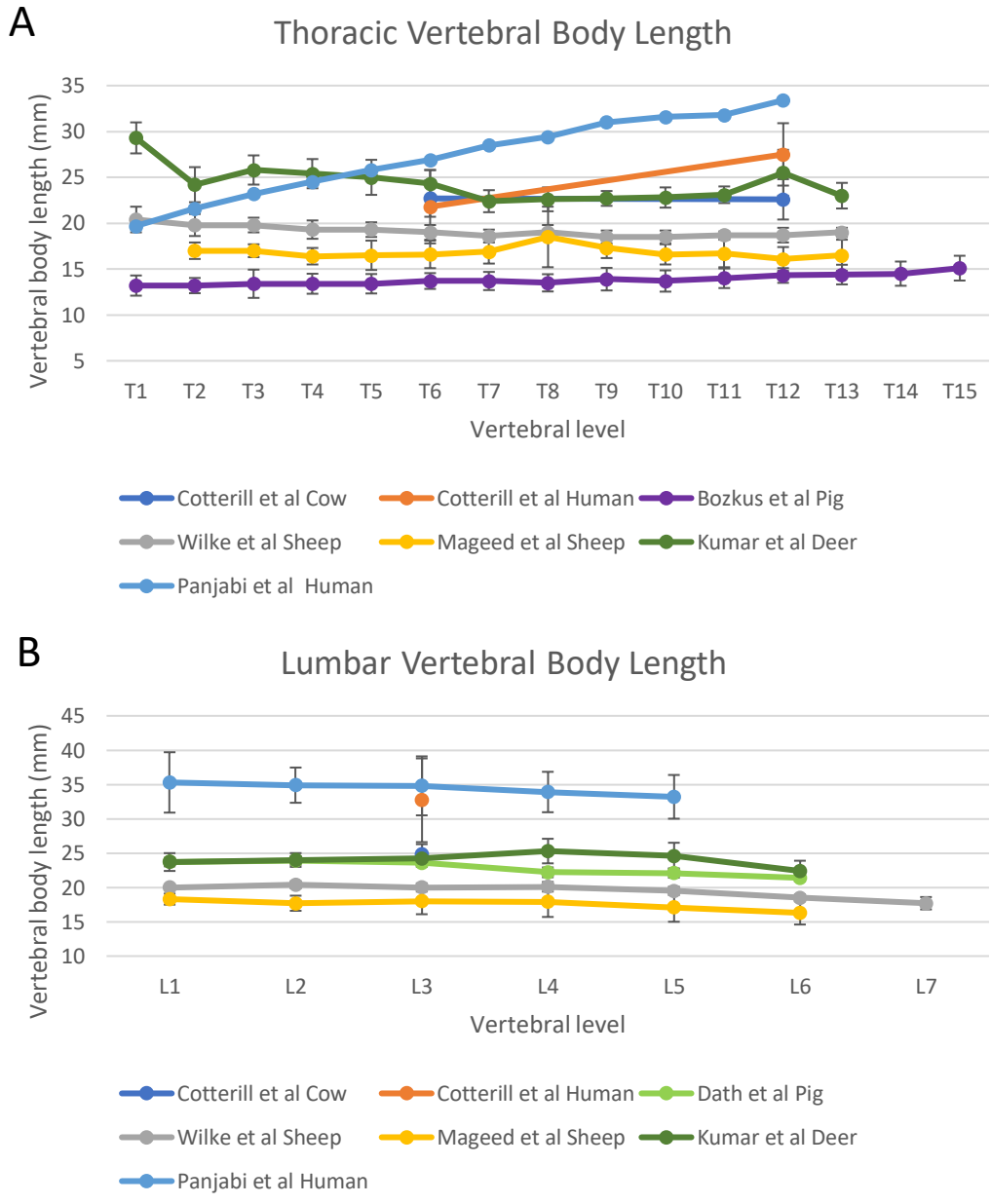
Figure 2.7 – Scatter plot of mean anteroposterior vertebral body length (mm) and standard error bars, taken from the studies included from the database search for cow, sheep, humans, deer and pig vertebrae. A – Thoracic spine vertebral body length. B – Lumbar spine vertebral body length.

A Thoracic Pedicle Height

Legend:
- Bozkus et al Pig
- Wilke et al Sheep
- Mageed et al Sheep
- Kumar et al Deer
- Panjabi et al Human

B Lumbar Pedicle Height

Legend:
- Dath et al Pig
- Wilke et al Sheep
- Mageed et al Sheep
- Kumar et al Deer
- Panjabi et al Human
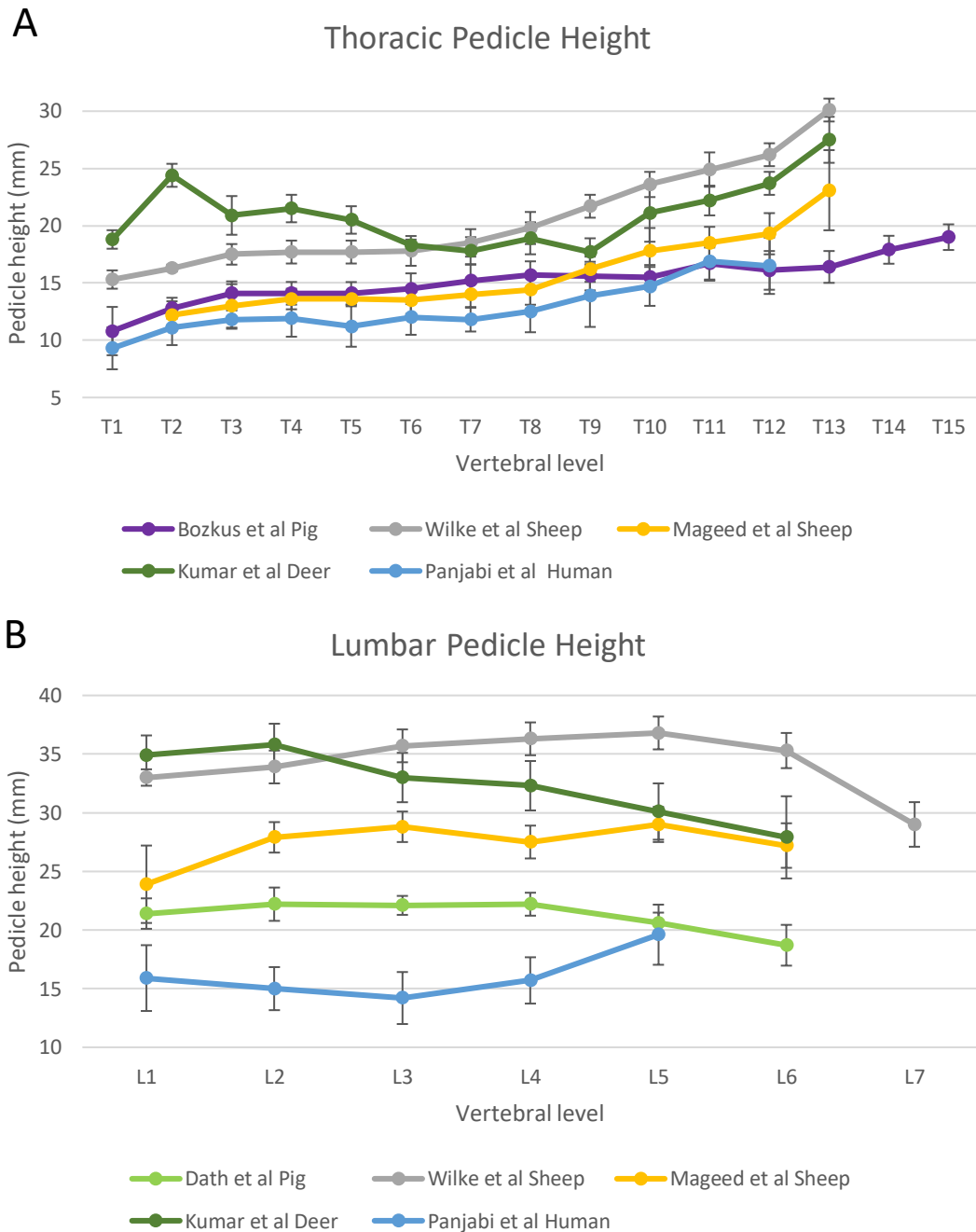
Figure 2.8 – Scatter plot of mean pedicle height (mm) and standard error bars, taken from the studies included from the database search for cow, sheep, humans, deer and pig vertebrae. A – Thoracic spine pedicle height. B – Lumbar spine pedicle height.

A

Thoracic Pedicle Width

Pedicle width (mm) vs Vertebral level (T1–T15)

Legend:
- Cotterill et al Cow
- Cotterill et al Human
- Bozkus et al Pig
- Wilke et al Sheep
- Mageed et al Sheep
- Kumar et al Deer
- Panjabi et al Human

B

Lumbar Pedicle Width

Pedicle width (mm) vs Vertebral level (L1–L7)

Legend:
- Cotterill et al Cow
- Cotterill et al Human
- Dath et al Pig
- Wilke et al Sheep
- Mageed et al Sheep
- Kumar et al Deer
- Panjabi et al Human

Figure 2.9 – Scatter plot of mean pedicle width (mm) and standard error bars, taken from the studies included from the database search for cow, sheep, humans, deer and pig vertebrae. A – Thoracic spine pedicle width. B – Lumbar spine pedicle width.

	Yingling et al. (Pig C3 - C7)		Nissan and Gilad (Human L1-5)	White and Panjabi (Human T12)	Cotterill et al. (Human L3)	Berry et al. (Human L1 - L5)	
Upper Vertebral Body Length	22.28 (2.54)		L1: 33.5 (2.9) L2: 34.4 (2.9) L3: 34.7 (2.7) L4 34.4 (2.7) L5: 34.2 (2.7)	32.8	32.7 (6.1)	N/A	
Lower Vertebral Body Length	22.53 (2.67)		L1: 34.1 (2.9) L2: 34.7 (3.0) L3: 34.6 (2.8) L4: 34.9 (2.8) L5: 33.9 (2.7)	33.4	N/A	N/A	
Pedicle Width	*Right:* 8.67 (1.21)	*Left:* 8.91 (0.95)	N/A	8.8	8.4 (2.0)	*Right:* L1: 7.0 (1.9) L2: 7.4 (1.6) L3: 9.2 (1.3) L4: 10.3 (1.6) L5: 10.9 (3.4)	*Left:* L1: 6.9 (1.7) L2: 7.5 (1.5) L3: 9.1 (1.6) L4: 10.4 (1.6) L5: 10.5 (2.9)

Table 2.2 – Comparison of mean pig C3-C7 vertebral measurements from Yingling et al. (185) with human vertebral measurements from other studies referenced by Yingling et al.: Nissan and Gilad (194), White (195) and Panjabi (193), Cotterill et al (184), Berry et al (196). Selected measures based upon availability of data for comparison across studies, in mm with standard deviations in parentheses where available.

2.3.1 COW

There is only one study comparing cow and human thoracolumbar vertebrae (184). The authors selected three vertebral levels: T6, T12 and L3. They found that there were significant differences in measurements for several areas. For example, at T6 the spinous process length was greater in the cow, but at L3 it was longer in humans. Of the measurements of particular relevance to vertebroplasty, there was no significant difference in VBL or VBW at T6, but at T12 and L3 the human VBL and VBW were significantly greater. At T6, the VBH was greater in cow vertebrae, but at T12 and L3 there were no significant

differences. Cow pedicles were significantly wider at T6, but there was no significant difference at T12 or L3.

2.3.2 PIG

Of the four studies assessing pigs, one looked at the cervical spine, one at the thoracic spine, one at the lumbar spine, and one at the whole spine. A fifth study compared the L4 level across several species including humans.

Bozkus et al (186) showed that T3-6, T8 and T12 had significant differences in posterior vertebral body height. They also showed significant differences in body width and length at all thoracic levels, with human vertebrae being larger in these dimensions. The width and length also remained relatively similar throughout the pig thoracic spine, whereas these increased in size in human spines.

Pedicle heights were greater in pig spines from T2 – T9, and in human spines at T11 and T12 (when compared with T11 – T15 in the pig spine). The left and right pedicle widths from T1 – T9 mostly did not show any significant differences. From T10 – T12, the human pedicles were significantly wider.

Dath et al (187) found the pig lumbar vertebrae to have larger body height than humans, but smaller body width and length. They also found that pedicle height and width were greater in pig vertebrae at all levels except L4 and L5 where human pedicles were wider.

Busscher et al (142) used CT measurements to compare whole pig and human cadaveric spines. They divided the spines into regions: cervical, high thoracic, low thoracic, and lumbar (though high or low thoracic are not defined). They considered absolute measurements of a region "comparable" if at least half the vertebrae did not show significant differences between species. Additionally, they calculated the ratios of the human and pig measurements, which they considered comparable if the variance of these ratios was less than 20% for each region. These criteria are arbitrary, with "comparable" being difficult to define consistently in the literature.

They state that anterior and central body height is comparable between species in all regions, but posterior height is only comparable in the cervical and high thoracic regions. Pedicle width is said to be comparable in the lower thoracic and lumbar regions, and pedicle height in the lumbar region. They also calculated the pedicle angle, which is comparable in the thoracic but not lumbar spine.

Yingling et al (185) compared the pig cervical spine from C3 – C7 with human L1 – L5. They found similar biomechanics in vertebral motion segments and loading failure mechanisms, albeit the pig forces requiring scaling up to match the human values. They also noted that vertebral body dimensions in human lumbar vertebrae were mostly larger than in pig cervical vertebrae. This would suggest that pig cervical spines would represent a useful alternative to human cadaveric spines when modelling injury patterns in young, healthy humans. However, for the purposes of testing spinal interventional equipment and techniques, the pig cervical spine is less suitable than the lumbar spine of the pig, or other large quadrupeds.

McLain et al (191) looked specifically at the L4 level, and showed no significant difference in VBH between immature standard farm pigs and mature Yucatan micropigs, and humans, but significantly greater VBW and VBL in humans. There was no significant difference between standard pig or human PW. The micropig PW was smaller than in humans. The pedicle angle was significantly greater in micropigs and standard farm pigs when compared to humans (i.e. more lateral distal to the vertebral body, and with a steeper medial approach to the vertebral body).

2.3.3 SHEEP

There were two studies included on sheep. One of these compared human and sheep thoracolumbar spines, and one compared whole spines. A third study compared sheep and human L4 vertebrae.

Wilke et al (188) found sheep vertebral body height to be greater than human, but length and width to be smaller. Pedicle height is suggested to be greater in sheep than humans, particularly in the lumbar spine. Thoracic pedicle width is also greater in sheep but is comparable from T12 and below.

Mageed et al (189) calculated several spinal indices using ratios of various measurements in order to overcome the heterogeneity of measurement techniques in the literature from which they obtained their human data. These included concavity index (ratio of anterior and posterior vertebral body height), endplate index (ratio of superior endplate length and

width), and the pedicle index (ratio of width and height). They did not include formal statistical comparison of the absolute values, but their data suggested that sheep vertebrae have greater vertebral body height but smaller width and length than human vertebrae. They also state that sheep pedicles are narrower, taller and more laterally angled than in humans.

At the L4 level, McLain et al. (191) showed no significant difference in vertebral body height, but the width and length were greater in humans. They found no difference in the pedicle width but agreed with Mageed et al. (197) that sheep pedicles show greater lateral angulation.

2.3.4 DEER

To date, there has been a single study comparing the measurements of the deer and human spines.

Kumar et al (190) compared whole spines between species. They found that deer vertebral body height was greater at all spinal levels. Vertebral body height and width were greater in deer at T1-T4, but below T5 that trend reversed, and the dimensions were greater in human vertebrae. The authors state that deer pedicles were taller than human pedicles at all levels, though they have not included formal statistical comparison. Similarly, although they conclude that pedicle width is comparable at the lower thoracic and lumbar spines, their presented data suggest that lower lumbar pedicles are rather wider in humans than deer, but it is unknown whether these differences are statistically significant or not.

2.4 DISCUSSION

Cows, pigs, sheep, deer and goats are the most commonly used animal models in spinal research. The available evidence demonstrates various areas of similarity and difference between humans and these species, though there are limitations to the published studies. In particular, the small number of studies, which themselves have low sample sizes, and the heterogeneity of the methodology in the available literature makes comparison difficult.

General methodology varied in terms of measurement. In particular, to the best of my knowledge, no method comparison between measurements using analogue callipers, digital callipers, hand-held micrometers, plain radiography with digitised rulers, and CT, has been performed.

Some studies examined human cadaveric vertebrae, while others used data from the established literature. This raises the possibility of errors being introduced via differing methodology within the same study.

Other than Dath et al (187), none of the included studies mentioned how many repetitions were performed for each measurement, which is a useful method for increasing reliability. Dath et al. used 3 repetitions at each measurement.

Regarding any attempted comparisons between various species, this is limited by the fact that in several studies, raw data are not provided for certain measurements. As a result,

when combined with the incomplete data for some species, it is not possible to perform a meta-analysis to reach any meaningful conclusion.

The general trends that can be seen from the included studies are that quadruped vertebral bodies tend to be taller, narrower and shorter in AP dimension than human vertebrae. Pig and cow lumbar and thoracic vertebrae are perhaps the closest to human in terms of vertebral body height, width and length, though deer may be closer when specifically considering upper thoracic vertebral body length (Figure 2.7).

The existing data suggest that in the mid-thoracic region, cows have greater vertebral body height than humans, but with comparable vertebral body width and length. In the lower thoracic or lumbar regions, humans have greater vertebral body width and length but there is comparable VBH.

Animal pedicles are generally narrower and taller than human pedicles. Once again, the literature suggests that pig pedicles are closest to humans regarding pedicle height (Figure 2.8). The data for pedicle width indicate much more overlap between species (Figure 2.9). Where available, the data suggest that animal pedicles are also more laterally angulated.

In contrast to the general trend of quadrupedal pedicles being narrower than in humans, cows appear to have wider pedicles at T6 region, but show no significant difference at T12 or L3.

Further inter-species comparison using data obtained by such varying methodology is unlikely to be helpful. There are also several important limitations to the available studies.

It must be noted that the data comparing cow and human spines are limited to a single study which only looked at three vertebral levels. It is difficult to know whether the selected vertebrae are representative of the remainder of the spine. Furthermore, pedicle height and angle are not included in this study.

The authors have not specified whether they assessed the left or right pedicle or took the mean of both sides. Nor have they specified where on the vertebral body they measured VBW, VBL or VBH; subsequent studies such as Yingling et al (185) appear to have assumed VBL was measured at the upper endplate; they may have contacted the authors for clarification, but this has not been stated. These are of relevance when making comparisons with other studies.

The pig data are the most abundant, and also the most conflicting. This is likely to be at least in part due to the use of specimens of different breeds, weights and ages. For example, as noted by Busscher et al (142), their data show smaller pedicles in the pig lumbar vertebrae than Dath et al (187). They suggest that this is likely because Dath et al. used older, heavier specimens.

Dath et al (187) did not perform any formal statistical comparison, stating that the differences between their pig measurements and selected human measurements from the available literature were self-evident. This is borne out in part by their data. Additionally, they did not specify whether they measured the left or right pedicle.

Busscher et al (142) do not provide any raw data beyond their measurements for pig and human VBH and intervertebral disc height. The authors have provided data on whether they felt that a spinal region was comparable between species, however they have not defined their subdivision of thoracic into high and low thoracic. They also have not provided any justification for their calculation of comparability, setting a seemingly arbitrary limit of 50% of the vertebrae of a region. This may not adequately take into account intra-regional variation.

Yingling et al (185) had a small sample size of only 3 spines. They provided only mean dimensions from all the vertebrae combined. They state that their small standard deviations suggest that a larger sample size was not required. However, it is interesting to note that other studies show significant differences in vertebral dimensions within the same segment; for example, Panjabi et al. (193) demonstrated significant differences in human VBL between L1 and L4 or L5.

Given the smaller dimensions of the pig cervical vertebrae, these are less suitable for testing transpedicular needles designed for use in humans. Although pedicle widths were similar between the species, the shorter vertebral body length could affect anterior needle placement and cement filling. In addition, the authors have not included data on vertebral body or pedicle height.

The sheep data are in agreement that sheep tend to have taller, but narrower vertebrae. They also have taller pedicles than humans. However, there is some disagreement regarding pedicle width. Mageed et al (189) state that sheep pedicles are narrower at all levels. Wilke

et al (188) in contrast showed that sheep thoracic vertebral pedicles are wider than humans from T1 – T12, below which level they are comparable. This is corroborated in part by McLain et al (191) who found no significant difference in pedicle width at L4.

Once again, these differences could be partly related to the use of different size animals, though interestingly McLain et al (191) used the smallest specimens and Wilke et al (188) the largest. Both Wilke et al (188) and Mageed et al (189) used female merino sheep. McLain et al. did not specify the breed.

Mageed et al (189) do not provide raw data for comparison. Though they state that sheep pedicles are narrower and taller than human pedicles, there are no numerical data. They also mention in their discussion that pedicle screws may encounter issues, but other transpedicular techniques such as vertebroplasty, kyphoplasty or percutaneous discectomy do not use pedicle screws. This makes it hard to assess whether sheep pedicles would be appropriate for use in these techniques.

The results from Kumar et al (190) suggest that deer follow the general trend of having narrower vertebrae from T5 and below, and that their pedicles are also narrower than humans. They also found that lower thoracic vertebral pedicle width may be comparable between the species. However, as mentioned earlier in the results, they do not include any formal analysis to suggest whether these differences are statistically significant.

The human data they used for comparison was taken from Panjabi et al (192, 193). It should be noted that the methods used to make vertebral measurements in these studies was

quite different. Kumar et al used a hand-held micrometer, whereas Panjabi et al used a specially designed 3-dimensional morphometer.

The question remains, which species is the "best" fit for modelling a human spine? The heterogeneity of methods of measurement, selected breed of animal species, and differences in sample group ages and weights in the available literature means that this is a difficult question to answer. The findings of the 9 papers I have reviewed would suggest that the best species would depend on the particular qualities required for the specific test being performed. For example, in the case of transpedicular percutaneous cement augmentation, the most important gross morphological features would include pedicle height, width, angle and coronal plane shape, and the length of the vertebral body.

However, other characteristics beyond gross topology will clearly also play a role; in the example of cement augmentation procedures, a similar trabecular structure would be important if assessing cement spread. This is discussed in greater detail in Chapter 4. Other procedures may warrant an evaluation of biomechanical factors.

It is clear that while no single animal model will be able to provide a perfect analogue of a live human spine, this is also not required for most early phase research. A reproducible model with wide availability and similarity in the requisite aspects, should suffice for the majority of investigations.

Future exploration in the area of animal models for spinal research should be tailored to specific purposes. Additionally, if evaluating a single species, attempts should be made to

maintain methodological consistency where possible. This will allow for future comparisons and meta-analyses between species. This has already been achieved to an extent, since certain measurements are widely performed throughout all the studies reviewed.

More studies may be required on deer, and cows in particular, due to the limited data currently available. Cows may not represent a particularly useful model in the UK due to restrictions on the use of cow spinal materials, and of the two deer may therefore represent the more practical choice.

pig and sheep data are a little more abundant, but given the contradictory nature of the evidence, further study is warranted. In particular, methodological rigour will help provide a more robust comparison and help in the selection of an animal model.

2.5 SUMMARY

- The available evidence suggests that pigs may provide the closest approximation for the human lumbar spine, in particular when considering transpedicular techniques

- In the thoracic spine, sheep, pigs and deer might all be appropriate candidates

- There is little consistency in the literature regarding methods of measurement or age of animal or human samples for comparison. This makes direct comparison between studies difficult.

- Further work into this area could consider a comparison between humans and multiple other species, using the same techniques for measurement, and thus directly comparing the differences between more than one animal and the human. This would allow the selection of a closest animal model for a variety of procedures, including percutaneous surgical techniques and open surgical techniques, depending on the specific features requiring assessment.

CHAPTER 3:
COMPARATIVE VERTEBRAL MORPHOMETRICS

3.1 INTRODUCTION

Human cadavers have an established role in research as a model for live human pathology, as discussed in Chapters 1 and 2; in the spine, several studies have used human cadaveric vertebrae to model fractures (198-201). However, human cadavers are not without drawbacks as models for *in vivo* processes and procedures, and they are an expensive and limited resource. As such it can be difficult to obtain the required numbers for a sufficiently powered study.

It is therefore unsurprising that animal models are often used as an alternative. Quadrupedal mammalian spines are known to undergo axial loading, as suggested by their endplate to endplate configuration, and *in vivo* axial compressive forces demonstrated by intradiscal pressure sensors (141, 202, 203). Pig, cow, and sheep spines are already used as models in the literature (180-182).

Pigs have historically been favoured, due to similarities in vertebral size and shape (141), but there is limited literature available providing a robust comparison between species. There have been some morphometric studies performed on a variety of quadrupeds, but there is no consensus as to whether there are any practically meaningful differences between these animal species, or whether any one species is closest to the human, for the purposes of modelling human vertebrae in the testing of surgical techniques.

The established literature shows certain trends in measurement sizes that might suggest the use of different species may be more appropriate in the thoracic spine compared to the lumbar spine. However, these studies are not without limitations, as detailed in Chapter 2.

In particular, small sample sizes, especially for humans, and the use of different methods of measurement, for example, direct visualisation measurements using electronic callipers, or Computed Tomography (CT) measurements.

The currently available literature also shows significant differences between male and female human vertebral size in terms of morphometry (204). To the best of our knowledge, no comparison has been performed to assess whether there are any significant age-related differences, other than vertebral height - in 1987, Twomey and Taylor (205) showed increased vertebral endplate concavity with increased age. If statistically significant differences are returned, it would also be useful to know whether these are practically meaningful when performing a transpedicular procedure with currently available equipment.

This chapter describes a study to address these issues in the literature. Firstly, a methodological comparison will be performed of measurements under direct visualisation, with measurement of CT images. The morphometries of male and female human vertebrae will be compared to reproduce the findings of the existing evidence, and analysis will also be performed to compare young and old vertebrae to assess whether there are any significant morphometric differences based on age. The morphologies of quadrupedal spines will then be compared with a human sample, with a view to selecting the most appropriate model for percutaneous transpedicular procedures.

3.1.1 RESEARCH QUESTIONS

1. Is radiological measurement as reproducible as measurement under direct
   visualisation, and do the results correlate? - Method comparison study between
   measurements obtained using direct visualisation and radiology to compare
   standard errors between the two techniques
2. Are there statistically significant differences between male and female, and young
   and old, human vertebral morphometries?
3. Which animal vertebrae provide the closest approximation with respect to vertebral
   cement augmentation, bearing in mind the transpedicular approach.

3.2 MATERIALS AND METHODS

3.2.1 ANIMAL SAMPLE SELECTION

For the animal samples, I selected species which were widely available and easily obtained. I
selected pigs and sheep as they fit these criteria in the UK. Whole cow spines were not
obtainable locally due to spinal material restrictions in the UK, and I therefore elected to
exclude them.

Two animal species and breeds were selected for harvesting as discussed in the introduction
to this chapter. I selected charolais sheep breeds, as these were the most easily obtained
from my local abattoir. Most available pig specimens in the UK are Large White hybrids,
which were also the breed provided by my local abattoir.

Pig specimens were male, between 3 – 6 months, and 55-60kg in weight. Sheep specimens
were male, between 3 – 6 months old, and 35 – 45 kg in weight.

Specimens were excluded if there was any existing spinal fracture or malignancy
demonstrated on the subsequent CT scans.

3.2.2 HUMAN SAMPLE SELECTION

A sample size of 44 was determined by a power calculation based on the available literature (see Statistics). Vertebral dimension measurements were performed on retrospectively selected studies of adult patients who underwent spinal CT imaging including the thoracic and lumbar spine.

Inclusion criteria:

- CT studies including the thoracic spine and lumbar spine from T1 – L5 with bone reconstructions
- Adult patients age >18

Exclusion criteria:

- Known malignancy
- Evidence of metastatic bone disease
- Spinal fractures
- Metabolic bone disease
- Spinal osteoarthritis resulting in deformity (as defined by the presence of any of the established features as follows: subchondral cyst formation, subchondral sclerosis, joint space loss, osteophyte formation, intervertebral disc height loss)
- Previous spinal surgery or cement augmentation
- Congenital segmentation anomalies

The human sample consisted of 29 male and 15 female patients, with a mean age of 59.7 years. The sample was divided into two groups based on the median age of 57. There were 21 specimens <57 years old, and 23 specimens ≥57 years old.

3.2.3 TECHNIQUE

3.2.3.1 ANIMAL SPINE HARVESTING

Animals were locally sourced from an abattoir in Norwich, Norfolk. Freshly harvested thoracolumbar spines were received from animals slaughtered the same morning with the adjacent soft tissues intact in a long, combined sirloin/loin and rib cut. This included paraspinal muscles and back muscles (sirloin and loin cuts) and ribs (rib cut). The skin, subcutaneous fat, fascial layers and paraspinal muscles were manually dissected. Paraspinal ligaments and intervertebral discs were also removed.

Pigs have 13-15 thoracic and 5-7 lumbar vertebrae. Sheep have 13-14 thoracic and 6-7 lumbar vertebrae.

Where extra vertebrae exist, I considered the junctional vertebrae to be equivalent to the respective junctional level in humans (for example, pig L6 compared with human L5 as both, on average, represent lumbosacral junctional vertebrae), and counted up or down from these.

Four spines of each species were harvested.

3.2.3.2 ANIMAL IMAGE ACQUISITION

CT was performed with a Siemens Somatom Definition AS plus 128 slice Computed Tomography machine. Images were acquired with the following parameters: Field of View (FOV), pixel matrix 512 x 512, Siemens B70 ultrasharp bone kernel + soft tissue kernel, 0.6 mm slice thickness. Multiplanar reconstruction (MPR) was performed at a diagnostic workstation for measurements (4MP Barco™ monitor).

3.2.3.3 HUMAN IMAGE ACQUISITION

Retrospective human CT images were selected sequentially from my hospital trust PACS (Picture Archiving and Communication System) database of clinical studies between 2010 and 2018, until I achieved a sample size of 44. The studies were performed with a Siemens Somatom Definition AS plus 128 slice scanner or a Siemens Somatom Definition AS 64 slice scanner using a 512 x 512 pixel matrix. The field of view was variable depending on patient habitus. Siemens B70 ultrasharp bone kernel, 2 mm slice thickness.

3.2.3.4 DATA EXTRACTION

Following dissection, animal vertebrae were first measured under direct visualisation using a vernier caliper and afterwards using digital calipers on CT images. Newly acquired animal spinal images and retrospectively acquired human spinal images were reviewed on a 3-megapixel imaging workstation, where measurements were taken using the Fuji SYNAPSE PACS.

Measurements were taken of each level from T1 – L5 using Fuji SYNAPSE PACS measurement tools, by a single operator.

The linear vertebral measurements were: maximal total craniocaudal height, axial length (anteroposterior dimension) and axial width (transverse dimension), vertebral body height, length and width, pedicle height, length and width, lamina height, length and width, and spinal canal axial length and width (Figure 2.2). Four repeat measurements were performed at each vertebral dimension. The rationale for the number of repetitions is discussed below in the statistics section.

3.2.4 STATISTICS

3.2.4.1 ANIMAL SAMPLE SIZE

The animal spine sample sizes were sample sizes of convenience, limited by my ability to acquire freshly harvested, whole spines from my local abattoir. Usual butchery practise is to bisect the spine, and therefore I was required to purchase whole spine cuts, and these were relatively limited in their availability.

3.2.4.2 HUMAN SAMPLE SIZE

My sample size for the retrospective study of vertebral dimensions was based on a power calculation using the data from the existing literature (192). Using their measurements for transverse process width gave a range of confidence intervals from ±1.76 mm to ±7.39 mm. I used the mean confidence interval range for my power calculation as follows:

$$N = \frac{4\sigma^2(Z_{crit})^2}{D^2} \tag{3.1}$$

Where N = sample size, σ = Standard Deviation, Z_{crit} = standard normal deviate, D = total width of the expected confidence interval. Statistical significance was set at 5%, therefore Z_{crit} = 1.96 (206). The required sample size is 44. My sample consisted of 29 male and 15 female patients, with a mean age of 59.7 years.

3.2.4.3 MEASUREMENTS

The mean, standard deviation and standard error of the mean were calculated for each morphological measure under direct visualisation and CT.

Measurements under direct visualisation were made by a single operator. The number of repetitions required was calculated from a desired standard error of the within-subject standard deviation. This is often set as 10% (95%CI $\pm$ 10%) (207).

To clarify an acceptable degree of standard error of the within-subject standard deviation, a single operator (TA) performed initial measurements to allow for 95%CI $\pm$ 5%, 10% and 20%. These initial measurements were performed on a pig spine at the left and right transverse processes from T3 – T10. The transverse processes of T3 – T10 were selected on the basis of similarity in length between the levels in the existing literature, to allow a preliminary calculation of the number of repetitions per measurement required by the single operator.

The number of repetitions for each of these degrees of standard error was calculated with the following formula (207):

First, I take the width of the confidence interval to be:

$$Z_{crit} \frac{S_w}{\sqrt{2n(m-1)}} \tag{3.2}$$

Where Z_{crit} = 1.96 for 95% CI, S_w = standard error of the within subject standard deviation, n = total sample size, m = number of repetitions per measurement.

The number of measurements to give a particular percentage of S_w is calculated as follows:

$$1.96 \frac{S_w}{\sqrt{2n(m-1)}} = xS_w \tag{3.3}$$

Where x = percentage of S_w. Since n = 4, the following measurement repetitions were calculated.

To assess 5% standard error required 49 measurements at each level, 10% standard error required 13 measurements, and 20% standard error required 4 measurements.

I selected a standard error which allowed for a combination of practicality and accuracy with n=4; although the thoracic vertebral transverse process lengths are comparable, the existing literature suggests that most other dimensions are more variable, and therefore I did not combine results between levels.

Direct and CT measurements were performed by a single operator. Intra-class correlation (ICC) was performed for single fixed raters for consistency of both direct and CT pig measurements, and sheep CT measurements. ICC was calculated using R software (208).

The mean, standard deviation, and standard error of the mean were calculated for all measures. Normality of these measures was assessed using both the Shapiro-Wilk test, and visual inspection of histograms and Q-Q plots. Method comparison data between direct visualisation and CT was analysed by assessing the mean differences and using scatter plots.

The interspecies comparison was performed via mean differences and visual assessment of scatter plots. Significance was assessed using a two-tailed T-test. In cases where a normal distribution could not be assumed, the Mann-Whitney U-test was applied.

3.3 RESULTS

3.3.1 METHOD COMPARISON

The intraclass correlation coefficient (ICC) for a single observer performing 4 repeat observations, for both direct and CT measurements on the pig, was close to 1, and reported as 1 by the software due to rounding.

	VBH		VBW		VBL	
	Mean (mm)	(SD)	Mean (mm)	(SD)	Mean (mm)	(SD)
Mean Difference	1.71	(0.95)	1.37	(0.77)	2.44	(0.44)

Table 3.1 – Results of the method comparison between direct and CT measurements. Mean values and standard deviations of the absolute mean differences between direct and CT measurements of pig vertebrae. VBW = vertebral body height, VBW = vertebral body width, VBL = vertebral body length

	TPW		SCW		SCL		TL	
	Mean (mm)	(SD)	Mean (mm)	(SD)	Mean (mm)	(SD)	Mean (mm)	(SD)
Mean Difference	2.22	(1.29)	1.95	(0.83)	1.23	(0.65)	1.14	(0.56)

Table 3.2 – Results of the method comparison between direct and CT measurements. Mean values and standard deviations of the absolute mean differences between direct and CT measurements of pig vertebrae. TPW = transverse process width, SCW = spinal canal width, SCL = spinal canal length, TL = total length

The greatest mean differences were noted in vertebral body length (Table 3.1), transverse process width, and spinal canal width. Figures 3.1 and 3.2 show the mean direct and CT measurements, and demonstrate that both measurement techniques follow the same trends with comparable sizes. The Bland Altman plot in Figure 3.3 shows that the largest differences tended to be observed in the measurements with the largest dimensions.

A Vertebral Body Height

B Vertebral Body Width

C Vertebral Body Length
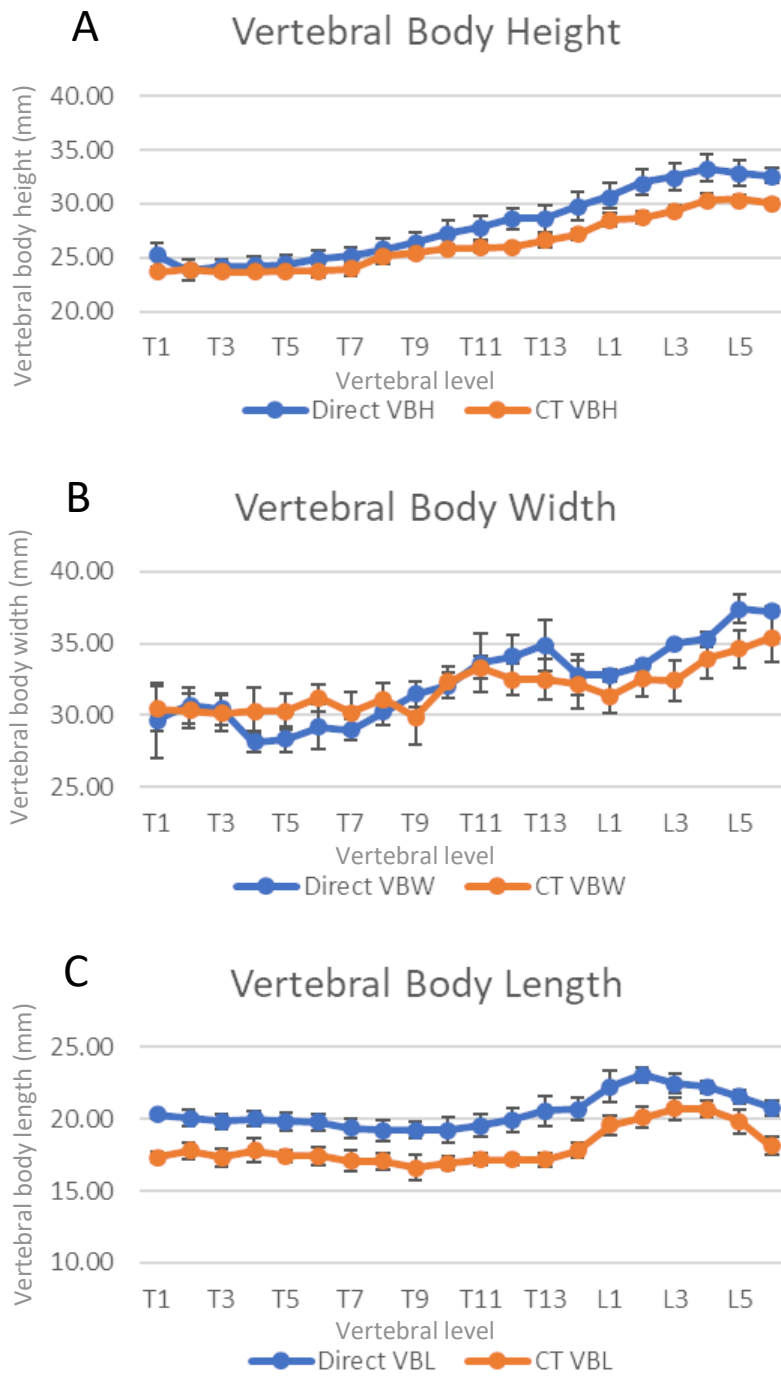
Figure 3.1 - Scatter plot of vertebral body dimensions (mm) and standard error bars, with measurements performed directly and on CT. A – Vertebral body height. B – Vertebral body width. C – Vertebral body length
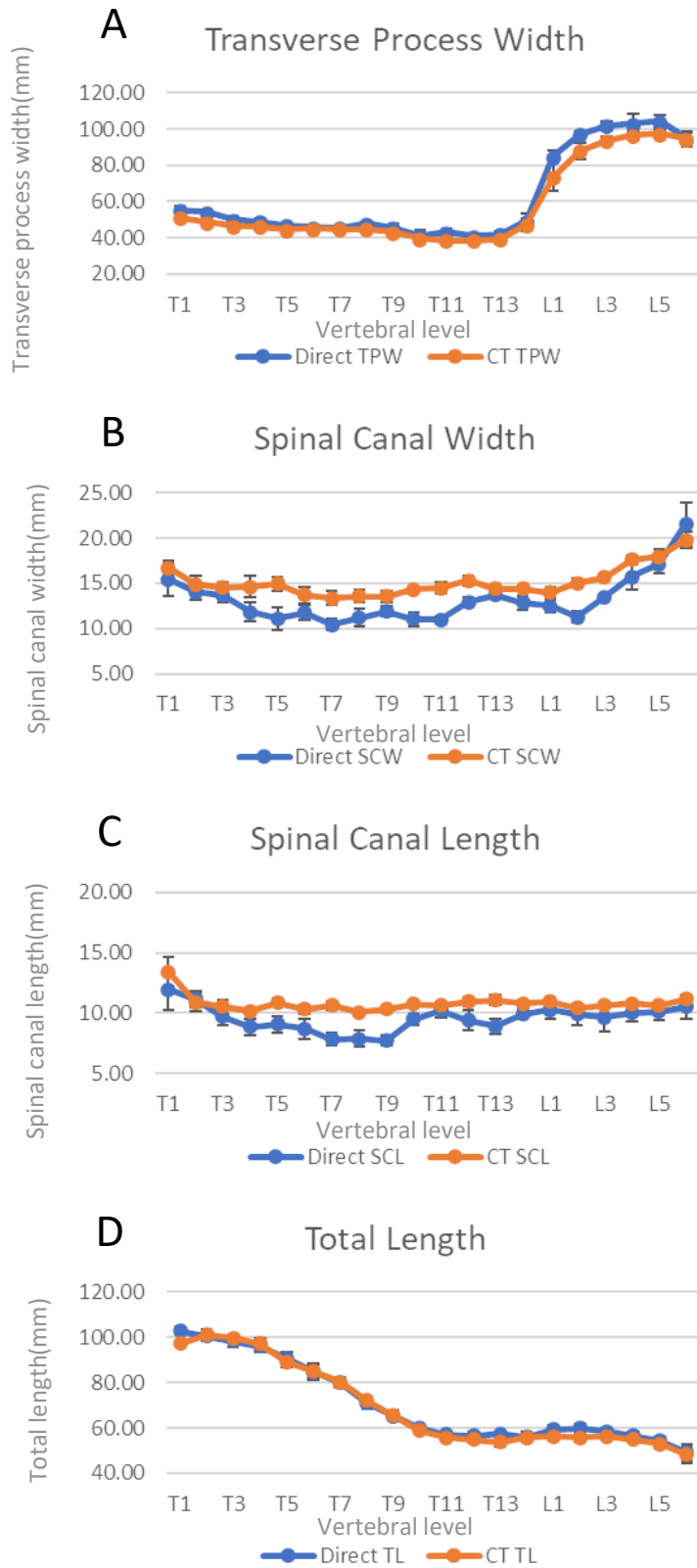
Figure 3.2 - Scatter plot of vertebral posterior element dimensions (mm) and standard error bars, with measurements performed directly and on CT. A – Transverse process width. B – Spinal canal width. C – Spinal canal length. D – Total anteroposterior length

Direct vs CT Measurements
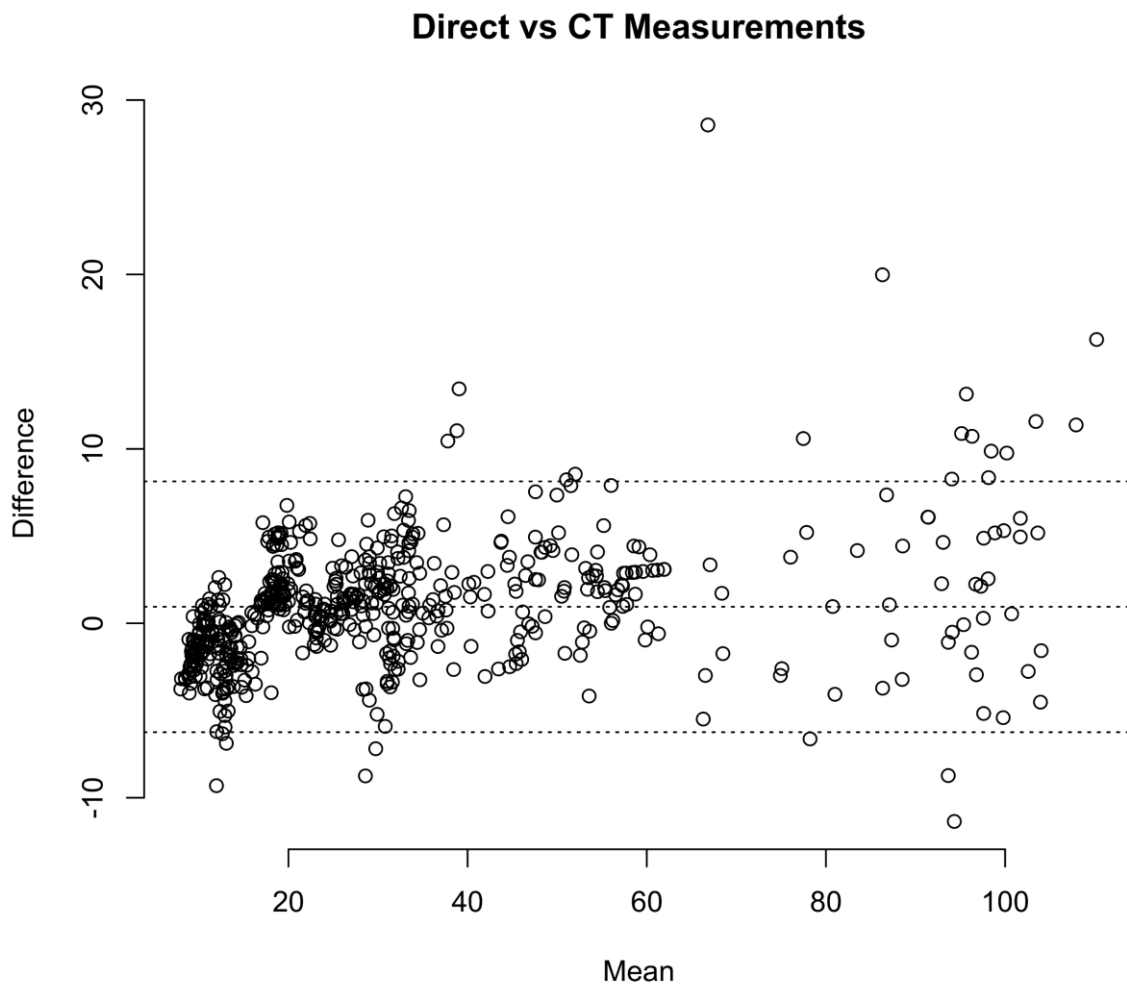
Figure 3.3 – Bland Altman plot of the differences between all the morphometric direct and CT measurements in pig vertebrae.

The human data mostly conform to normal distributions. The sample size of the animal data make assessment of distribution difficult. Histograms visually representing the human and animal data distribution are provided in Appendix B. Q-Q plots and Shapiro Wilk tests of the human and animal data are provided in Appendix C and Appendix D respectively.

3.3.2 HUMAN VERTEBRAL SIZE GENDER COMPARISON

Figures 3.4 – 3.8 show the human male and female mean vertebral morphometric measurements in scatter plots. Tables are included in Appendix F with the mean measurements, standard deviations, 95% confidence intervals, and mean differences with statistical differences. The male mean measurements are larger than female mean measurements at all vertebral levels. These differences are statistically significant.
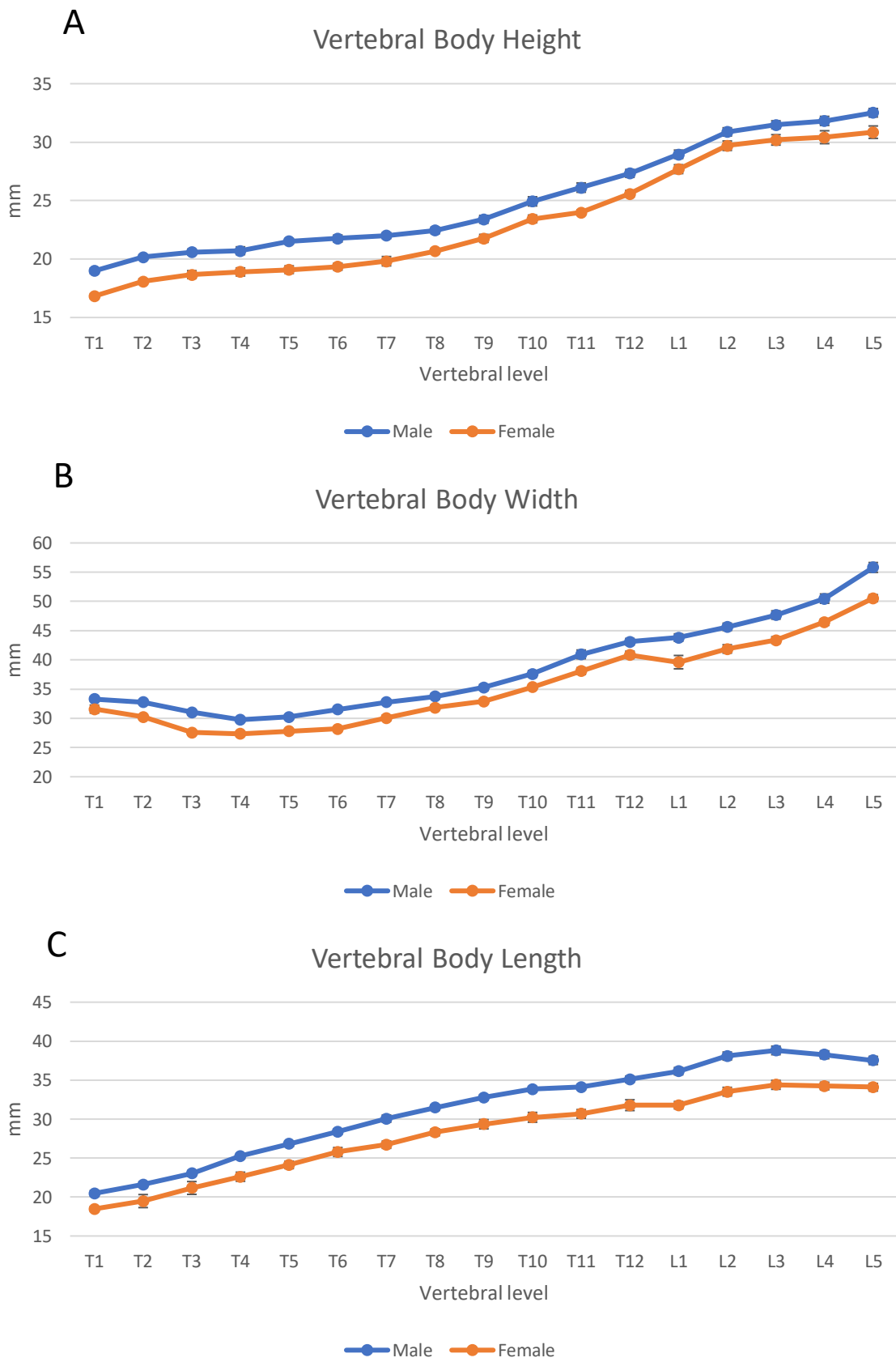
Figure 3.4 – Scatter plot of human male and female vertebral body dimensions (mm) measured on CT. A – Vertebral body height. B – Vertebral body width. C – Vertebral body length

Transverse Process Width
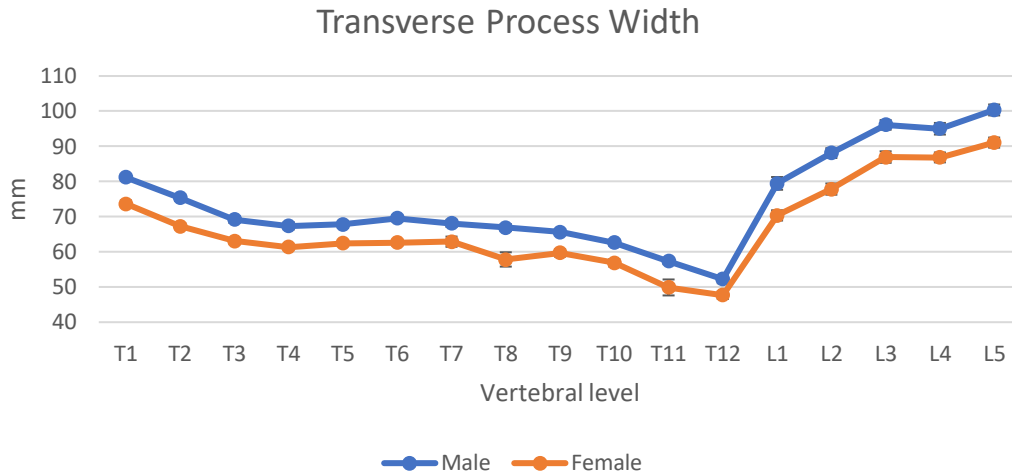
Figure 3.5 – Scatter plot of human male and female transverse process width (mm) measured on CT

A

Spinal Canal Width

B

Spinal Canal Length
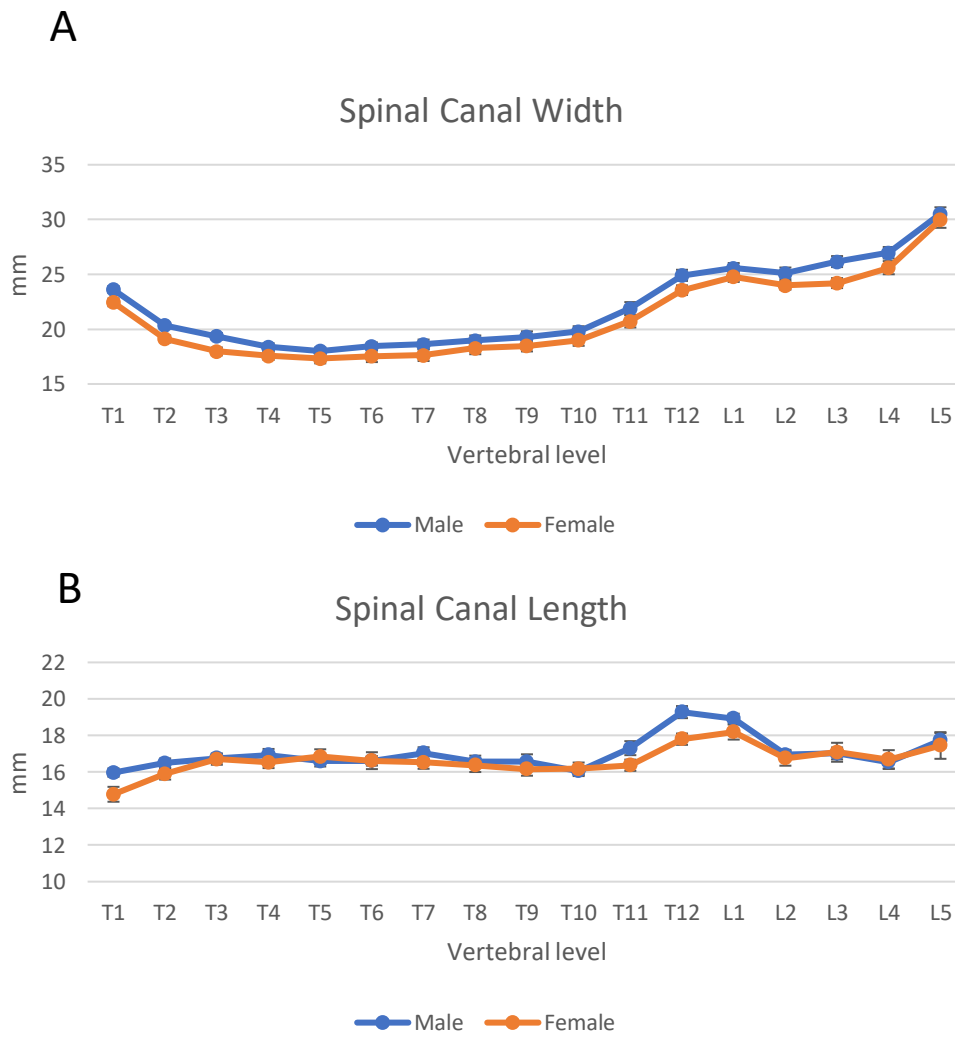
Figure 3.6 - Scatter plot of human male and female spinal canal dimensions (mm) measured on CT. A – Spinal canal width. B – Spinal canal length.

Total Anteroposterior Length
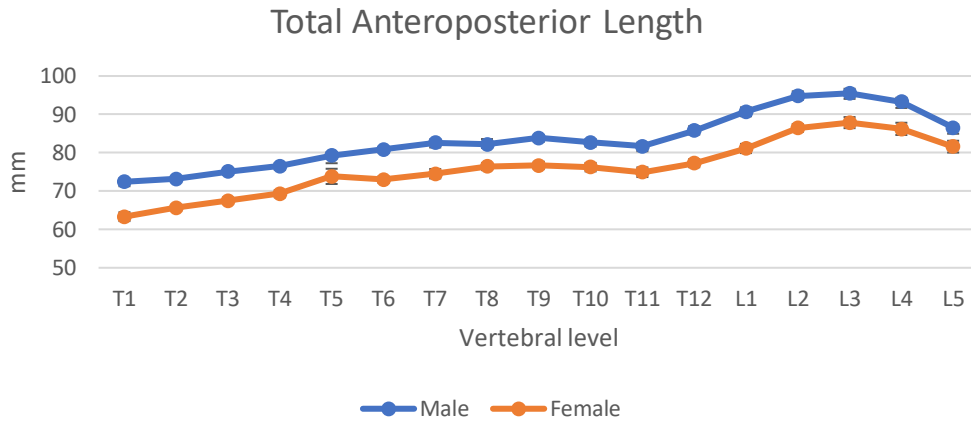
Figure 3.7 – Scatter plot of human male and female total anteroposterior length (mm) measured on CT.
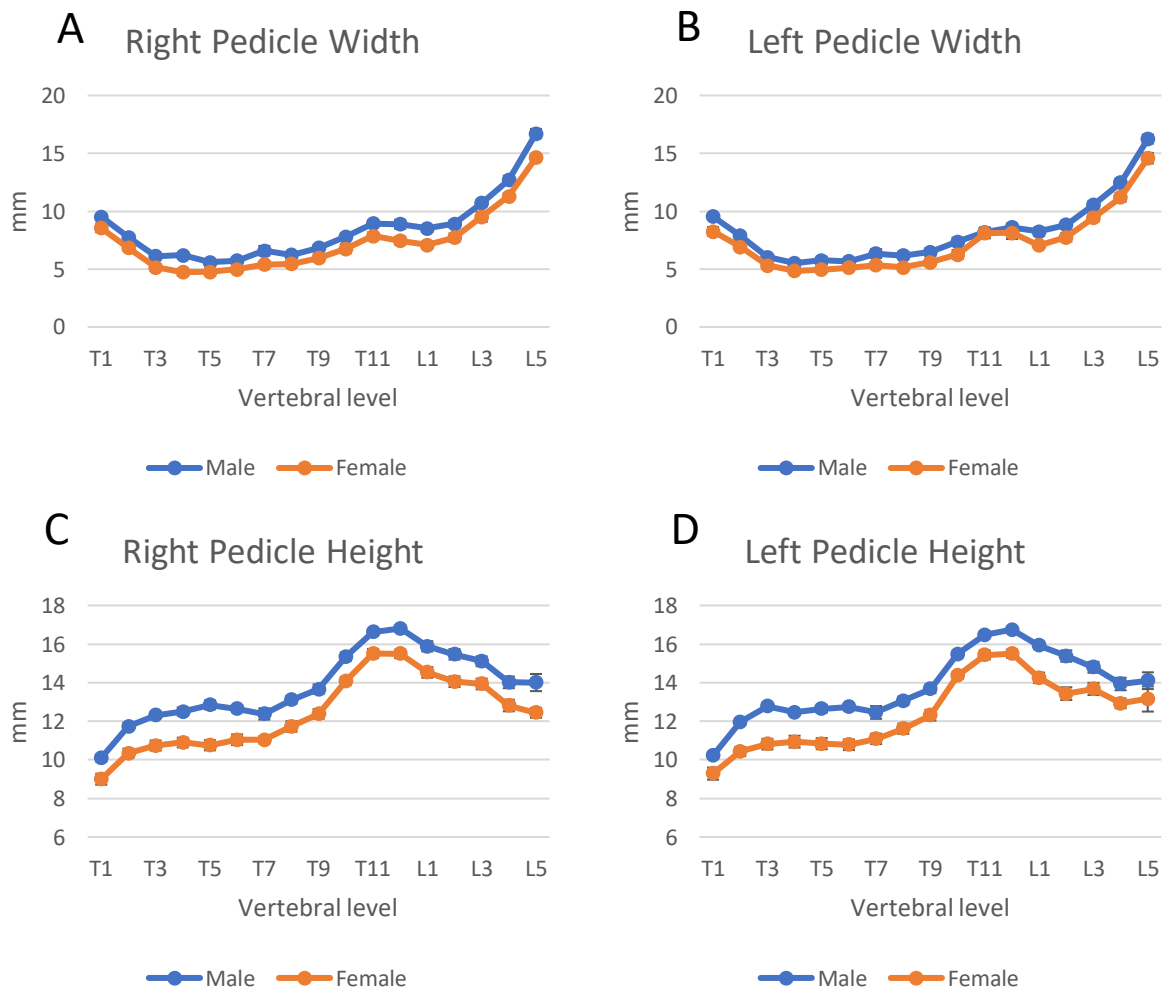
Figure 3.8 – Scatter plot of human male and female pedicle dimensions (mm) measured on CT. A – Right pedicle height. B – Left pedicle height. C – Right pedicle width. D – Left pedicle width.

3.3.3 HUMAN VERTEBRAL SIZE AGE COMPARISON

Figures 3.9 – 3.13 show human vertebral morphometric measurements for the two age groups, <57 years old and ≤57 years old, in scatter plots. Tables are included in Appendix G with the mean measurements, standard deviations, 95% confidence intervals, and mean differences with statistical differences.

The data do not show any statistically significant differences in any of the vertebral measurements between the older and younger groups, at any of the vertebral levels.
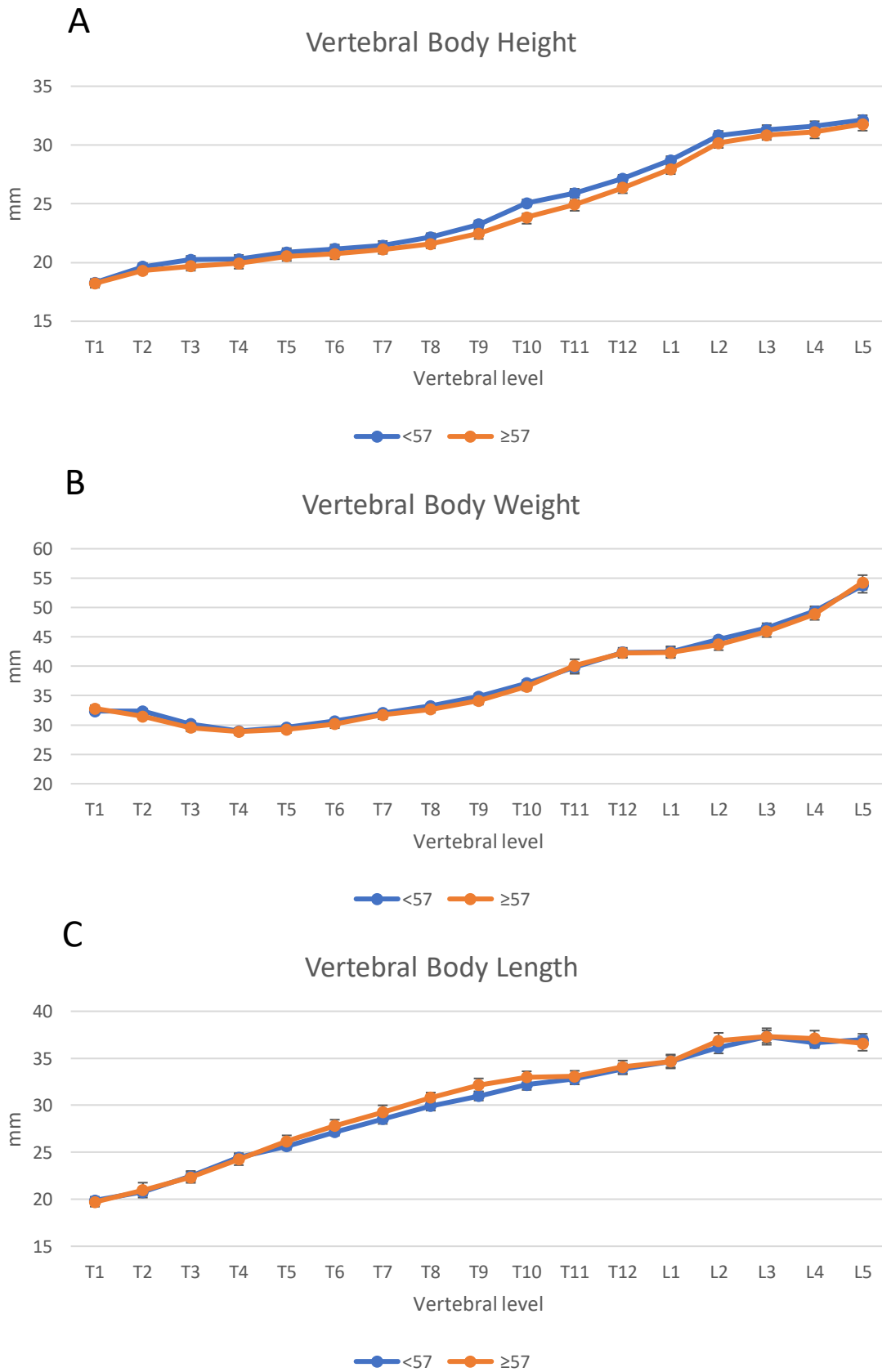
Figure 3.9 – Scatter plot of human older and younger vertebral body dimensions (mm) measured on CT. A –
Vertebral body height. B – Vertebral body width. C – Vertebral body length

Transverse Process Width
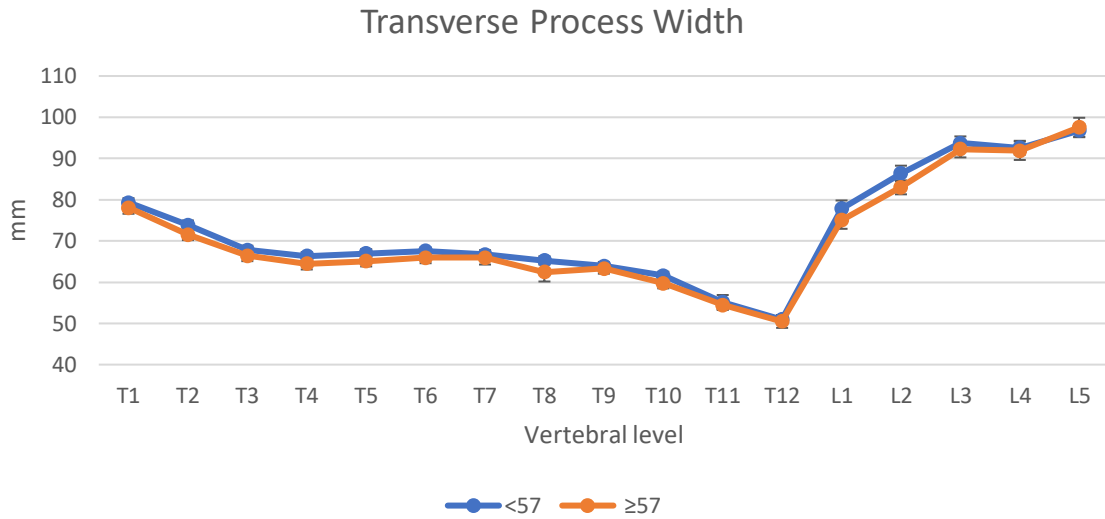
Figure 3.10 – Scatter plot of human older and younger transverse process width (mm) measured on CT

A Spinal Canal Wdith

B Spinal Canal Length
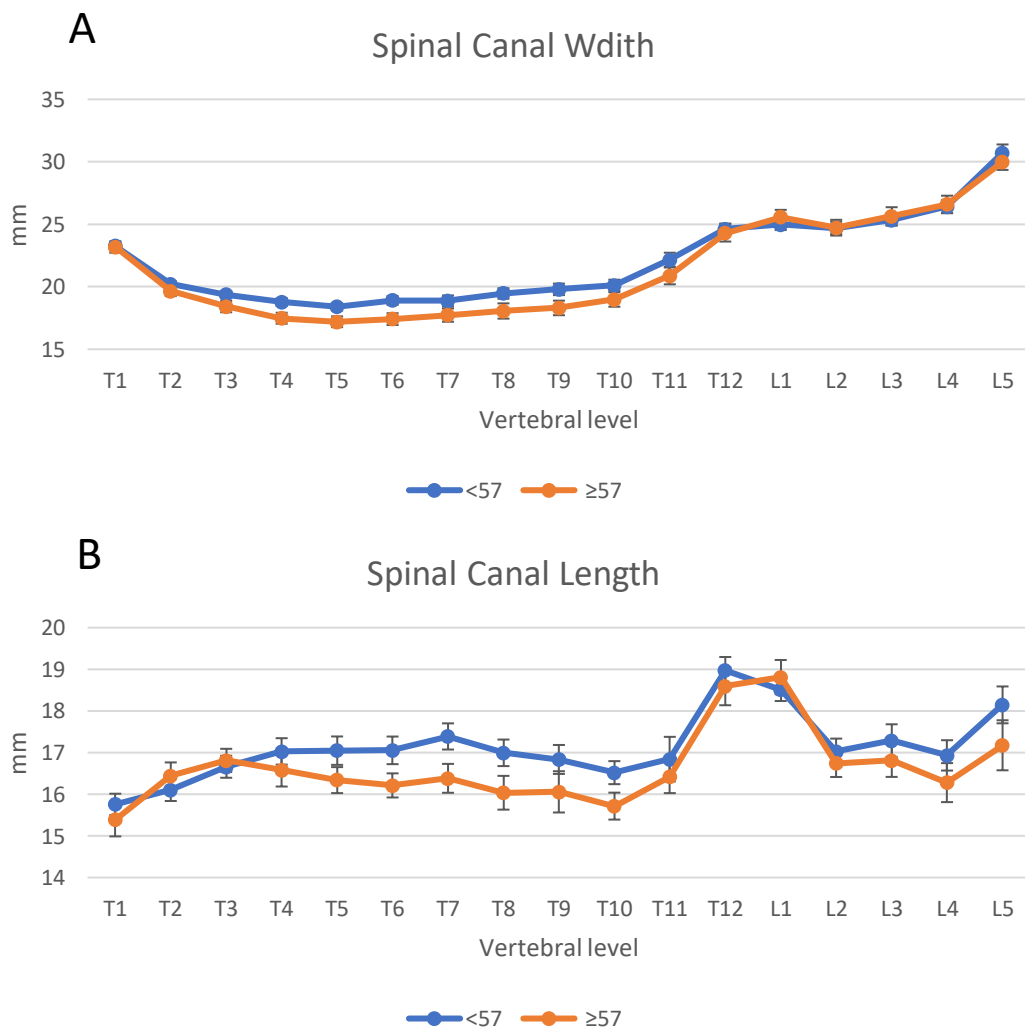
Figure 3.11 - Scatter plot of human older and younger spinal canal dimensions (mm) measured on CT. A – Spinal canal width. B – Spinal canal length.

Total Anteroposterior Length
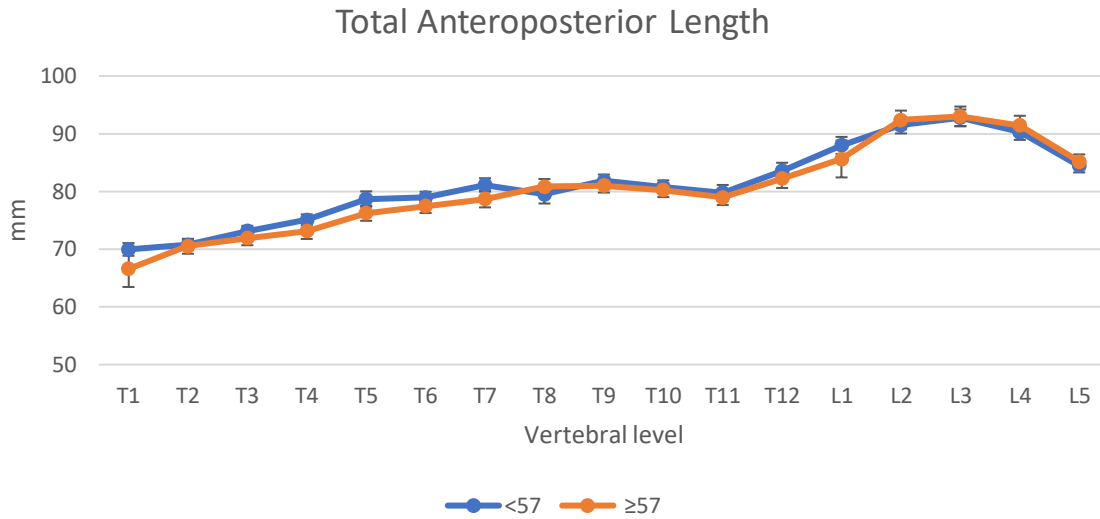
Figure 3.12 – Scatter plot of human older and younger total anteroposterior length (mm) measured on CT.

A Right Pedicle Width

B Left Pedicle Width

C Right Pedicle Height

D Left Pedicle Height
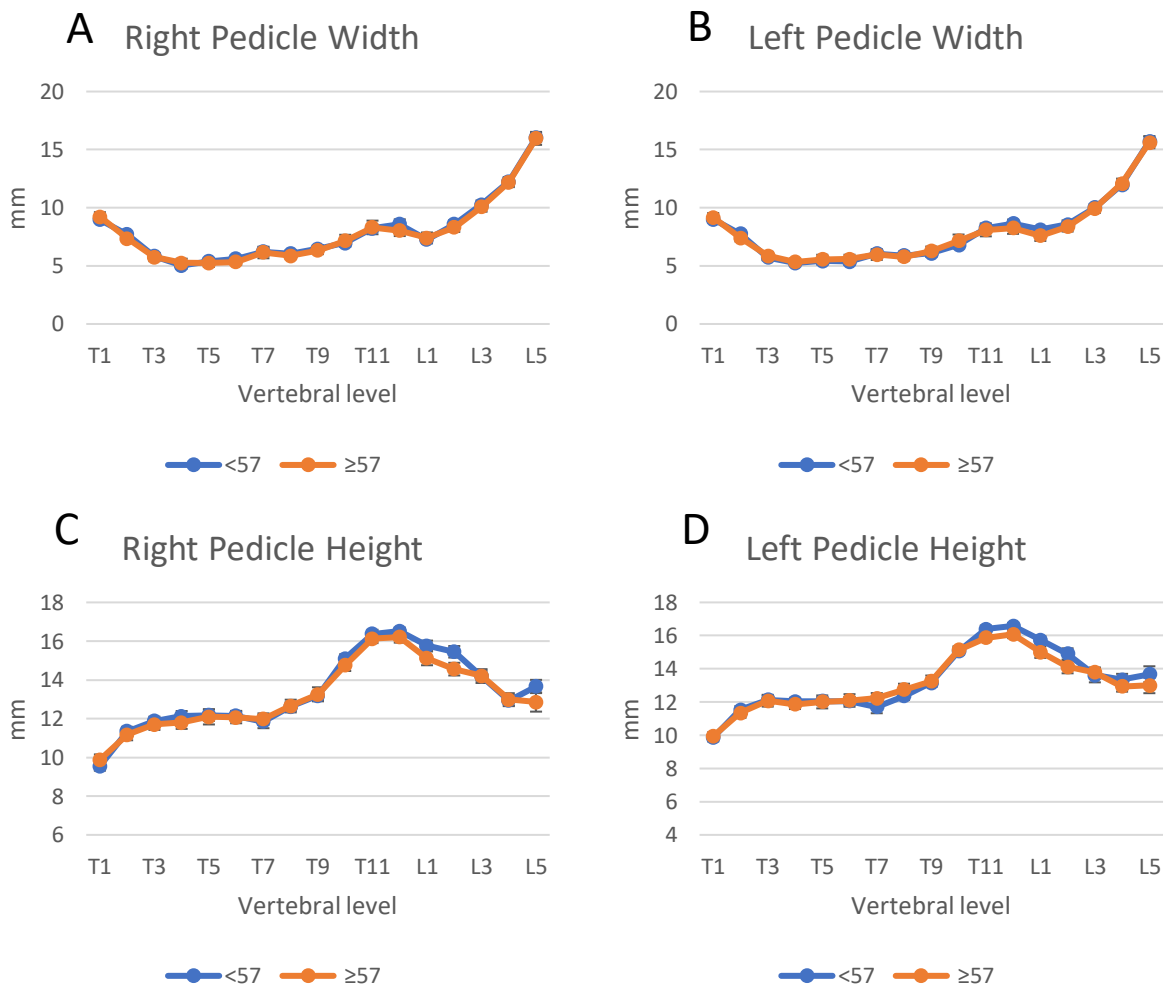
Figure 3.13 – Scatter plot of human older and younger pedicle dimensions (mm) measured on CT. A – Right pedicle height. B – Left pedicle height. C – Right pedicle width. D – Left pedicle width.

3.3.4 INTERSPECIES COMPARISON

Figures 3.14 – 3.18 provide a visual representation of the species mean measurements in scatter plots. Tables E.1 – E.11 in Appendix E show the species mean measurements, standard deviation, 95% confidence intervals, and the mean differences with statistical significance calculated via a two tailed t-test.
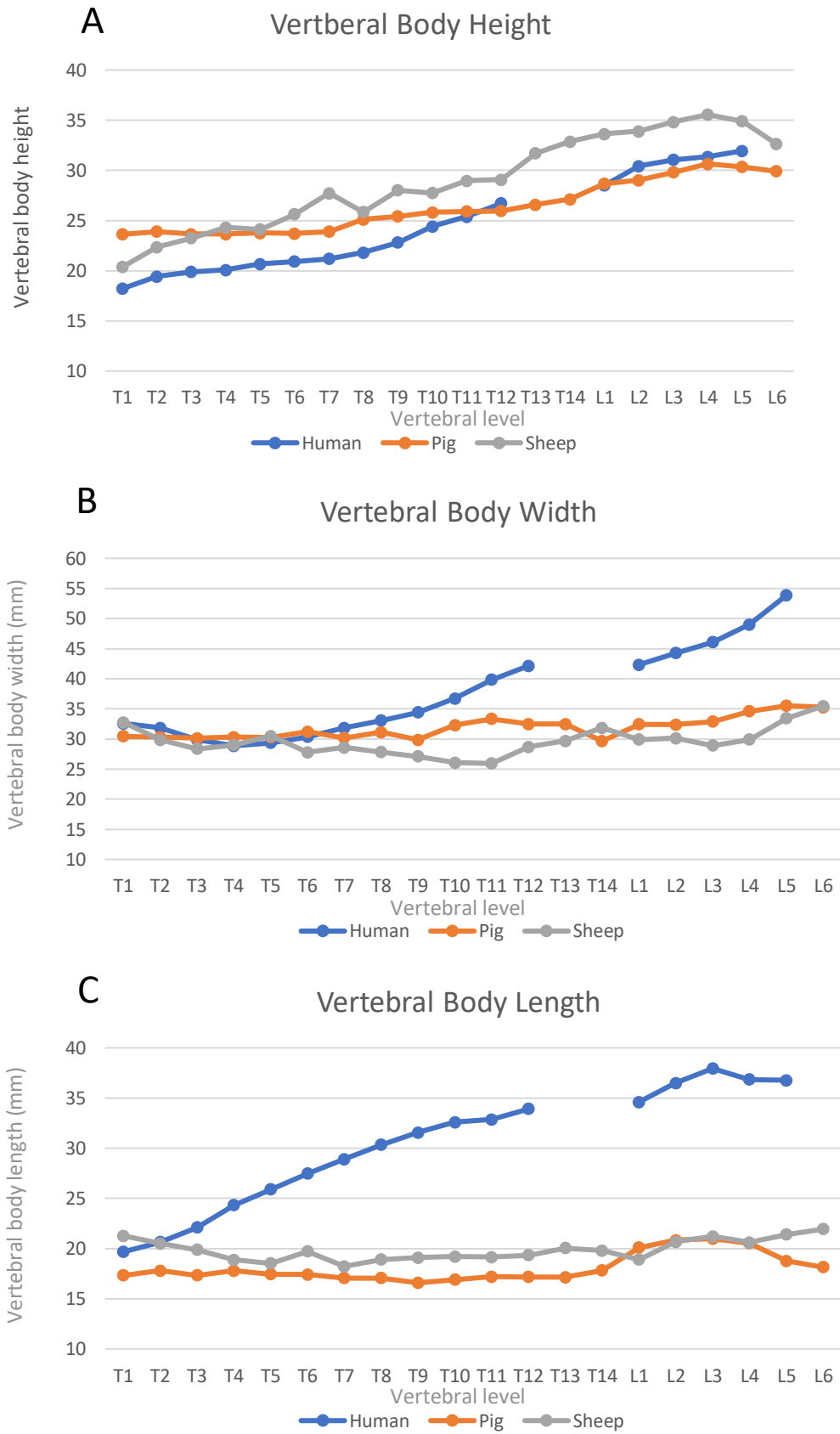
Figure 3.14 – Scatter plot of human, pig and sheep vertebral body dimensions (mm) measured on CT. A – Vertebral body height. B – Vertebral body width. C – Vertebral body length
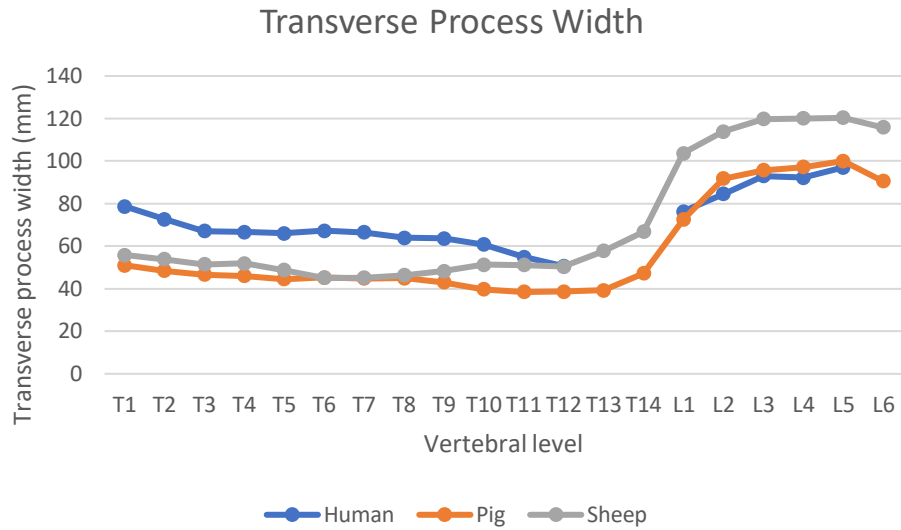
Figure 3.15 – Scatter plot of human, pig and sheep transverse process width (mm) measured on CT.
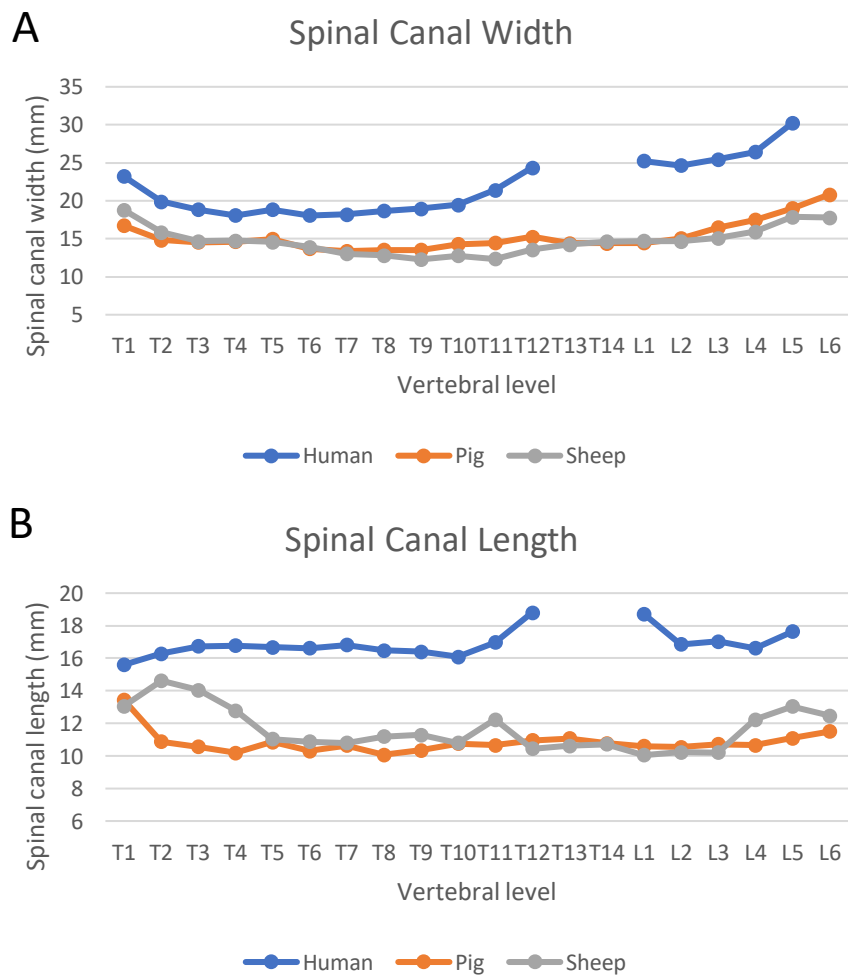
Figure 3.16 - Scatter plot of human, pig and sheep spinal canal dimensions (mm) measured on CT. A – Spinal canal width. B – Spinal canal length.

Total Anteroposterior Length
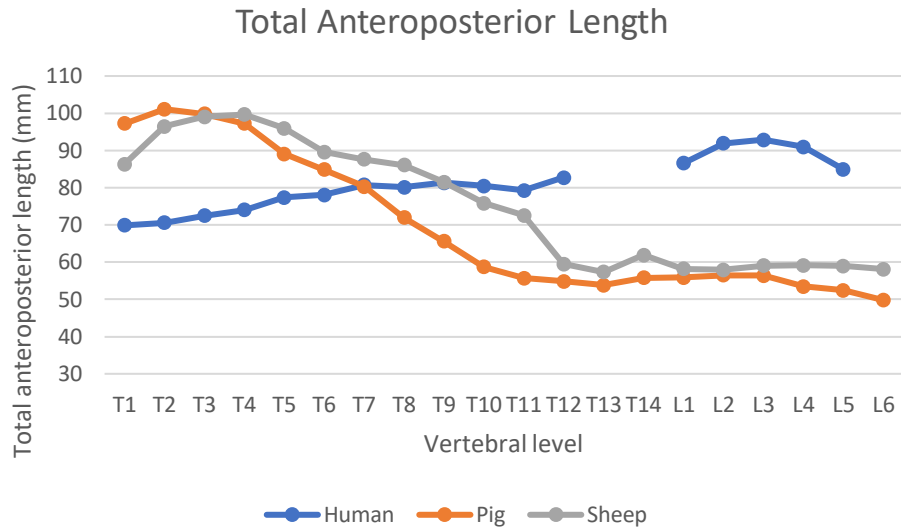
Figure 3.17 – Scatter plot of human, pig and sheep total anteroposterior length (mm) measured on CT.
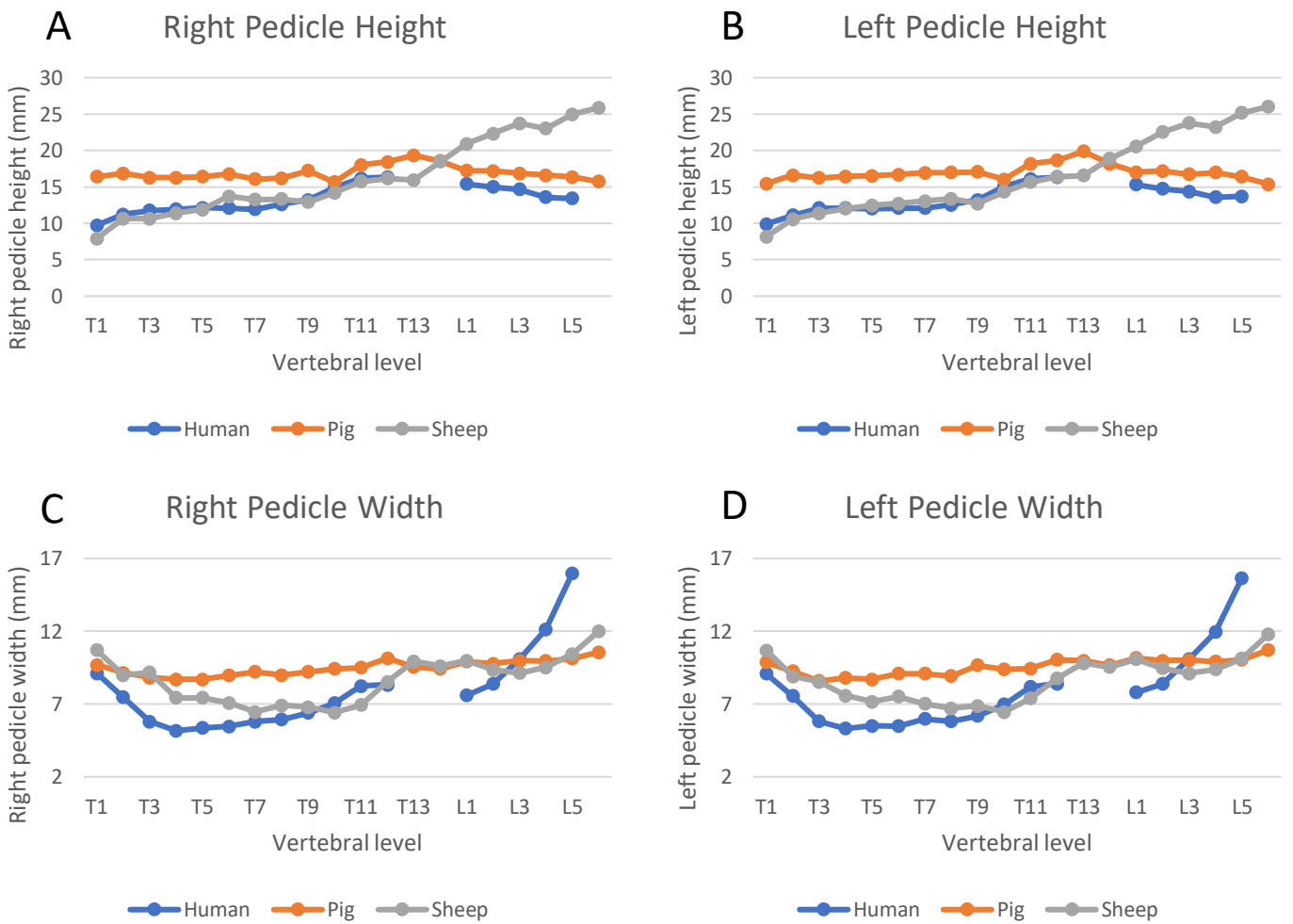
Figure 3.18 – Scatter plot of human, pig and sheep pedicle dimensions (mm) measured on CT. A – Right pedicle height. B – Left pedicle height. C – Right pedicle width. D – Left pedicle width.

3.3.4.1 VERTEBRAL BODY DIMENSIONS

The overall trend for vertebral body dimensions in all three species is of increasing height and width from cranial to caudal.

Pig and sheep vertebral bodies are taller in the thoracic spine, with statistically significant differences. The difference between pigs and humans lessens at lower thoracic vertebrae, and at T12 is no longer statistically significant. Sheep vertebrae remain taller than human vertebrae throughout.

All three species have similar vertebral body width in the upper thoracic spine, with no significant difference between human and pig vertebral width from T1 – T8. Below this level, human vertebrae increase markedly in width, whereas pig vertebrae do not increase to the same degree, and are significantly narrower. Sheep vertebrae are significantly narrower than humans throughout the spine.

Human vertebrae show marked increase in body length from cranial to caudal, and are significantly longer than pig vertebrae throughout. Sheep vertebral bodies are longer than humans at T1, with no significant difference at T2, and below this level, are significantly shorter. This difference is most marked in the lower thoracic and lumbar spine.

3.3.4.2 TRANSVERSE PROCESS WIDTH

Intertransverse process dimension follows a similar trend in all three species, with a gradual decrease in size along the thoracic spine from T1 -T12/T14, followed by a marked increase in size from the final thoracic vertebra to the first lumbar vertebrae. Human thoracic vertebrae are significantly larger in intertransverse dimension than pigs, and also sheep until the T12 level, where there is no significant difference between humans and sheep. In the lumbar spine, sheep vertebrae are significantly larger than humans in intertransverse process length. Human and pig vertebrae are similar in lumbar intertransverse dimension, with no

significant differences except at L2 where pig verterbrae were slightly larger, and between human L5 and pig L6, where the pig L6 vertebra is significantly smaller than the human L5.

3.3.4.3   SPINAL CANAL DIMENSIONS

The human spinal canal width and length are significantly larger than in pigs or sheep throughout the spine.

3.3.4.4   TOTAL LENGTH

Pig and sheep vertebrae demonstrate a different total anteroposterior length trend than human vertebrae. The quadrupedal vertebrae show an overall decrease in size from T1 to L6, whereas humans show a gradual increase from T1 to the mid lumbar spine.

3.3.4.5   PEDICLE DIMENSIONS

Human and pig vertebrae have similar pedicle widths at T1. However, throughout the remainder of the thoracic spine, human pedicles are significantly narrower than pigs. In the lumbar spine, pig pedicle width remains relatively constant, but human pedicle width shows a dramatic increase in size. At the L1 and L2 levels, human pedicles are again narrower than pigs, however at L3 there is no statistically significant difference, and the human L4 and L5 vertebrae are significantly wider than in pigs.

Sheep pedicles are wider than humans in the upper and mid thoracic spine, until the T9 level where there is no statistically significant difference. From T10 – T12, human pedicles are significantly wider than sheep.

All three species show a trend of increasing pedicle height in the thoracic spine. Pig pedicles are significantly taller throughout the spine except at the T10 level.

Sheep pedicles are similar in height to human pedicles throughout the thoracic spine. However, whereas human pedicle height levels out in the lumbar spine, sheep pedicles

continue to increase in size, and are significantly taller than humans throughout the lumbar spine.

Although both quadruped spines have greater pedicle heights than humans in the lumbar spine, the difference is less between humans and pigs than between humans and sheep.

3.4 DISCUSSION

My results show that CT measurements are at least as reliable as measurements under direct visualisation, and can therefore be used as an alternative method of measurement. The currently established literature uses a mixture of CT and direct measurements, but to my knowledge, no such methodological assessment has been performed before.

The human vertebral gender comparison revealed statistically significant differences between male and female specimens. The male vertebral measurements were larger than females, which is consistent with the established literature. However, these differences are small relative to the sizes of existing transpedicular needles and screws. This is unlikely to be practically meaningful beyond confirming that the current range of equipment sizes is required, which is considered to be evident in clinical practice.

The comparison between older and younger human vertebrae did not reveal any statistically significant differences in morphometry. In particular, there were no differences in vertebral body height. Given the known loss of stature with increasing age, this the morphometric variable that was considered most likely to show a difference with age. The findings are still consistent with those of Twomey and Taylor (1987), who showed increased concavity of the endplates with older age, whereas our measurements were specifically taken at the posterior vertebral body.

The main limitations of the age and gender comparisons relate to the relatively small sample sizes. The gender sample sizes were also uneven, with more male than female

specimens. It should also be noted that the gender comparison was not controlled for age, and the age comparison was not controlled for gender. Neither comparison controlled for other potential confounding variables such as body mass index (BMI), ethnicity, or activity or growth hormone and insulin-like growth factor levels during the childhood and adolescent growth spurts.

Simple visual inspection of the dissected animal vertebrae, and the imaged human and animal vertebrae, reveals many morphological similarities. Figure 3.19 shows a diagramatic representation of human, pig and sheep vertebrae with the major surface anatomical structures labelled. All three animals demonstrate a similar configuration, with several structures consistent between the species, including an ovoid vertebral body, pedicles, transverse processes, lamina, spinous processes, and articular facets.

An important difference between the pig and other species in the thoracic is the presence of an intrapedicular transverse foramen. This had been noted in a previous comparative study by Bozkus et al (186). As a result, pig pedicles tend to be taller than sheep or human pedicles in the thoracic spine.

My measurements show that human vertebrae tend to have longer and wider vertebral bodies than sheep or pigs. Vertebral body height is greater in animals than in humans in the thoracic spine. This trend is reversed for humans and pigs in the lumbar spine.
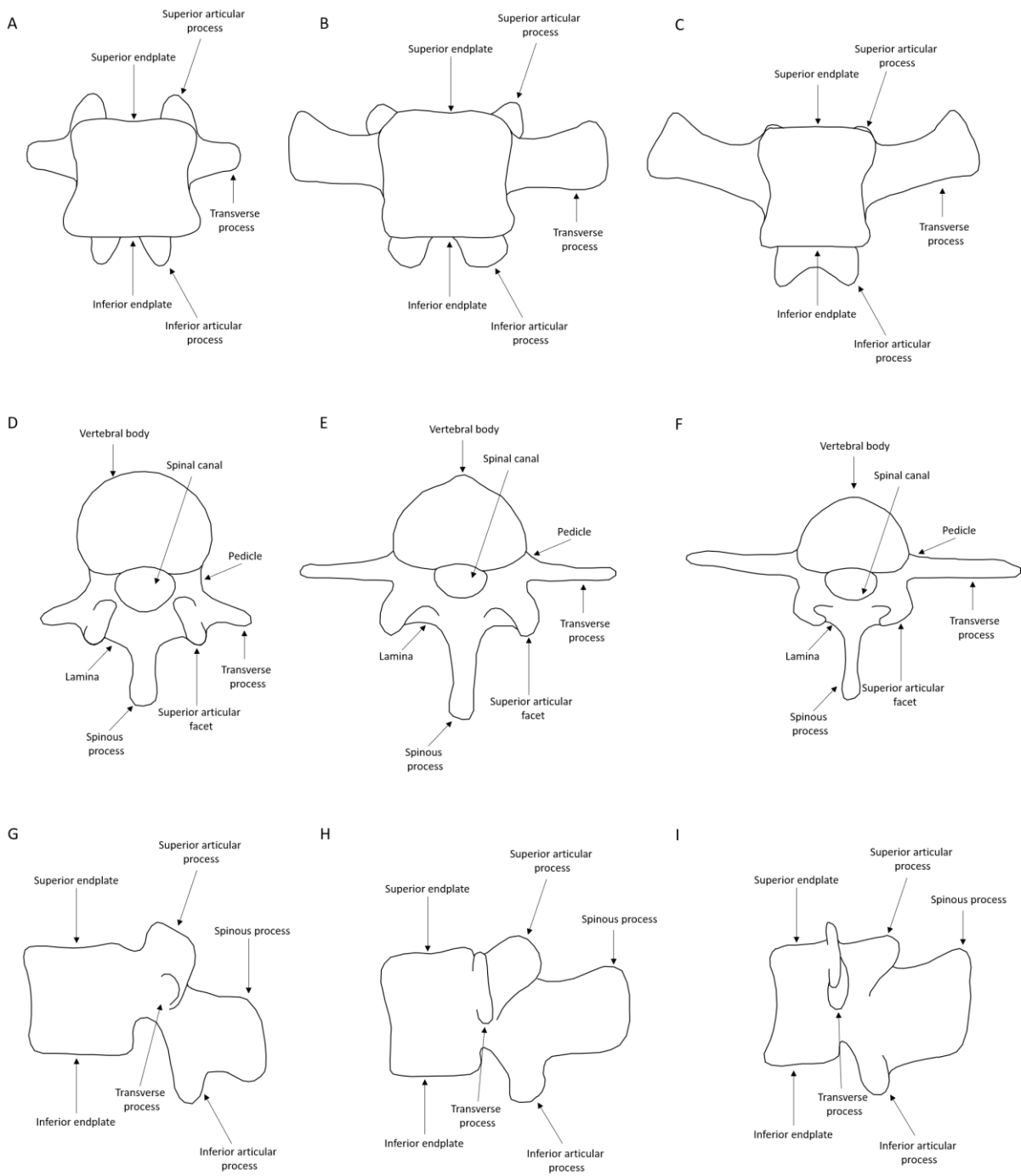
Figure 3.19: Diagram showing the main anatomical structures of human and animal vertebrae. A - Human vertebra anterior view, B – Pig vertebra anterior view, C – Sheep vertebra anterior view, D – Human vertebra superior view, E – Pig vertebra superior view, F – Sheep vertebra superior view, G – Human vertebra lateral view, H – Pig vertebra lateral view, I – Sheep vertebra lateral view

Human spinal canal dimensions are greater than in the sampled animals. It is possible that this is due to increased demands on the motor and proprioceptive spinal tracts in coordinating bipedal locomotion, which are known to be larger and more complex in humans than other mammals (209).

Interestingly, both vertebral body and total anteroposterior length are greater in the human lower thoracic and lumbar spine. This may relate to the differences in muscular forces exerted on quadrupeds compared to bipeds.

The pedicular dimensions are of particular interest when considering a model for percutaneous transpedicular procedures. In terms of height, sheep pedicles are closer to human in the thoracic spine, whereas pigs are more similar in the lumbar spine.

The relationship between the species' pedicle widths is more complex. Both sheep and pig pedicles are wider than humans in the upper and mid thoracic spine, though sheep are closer to humans than pigs. In the lower thoracic spine, sheep and human pedicle widths are comparable. In the lumbar spine, both quadruped species' pedicle widths remain fairly constant with a slight increase in sheep pedicle width at L6. However, human pedicle widths start off smaller than both animals at L1, but show a marked increase from L1 to L5, and at L4 and L5 are significantly larger than either animal. At L3, there is no significant difference between humans and pigs.

Some of my data are consistent with the established literature in terms of dimensions (142, 186-189, 191-193). As discussed in more detail in Chapter 2, the general trends shown in these studies are of quadruped vertebral bodies being taller, narrower and shorter in AP dimension than in humans.

My data also show similarities in the relationships between pedicle dimensions, such as human lumbar pedicle height being smaller than in animals, but closer to pigs than sheep. The increase in human lumbar pedicle width from being narrower than the animal specimens at L1 to wider at L4 and L5, is also consistent with my data.

There are some differences between the literature and my data, however. For example, the thoracic pedicle height and width of sheep demonstrated by Wilke et al (188) are larger than both humans and sheep. This difference is likely due to the relatively advanced age and high weight of the sheep samples used by Wilke et al. Indeed, Mageed et al. (189) used sheep closer in age and weight to my sample, and the trends are much more closely recreated when looking at their data.

This serves as an example of the importance of sample selection when assessing the role of my data in the wider literature.

This study used a single observer performing 4 repetitions of each animal measurement, as described earlier in the materials and methods section. This allowed me to assess reliability with intra-class correlation statistics which showed an excellent intra-observer correlation with an ICC coefficient estimate close to 1. It should be noted that visual assessment of the data shows that despite the ICC coefficient estimate close to 1, the correlation is not perfect, and this is likely to represent an overestimate. However, representations of this data with scatter plots visually confirms the strong correlation.

By using a sufficiently large human sample size, I also overcome two of the main limitations in the literature. Firstly, several studies did not perform human measurements themselves, and used previously available human data, however their animal measurements were performed using different methods than those older human studies. Secondly, those studies that did perform their own human measurements were often hampered by small sample sizes.

In contrast, the animal sample size was limited due to a combination of difficulty in acquiring animal spines from the abattoir within a limited timeframe and storage space constraints which required me to perform vertebral harvesting and scanning for each specimen before obtaining a new one. In the established literature, animal sample sizes varied from 3 to 10, and the sample size of 4 lies at the lower end of this scale. Although I attempted to improve reliability by performing multiple repetitions of each measurement, I opted to compromise between optimising the standard error of the within-subject standard

deviation, and a reasonable number of repetitions. With 4 repetitions, the standard error of the within-subject standard deviation was relaxed to 20%. This is usually (albeit somewhat arbitrarily) set at 10%, however, this would have required 49 repetitions of each measurement. Due to time constraints with the lab, this would not have been feasible.

The sheep samples were younger and of lower weight than the pig specimens. This limitation was due to spinal material restrictions in place in the UK for mature sheep. However, as demonstrated by the results, in spite of being lower in weight, the vertebral dimensions of the sheep sample were in general either similar to or larger than the pig sample.

One of the limitations of this study was the lack of repeat observations on the human data. Without this, it is not possible to comment on the reliability of this data. This was simply an oversight and was not planned. To address this by applying Equation (3.3), the human sample would require 2 repetitions of each measurement to achieve 20% standard error, as with the animal samples.

I did not to perform pedicle angle or pedicle length measurements on the CT data. However, they have been performed in the literature, for example Busscher et al (142) assessed pedicle angles. These dimensions would be of relevance when selecting a model for percutaneous transpedicular procedures. Given the difficulty of implementing them, I opted to leave these analyses to the statistical shape modelling study.

Another weakness of the study lies in the human sample size lacking an upper age exclusion criterion. Although I excluded any cases with significant osteoarthritis (as discussed in the Materials and Methods section), the likelihood is that there may be subtle or early osteoarthritis changes which could affect certain measurements.

I have also not performed any assessment of bone density in this study. Quadruped spines are known to have higher bone densities than human spines, due to their greater loads (141, 203). This will undoubtedly affect the placement and subsequent loosening of implements such as pedicle screws.

Historically, pig spines have been considered to be the closest analogy to the human spine as an *in vivo* model. Although other quadruped spines have been morphologically assessed, no consensus exists as to the closest model. The morphology results suggest that when considering percutaneous transpedicular procedures, the sheep spine is more appropriate in the thoracic spine, whereas the pig is more appropriate in the lumbar spine.

Although some there is some controversy regarding vertebroplasty, other transpedicular procedures such as kyphoplasty, transpedicular bone biopsies, vertebral body tumour ablation, remain relevant and continue to develop. These findings should be of benefit in preclinical, early phase trials of surgical pedicle screws, transpedicular needles and cements, as well as in the selection of animals for physician and surgeon training courses.

3.5 SUMMARY

- This chapter deals with the methodological comparison of direct and CT measurements, and the morphological assessment of human, pig, and sheep vertebrae

- I show that when selecting a model for transpedicular procedures, sheep are closer to humans in the thoracic spine, and pigs are closer to humans in the lumbar spine

- Currently, pig spines are generally used to model the human spine. I propose that sheep spines should be used if the area of consideration is the thoracic spine, with respect to transpedicular access.

- The study was robust with a large human sample size, and excellent reliability

- However, the animal sample size was limited, and I omitted pedicle angle and length measurements. Additionally, I have not addressed differences in bone density in this study.

CHAPTER 4:
VERTEBRAL TEXTURE ANALYSIS

4.1 INTRODUCTION

As discussed in Chapter 1, CT texture analysis provides a non-invasive method for examining the internal architecture of bone. In short, a bone consists of a cortex of dense cortical bone, and an internal medulla. The medulla itself comprises marrow tissue, which is a mixture of haematopoietic cells, adipocytes and stromal cells, and trabecular bone. Trabecular bone is arranged in networks of channels which tend to run in parallel to the long axis of a bone, essentially in alignment with mechanical stresses upon the bone during development (12-14).

The internal trabecular microarchitecture is of importance in the role of vertebral strength, and the loss of trabecular plates in osteoporosis is considered an additional factor for vertebral fragility (210).

Of particular relevance to my thesis, however, is the impact of trabecular architecture on the loading forces on bone cement. Studies have shown that the bone-cement interface is the main site of loading, with computer modelling suggesting that it is specifically in the areas of partial interdigitation of cement through the inter-trabecular spaces (144, 146).

CT texture analysis uses statistical analyses based on the work of Haralick (148, 150) to deduce information about the internal structure of an organ. As described in Chapter 1, the terminology used in the field of CT texture analysis evolved from traditional histomorphometry; to briefly reiterate, the most relevant terms to this study are those relating to first order statistics, namely bone volume (BV), total or tissue volume (TV), apparent bone fraction (BV/TV), apparent trabecular thickness (Tb.Th), apparent trabecular

separation (Tb.Sp), and apparent trabecular number (Tb.N). These terms are discussed in more detail in Chapter 1.

Although micro-CT is the preferred imaging technique for bone texture analysis, high resolution clinical CT has been shown to be adequate (152, 154).

Given the importance of trabecular architecture in cement loading, I would propose that the internal structure of bone should be considered when selecting an animal vertebra to model the human for the purposes of bone cement injection.

This chapter describes a study which compared the trabecular microarchitecture of human, pig and sheep L1 vertebrae, using images acquired for Chapter 3.

4.1.1 RESEARCH QUESTION

This study describes the mean apparent bone fraction, apparent trabecular thickness, apparent trabecular separation, and apparent trabecular number for human, pig, and sheep L1 vertebral bodies. It is designed to decide which animal has textural features that most closely resemble the human.

4.2 MATERIALS AND METHODS

4.2.1 SAMPLE SELECTION AND IMAGE ACQUISITION

The image data used in this study is the same as used in Chapter 3.

I examined 4 pig, 4 sheep, and 44 human spines. The rationale behind species selection and sample size is explained in further detail in the Materials and Methods section of Chapter 3. To summarise, the animal sample sizes were samples of convenience, based on the number of animal spines I was able to acquire. The human data were selected from a clinical imaging

database, and 44 studies were chosen based on a power size calculation using data from human vertebral measurements performed under direct visualisation (192).

4.2.2 TEXTURE ANALYSIS

Texture analysis was performed using the BoneJ plugin for Fiji software (211, 212). Rectangular regions of interest (ROI) of 10 x 5 mm were created centrally within the vertebral bodies. This ROI size was chosen after a pilot testing on pig and sheep vertebrae, and a random sample of human vertebrae, to ensure that an adequate volume of medullary bone was sampled, and to avoid including any cortical bone (Figure 4.1).
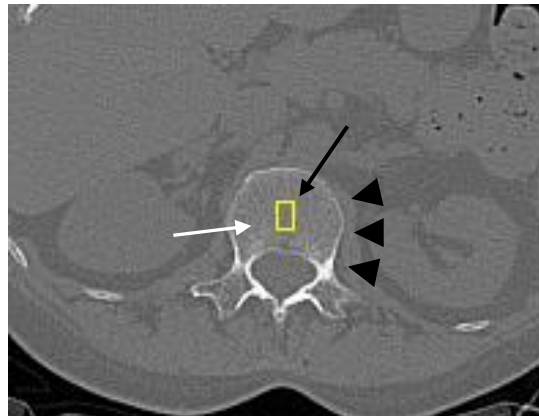
Figure 4.1 – Computed Tomography axial slice through the mid-section of a human L1 vertebra, with an example of ROI placement (indicated by the narrow black arrow) within medullary bone (indicated by the narrow white arrow), avoiding the outer cortical bone (indicated by the black arrow heads).

Trabecular segmentation was performed by creating binarized images using adaptive thresholding (Figure 4.2). Human thresholds were between 180 – 200 Hounsfield Units (HU). Pig thresholds were 350 HU. Sheep thresholds were 400 HU. The BoneJ plugin was used to calculate the bone volume, tissue volume, apparent trabecular apparent bone fraction, apparent trabecular thickness, and apparent trabecular separation for human, pig, and sheep L1 vertebral bodies, using three-dimensional image thickness calculations (213, 214).
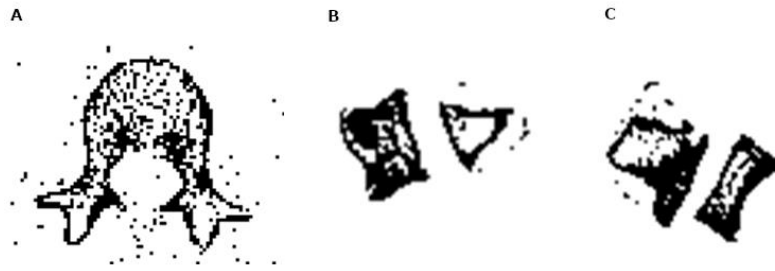
Figure 4.2 – Images from the FIJI software with examples of single slice binarised images produced using adaptive thresholding as described above. A - human, B - pig, C- sheep vertebrae.

ROIs were drawn by a single operator. Two repetitions were performed on each vertebra to allow assessment of intra-observer correlation.

4.2.3 STATISTICS

Basic statistical analysis was performed on the measurements, with calculation of the mean, standard deviation, and standard error for BV/TV, Tb.Th, Tb.Sp, and Tb.N. The distribution of these measures was assessed using both the Shapiro-Wilk test, and visual inspection of histograms and Q-Q plots.

Intra-class correlation coefficients were estimated for all measurements for single fixed raters for consistency.

Due to difficulties relating to assumption of normal distribution for the smaller animal sample sizes as detailed in Chapter 3, statistical significance was assessed using both a two-tailed T-test and the Mann-Whitney U-test.

Statistics were performed on R software (208).

4.3 RESULTS

4.3.1 DATA DISTRIBUTION

The human data showed parametric distribution with visual assessment of histograms and Q-Q plots. The pig and sheep data could not be well assessed due to the sample sizes (Figures 4.2 – 4.7).
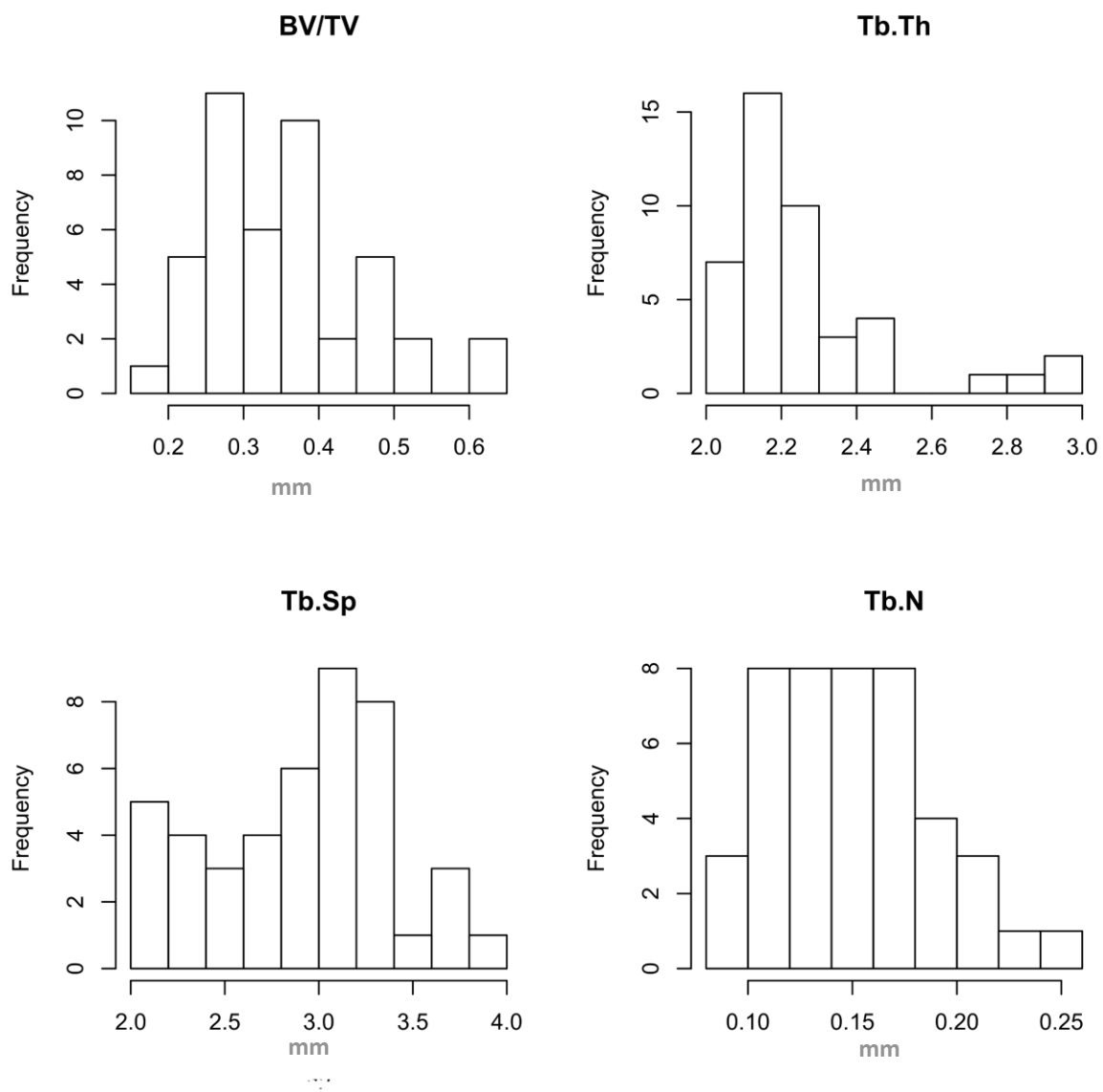
Figure 4.3 – Human data - Histograms demonstrating the distribution of human data for apparent bone fraction (BV/TV), trabecular thickness (Tb.Th), trabecular separation (Tb.Sp), and trabecular number (Tb.N)
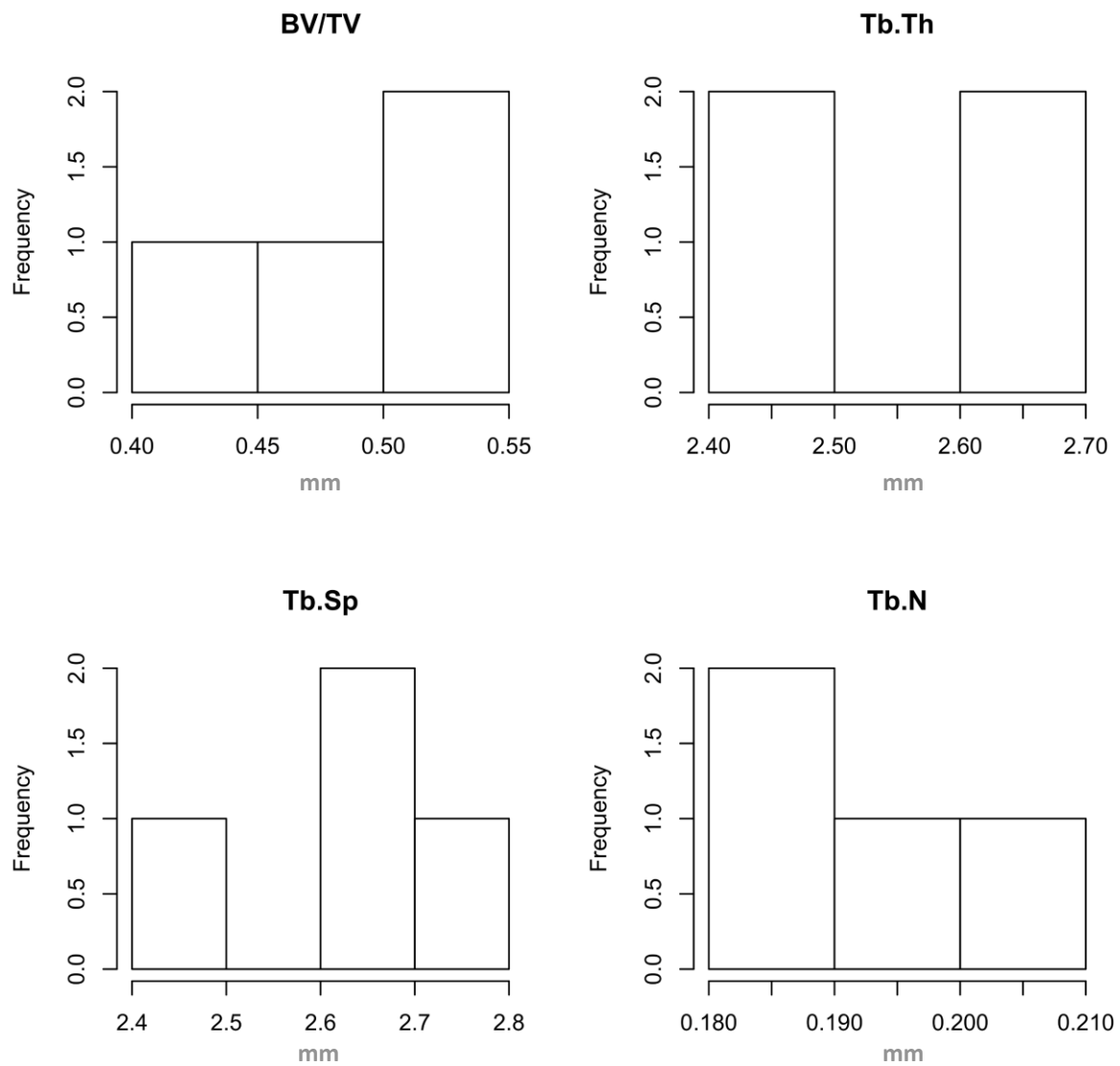
Figure 4.4 –Histograms demonstrating the distribution of pig data for apparent bone fraction (BV/TV), trabecular thickness (Tb.Th), trabecular separation (Tb.Sp), and trabecular number (Tb.N)
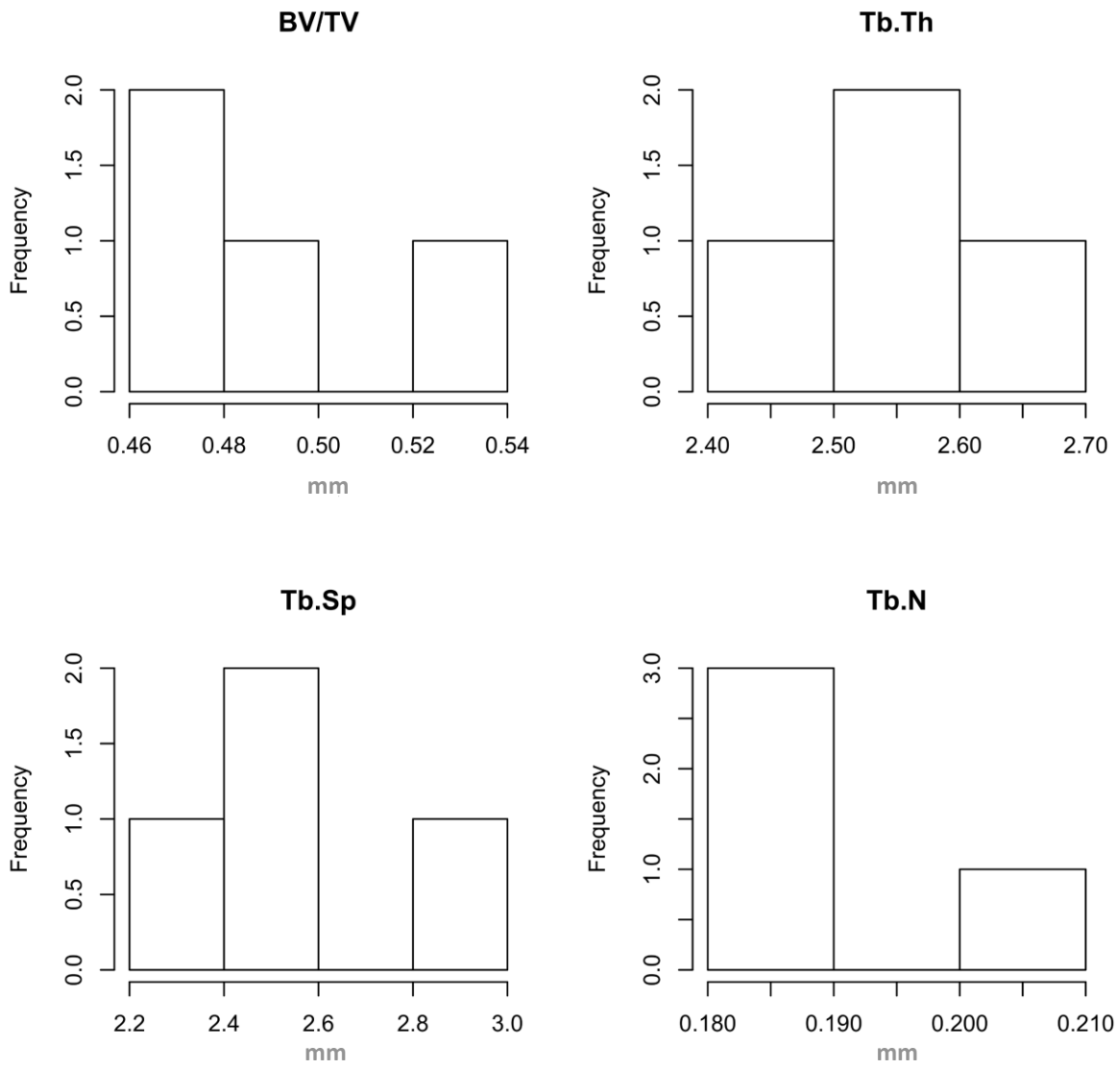
Figure 4.5 – Sheep data - Histograms demonstrating the distribution of sheep data for apparent bone fraction (BV/TV), trabecular thickness (Tb.Th), trabecular separation (Tb.Sp), and trabecular number (Tb.N)
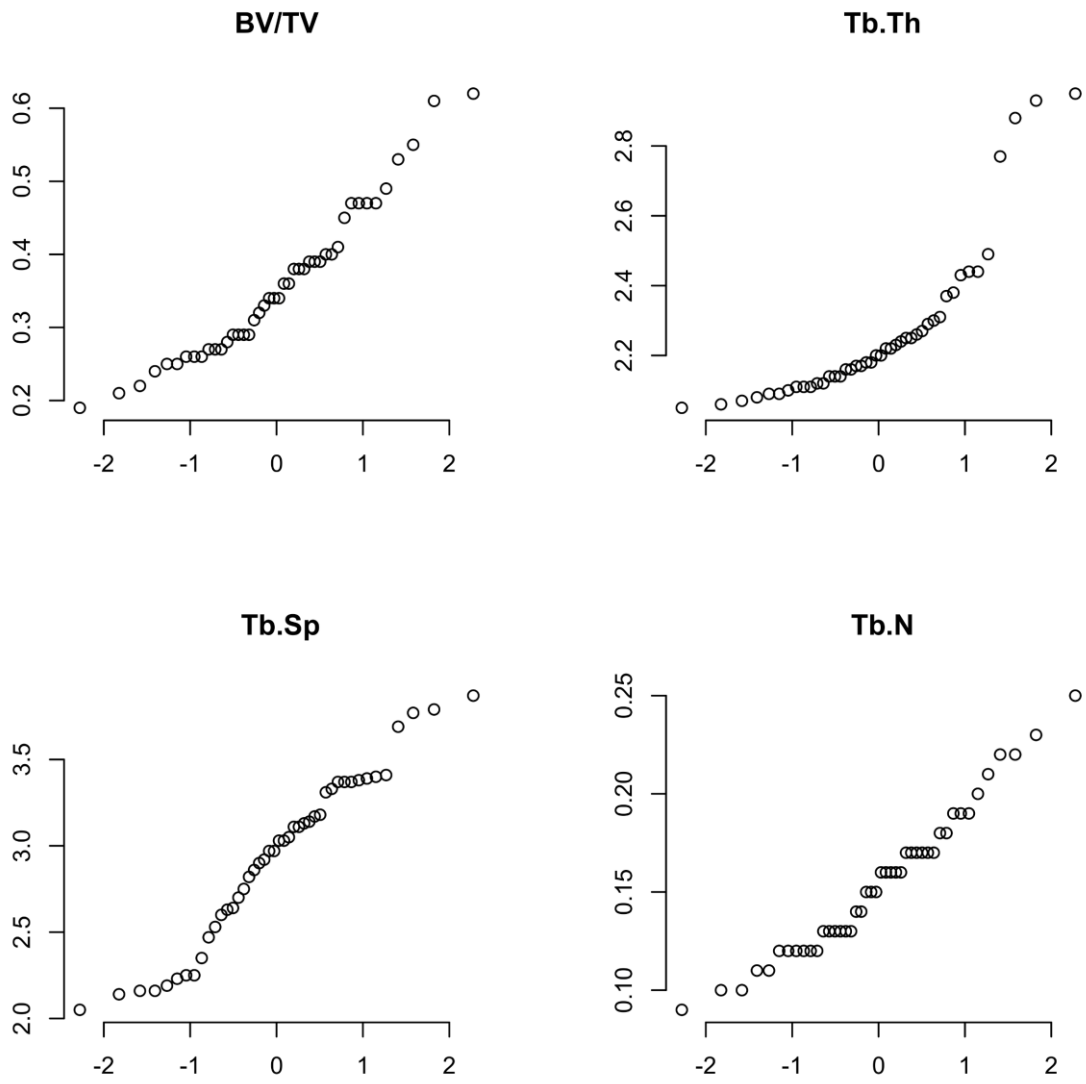
Figure 4.6 – Human Q-Q plots for apparent bone fraction (BV/TV), trabecular thickness (Tb.Th), trabecular separation (Tb.Sp), and trabecular number (Tb.N)
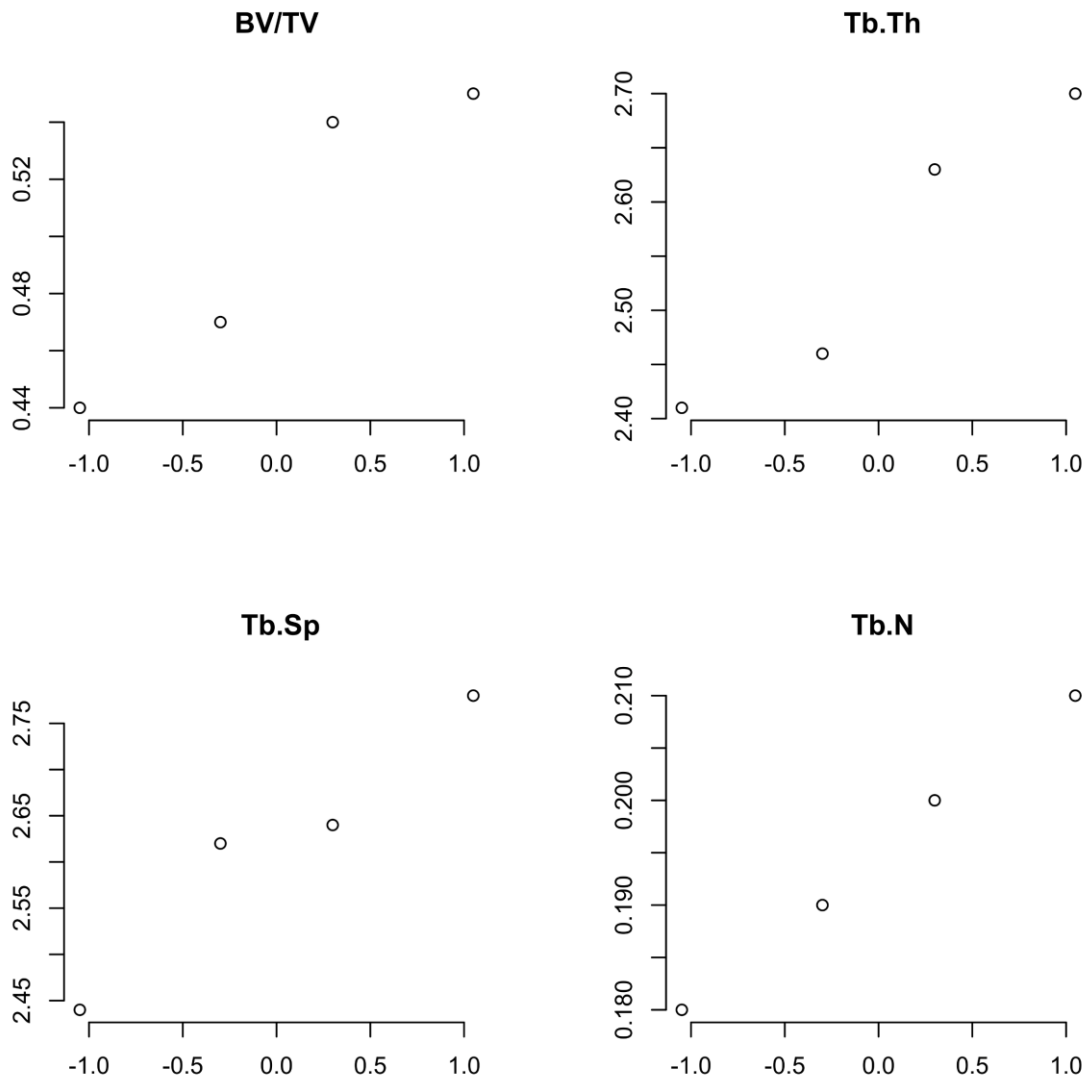
Figure 4.7 – Pig Q-Q plots for apparent bone fraction (BV/TV), trabecular thickness (Tb.Th), trabecular separation (Tb.Sp), and trabecular number (Tb.N)
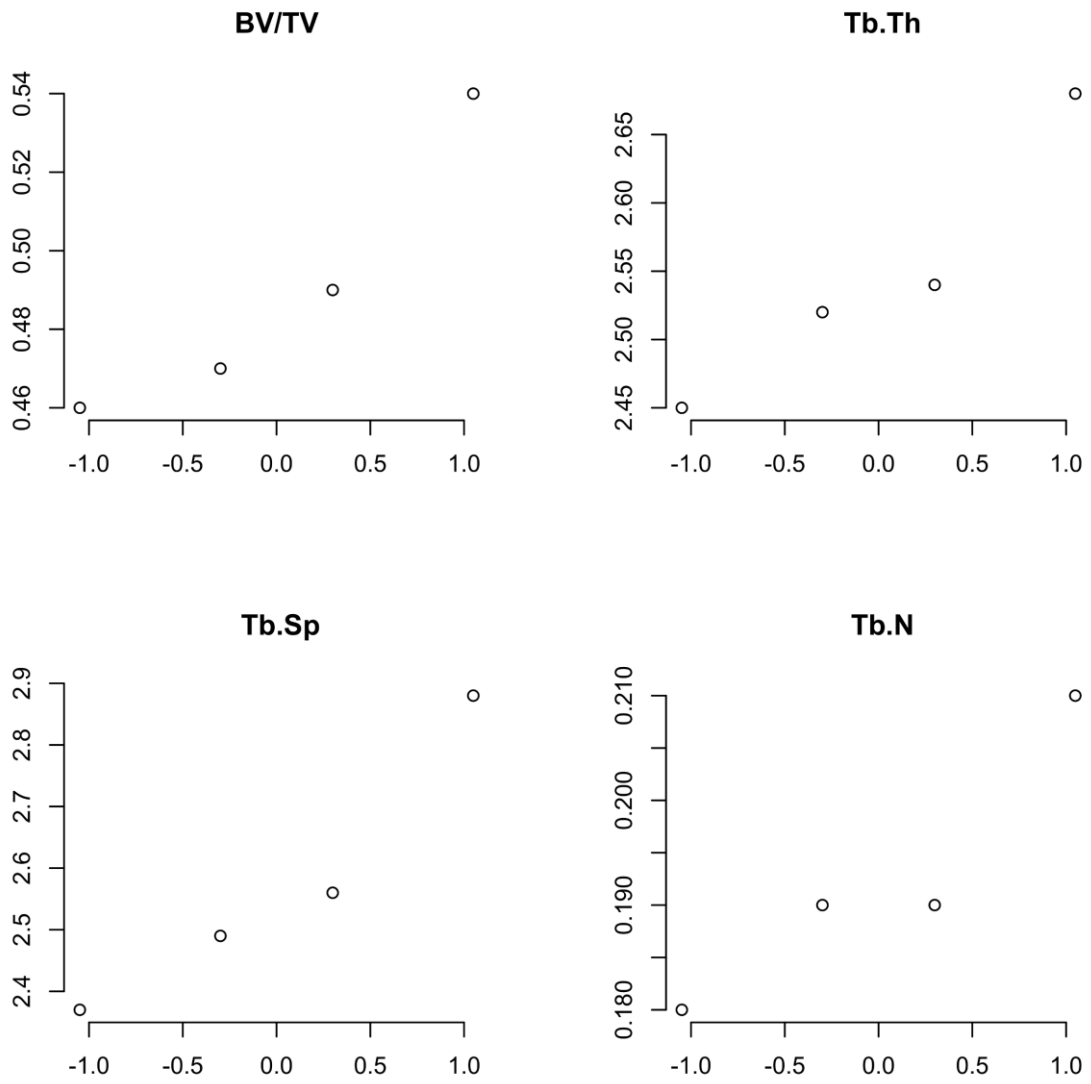
Figure 4.8 – Sheep Q-Q plots for apparent bone fraction (BV/TV), trabecular thickness (Tb.Th), trabecular separation (Tb.Sp), and trabecular number (Tb.N)

4.3.2 INTRAOBSERVER CORRELATION

The intraclass correlation coefficient for single fixed rater for consistency, for a single observer performing two repetitions was at least 0.93 (Table 4.1).

	ICC	CI	p
Human	0.93	0.91 - 0.95	<0.01
Pig	0.99	0.98 - 1.00	<0.01
Sheep	0.96	0.90 - 0.99	<0.01

Table 4.1 – Intraclass Correlation Coefficient and 95% confidence intervals for a single fixed rater for consistency, for human, pig, and sheep data for two repetitions performed by a single observer

4.3.3 INTERSPECIES COMPARISON

Human apparent bone fraction and trabecular thickness were significantly lower than either sheep or pigs. No statistically significant difference in trabecular separation or trabecular number was demonstrated between humans and either animal species (Table 4.2).

95%

	Human		Pig					Sheep				
	Mean (SD)	CI	Mean (SD)	CI	Mean Difference	CI	p	Mean (SD)	CI	Mean Difference	CI	p
BV/TV	0.36 (0.10)	0.33 - 0.39	0.50 (0.05)	0.45 - 0.55	0.14	0.03 - 0.24	<0.01	0.49 (0.04)	0.46 - 0.52	0.13	0.03 - 0.23	0.01
Tb.Th (mm)	0.22 (0.02)	0.22 - 0.23	0.26 (0.01)	0.24 - 0.27	0.04	0.004 - 0.05	0.02	0.25 (0.01)	0.25 - 0.26	0.03	0.003 - 0.05	0.03
Tb.Sp (mm)	0.29 (0.05)	0.28 - 0.31	0.26 (0.01)	0.25 - 0.28	-0.03	-0.08 - 0.02	0.17	0.26 (0.02)	0.24 - 0.28	-0.03	-0.09 - 0.02	0.18
Tb.N (/mm)	1.60 (0.40)	1.4 - 1.7	2.03 (0.13)	1.8 - 2.1	0.43	-0.14 - 0.85	0.14	1.92 (0.11)	1.86 - 2.02	0.32	-0.17 - 0.75	0.14

Table 4.2 – Mean apparent bone fraction (BV/TV), trabecular thickness (Tb.Th), trabecular separation (Tb.Sp), and trabecular number (Tb.N) of human, pig, and sheep data (standard deviation), 95% confidence intervals (CI), and mean differences with statistical significance (p).

4.4
4.4 DISCUSSION

The results demonstrate that at the L1 level, human vertebrae have lower apparent bone fraction than pigs or sheep. This suggests a lower proportion of bone matrix relative to total volume. Human trabecular thickness is also significantly lower than that of pigs or sheep. Interestingly, human trabecular separation and number were not significantly different from either quadruped.

This implies that all three species have comparable numbers of trabeculae which are similarly spaced, but that quadruped trabeculae are generally thicker. However, while these differences in trabecular thickness and apparent bone fraction are statistically significant, it is questionable whether these differences are truly meaningful. In absolute terms, the differences are small, and it is unclear whether they would have any meaningful effect on cement spread and interdigitation.

These findings corroborate previous studies which show higher trabecular thickness and bone volumes in sheep and pigs than humans.

Inui et al (215) performed CT texture analysis on micropigs of various ages to assess changes in trabecular microarchitecture with aging. Although they did not perform a direct comparison to human vertebrae, their results at 3 months were comparable to ours, allowing for differences in breed and age. Their two male 3 month old pigs had a mean apparent bone fraction of 44% (SD = 0.01), mean trabecular thickness of 0.20mm (SD = 0.03), mean trabecular separation 0.13mm (SD = 0.02), and mean trabecular number 4.43 (SD = 0.72). This is compared to the pig sample mean apparent bone fraction of 50% (SD = 0.05), mean trabecular thickness of 0.26mm (SD = 0.01 mm), mean trabecular separation 0.26 mm (SD = 0.01 mm), and mean trabecular number 2.03 (SD = 0.13).

A previous study using two-dimension high resolution stereo microscopy images compared 5 adult human lumbar spines with 5 mature sheep spines, combining results from all vertebral levels. They showed a mean human trabecular thickness of 0.27 mm (SE = 0.008

mm) and mean sheep trabecular thickness of 0.29 mm (SD = 0.005 mm0 (216), which they found to be statistically significant. These findings are comparable to ours, and show a similar trend.

A vertebral histomorphometric study of humans, pigs, rhesus monkeys and beagles using a scanning microscope to assess radiographs of bone tissue samples (217) included a comparison of human and pig bone volumes. They found a human bone volume of 15.3% compared to micropig bone volume of 52.7%. Bone volume is analogous to apparent bone fraction. Although their absolute values for human bone volume are lower than the apparent bone fraction, the trend remains the same, with a lower value in humans. The differences in values may be explained in part by the differences in methodology.

Although CT bone texture analysis comparison of humans and non-human primates, rodents, and dogs have been performed, to the best of my knowledge no such comparison of humans with sheep or pig vertebrae has been made. These results provide additional data to the established literature: that human trabecular thickness is lower than either quadruped, but trabecular separation is not statistically different.

These findings correlate with the established literature that quadrupeds have higher vertebral bone mineral density than humans (218). As discussed in Chapter 1, bones undergo remodelling depending upon applied forces (11) (Clarke 2008). It could therefore be assumed that quadrupedal vertebrae may in fact undergo higher axial loads than human vertebrae, but no comparative studies have been performed to confirm this.

The main strengths of this study are the large human sample size compared to the studies in the established literature, and the high intra-observer correlation.

There are a number of limitations to this study. My analyses were performed using clinical CT machines, rather than micro-CT. As such, the results were affected by partial volume artefact since the pixel resolution was low, and there would therefore be inevitable blurring of boundaries between tissues of differing densities.

The human sample, although larger than most similar comparison studies, was heterogeneous in terms of age and gender, with no upper age limit. Although osteoarthritis was an exclusion criterion, osteopaenia and osteoporosis were not readily assessed on clinical CT, and therefore these were not necessarily excluded. However, this may not have a large an impact on the trabecular architecture analyses, as I used adaptive thresholding to account for variance in density, and as discussed in Chapter 1 regarding osteoporosis, this affects bone mineral density more than trabecular architecture.

As discussed in Chapter 3, the animal sample sizes were limited. This not only affected the statistical power of the findings, but also made assessment of data distribution difficult. I was not able to assume a normal distribution, and therefore statistical significance was assessed on the assumption that data were not Normally distributed.

Additionally, the analyses were performed at a single vertebral level. It is uncertain whether these findings can necessarily be applied to other spinal levels.

The findings corroborate and build upon the established literature in this field. The fact that there is no statistically significant difference in trabecular separation between humans and pigs or sheep is potentially of relevance when considering vertebral cement spread and interdigitation. As the cement-trabecula interface appears to be the most important site for loading, cement fracturing, and stress shielding (144-146), it is possible that the similarity between these species in terms of trabecular separation means that either sheep or pigs would represent a suitable animal model for testing vertebral cement spread. However, this requires additional testing with direct comparison of cement injection and quantitative analysis of the subsequent cement patterns. Indeed, it is not clear whether even the statistically different findings would result in any meaningful differences in practice, and further assessment with cement injection studies is needed.

Additionally, the lower trabecular thickness and lower bone mineral density of human vertebrae may impact the pattern of fracturing/cracking of cement, and additional studies are needed to assess this. Specifically, studies comparing cement fracturing/cracking and cement failure between human, pig, and sheep vertebrae are required.

I have not performed any higher order statistical analysis, such as run length matrices. This could be addressed by performing second order statistical analyses on the data.

In combination with the results from Chapter 3, I propose that sheep vertebrae be used to model the human thoracic spine, and pig vertebrae be used to model the human lumbar spine. The evaluation of cement spread may be similar, but assessment of fracturing following cementation should be viewed with caution as this study has not directly examined this.

4.5 SUMMARY

- This chapter deals with bone texture analysis of human, pig, and sheep vertebrae

- I show that when selecting a model for vertebral cement procedures, the trabecular separation shows no statistically significant difference between humans and either quadruped which suggests that both pigs and sheep may demonstrate similar cement spread

- The study was robust with a large human sample size, and excellent reliability.

- The animal sample size was limited, and the images were obtained using a high-resolution clinical scanner, rather than micro CT

- Further work is required to assess whether vertebral cement spread and interdigitation is similar between species in practice

CHAPTER 5:
STATISTICAL SHAPE ANALYSIS

5.1 INTRODUCTION

Statistical Shape Analysis (SSA) provides a different method for comparing shape than manual morphometric measurements. As discussed in Chapter 1, rather than taking individual measurements in isolation, SSA considers all the geometric information of the objects being compared.

This study uses similarity and affine transformations, thin plate spline (TPS) deformations, full generalised Procrustes analysis (GPA) and principal component analysis (PCA). These techniques are applied to create a statistical shape model, which provides a visual representation of the shape variation between the objects being compared.

These concepts are discussed in more detail in Chapter 1, and a full description of the mathematics involved can be found in *Statistical Shape Analysis 2nd Edition* (155). A brief summary is provided below as a reminder for the reader.

5.1.1 DEFINITIONS

The definition of shape used by Kendall (156) has subsequently become widely used in statistical shape analysis. Kendall defined shape as "*all the geometric information that remains when location, scale, and rotational effects are removed from an object*".

Landmarks are points placed on the surface of an object, that corresponds between objects being compared. I used scientific, or anatomical landmarks, which are points assigned based on an anatomically meaningful way, such as the apex of an anatomical structure.

Semilandmarks are a set of points used to conform to a curved surface that cannot be described with a single point landmark (157). I have used semilandmarks, as vertebrae are complex objects with many curved surfaces.

I have used Dryden and Mardia's definitions of centroid and centroid size. The centroid coordinate simply the mean of all the object coordinate values and is a computable equivalent to the centre of gravity of the object. Centroid size defined as "*the square root of the sum of squared Euclidean distances from each landmark to the centroid*".

5.1.2 AFFINE AND SIMILARITY TRANSFORMATIONS, AND THIN PLATE SPLINES

Affine transformations are the simplest method of changing shape, and work by preserving parallel lines and planes between objects.

Similarity transformations change a shape by rotation, scaling, translating and reflecting. They therefore do not affect "shape" as defined by Kendall. I used similarity transformations during multiple steps within the methodology, to remove non-shape related information.

A thin plate spline (TPS) is a function that allows one shape to be deformed to another while minimising the bending energy. TPS functions are used with landmarks and sliding semilandmarks to interpolate the space between landmarks. TPS allows matching between objects that affine transformations would not be able to. The average objects of each species were too dissimilar in morphology for affine transformation but had consistent

topology. I was therefore able to use TPS to register the average human shape to the average animal shapes.

5.1.3 PROCRUSTES ANALYSIS AND PRINCIPAL COMPONENT ANALYSIS

The general Procrustes analysis matches shapes using a sum-of-least-squares technique. It involves using a similarity transformation to remove non-shape related information, and then minimising the sum of squared differences between the vertex points of each object.

Once GPA has been performed, principal component analysis may be used to create a statistical shape model which describes variation from the mean shape.

Principal component analysis (PCA) allows for the reduction of the number of dimensions when assessing multi-dimensional data. It allows the selection of the principal component, which is the component with the greatest effect on the data. In SSA, it is used to generate a mean shape, and then produce eigenvectors and eigenvalues to define shape modes. Shape modes are orthogonal patterns of variation in shape around the mean.

5.2 MATERIALS AND METHODS

5.2.1 SAMPLE SELECTION AND IMAGE ACQUISITION

The image data used in this study are the same as used in Chapters 3 and 4.

I examined the L1 vertebrae of 4 pigs, 4 sheep, and 42 human spines. Two human specimens were excluded as on visual assessment of the 3D objects, they appeared to demonstrate superior endplate collapse. The animal sample size was one of convenience, based on

availability of whole spines from the abattoir, from which vertebrae were harvested. The human sample was taken sequentially from a clinical imaging database. The sample size was calculated from established work in the literature on the morphometry of human vertebrae. The rationale behind species selection and sample size is explained in further detail in the Materials and Methods section of Chapter 3.

Previous work by Tümer et al. in 2016 showed that a sample size of 35 was sufficient to create a robust SSM (219) for the articular surface of the talus. This was assessed by performing a bootstrap analysis (220) which involves rebuilding the SSM multiple times using resampled data. The resulting models may then be assessed qualitatively by comparing coloured model meshes. Quantitative assessment can also be performed by calculating the variance of the object vertices from the mean shape.

Whole vertebrae are more complex shapes, and therefore it is difficult to assume that a sample size of 35 would prove sufficient for an accurate SSM. I have not performed a bootstrap analysis as I am not using the SSM for any specific application. Instead, I simply require the mean object of the sample population to analyse the shape variation within the sample, accepting that this variation may not be representative of any other sample population.

5.2.2   3D OBJECT CREATION

3D objects of the L1 vertebrae were created using the open access software Stradwin (221). The vertebrae were contoured automatically with manual correction, and the objects were generated by the software using a distance transform and regularised marching tetrahedra (222). Figure 5.1 shows examples of the contouring and Figure 5.2 the subsequent 3D object.
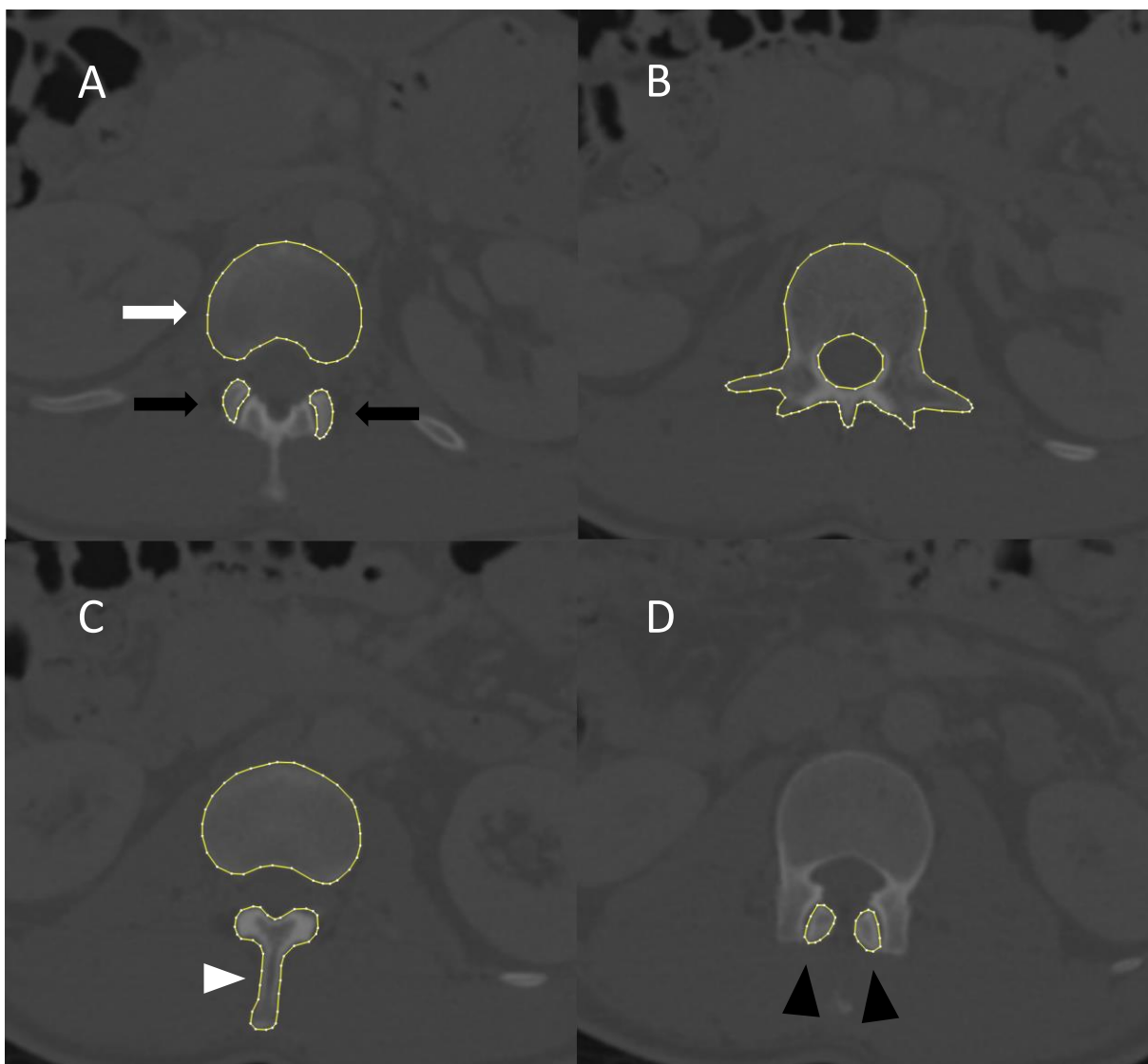
Figure 5.1: Representative slices of CT through a human L1 vertebra. The yellow outline denotes contouring performed on Stradwin. A – Slice through the superior aspect of the L1 vertebral body (white arrow) and the superior articular facets (black arrows). B – Slice through the upper third of the L1 vertebral body. C – Slice through the lower third of the vertebral body with the spinous process posteriorly (white arrowhead). D – Slice showing the inferior articular facets (black arrowheads).

A
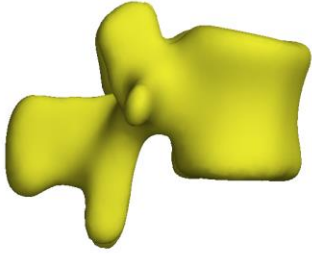
B
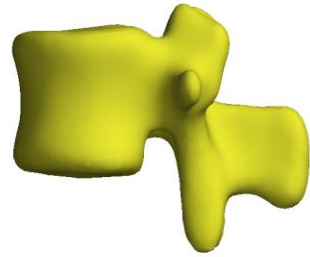
C

D
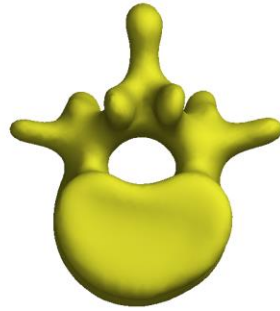
E
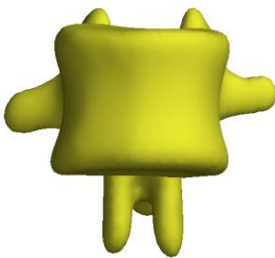
F
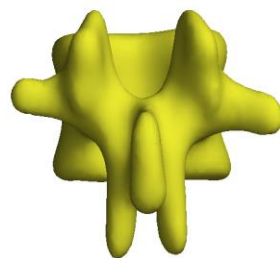
Figure 5.4: 3D object of the human L1 vertebra which was contoured in Figure 5.1, created using Stradwin, showing A. left lateral, B. right lateral, C. superior, D. inferior, E. anterior, F. posterior views

5.2.3 GENERATION OF STATISTICAL SHAPE MODEL

The 3D objects were analysed using another open access software, wxRegSurf (223).

Landmarks and semilandmarks, referred to as landcurves in wxRegSurf, were placed on corresponding sites on all vertebrae (Figure 5.3). I placed 24 landmarks and 24 semilandmarks on each vertebral object.

For each species, a single object was selected as an "average" appearance, based on subjective observation. This object was aligned to the centroid and registered to each of the other vertebrae of that species, using a similarity transformation, affine transformations, called locally affine deformation (LAD) in wxRegSurf, and GPA, to create an average shape for that species. Objects of the same species were similar enough in morphology that LAD was able to adequately match them.

This average object for each species was named the "canonical" by convention of the software. To optimise the registrations, this canonical object was then re-registered with each vertebral object of its species, and this was used to create a "true canonical", using similarity transformation, LAD, and GPA.

These "true canonicals" were used as average shape representations of each species.
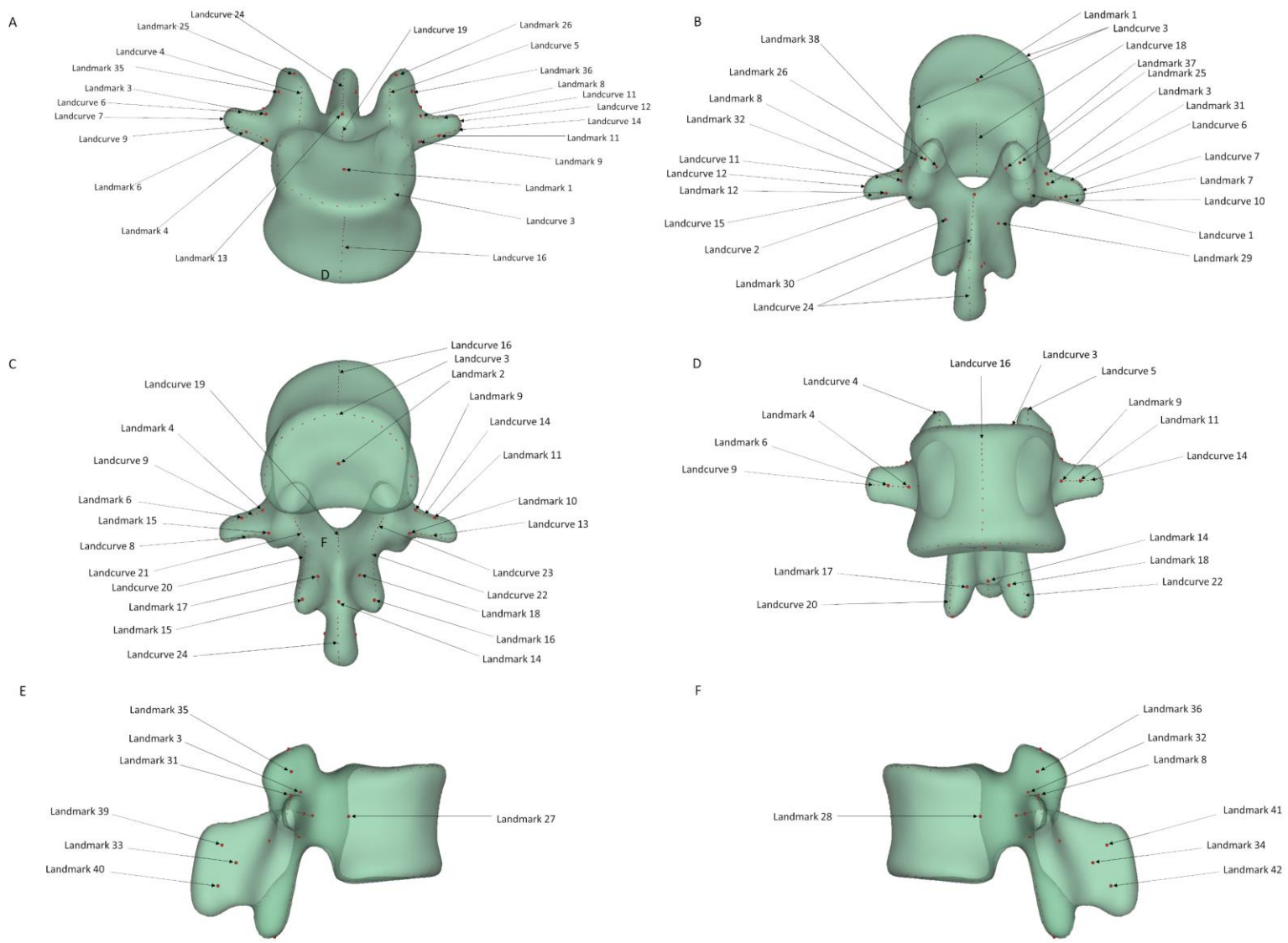
Figure 5.5: Landmark and semilandmark (named "landcurves" as per wxRegSurf naming convention) placements on a human L1 vertebra for shape matching. The landmarks are indicated by single red dots. The semilandmarks are indicated by red dashed lines. A - Anterior superior oblique view; B - Anterior view; C - Anterior inferior oblique view; D - Posterior superior oblique view; E – Right lateral view, F – Left lateral view

5.3 EXPERIMENTS

5.3.1 HUMAN SHAPE VARIATION

To assess human L1 vertebral shape variation within the study population, I created an SSM.

The software applied PCA to the human "true canonical" to generate an SSM with shape modes. Horn's parallel analysis (224) was performed to assess the number of shape modes to consider as significant by judging how many modes are more relevant in their contribution to shape than background noise in the PCA coefficient matrix (generated by randomisation of the matrix and repeating PCA). As shape mode 1 is mostly scale information, I performed Horn's parallel analysis both including and excluding shape mode 1. The analysis was performed using a custom MATLAB 2018a (225) script written by Professor T Turmezei.

5.3.2 COMPARISON OF HUMAN AND ANIMAL VERTEBRAE

The human "true canonical" was deformed to the pig and sheep "true canonicals". First the objects were automatically aligned to the centroid. Manual alignment was then performed by making the superior and inferior endplates parallel on the lateral view, and aligning the pedicles, transverse processes and spinous processes for vertical and horizontal symmetry on the anterior view (Figure 5.4). No scaling was performed prior to deformation, as scale is considered relevant to the comparison between species.

The deformation was performed by the software using TPS, as the objects were too dissimilar to use basic LAD. During the registration of human to pig and human to sheep objects, I noted difficulties in matching certain anatomical structures. The superior articular facets were poorly matched, due to a hooked configuration of the quadruped facet,

compared to the relatively broader human facet. The transverse processes also proved difficult to match, as the quadruped processes were markedly longer and broader than the human.

To address this issue, I added several extra landmarks around these structures, which proved effective in allowing TPS deformation with adequate matching of objects.

Using another custom MATLAB 2018a (225) script written by Professor Turmezei, point displacement magnitude vectors were calculated for human to pig and human to sheep deformations. As the objects are constructed of vertices defining the corners within a triangular mesh, the displacement of a vertex by the TPS deformation can be described as a vector. These vectors therefore effectively describe the direction and magnitude of displacement corresponding vertices between the animal and human objects.
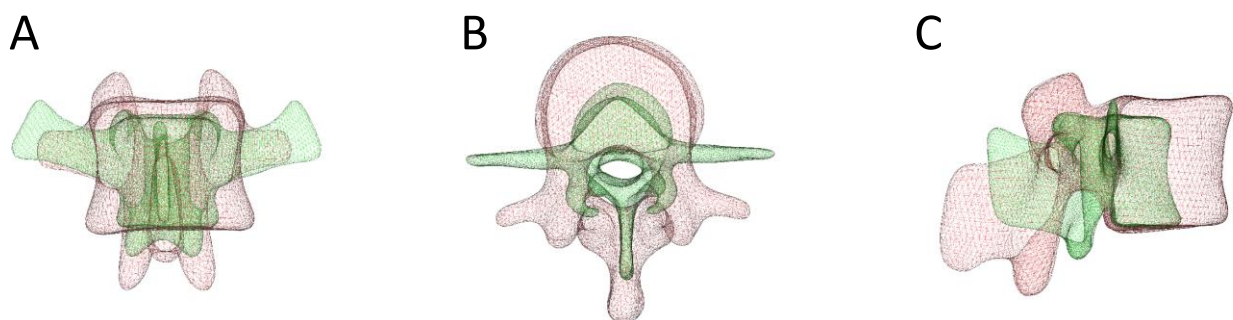
Figure 6.4: Demonstration of object alignment in wxRegSurf. The human vertebral object (red mesh) and sheep vertebral object (green mesh) are overlaid, aligned to the centroid with manual alignment subsequently performed by making the superior and inferior endplates parallel on the lateral view, and aligning the pedicles, transverse processes and spinous processes on the anterior view. A - anterior view. B - superior view. C - lateral view

5.4 RESULTS

5.4.1 HUMAN SHAPE VARIATION
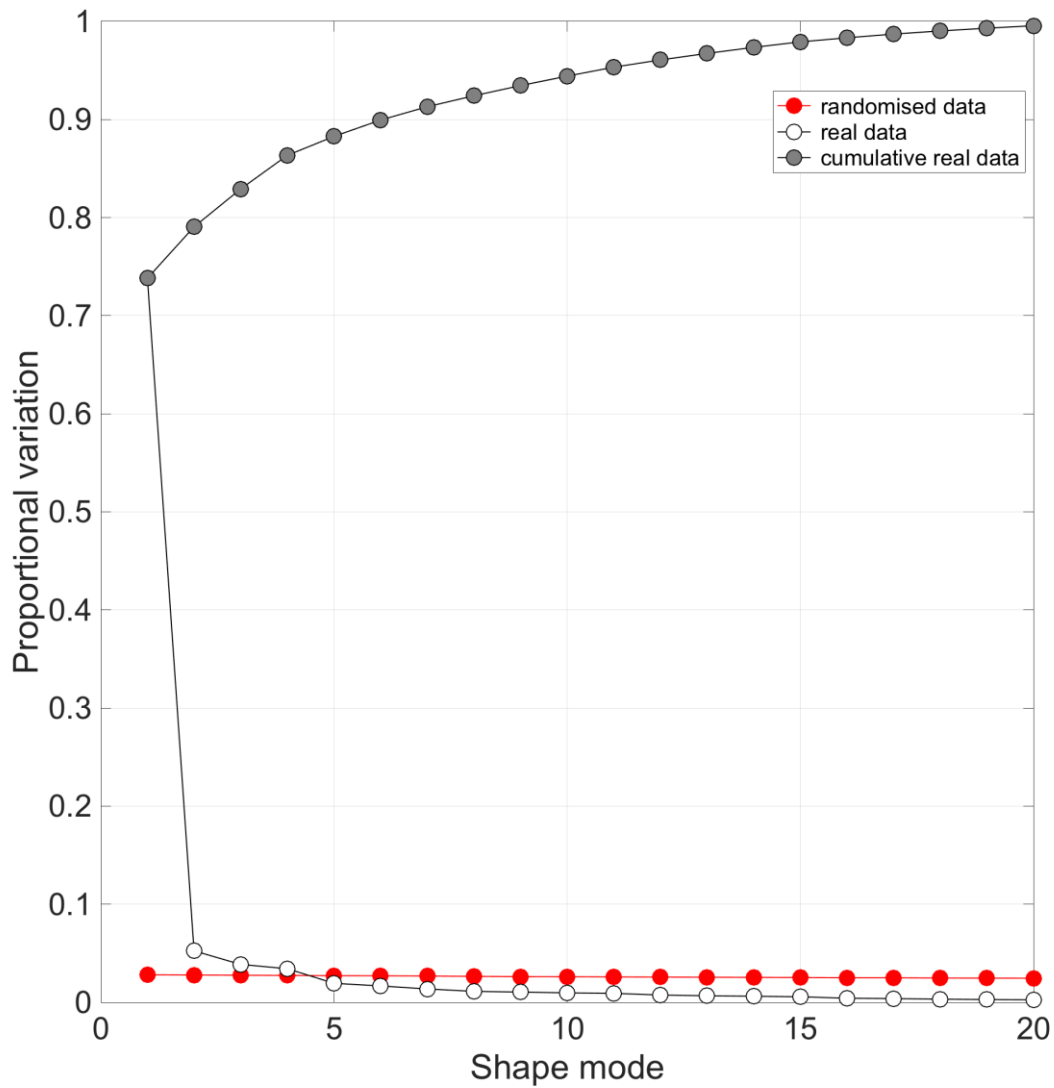
Figure 5.7: Horn's parallel analysis of human object principal component analysis with scale (i.e. shape mode 1) included. The proportional variation is along the y-axis. The shape modes are along the x-axis. The randomised data variation is in red. The cumulative real data are in grey. The real data are in white. The point along the x-axis at which the real data trend line crosses the randomised data line represents the number of shape modes which are considered to be significant.
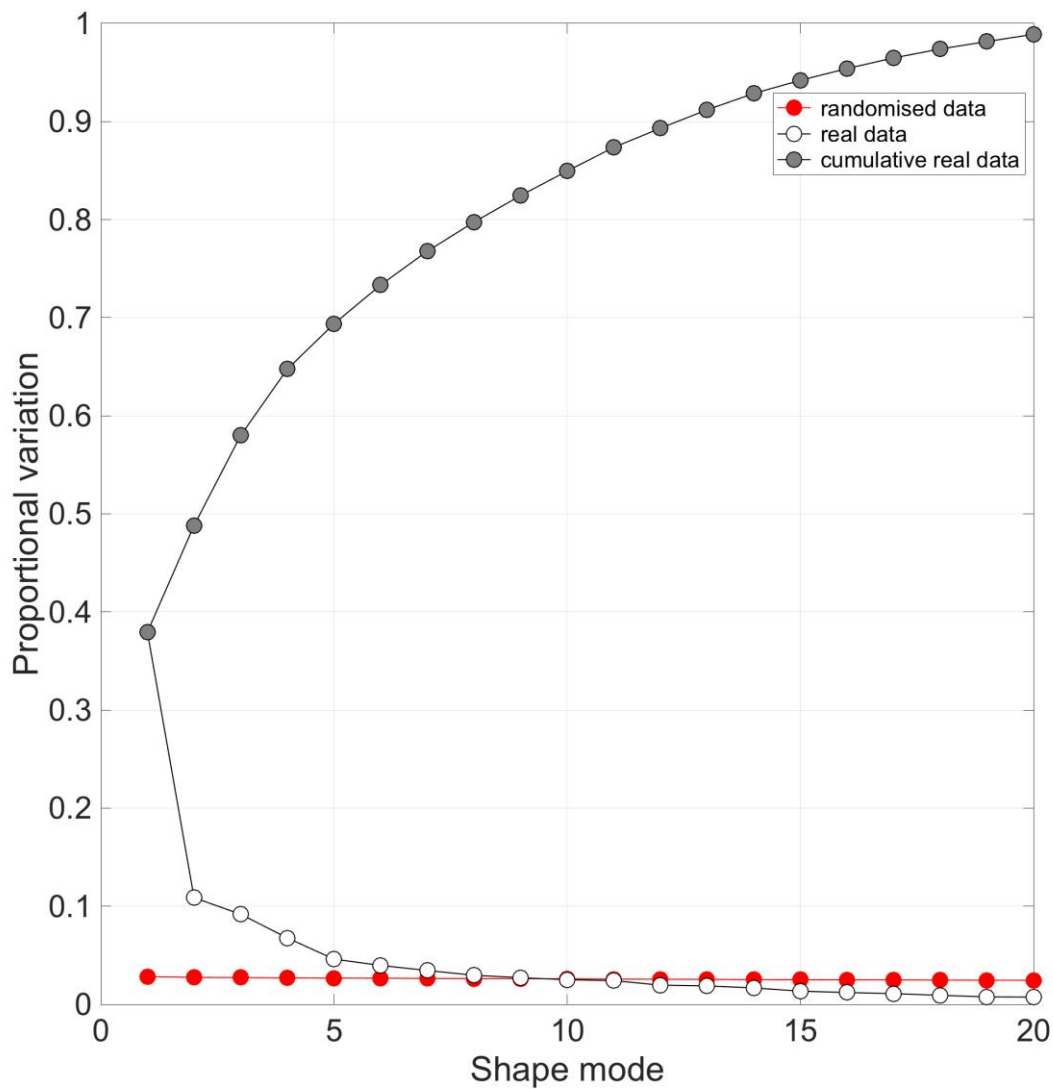
Figure 5.8: Horn's parallel analysis of human object PCA with scale (i.e. shape mode 1) excluded. The proportional variation is along the y-axis. The shape modes are along the x-axis. The randomised data variation are in red. The cumulative real data are in grey. The real data are in white. The point along the x-axis at which the real data trend line crosses the randomised data line represents the number of shape modes which are considered to be significant.

Horn's parallel analysis was performed with shape mode 1, which is predominantly scaling information, both included (Figure 5.5) and excluded (Figure 5.6). When shape mode 1 was included, the analysis suggests that the first 5 shape modes are most significant. These shape modes are the first 5 components of shape variation, calculated on the basis of total variation explained while being unrelated to one another. When shape mode 1 was excluded, the following 9 shape modes, i.e. shape mode 2 – 10, were most significant. I have

therefore opted to include shape modes 1 – 10 in the discussion. Due to the complexity of the shape of the vertebral object, it is unsurprising that a large number of significant shape modes exist.
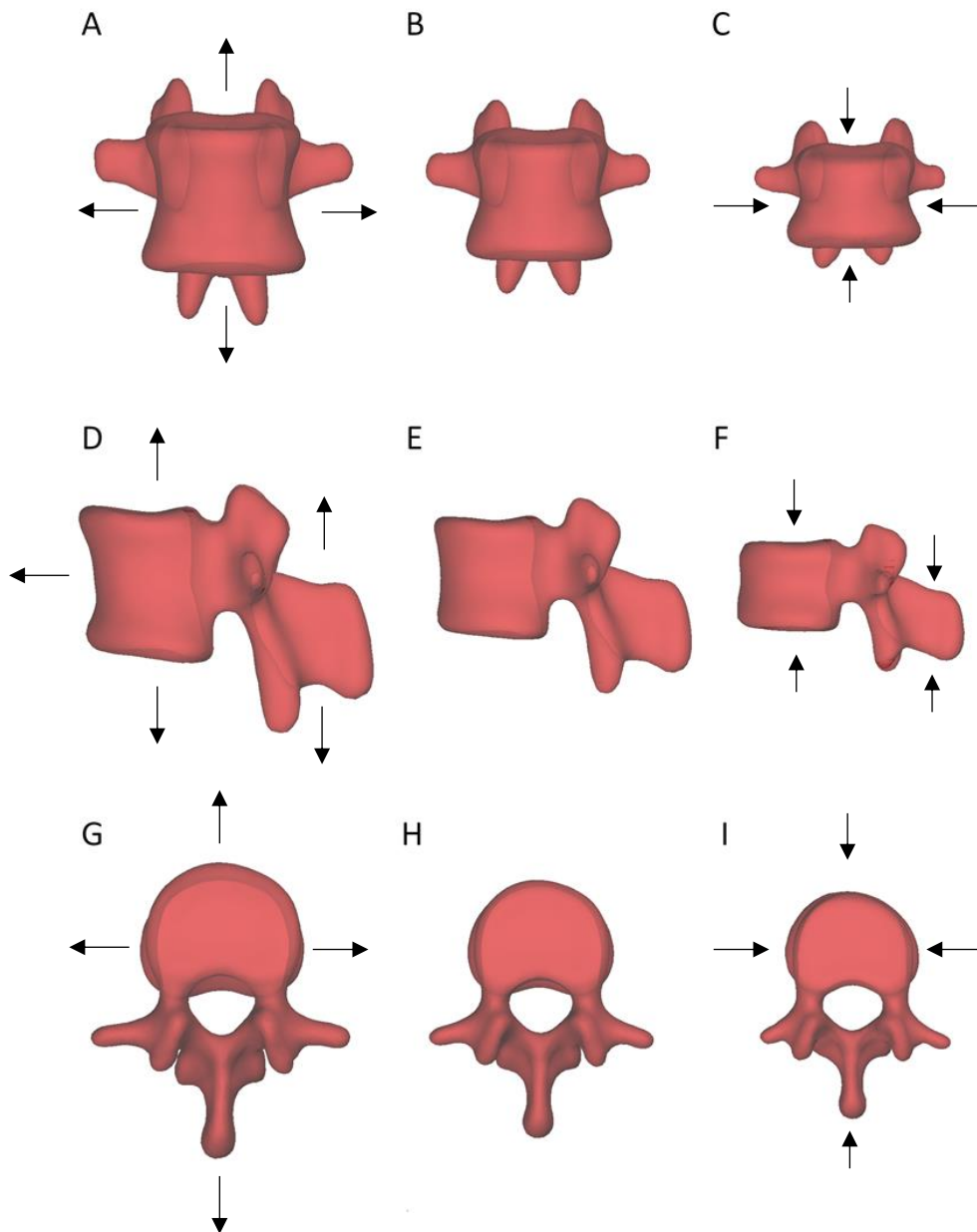
Figure 5.9: Human SSM showing shape mode 1. A,D,G: -1 standard deviation of variation in the shape mode, B,E,H: mean shape, C,F,I: +1 standard deviation of variation in the shape mode. Anterior (A-C), lateral (D-F) and superior views (G-I). Black arrows show the major directions of shape change from the mean shape. In the case of shape mode 1, this is scale.

Shape mode 1 (Figure 5.7) describes mostly scaling, and there is also slight anteroposterior (AP) skewing of the vertebral body as scale increases.
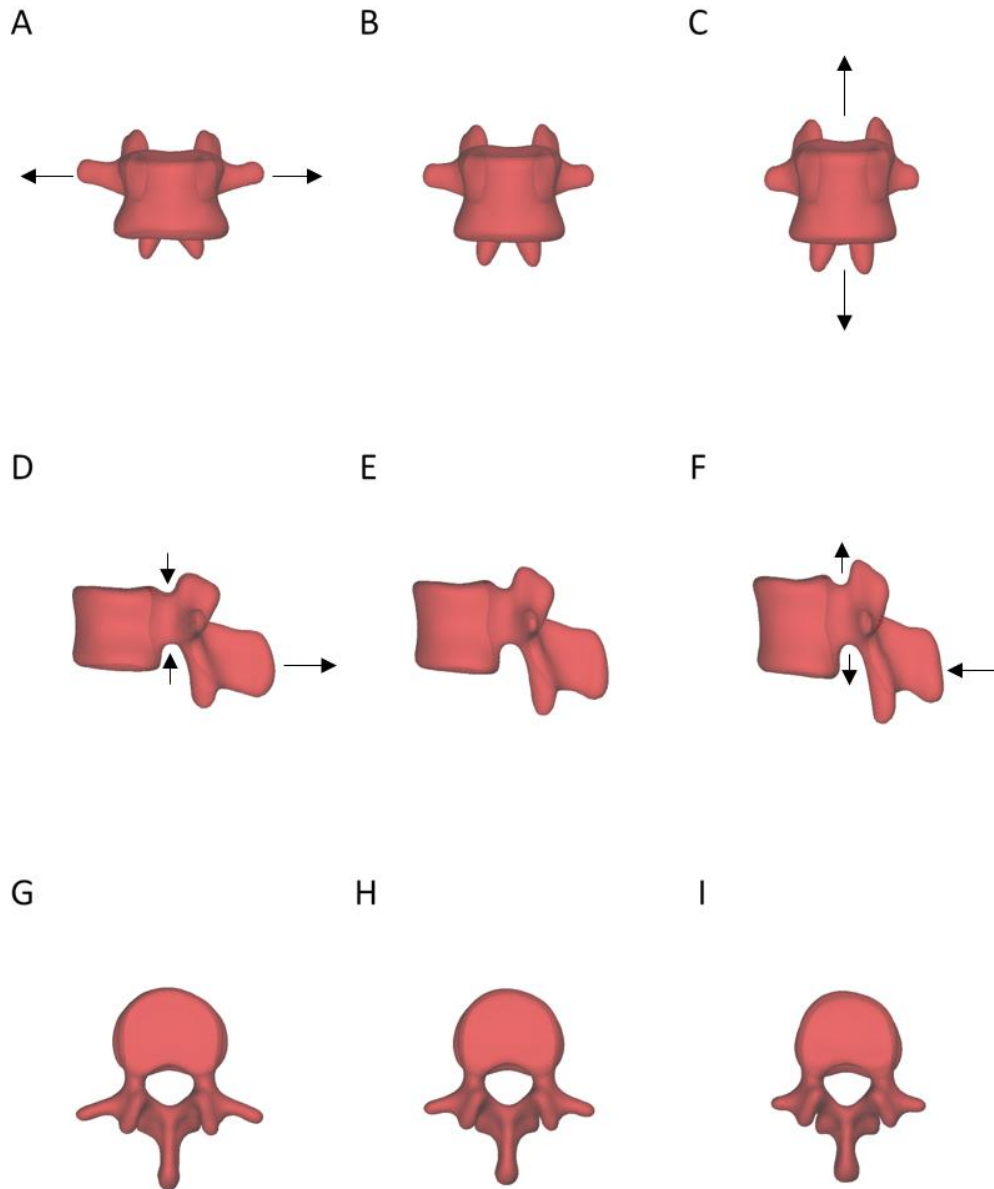
Figure 5.10: Human SSM showing shape mode 2. A,D,G: -1 standard deviation of variation in the shape mode, B,E,H: mean shape, C,F,I: +1 standard deviation of variation in the shape mode. Anterior (A-C), lateral (D-F) and superior views (G-I). Black arrows show the major directions of shape change from the mean shape.

Shape mode 2 (Figure 5.8) describes variation of the transverse process and spinous process length, with widening and shortening of vertebral body width and height as the processes become longer. Shape mode 2 also shows the greatest variation in pedicle height; as vertebral height increases, so too does pedicle height.
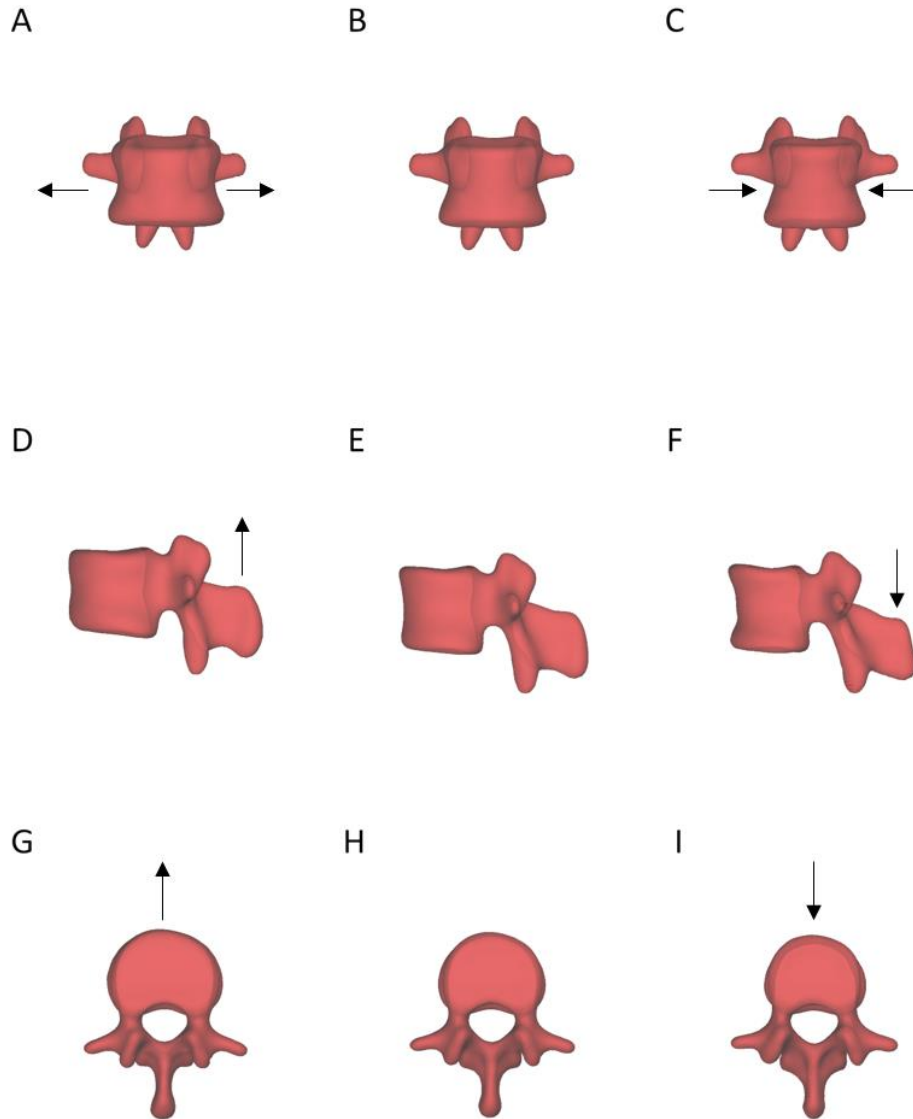
Figure 5.11: Human SSM showing shape mode 3. A,D,G: -1 standard deviation of variation in the shape mode, B,E,H: mean shape, C,F,I: +1 standard deviation of variation in the shape mode. Anterior (A-C), lateral (D-F) and superior views (G-I). Black arrows show the major directions of shape change from the mean shape.

Shape mode 3 (Figure 5.9) shows variation of vertebral body width and AP length. As the vertebral body becomes narrower and shorter, the superior articular facets become broader, and the spinous process becomes more caudally angled. The pedicles also become more medially angled and narrower as they join the vertebral body, and the transverse processes become less posteriorly angled. The inferior articular processes become more posteriorly angled.
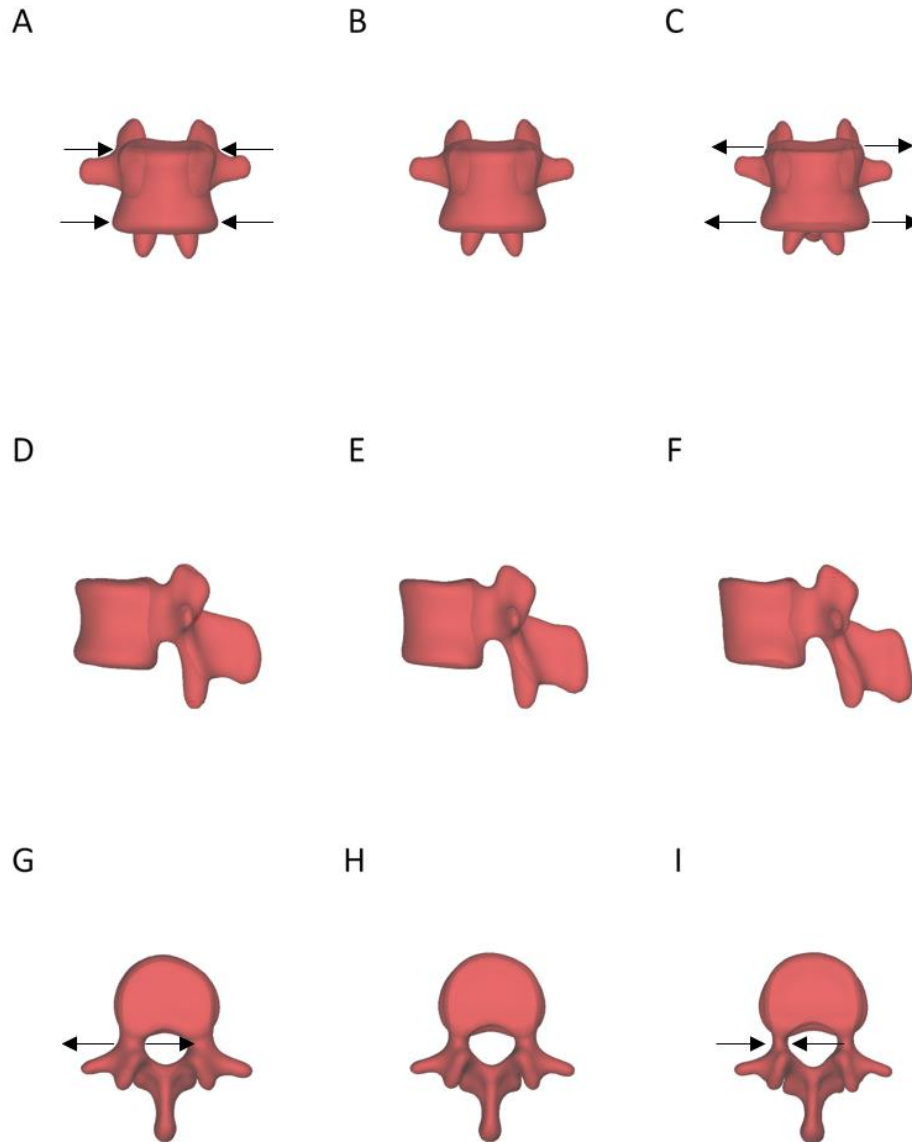
Figure 5.12: Human SSM showing shape mode 4. A,D,G: -1 standard deviation of variation in the shape mode, B,E,H: mean shape, C,F,I: +1 standard deviation of variation in the shape mode. Anterior (A-C), lateral (D-F) and superior views (G-I). Black arrows show the major directions of shape change from the mean shape.

Shape mode 4 (Figure 5.10) describes significant variation in pedicle width with a much lesser degree of variation in pedicle height. There is also a widening of the superior and inferior endplates with a narrowing at the mid-level of the vertebral body. The transverse processes become shorter, and the posterior aspect of the spinous process becomes thicker. The superior and inferior articular facets become thinner.
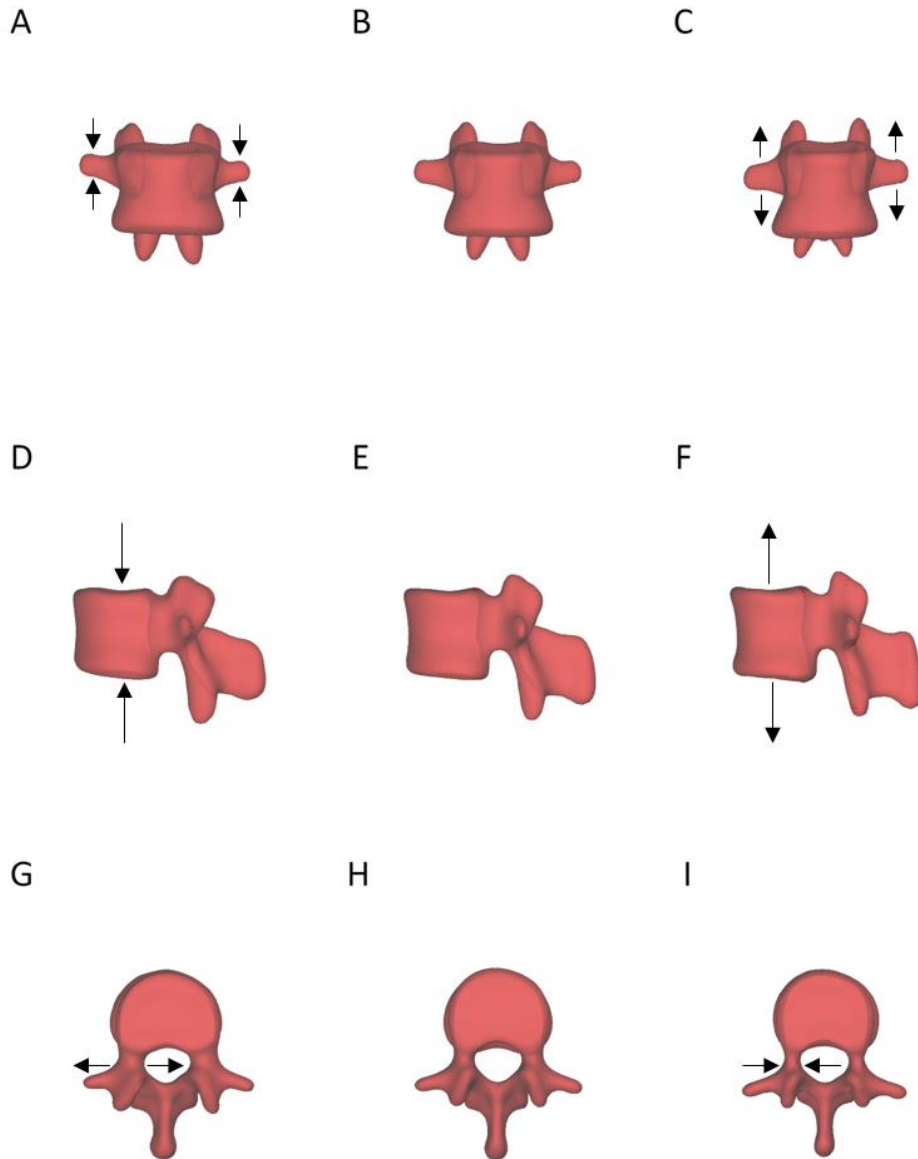
Figure 5.13: Human SSM showing shape mode 5. A,D,G: -1 standard deviation of variation in the shape mode, B,E,H: mean shape, C,F,I: +1 standard deviation of variation in the shape mode. Anterior (A-C), lateral (D-F) and superior views (G-I). Black arrows show the major directions of shape change from the mean shape.

Shape mode 5 (Figure 5.11) also describes marked variation in pedicle width. As the pedicles become wider, the transverse processes become shorter, vertebral body height decreases, inferior articular processes become longer inferiorly, and the craniocaudal (CC) height of the apex of the spinous process becomes shorter. This shape mode describes spinal canal width and length as well.
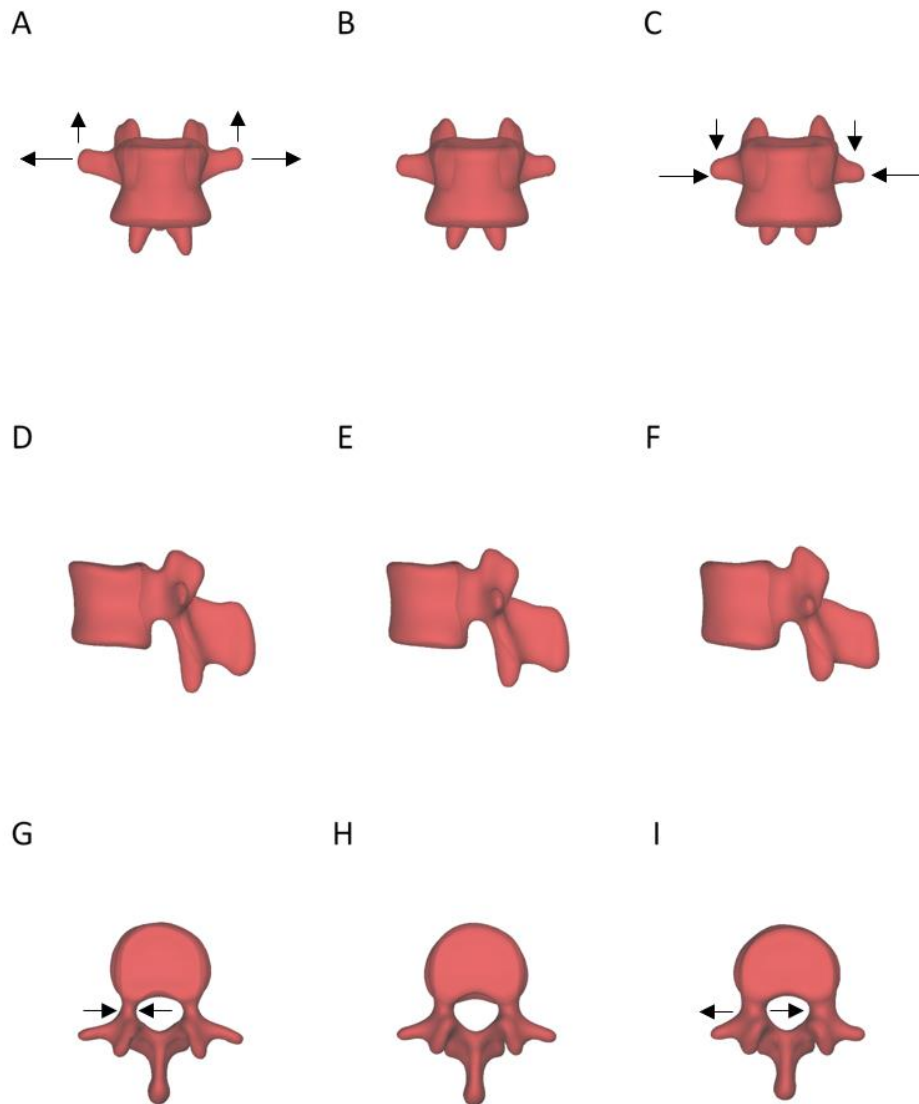
Figure 5.14: Human SSM showing shape mode 6. A,D,G: -1 standard deviation of variation in the shape mode, B,E,H: mean shape, C,F,I: +1 standard deviation of variation in the shape mode. Anterior (A-C), lateral (D-F) and superior views (G-I). Black arrows show the major directions of shape change from the mean shape.

As with shape modes 4 & 5, shape mode 6 (Figure 5.12) shows a substantial variation in pedicle width. There is also variation in transverse process length and craniocaudal plane angulation. As the pedicles become wider, the spinous process becomes shorter in craniocaudal dimension, and the inferior articular processes become shorter.
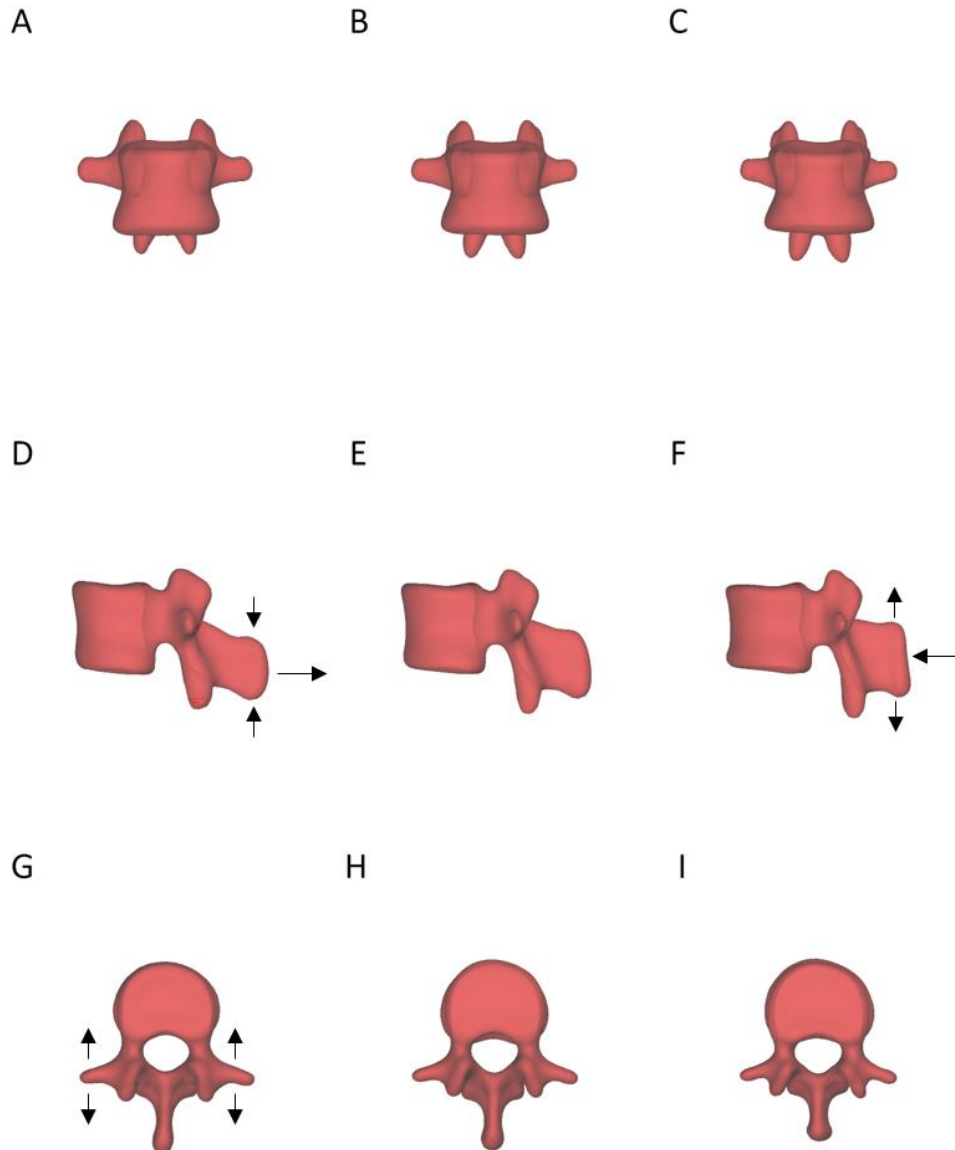
Figure 5.15: Human SSM showing shape mode 7. A,D,G: -1 standard deviation of variation in the shape mode, B,E,H: mean shape, C,F,I: +1 standard deviation of variation in the shape mode. Anterior (A-C), lateral (D-F) and superior views (G-I). Black arrows show the major directions of shape change from the mean shape.

Shape mode 7 (Figure 5.13) describes variation of transverse process length and thickness, and spinous process length and CC height. As the transverse processes and spinous processes become shorter, the inferior articular processes become longer, and the superior articular facets become more steeply angled in the coronal plane.
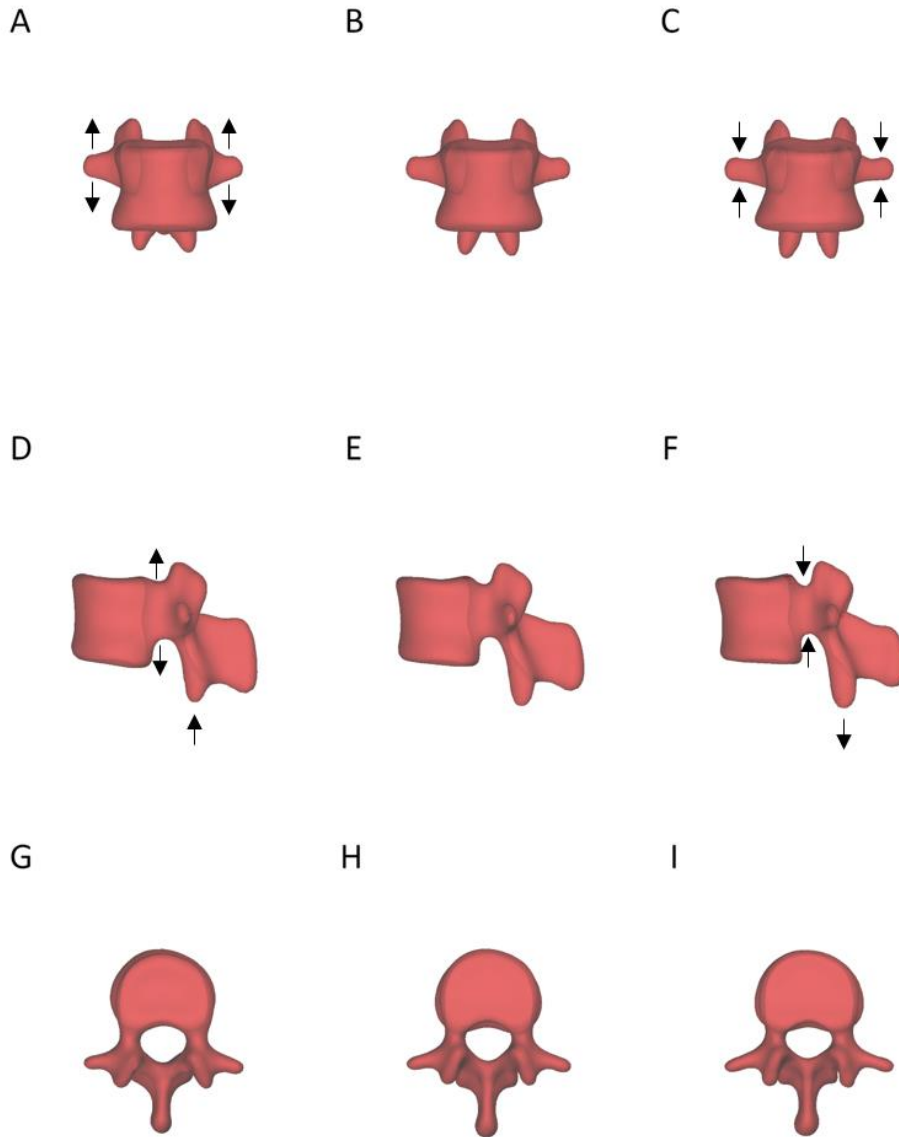
Figure 5.16: Human SSM showing shape mode 8. A,D,G: -1 standard deviation of variation in the shape mode, B,E,H: mean shape, C,F,I: +1 standard deviation of variation in the shape mode. Anterior (A-C), lateral (D-F) and superior views (G-I). Black arrows show the major directions of shape change from the mean shape.

Shape mode 8 (Figure 5.14) shows variation in pedicle height. As pedicle height increases, transverse process length decreases and craniocaudal height increases, and inferior articular process length decreases.
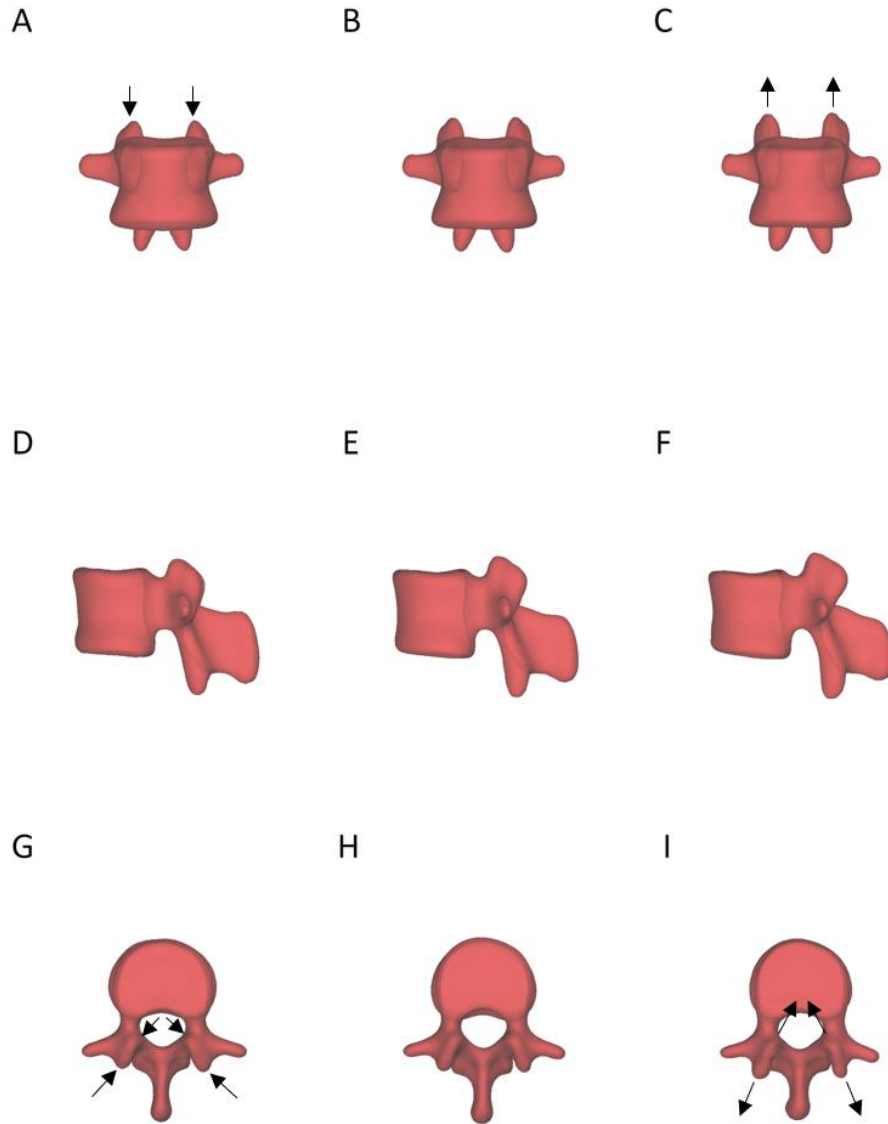
Figure 5.17: Human SSM showing shape mode 9. A,D,G: -1 standard deviation of variation in the shape mode, B,E,H: mean shape, C,F,I: +1 standard deviation of variation in the shape mode. Anterior (A-C), lateral (D-F) and superior views (G-I). Black arrows show the major directions of shape change from the mean shape.

Shape mode 9 (Figure 5.15) predominantly describes variation in superior articular process craniocaudal and anteroposterior length. As the superior articular processes increase in CC and AP length, the apex of the spinous process becomes shorter in CC height, and the transverse processes become shorter. The inferior articular processes also become slightly broader.
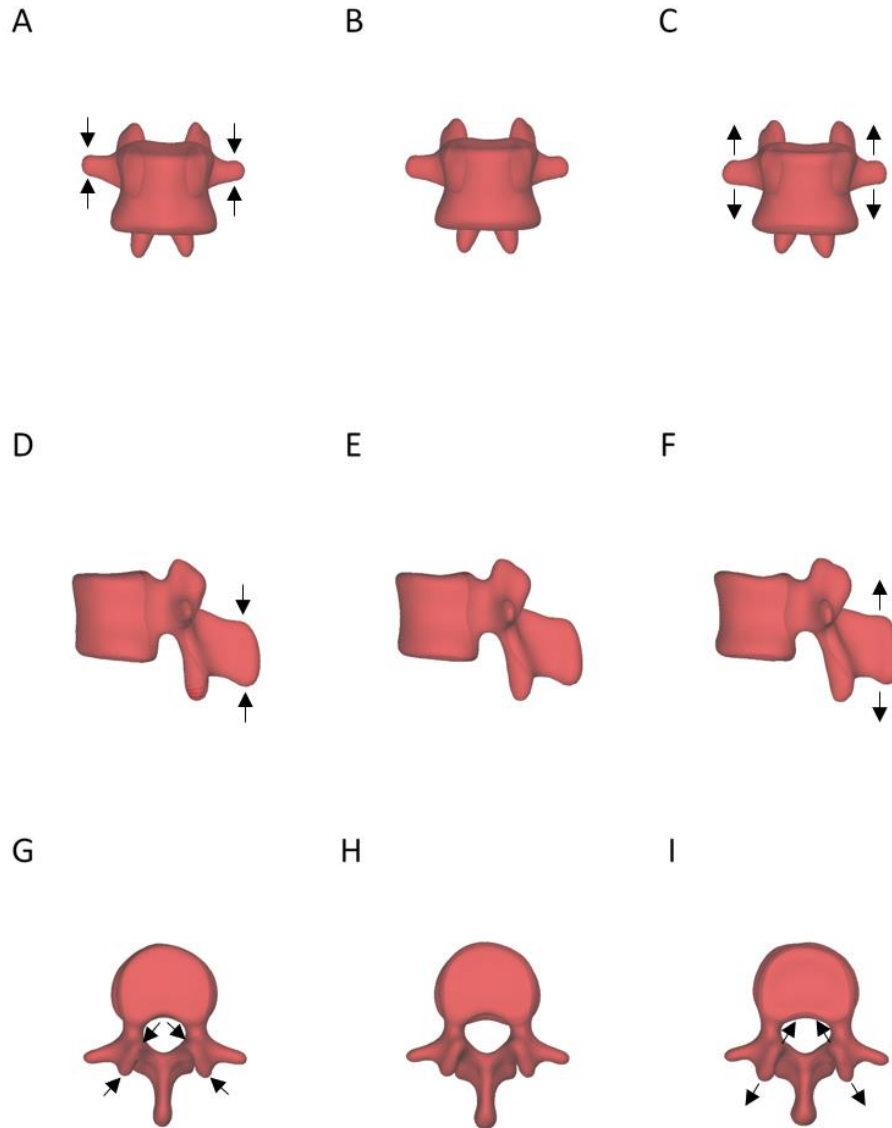
Figure 5.18: Human SSM showing shape mode 10. A,D,G: -1 standard deviation of variation in the shape mode, B,E,H: mean shape, C,F,I: +1 standard deviation of variation in the shape mode. Anterior (A-C), lateral (D-F) and superior views (G-I). Black arrows show the major directions of shape change from the mean shape.

Shape mode 10 (Figure 5.10) shows variation in superior articular process AP length, transverse process CC height, and spinous process apical CC height.

5.4.2 COMPARISON OF HUMAN AND ANIMAL VERTEBRAE
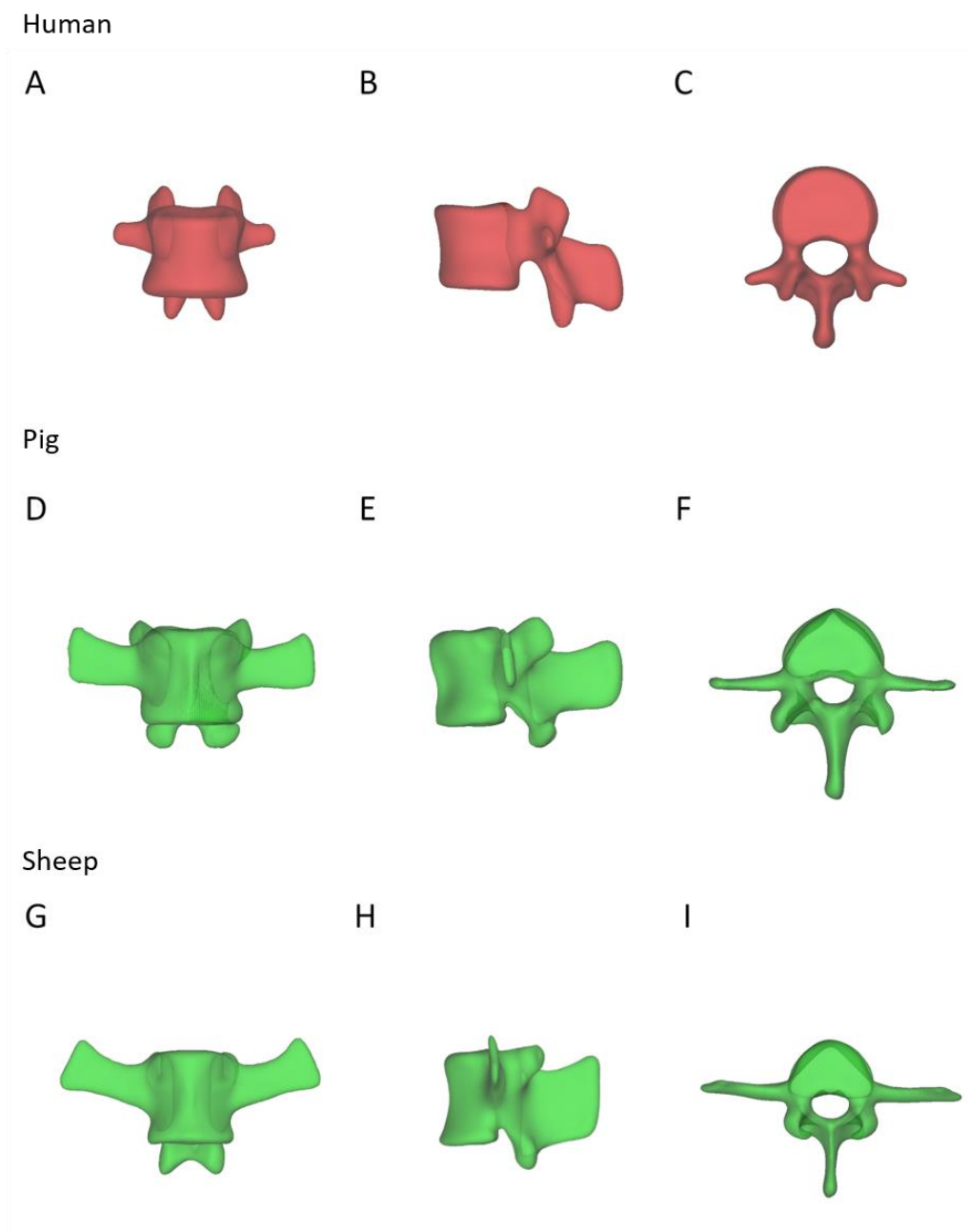
Human

Figure 5.19: Average shape objects of the L1 vertebra of the human (A - C), pig (D - F), and sheep (G - I). Shown are anterior (A,D,G), lateral (B,E,H), and superior (C,F,I) views of the vertebral objects.

Subjective visual assessment of the three-dimensional objects of the average shape of each species shows some clear differences (Figure 5.17), prior to any analysis. The objects are anchored to each other by their centroid, with no scaling performed prior to TPS. The

human L1 vertebral body is shorter than either quadruped in CC vertebral height, and wider and longer in AP dimension.

The human transverse processes are also shorter and markedly shorter than in the quadruped. Additionally, the spinal canals show a more oblique orientation in the animal objects, likely due to the alignment being based upon peripheral structures such as the endplates and transverse processes.
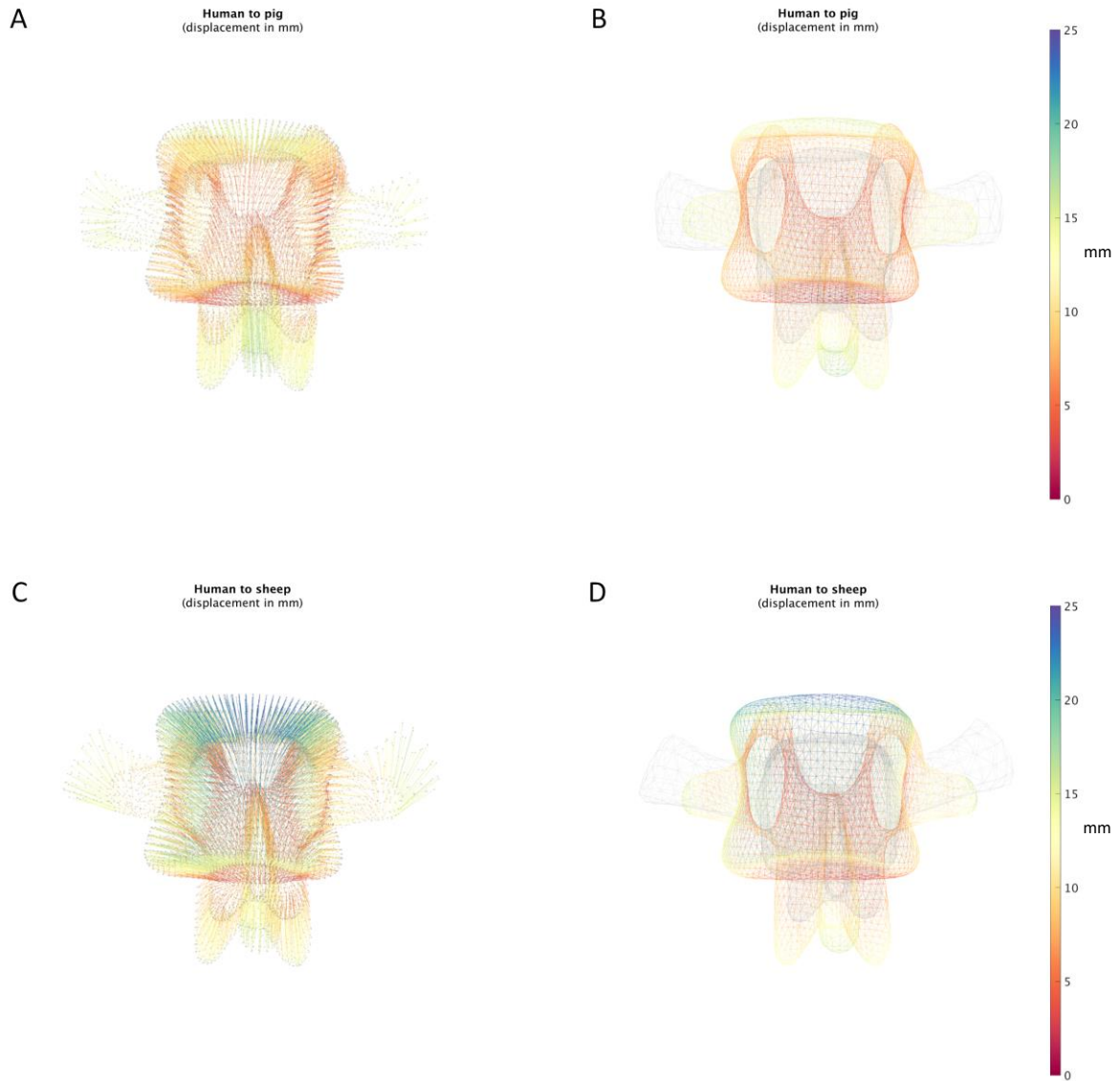
Figure 5.20: Human vertebral object matched to the pig and sheep vertebral objects. Anterior view of vertex displacement vectors for human to pig (A,B) and human to sheep deformations (C,D). A & C show direction of vertex displacement with vectors as lines, with magnitude of millimetres of displacement represented by colour. B & D show animal and human object meshes overlaid, with animals in grey, and human vertices in colour representing the magnitude of vertex displacement.
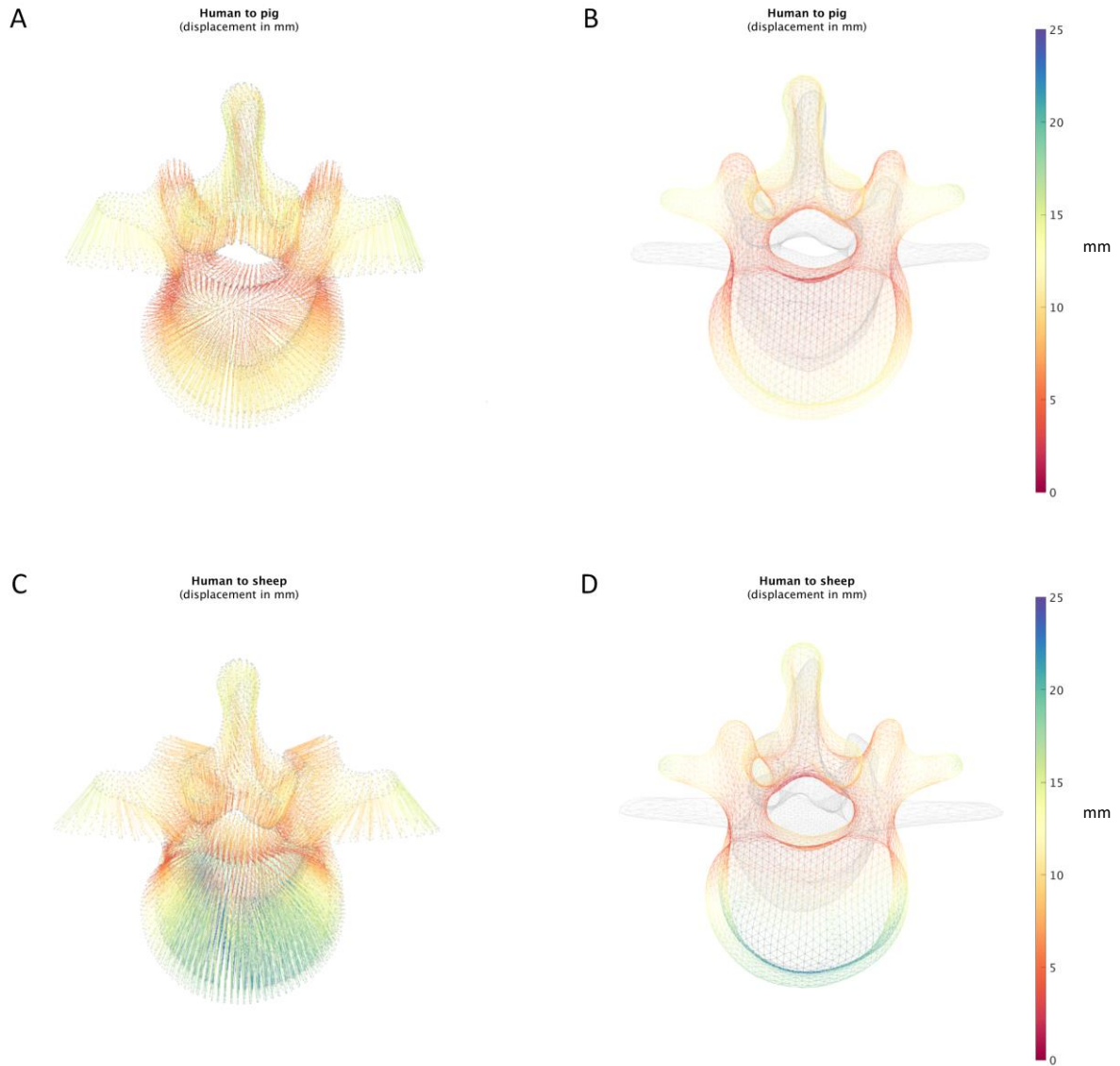
Figure 5.21: Human vertebral object matched to the pig and sheep vertebral objects. Inferior view of vertex displacement vectors for human to pig (A,B) and human to sheep deformations (C,D). A & C show direction of vertex displacement with vectors as lines, with magnitude of millimetres of displacement represented by colour. B & D show animal and human object meshes overlaid, with animals in grey, and human vertices in colour representing the magnitude of vertex displacement.
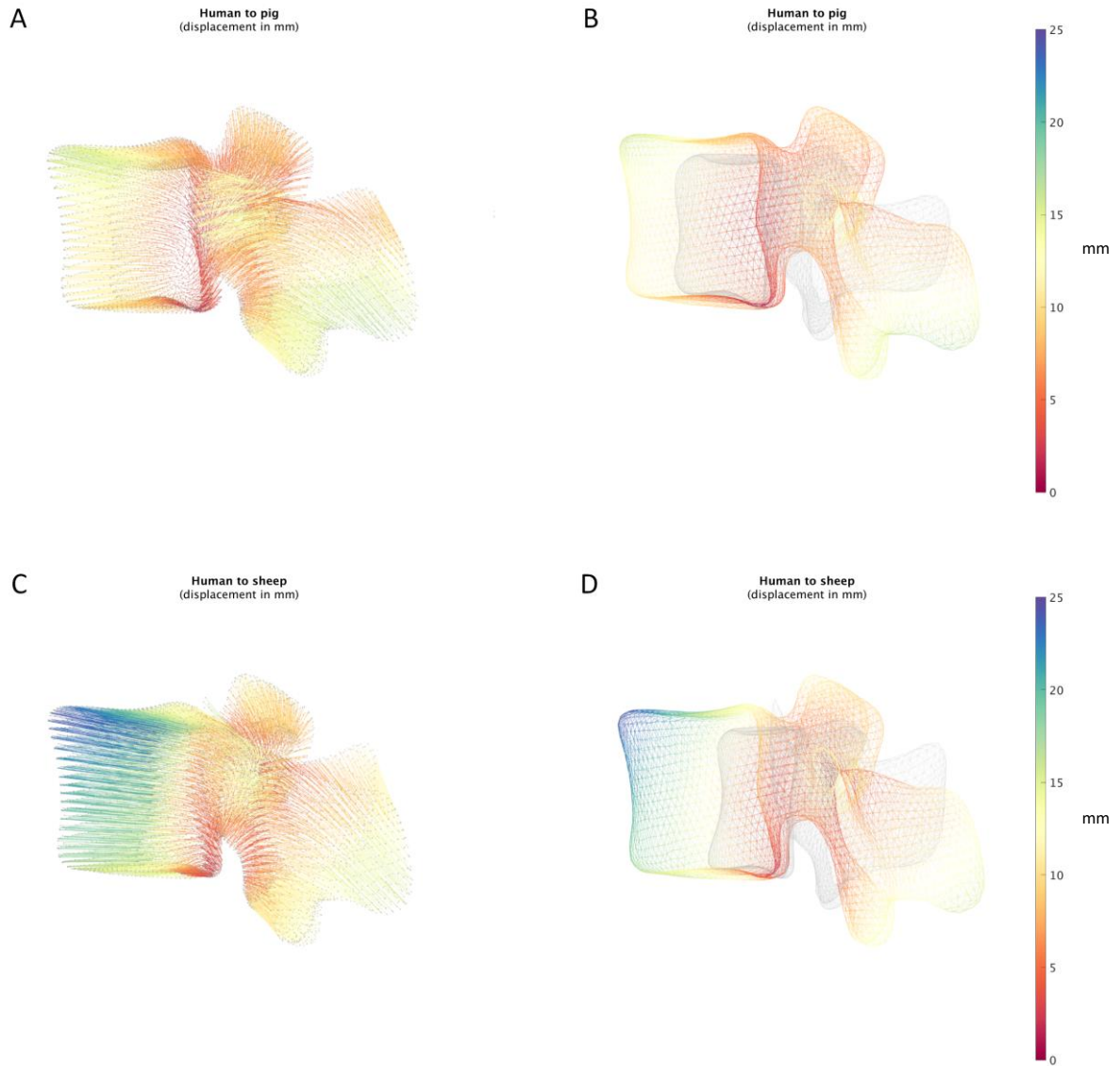
Figure 5.22: Human vertebral object matched to the pig and sheep vertebral objects. Left lateral view of vertex displacement vectors for human to pig (A,B) and human to sheep deformations (C,D). A & C show direction of vertex displacement with vectors as lines, with magnitude of millimetres of displacement represented by colour. B & D show animal and human object meshes overlaid, with animals in grey, and human vertices in colour representing the magnitude of vertex displacement.
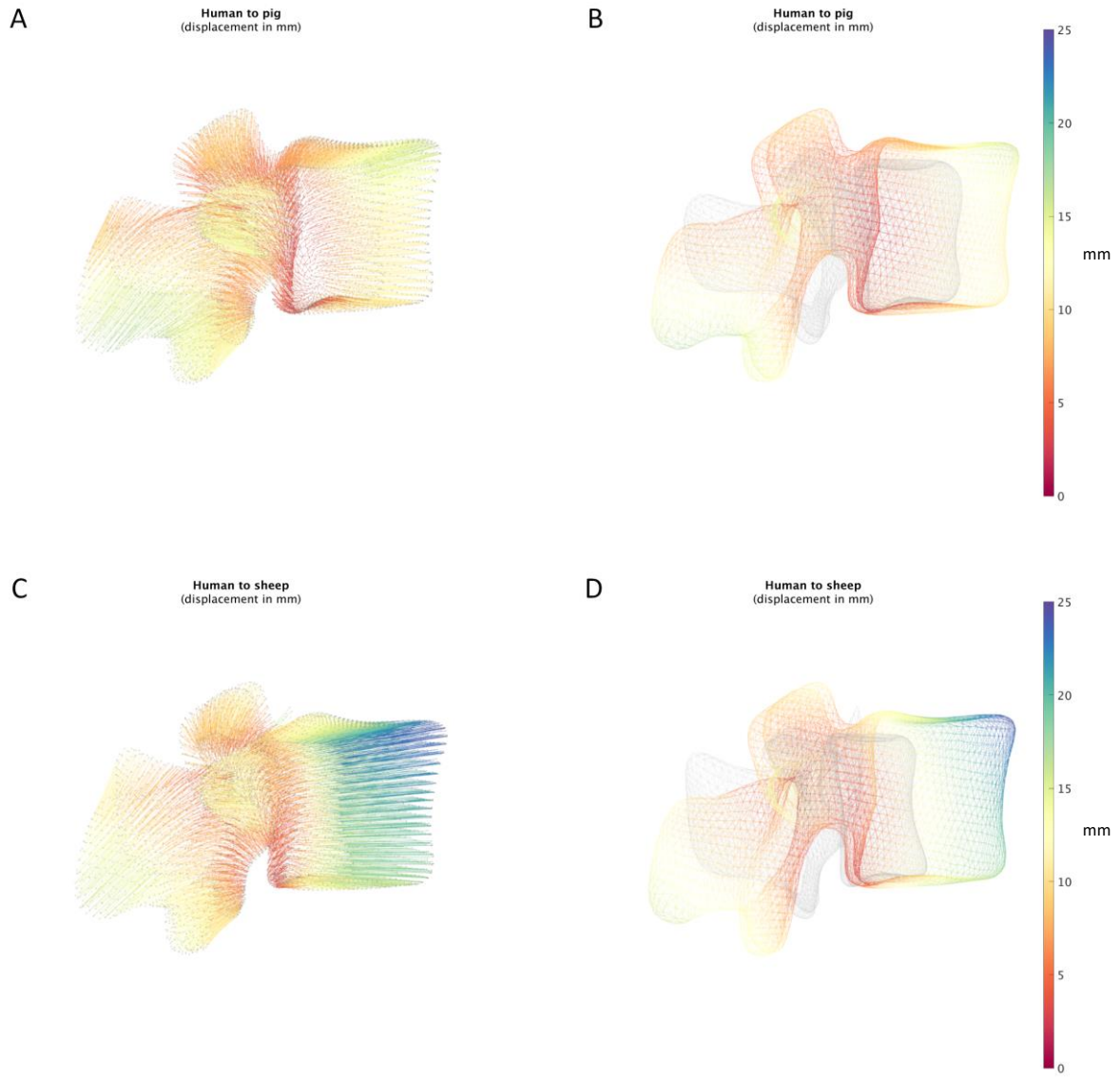
Figure 5.23: Human vertebral object matched to the pig and sheep vertebral objects. Right lateral view of vertex displacement vectors for human to pig (A,B) and human to sheep deformations (C,D). A & C show direction of vertex displacement with vectors as lines, with magnitude of millimetres of displacement represented by colour. B & D show animal and human object meshes overlaid, with animals in grey, and human vertices in colour representing the magnitude of vertex displacement.
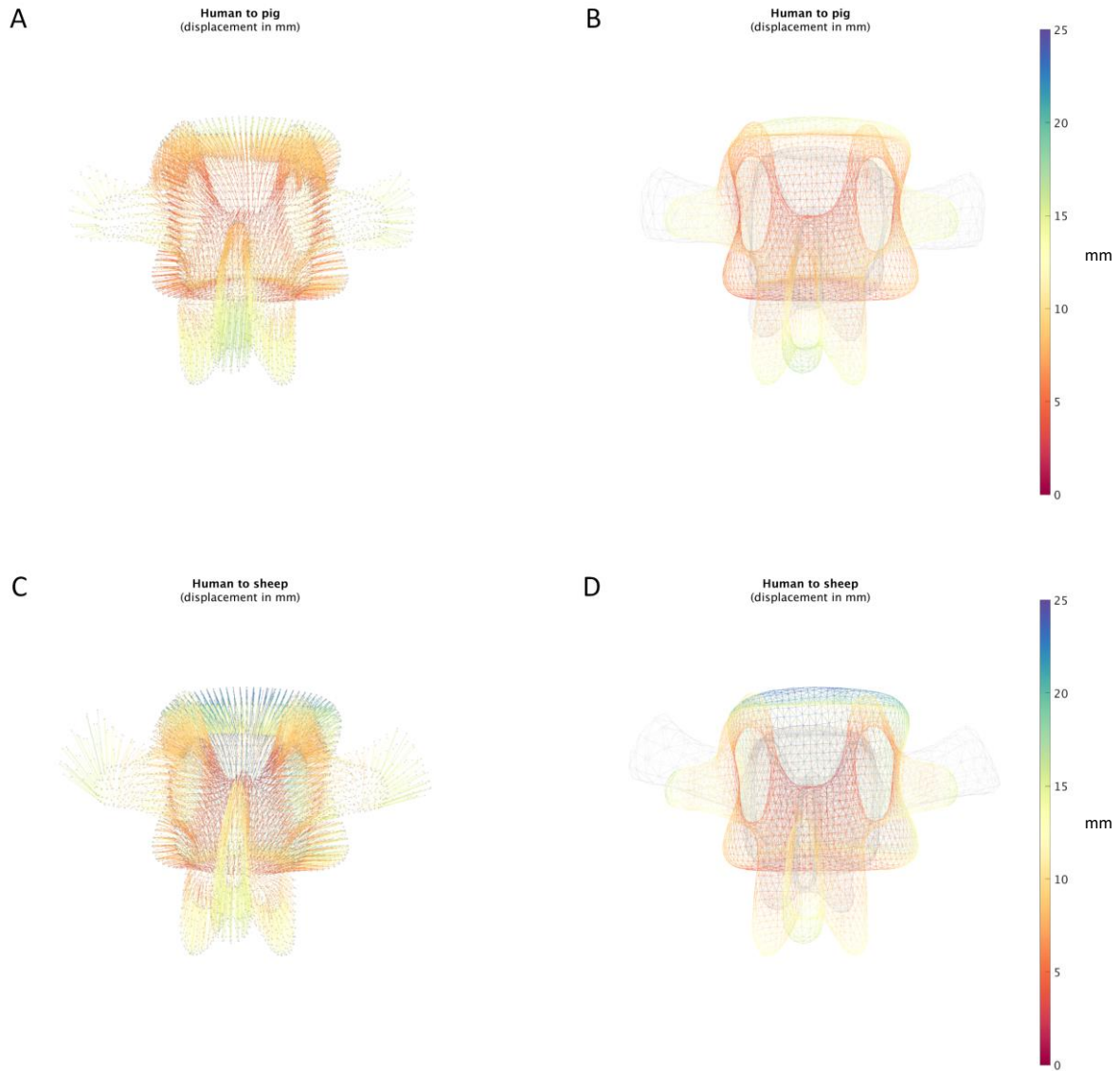
Figure 5.24: Human vertebral object matched to the pig and sheep vertebral objects. Posterior view of vertex displacement vectors for human to pig (A,B) and human to sheep deformations (C,D). A & C show direction of vertex displacement with vectors as lines, with magnitude of millimetres of displacement represented by colour. B & D show animal and human object meshes overlaid, with animals in grey, and human vertices in colour representing the magnitude of vertex displacement.
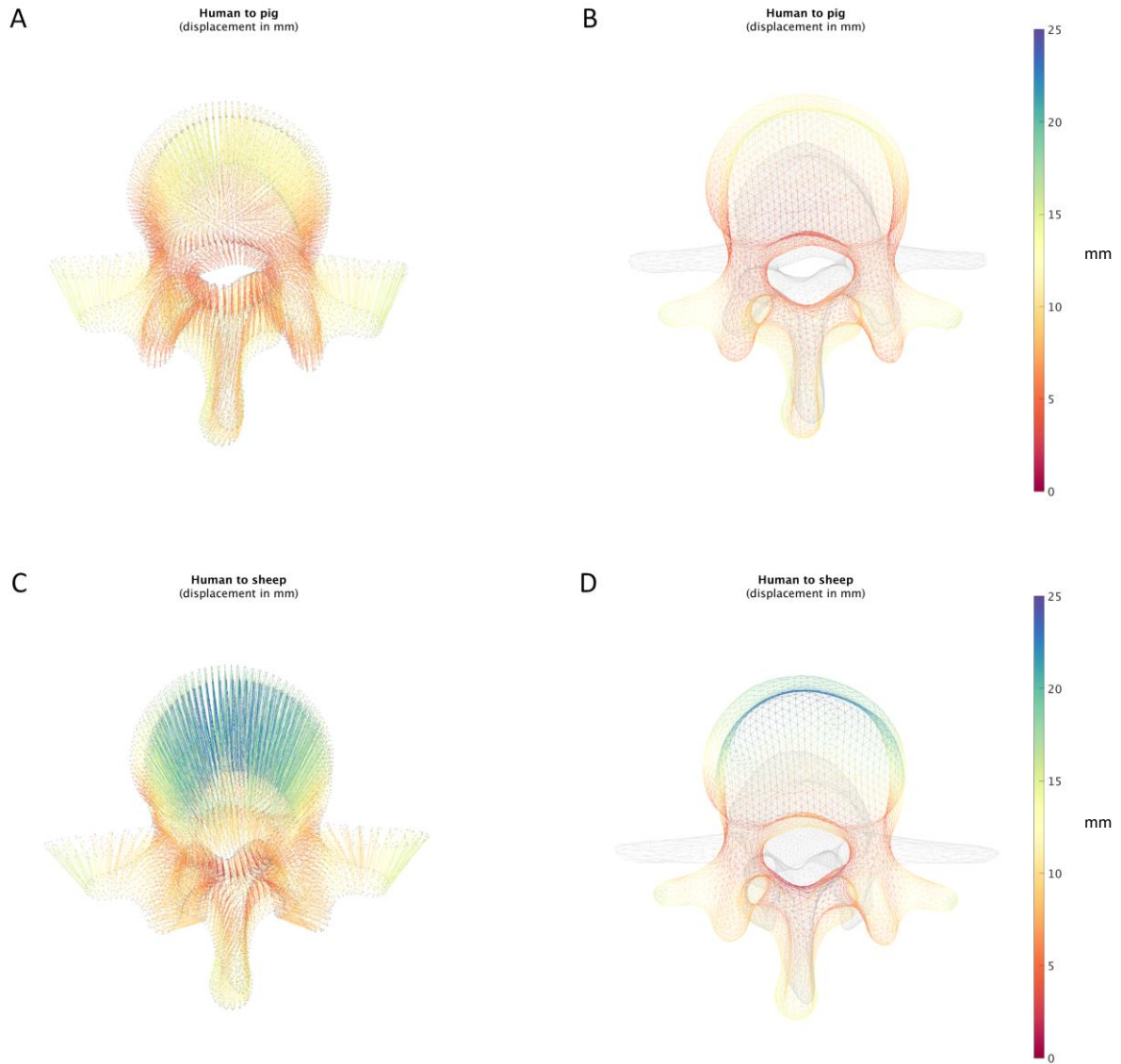
Figure 5.25: Human vertebral object matched to the pig and sheep vertebral objects. Superior view of vertex displacement vectors for human to pig (A,B) and human to sheep deformations (C,D). A & C show direction of vertex displacement with vectors as lines, with magnitude of millimetres of displacement represented by colour. B & D show animal and human object meshes overlaid, with animals in grey, and human vertices in colour representing the magnitude of vertex displacement.

The vertex displacement vector diagrams (Figures 5.18 – 5.23) are visual representations of the magnitude and direction of the displacement of the constituent vertices of the canonical human object when deformed to match the canonical animal object.

The vertices at the anterior surface of the human vertebral body show significant displacement magnitude posteriorly towards the centroid in the human to sheep comparison. The magnitudes are more pronounced superiorly. The vertices at the lateral aspects of the vertebral body show progressively smaller magnitudes of displacement towards the centroid, as the lateral surface of the vertebral body approaches the junction with the pedicle.

At the junction with the pedicle and the posterior vertebral body surface at the spinal canal, the displacement magnitudes are relatively small, best seen on Figures 5.19 & 5.23. After alignment, the posterior vertebral body wall of the sheep lies posteriorly to the human, and the human vertices are therefore displaced posteriorly towards the centroid.

The mesh overlays show that the pedicles are well aligned after centroid alignment and subsequent manual alignment, though subjective visual observation suggests that sheep pedicles are much shorter in anteroposterior length than humans. Sheep pedicles are slightly wider and taller than humans, with small vector displacement magnitudes. The direction of displacement is outwards from the human mesh position to the sheep mesh position.

Human transverse processes are shorter and less broad than sheep. As a result of longer pedicles in humans, the transverse processes also lie posteriorly and are relatively posteriorly angled. There is moderate magnitude vector displacement at the tips of the transverse processes, which lie furthest from their corresponding points in the sheep. Human transverse processes also become narrower towards their apices, whereas the sheep transverse process tends to become broader. The vector displacements at the apices

of the transverse processes travel anteriorly, as well as superiorly and inferiorly at the superior and inferior aspects of the process respectively.

Due to their position, the laminae are even more difficult to assess visually than the pedicles. The sheep laminae lie anterior to the human laminae, and the vertices are predominantly displaced anteriorly. The visible laminar vertex displacements are of small magnitude.

The vertex displacements at the superior articular process are of relatively small magnitude. The human superior articular process is taller and broader than the sheep, and lies in a more lateral position compared to the sheep. The direction of displacement vectors tends to be medial.

The inferior articular processes in the human are longer than the sheep, and lie relatively posteriorly. For much of the superior and mid portions of the inferior articular process, the vector displacements are anterior and of small magnitude. However, at the inferior aspects and the articular facet, the displacements are of greater magnitude, and with an anterosuperior direction.

The human spinous process extends further posteriorly than the sheep, and is taller and wider, and lies predominantly inferiorly in comparison. The vertex displacements are of greatest magnitude inferiorly, in an anterosuperior direction.

5.4.2.2   HUMAN TO PIG DISPLACEMENT

The human to pig vertex displacements follow a similar pattern to the human to sheep displacements, but in general are of smaller magnitude.

The greatest magnitude of displacement is seen at the anterosuperior vertebral body with a posterior and slightly inferior direction, but these magnitudes are smaller than in the sheep. As with the sheep, these displacement magnitudes become gradually smaller along the lateral surface of the vertebral body towards the junction with the pedicle, and are smallest at the inferior aspect of the posterior vertebral body and the inferior laminae.

The pedicles are again well aligned, and as with the sheep, the pig appears to have shorter pedicles than the human on visual inspection of the overlaid object meshes. Again, like the sheep, the pig pedicles are taller and wider than the human. This difference is most pronounced in height with the greatest magnitudes of pedicle vertex displacement being at the inferior surface of the pedicle with displacement in an inferior direction, as part of the pig pedicle lies inferior to the human.

The pig superior and inferior articular processes show similar magnitude and direction of vertex displacement to the sheep. This is again most pronounced at the posterior and inferior aspect of the inferior articular processes, with anterior vertex displacement.

A similar magnitude of displacement is seen at the inferior surface of the spinous process as at the anterosuperior vertebral body. As in the sheep, the pig spinous process lies superiorly to the human, and extends less far posteriorly. It is also shorter in craniocaudal dimension. The majority of vertex displacements are in an anterior direction.

5.5 DISCUSSION

5.5.1 HUMAN SHAPE VARIATION

The human SSM provides information on shape variation in the sample around the mean shape. The most significant shape mode was shape mode 1, as reflected by the results of Horn's parallel analysis when run with and without shape mode 1. I opted to include up to shape mode 10 as per the results of the analysis without shape mode 1, for the sake of a more complete discussion. However, since scale is the predominant factor of variation, it may be that only shape modes 1 – 5 are of experimental or practical importance.

Shape mode 1 describes mostly scale information, accounting for approximately 73% of variation. This is likely largely as a result of the fact that the sample population was not controlled for height, weight or gender. Marked vertebral body height, width and length, pedicle height, transverse process length, and spinous process length variation is found in shape mode 1, with the most significant variation of vertebral body height out of all assessed shape modes. There is not much in the way of pedicle width variation in shape mode 1, which is perhaps surprising, and it is unclear as to why this is the case. One possibility is that the predominant forces being applied to the pedicle in humans are in a craniocaudal direction, and therefore pedicle height is more prone to variation in growth depending upon the weight of the subject.

Shape mode 2 suggests that transverse and spinous process length and pedicle height are the next most variable shape differences. With shape mode 1 excluded, shape mode 2 accounts for approximately 37% of variation. Pedicle width is not significantly described by a shape mode until modes 4,5&6, which account for approximately 9%, 7% and 5% of variation respectively. This suggests that in the sample population, at least, pedicle height is a more variable feature than pedicle width. Indeed, pedicle angulation as described by shape mode 3, approximately 11% of variation, is also more variable than pedicle width.

As transpedicular access devices and pedicle screws tend to be roughly cylindrical, this difference in variability between height and width is unlikely to be of any great importance when designing these tools.

Additionally, while pedicles form the superior and inferior boundaries of the intervertebral foramina, and therefore size variation could be expected to play a role in the development of foraminal stenosis and radiculopathy, the evidence suggests that vertebral body height is actually the key factor and that pedicle height does not contribute (226).

Vertebral body width and AP length, superior articular facets broadness, spinous process sagittal plane angulation and pedicle axial plane angulation are described by shape mode 3, and the next most significant variation (approximately 11% of variation). Pedicle angulation is of relevance to percutaneous transpedicular techniques, as devices must be aligned along the AP axis of the pedicle and avoid breaching the medial pedicle wall (vertebroplasty technique is reviewed in more depth in Chapter 1), and it is interesting to note that it is among the more variable aspects of human vertebrae.

As well as marked variation of pedicle width, shape mode 4 also describes widening of the superior and inferior endplates with a narrowing at the mid-level of the vertebral body. Although I attempted to exclude cases with observed degenerative changes, it is possible that some of this endplate width variation is due to early degeneration.

Shape mode 5 shows variation in pedicle width as well as transverse process length, vertebral body height decreases. It also shows the most evident inferior articular process length variation other than shape mode 1.

Shape modes 6 - 10 describe variation in spinous process CC height and thickness, transverse process angulation, length and thickness, superior articular facet broadness and coronal plane angulation, and inferior articular facet broadness. These aspects of shape are therefore less variable than vertebral body and pedicle dimensions, and when scale is considered, they are unlikely to meaningfully affect the shape variation of human vertebrae.

To know whether these findings can be extrapolated to a general population, a bootstrap analysis of the data could be performed in the next stage of analysis, and the sample population size increased accordingly.

5.5.2 COMPARISON OF HUMAN AND ANIMAL VERTEBRAE

Overall, the vertices closer to the centroid of the objects tend to have lower displacement compared to those further out. This is borne out by subjective visual assessment which also suggests that the shape of these structures is similar between human and animal vertebrae.

The regions of greatest magnitudes of displacement between human and either quadruped, the anterior vertebral body surface and posteroinferior spinous process, and these appear visually different in shape between human and animal vertebrae. This could represent differences in ligamentous attachments and forces between bipedal and quadrupedal gait.

This is an important point to note when considering an animal model. Clearly there are marked differences in shape that basic morphometrics (such as the findings in Chapter 3) underestimate. However, I am selecting an animal model for early phase testing of equipment, and it is understood that the morphologies will be different. My aim is to find the closest approximation, and in this regard, the model does not need to be identical to the human.

The directions of vertebral body vector displacements are similar for the human to pig and human to sheep deformations. The magnitude of these displacements is less for the human to pig than the human to sheep deformation, which corroborates both the established literature discussed in Chapter 2, and the findings in Chapter 3, where it is shown that vertebral body length is significantly greater in the human L1 than either quadruped, and that this difference is marginally greater between human and sheep than human and pig. I found a mean human vertebral body length of 34.59 mm (SD = 3.06 mm). The mean pig vertebral body length was 20.10 mm (SD = 0.78 mm), and the mean sheep vertebral body length was 18.89 mm (SD = 0.39 mm).

However, the morphometry in Chapter 3 suggested that there was no statistically significant difference between the pig and sheep vertebral body length, and that the degree of difference was smaller than the findings here. The morphometric mean difference between human and sheep vertebral body length at the superior endplate was 8.68 mm, whereas the vertex displacement magnitudes at the anterosuperior vertebral body are >20 mm based on subjective assessment of visual colour scale.

This represents the fundamental differences in the nature of these two analyses. Whereas morphometry considered vertebral body length as an isolated measurement, SSA takes into account the entire object, and the vertex displacement vectors are calculated from vertex to vertex. Therefore, although both methods convey similar information in some regards, they are not directly comparable beyond showing similar trends.

Subjective visual observation of the meshes in Figures 5.19 & 5.23 suggests that human pedicles are longer than either quadruped. However, due to the position of the pedicles, it is difficult to assess displacement vector magnitudes, and therefore I cannot draw a conclusion as to whether either quadruped is closer to the human than the other.

Both pig and sheep pedicles were slightly wider and taller than in the human, with similar degrees of displacement vector magnitude and patterns of displacement vector directions. The colour scale representation suggests that there may be a slightly greater magnitude of vector displacement around the human to sheep deformation than the human to pig deformation in all directions. This would again correlate with the background literature and the findings in Chapter 3. The morphometric analysis showed that at the L1 level, pig pedicle width and height were closer to humans than sheep. For example, I found a mean human right pedicle width of 7.60 mm (SD = 1.70 mm) and right pedicle height of 15.42 mm (SD = 1.42 mm). The mean pig right pedicle width was 9.91 mm (SD = 0.76 mm) and mean right pedicle height was 17.23 mm (SD = 0.70 mm). The mean sheep right pedicle width was 9.98 mm (SD = 0.51 mm) and mean height was 20.91 mm (SD = 0.61 mm). These differences were statistically significant.

The differences between human and quadruped vertebrae as depicted by vertex displacement provides an alternative description to basic morphometric measurements, some of which corroborate my earlier findings. There are also new findings provided by SSA which do not have corresponding morphometry in Chapter 3.

For example, the trend of decreasing vertex displacement magnitude at the lateral aspects of the vertebral body, from anterior to posterior, is not described by a single vertebral body width measurement, nor is the fact that the greatest vertex displacement magnitudes are found at the anterosuperior vertebral body accounted for by my vertebral length morphometric measurements, though I do have to accept that these trends may in part be affected by how I have aligned the average shape objects prior to deformation. The morphometric measurements also do not take into account the differing angulation of transverse processes, whereas SSA shows that human transverse processes lie relatively posteriorly and are slightly posteriorly angled with respect to the centroid.

Of the novel information provided, the fact that the greatest vertex displacement magnitudes are found at the anterosuperior vertebral body is relevant in the selection of an animal model for testing vertebroplasty and kyphoplasty in particular. The access cannulae are positioned with a slight inferior angulation, and the optimal position for the needle tip is considered to be close to the anteroinferior vertebral body wall. Although I have found that pigs have lesser magnitudes of displacement than sheep at the anterosuperior vertebral body, the displacement is similar between species inferiorly as well as at the lateral aspects of the vertebral body. This suggests that the measurement of vertebral body length and width may be of less importance when considering which species to select as a model. However, they would still remain relevant when comparing against pedicular form.

Some of these additional findings are of limited relevance for the purposes of this thesis, such as transverse process position and angulation, spinous process height, angulation and apical thickness, and superior and inferior articular process broadness and length, as these structures are not directly involved in transpedicular techniques.

Combining the findings here with the morphometric findings of Chapter 3, and given no significant differences shown in trabecular microarchitecture between sheep or pigs at L1 in Chapter 4, I would suggest that at L1, the pig offers a closer analogue to the human than does the sheep, in terms of pedicle shape and dimension.

5.5.3 STRENGTHS AND LIMITATIONS OF THIS STUDY

SSA provides additional information compared to basic morphometry, some of which is of direct relevance to this thesis, in particular the corroboration of pedicle dimension differences found in Chapter 3, as well as the new finding that the majority of vertebral body vertex displacement is at the anterosuperior aspect with similar displacements at the lateral and posterior vertebral body surfaces in both pigs and sheep. This suggests that

differences in vertebral body morphometric measurements are less likely to be useful in selecting an animal model.

Some of the findings are of less direct relevance to selecting an animal model, such as the human shape mode variation, though these are more likely to be of use when considering the development of novel instruments. There is also the potential to use this shape model, if sufficiently robust (see below), to assess the quantitative relationship between fracture risk and shape.

The main limitation of the study is the low animal sample size. Although it allowed me to create an average shape for the sample population which was sufficient for my purposes, it is far too small to allow extrapolation of the model to a general animal population. A similar problem may be present for the human sample.

A logical next step would be to perform a bootstrap analysis of the human sample, to determine whether the shape model is sufficiently robust, and therefore whether the shape mode variations are applicable to a general human population.

I have also only assessed the L1 vertebra between species. The Chapter 3 morphometry data suggest that sheep are likely to be closer to humans in terms of pedicle dimension in the thoracic spine, and it would be interesting to extend this study to determine whether thoracic vertebral shape analysis corroborates this as well.

Additionally, in the lower lumbar spine, human vertebral bodies become increasingly wider and longer than pigs and sheep, and human pedicles become much wider than either animal, as shown by the data in Chapter 3. It would be useful to assess whether these morphometric differences have corresponding shape differences, and whether those differences would be expected to impact transpedicular techniques, and as such, whether they would affect the selection of an animal model.

It would also be of interest to compare shape differences between different lumbar and thoracic vertebrae within the same species. This would provide information on the applicability of findings at one level to another.

I also suspect that the use of L1 may have resulted in increased variability, due to the transitional nature of the T12 – L1 junction. It would be interesting to compare the shape mode variability of L1 with L2 or L3.

As mentioned in the methods above, I noted difficulty in matching the superior articular facets between humans and quadrupeds, due to the hooked shape of sheep and pig facets. This was more pronounced in the sheep than in the pig. I was able to overcome this by adding more landmarks to the objects.

5.6 SUMMARY

- The application of SSA in comparative anatomy of vertebrae is a relatively new technique using well established analytical methods.

- The results show that quadruped pedicles are taller and wider than human vertebrae at L1, despite the vertebral bodies being smaller. The greatest magnitudes of vector displacement are between vertebral body dimensions and transverse and spinous processes. This correlates with the findings in Chapter 3, and the background literature.

- At the L1 vertebra, pig vertebrae are more similar to humans than sheep.

- SSA provides more information than basic morphometry, some of which is directly relevant to this thesis. Other factors present interesting areas for novel work.

- The study was limited by sample sizes

CHAPTER 6:
SUMMARY

The main aim of this thesis was to choose an animal vertebra to model human vertebrae for transpedicular vertebral access.

The rationale for this thesis is based on the use of vertebroplasty as a technique for treating osteoporotic vertebral fractures, and the development of novel instruments and bone cements which require preclinical phase testing before being used in live human subjects.

This is of relevance in modern medical practice due to the difficulty in treating osteoporotic vertebral fractures, which remain a significant morbidity and mortality risk. Osteoporosis is a substantial health burden in the Western world. While complex and multifactorial, and despite the existence of preventative medical therapies, the relationship to age and sex hormones in combination with longer life expectancies, means that it remains a problem.

Various treatment options for osteoporotic vertebral fractures are currently available, but there is no consensus on guidelines for optimal management, with contradictory guidance from different medical bodies. This makes managing such patients, who are often elderly and present with multiple comorbidities, difficult in clinical practice. For patients with stable fractures, conservative medical management is usually the first line treatment option.

However, the existence of minimally invasive percutaneous techniques such as vertebroplasties means that additional treatment options exist. The efficacy of vertebroplasty is currently debated, with a meta-analysis of the literature suggesting that it offers no benefit over a sham procedure placebo effect. However, difficulty in patient

selection continues to be an issue for the large sham procedure-controlled trials. There continues to be an ongoing debate over the use of vertebroplasty. The authors of the largest and most recent sham procedure-controlled trial, VERTOS VI, stated that at their treatment centre, they would still use vertebroplasty for certain carefully selected patients.

As well as controversy with the clinical evidence for vertebroplasty, the development of newer equipment and cement is limited either by the difficulty in obtaining sufficiently large numbers of human cadaveric vertebrae, or by the use of an animal species without consideration as to whether it is indeed the closest alternative to human cadavers.

Although not without limitations, human cadaveric vertebrae offer the closest alternative to live human specimens. However, given the cost and limited availability, animal vertebrae would offer a practical alternative. Quadrupeds such as pigs, sheep, cows, goats, and deer are used both in research and in training of surgeons and radiologists in procedures. While comparative anatomy studies have been performed between humans and several quadruped species there is no consensus within the literature as to which species would be the closest to the human vertebra, especially in the specific context of transpedicular techniques.

To address this current deficit in the literature, I have performed three studies comparing pigs and sheep with humans. These two species were selected on the basis of availability from the local abattoir, and the existing evidence suggests that both are close to human vertebrae in basic morphometry, with sheep pedicles being closer to the human in the thoracic spine, and pig pedicles being closer to the human in the lumbar spine.

The first study established that radiological measurement of vertebral morphometric dimensions was at least as reproducible as, and correlated with, direct visual measurements using a vernier caliper.

The interspecies comparison showed that overall, when considering pedicle dimensions, sheep were closer to humans in the thoracic spine, whereas pigs were closer in the lumbar spine. Although pig pedicles were of similar width to humans in the thoracic spine, they are considerably taller due to the presence of an intrapedicular transverse foramen.

In the lumbar spine, pigs were closer to humans than sheep in terms of height, especially at the lower lumbar levels where sheep pedicles became much taller. However, it should be noted that neither quadruped species was overall particularly similar to humans in terms of pedicle width, except the pig at L3. Although human vertebrae start slightly narrower than either animal at L1, they increase significantly in width throughout the lumbar spine, and by L5, they are markedly wider than either species. The L3 vertebra was the point where the two trend lines intersected. This may not impact transpedicular instrument assessment as much as one might initially expect, as even the larger access needles at present are usually 8 gauge (3.2 mm internal diameter), such as the Kyphon™ Xpander II Osteo Introducers.

The quadruped vertebrae were taller than human vertebrae, whereas human vertebrae were wider and longer in AP dimension. The differences in height were smaller than the differences in vertebral body length, which was most pronounced in the lower thoracic and lumbar spine.

Spinal canal dimensions were larger in humans than either pig or sheep, and this may be due to increased size of spinal tracts coordinating bipedal locomotion.

Bone texture analysis allows the comparison of trabecular microarchitecture between species. The interface between cement and trabeculae is of importance in load transfer. As such, when assessing novel cements, it may be of use to select an animal which more closely approximates the human trabecular structure.

Bone texture analysis was performed on L1 vertebrae across species. At this level, I showed that human vertebrae have lower apparent bone fraction than either quadruped, which is consistent with findings in the literature using other techniques. The ability to calculate an estimate of trabecular thickness using CT texture analysis allowed me to demonstrate that human L1 trabeculae were significantly thinner than pigs or sheep. Importantly, however, there was no statistically significant difference in trabecular spacing between humans and sheep or pigs.

Since the interdigitation of cement occurs in the spaces between trabeculae, it would seem that when considering the internal microarchitecture, sheep and pig vertebrae would be equally close to humans, and therefore either might be a suitable choice to model cement spread patterns.

Statistical shape analysis is a powerful method of assessing shape variation. It is a geometric technique, unlike basic morphometric measurements, in that it takes into account all the geometric information of a shape, rather than simply comparing isolated dimensions.

SSA was performed on L1 vertebrae across species. The findings corroborated the morphometric findings for pedicle dimensions, showing that at this level, human pedicles were shorter and thinner than pigs and sheep. Pedicle shape between the species appeared quite similar, as demonstrated by the low magnitude of the displacement vectors around the pedicles. Additionally, much of the difference appeared to be due to scaling, suggesting that the innate object shapes of the pedicles are not too dissimilar.

The main sites of shape difference were at the anterior vertebral body, transverse processes or spinous process, where vector displacement magnitudes were greater. This again corresponds to the morphometric findings of measurements at these locations.

An important limitation throughout all three studies was, somewhat ironically, the availability of whole animal spines from which to harvest vertebrae. As such, the animal population numbers were much smaller than the human population. However, these were still much cheaper and easier to obtain than human cadaveric vertebrae. With a sufficient budget and time, these would be more easily obtained in larger numbers than human cadaveric vertebrae. The number of vertebrae I was able to obtain were sufficient for my purposes, and similar to other studies in the existing literature.

Combining the results from the three studies, I conclude that pig vertebrae are closer to humans than sheep in the lumbar spine, in particular in pedicle size and shape. Sheep vertebrae have more similar pedicle morphometry to humans than do pigs in the thoracic spine. At the L1 level, either the pig or sheep would represent similarly close approximations of human trabecular microarchitecture. Therefore I would suggest using pigs to model the human lumbar spine, and sheep to model the human thoracic spine.

These findings are in line with the Chapter 2 systematic review comparing studies assessing individual quadruped species. I have provided additional information by directly comparing pigs and sheep with humans, and performing statistical analyses to confirm this. I have also provided additional evidence to promote the pig over the sheep as a model for the lumbar spine with the closer trabecular microarchitecture at the L1 level. SSA at the L1 vertebra also corroborates the basic morphometry.

Further work might involve performing the same analyses using larger animal sample sizes, to overcome the overarching limitation throughout the studies I have performed.

I have not performed bone texture analysis or SSA at other vertebral levels, and this would perhaps be the next logical step in extending the work started here. SSA could also be

performed to compare similarities within species across vertebral levels; for example, looking at how an L1 vertebra differs from L5 in terms of shape modes. This might offer insight into how useful it is to test an instrument on one vertebral level and apply the findings to other levels.

I have also not performed 2nd order bone texture analyses due to user inexperience with the software, and time constraints. However, statistics such as run length matrices are useful additional parameters for comparison.

In conclusion the studies in this thesis compare pig and sheep vertebrae with humans, using basic morphometrics, bone texture analysis and statistical shape analysis. Based on the results of the studies, I would recommend the use of pigs to model the human lumbar spine, and sheep to model the human thoracic spine.

GLOSSARY

Affine transformation	The simplest method of changing a shape, preserving parallel lines and planes between objects
Bone mineral density (BMD)	Bone mineral density; a measure of bone mineral content which is related to bone strength
Centroid	Mean coordinate value of an object
Cortical bone	The dense outer layer of bones, consisting of columnar arrangement of osteons
Cortoss™	Proprietary bone cement produced by Stryker
Dual energy X-ray Absorptiometry (DEXA)	Dual energy X-ray Absorptiometry; a radiographic technique for assessing bone mineral density
Generalised Procrustes Analysis (GPA)	A method of matching shapes using a sum-of-least-squares technique
Morphometry	Basic non-geometric measurements of anatomic structures
Osteon	The basic unit of bone tissue, consisting of concentric layers of osteoblasts, osteoclasts and osteocytes in a mineralised extracellular matrix, around a central canal containing blood vessels and nerves.
Landmark	Points placed on the surface of objects at corresponding locations
Physis	The growth plate of developing bone
Principal Component Analysis (PCA)	A method of describing variability of multidimensional data
Semilandmark	A series of points describing a curved surface of an object that cannot be described by a single point
Shape	All geometric information that remains when location, scale and rotation is removed from an object
Similarity transformation	A method of changing an object using rotation, scaling, translation and reflection, therefore preserving shape as defined above
Trabecula	The longitudinal arrangement of osteons in cancellous or medullary bone
T-score	The mean bone mineral density for a young adult (and therefore presumed normal) population
Vertebral compression fracture (VCF)	A fracture of the vertebral body resulting in loss of height

ABBREVIATIONS

3D	Three dimensional
BMD	Bone mineral density; a measure of bone mineral
$Ca_{10}(PO_4)_6(OH)_2$	Calcium hydroxyapatite, the main inorganic component of bone
CT	Computed Tomography
DEXA	Dual energy X-ray Absorptiometry
EU27	The 27 sovereign nations of the European Union (prior to Brexit)
GPA	Generalised Procrustes analysis
MRI	Magnetic Resonance Imaging
PCA	Principal component analysis
PGE2	Prostaglandin E2
PMMA	Polymethylmethacrylate bone cement
PTH	Parathyroid hormone
PVP	Percutaneous vertebroplasty
RANK	Receptor activator of nuclear factor kappa-B, a cell surface receptor found on many cells including osteoblasts
RANKL	Receptor activator of nuclear factor kappa-B ligand, a cytokine which binds to RANK
ROS	Reactive oxygen species
SSA	Statistical shape analysis
SSM	Statistical shape model
TA	Texture analysis
TPS	Thin-plate spline
VCF	Vertebral compression fracture

APPENDICES

A – DIRECT VS CT MEASUREMENTS AND MEAN DIFFERENCES

	VBH									Mean Difference
	Direct		95% CI			CT		95% CI		
T1	25.23	(1.18)	22.92	–	27.55	23.64	(0.18)	23.28	–	23.99	1.59
T2	23.78	(0.98)	21.86	–	25.70	23.89	(0.24)	23.42	–	24.36	0.11
T3	24.16	(0.71)	22.76	–	25.55	23.66	(0.39)	22.90	–	24.43	0.49
T4	24.25	(0.83)	22.63	–	25.87	23.65	0.19)	23.28	–	24.02	0.60
T5	24.35	(0.88)	22.63	–	26.06	23.77	(0.28)	23.22	–	24.31	0.58
T6	24.88	(0.84)	23.23	–	26.52	23.72	(0.63)	22.49	–	24.96	1.15
T7	25.09	(0.90)	23.33	–	26.85	23.91	(0.69)	22.55	–	25.27	1.18
T8	25.77	(0.97)	23.87	–	27.67	25.13	(0.69)	23.77	–	26.48	0.64
T9	26.39	(0.95)	24.53	–	28.25	25.44	(0.49)	24.48	–	26.39	0.95
T10	27.21	(1.23)	24.80	–	29.63	25.83	(0.41)	25.02	–	26.63	1.38
T11	27.77	(1.13)	25.55	–	29.98	25.92	(0.47)	25.00	–	26.85	1.84
T12	28.62	(0.96)	26.74	–	30.51	25.98	(0.32)	25.36	–	26.59	2.64
T13	28.59	(1.24)	26.17	–	31.01	26.59	(0.64)	25.35	–	27.84	2.00
T14	29.77	(1.29)	27.23	–	32.30	27.13	(0.44)	26.26	–	28.00	2.63
L1	30.70	(1.19)	28.36	–	33.04	28.50	(0.61)	27.30	–	29.70	2.20
L2	31.96	(1.22)	29.58	–	34.34	28.71	(0.55)	27.63	–	29.79	3.25
L3	32.49	(1.30)	29.95	–	35.04	29.36	(0.48)	28.40	–	30.31	3.14
L4	33.31	(1.30)	30.75	–	35.87	30.39	(0.59)	29.23	–	31.55	2.92
L5	32.89	(1.18)	30.59	–	35.18	30.43	(0.44)	29.58	–	31.29	2.45
L6	32.58	(0.73)	31.16	–	34.00	30.08	(0.31)	29.48	–	30.68	2.50

Figure A.1 – Vertebral body height direct and CT measurements (mm)

	Direct		95% CI			CT		95% CI			Mean Difference
					VBW						
T1	29.65	(2.60)	24.56	–	34.74	30.46	(1.62)	27.29	–	33.63	0.81
T2	30.68	(1.22)	28.29	–	33.07	30.32	(1.22)	27.92	–	32.72	0.36
T3	30.44	(1.10)	28.29	–	32.59	30.12	(1.23)	27.70	–	32.53	0.33
T4	28.15	(0.69)	26.81	–	29.50	30.29	(1.61)	27.14	–	33.44	2.13
T5	28.35	(0.90)	26.58	–	30.11	30.25	(1.27)	27.76	–	32.74	1.90
T6	29.20	(1.56)	26.15	–	32.25	31.20	(0.90)	29.44	–	32.97	2.00
T7	28.97	(0.72)	27.57	–	30.38	30.17	(1.48)	27.27	–	33.06	1.19
T8	30.21	(0.89)	28.47	–	31.96	31.12	(1.13)	28.91	–	33.33	0.91
T9	31.46	(0.89)	29.72	–	33.21	29.87	(1.89)	26.17	–	33.58	1.59
T10	32.07	(0.87)	30.36	–	33.78	32.29	(1.09)	30.16	–	34.43	0.22
T11	33.63	(2.01)	29.69	–	37.57	33.33	(0.81)	31.73	–	34.92	0.30
T12	34.09	(1.44)	31.25	–	36.92	32.47	(1.10)	30.32	–	34.61	1.62
T13	34.86	(1.74)	31.45	–	38.26	32.47	(1.40)	29.71	–	35.22	2.39
T14	32.78	(1.43)	29.98	–	35.59	32.15	(1.70)	28.81	–	35.48	0.64
L1	32.78	(.044)	31.92	–	33.64	31.33	(1.19)	28.99	–	33.67	1.45
L2	33.44	(0.24)	32.97	–	33.92	32.52	(1.27)	30.03	–	35.01	0.92
L3	35.00	(0.30)	34.40	–	35.59	32.43	(1.42)	29.63	–	35.22	2.57
L4	35.30	(0.53)	34.28	–	36.33	33.94	(1.35)	31.29	–	36.60	1.36
L5	37.40	(0.95)	35.54	–	39.27	34.60	(1.29)	32.07	–	37.13	2.81
L6	37.25	(0.31)	36.64	–	37.86	35.41	(1.75)	31.99	–	38.84	1.84

Figure A.2 – Vertebral body width direct and CT measurements (mm)

	Direct		95% CI			CT		95% CI			Mean Difference
					VBL						
T1	20.29	(0.24)	19.82	–	20.76	17.34	(0.40)	16.55	–	18.14	2.95
T2	20.07	(0.61)	18.87	–	21.28	17.80	(0.60)	16.62	–	18.98	2.27
T3	19.84	(0.53)	18.81	–	20.87	17.32	(0.65)	16.04	–	18.60	2.52
T4	20.00	(0.54)	18.95	–	21.05	17.80	(0.82)	16.20	–	19.40	2.20
T5	19.84	(0.63)	18.60	–	21.08	17.43	(0.42)	16.60	–	18.26	2.41
T6	19.81	(0.58)	18.68	–	20.94	17.42	(0.65)	16.14	–	18.70	2.39
T7	19.35	(0.68)	18.02	–	20.68	17.06	(0.72)	15.65	–	18.48	2.29
T8	19.19	(0.73)	17.76	–	20.63	17.07	(0.60)	15.89	–	18.24	2.12
T9	19.23	(0.59)	18.08	–	20.38	16.59	(0.90)	14.83	–	18.35	2.64
T10	19.21	(0.88)	17.49	–	20.93	16.91	(0.45)	16.03	–	17.79	2.31
T11	19.52	(0.79)	17.97	–	21.07	17.20	(0.45)	16.32	–	18.07	2.33
T12	19.92	(0.83)	18.31	–	21.54	17.17	(0.35)	16.48	–	17.87	2.75
T13	20.55	(1.02)	18.55	–	22.55	17.15	(0.49)	16.19	–	18.11	3.40
T14	20.69	(0.82_	19.09	–	22.29	17.81	(0.51)	16.81	–	18.81	2.88
L1	22.24	(1.09)	20.10	–	24.38	19.56	(0.72)	18.14	–	20.97	2.68
L2	23.08	(0.55)	21.99	–	24.16	20.10	(0.74)	18.66	–	21.55	2.97
L3	22.47	(0.66)	21.19	–	23.76	20.74	(0.79)	19.18	–	22.29	1.73
L4	22.24	(0.39)	21.47	–	23.01	20.70	(0.59)	19.54	–	21.85	1.54
L5	21.56	(0.47)	20.64	–	22.47	19.82	(0.81)	18.23	–	21.41	1.73
L6	20.76	(0.50)	19.77	–	21.75	18.14	(0.67)	16.83	–	19.45	2.62

Figure A.3 – Vertebral body length direct and CT measurements (mm)

	Direct		95% CI			CT		95% CI			Mean Difference
						TPW					
T1	55.17	(2.07)	51.12	–	59.22	50.96	(2.10)	47.02	–	54.90	4.21
T2	54.08	(1.09)	51.95	–	56.20	48.51	(0.71)	47.13	–	49.89	5.56
T3	49.91	(1.90)	46.18	–	53.65	46.62	(0.37)	45.89	–	47.35	3.29
T4	48.90	(1.47)	46.01	–	51.79	46.07	(0.79)	44.52	–	47.62	2.83
T5	46.96	(1.16)	44.69	–	49.23	44.46	(1.13)	42.25	–	46.67	2.49
T6	45.85	(0.74)	44.40	–	47.30	45.30	(0.94)	43.47	–	47.14	0.55
T7	45.42	(0.49)	44.47	–	46.37	44.77	(1.22)	42.37	–	47.16	0.65
T8	48.00	(1.45)	45.16	–	50.83	44.98	(1.41)	42.23	–	47.74	3.01
T9	45.40	(2.30)	40.88	–	49.91	43.06	(1.57)	39.99	–	46.13	2.34
T10	41.17	(2.95)	35.40	–	46.94	39.76	(3.31)	33.27	–	46.26	1.41
T11	40.93	(2.11)	38.79	–	47.06	38.45	(2.60)	33.37	–	43.54	2.47
T12	41.05	(1.11)	38.88	–	43.22	38.65	(2.26)	34.23	–	43.07	2.40
T13	41.90	(1.84)	38.29	–	45.51	39.26	(2.78)	33.81	–	44.72	2.63
T14	49.32	(3.95)	41.57	–	57.07	47.23	(3.31)	40.74	–	53.72	2.09
L1	84.88	(3.20)	78.61	–	91.16	83.33	(7.68)	58.28	–	88.37	1.55
L2	97.08	(1.76)	93.63	–	100.53	96.02	(4.50)	79.19	–	96.84	1.06
L3	101.84	(2.51)	96.93	–	106.76	98.52	(2.15)	89.30	–	97.74	3.32
L4	101.22	(5.33)	92.77	–	113.67	99.66	(1.87)	92.99	–	100.33	1.56
L5	100.30	(3.34)	97.75	–	110.86	99.59	(1.79)	94.08	–	101.10	0.71
L6	94.54	(3.94)	86.82	–	102.27	94.81	(3.20)	88.53	–	101.08	0.26

Figure A.4 – Transverse process width direct and CT measurements (mm)

	Direct		95% CI			CT		95% CI			Mean Difference
					SCW						
T1	15.42	(1.79)	11.91	–	18.94	16.72	(0.73)	15.28	–	18.15	1.29
T2	14.01	(0.92)	12.21	–	15.81	14.84	(1.02)	12.84	–	16.84	0.83
T3	13.67	(0.82)	12.07	–	15.27	14.53	(0.56)	13.44	–	15.63	0.86
T4	11.81	(1.02)	9.80	–	13.81	14.62	(1.12)	12.43	–	16.82	2.82
T5	11.08	(1.32)	8.49	–	13.66	14.94	(0.74)	13.49	–	16.39	3.87
T6	11.75	(0.86)	10.07	–	13.44	13.70	(0.89)	11.95	–	15.44	1.95
T7	10.42	(0.61)	9.23	–	11.61	13.37	(0.73)	11.93	–	14.80	2.95
T8	11.20	(1.03)	9.17	–	13.22	13.54	(0.68)	12.21	–	14.86	2.34
T9	11.90	(0.54)	10.84	–	12.96	13.53	(0.60)	12.35	–	14.70	1.62
T10	11.00	(0.75)	9.53	–	12.47	14.30	(0.28)	13.76	–	14.84	3.30
T11	11.97	(0.40)	10.19	–	11.76	14.46	(0.59)	13.30	–	15.62	2.49
T12	12.89	(0.52)	11.88	–	13.90	15.26	(0.53)	14.22	–	16.29	2.37
T13	13.65	(0.36)	12.94	–	14.36	14.41	(0.33)	13.78	–	15.05	0.76
T14	12.81	(0.74)	11.37	–	14.26	14.40	(0.09)	14.22	–	14.57	1.58
L1	12.49	(0.67)	11.17	–	13.81	13.95	(0.61)	12.76	–	15.14	1.46
L2	13.26	(0.64)	10.01	–	12.52	15.00	(0.47)	14.08	–	15.92	1.74
L3	13.49	(0.28)	12.95	–	14.03	15.66	(0.33)	15.02	–	16.30	2.17
L4	15.71	(1.38)	13.01	–	18.41	17.62	(0.42)	16.79	–	18.45	1.91
L5	17.08	(0.95)	15.21	–	18.94	17.96	(0.83)	16.33	–	19.60	0.89
L6	21.53	(2.38)	16.87	–	26.20	19.78	(0.96)	17.91	–	21.65	1.75

Figure A.5 – Spinal canal width direct and CT measurements (mm)

	Direct		95% CI		CT		95% CI		Mean Difference
					SCL					
T1	11.95	(1.66)	8.70	– 15.20	13.43	(1.23)	11.02	– 15.83	1.48
T2	11.16	(0.70)	9.79	– 12.53	10.88	(0.78)	9.34	– 12.41	0.28
T3	9.71	(0.72)	8.30	– 11.13	10.56	(0.48)	9.61	– 11.50	0.84
T4	8.85	(0.70)	7.48	– 10.21	10.19	(0.12)	9.96	– 10.42	1.34
T5	9.05	(0.67)	7.72	– 10.37	10.86	(0.28)	10.30	– 11.42	1.81
T6	8.69	(0.81)	7.09	– 10.28	10.31	(0.35)	9.62	– 11.00	1.63
T7	7.81	(0.54)	6.76	– 8.86	10.65	(0.37)	9.92	– 11.38	1.83
T8	7.89	(0.63)	6.65	– 9.13	10.07	(0.13)	9.82	– 10.33	2.18
T9	7.73	(0.37)	7.00	– 8.47	10.34	(0.27)	9.82	– 10.87	2.61
T10	9.47	(0.50)	8.50	– 10.45	10.76	(0.32)	10.13	– 11.39	1.29
T11	10.21	(0.56)	9.11	– 11.31	10.66	(0.18)	10.31	– 11.01	0.46
T12	9.40	(0.84)	7.75	– 11.04	10.96	(0.38)	10.22	– 11.70	1.57
T13	8.91	(0.59)	7.74	– 10.07	11.06	(0.39)	10.30	– 11.83	2.16
T14	9.91	(0.40)	9.13	– 10.69	10.78	(0.31)	10.17	– 11.38	0.87
L1	10.26	(0.69)	8.91	– 11.60	10.96	(0.29)	10.39	– 11.54	0.71
L2	9.92	(0.88)	8.20	– 11.64	10.43	(0.14)	10.36	– 10.50	0.51
L3	9.63	(1.16)	7.36	– 11.90	10.62	(0.10)	10.47	– 10.76	0.99
L4	10.00	(0.68)	8.67	– 11.33	10.82	(0.30)	10.75	– 10.88	0.82
L5	10.12	(0.67)	8.80	– 11.44	10.62	(0.10)	10.42	– 10.81	0.50
L6	10.52	(1.02)	8.52	– 12.52	11.14	(0.31)	10.54	– 11.75	0.62

Figure A.6 – Spinal canal length direct and CT measurements (mm)

	TL									
	Direct		95% CI			CT		95% CI			Mean Difference
T1	102.95	(1.71)	99.59	–	106.30	101.20	(1.02)	95.20	–	99.20	1.75
T2	100.45	(1.72)	97.08	–	103.83	101.09	(2.57)	96.05	–	106.13	0.64
T3	98.41	(2.65)	93.23	–	103.60	99.79	(1.54)	96.78	–	102.80	1.37
T4	96.15	(2.77)	90.71	–	101.58	97.23	(2.58)	92.17	–	102.29	1.09
T5	90.86	(2.36)	86.24	–	95.48	89.06	(2.34)	84.47	–	93.65	1.80
T6	84.77	(3.76)	77.40	–	92.14	84.85	(2.95)	79.07	–	90.64	0.09
T7	79.98	(2.21)	75.65	–	84.31	80.31	(1.73)	76.92	–	83.70	0.33
T8	71.01	(2.90)	65.33	–	76.70	71.99	(1.97)	68.13	–	75.86	0.98
T9	65.22	(2.35)	60.62	–	69.82	65.57	(1.91)	61.83	–	69.31	0.35
T10	59.81	(0.54)	58.75	–	60.87	58.74	(1.29)	56.22	–	61.27	1.07
T11	56.97	(1.54)	53.95	–	59.99	55.67	(0.99)	53.74	–	57.61	1.30
T12	56.55	(1.84)	52.96	–	60.15	54.81	(1.68)	51.51	–	58.11	1.74
T13	57.21	(1.13)	54.99	–	59.43	55.81	(2.23)	49.44	–	58.19	1.40
T14	56.02	(2.43)	51.26	–	60.78	55.79	(1.42)	53.01	–	58.57	0.23
L1	57.21	(2.16)	54.97	–	63.45	56.20	(1.97)	52.34	–	60.06	1.01
L2	57.84	(1.58)	56.75	–	62.93	56.54	(1.94)	51.75	–	59.34	1.29
L3	58.51	(1.33)	55.91	–	61.11	56.24	(1.34)	53.63	–	58.86	2.27
L4	56.50	(1.84)	52.89	–	60.11	54.93	(1.25)	52.49	–	57.37	1.57
L5	54.18	(1.73)	50.79	–	57.58	52.81	(1.99)	48.92	–	56.70	1.37
L6	49.25	(3.49)	42.40	–	56.09	48.05	(3.53)	41.12	–	54.97	1.20

Figure A.7 – Total anteroposterior length direct and CT measurements (mm)

B – HISTOGRAMS OF DATA DISTRIBUTION FOR HUMAN, PIG AND SHEEP MORPHOMETRIC CT MEASUREMENTS
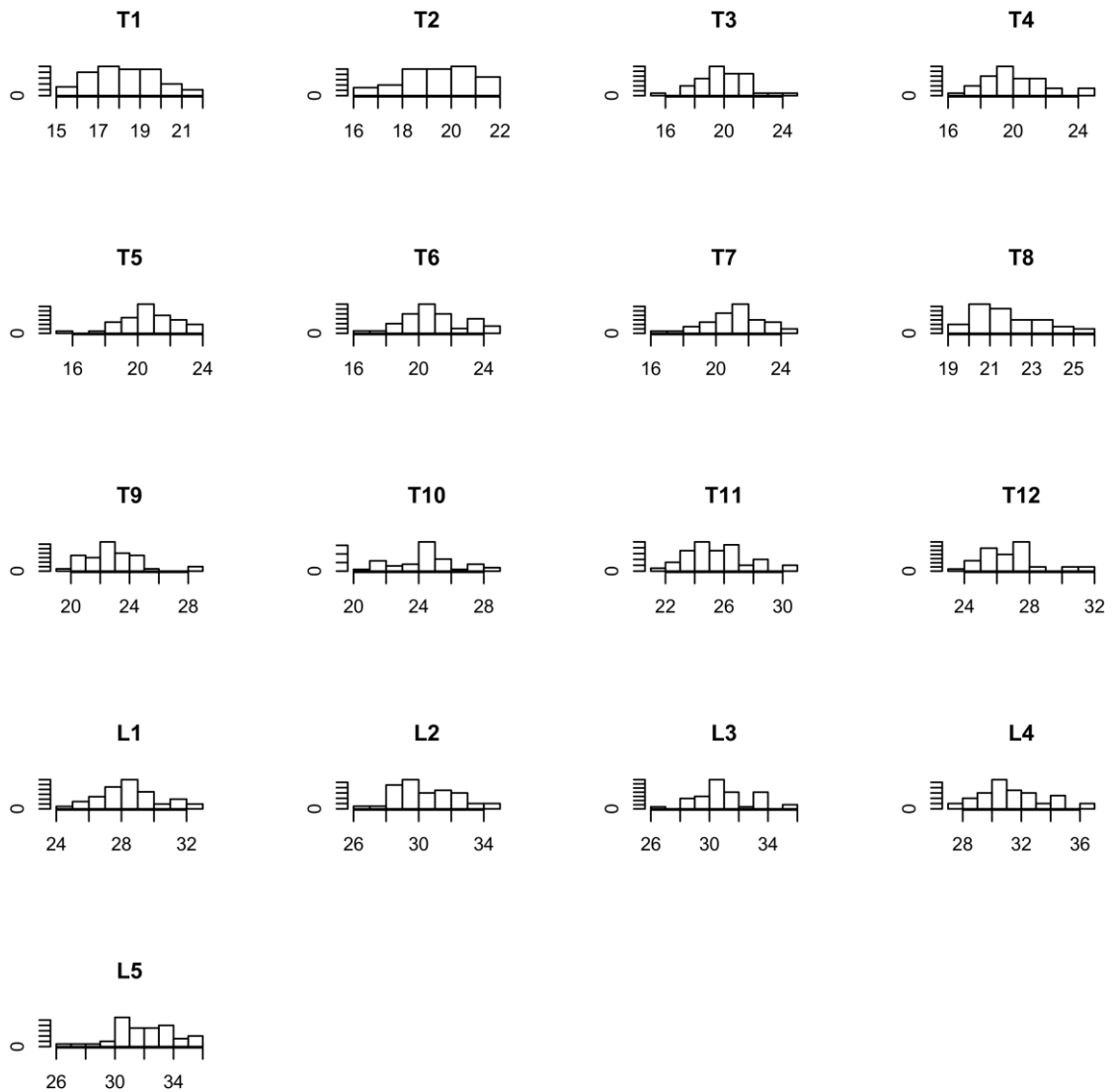
Figure B.1 – Histograms detailing human vertebral body height data distributions, with measurement size (mm) on the x-axis, and number of specimens on the y-axis
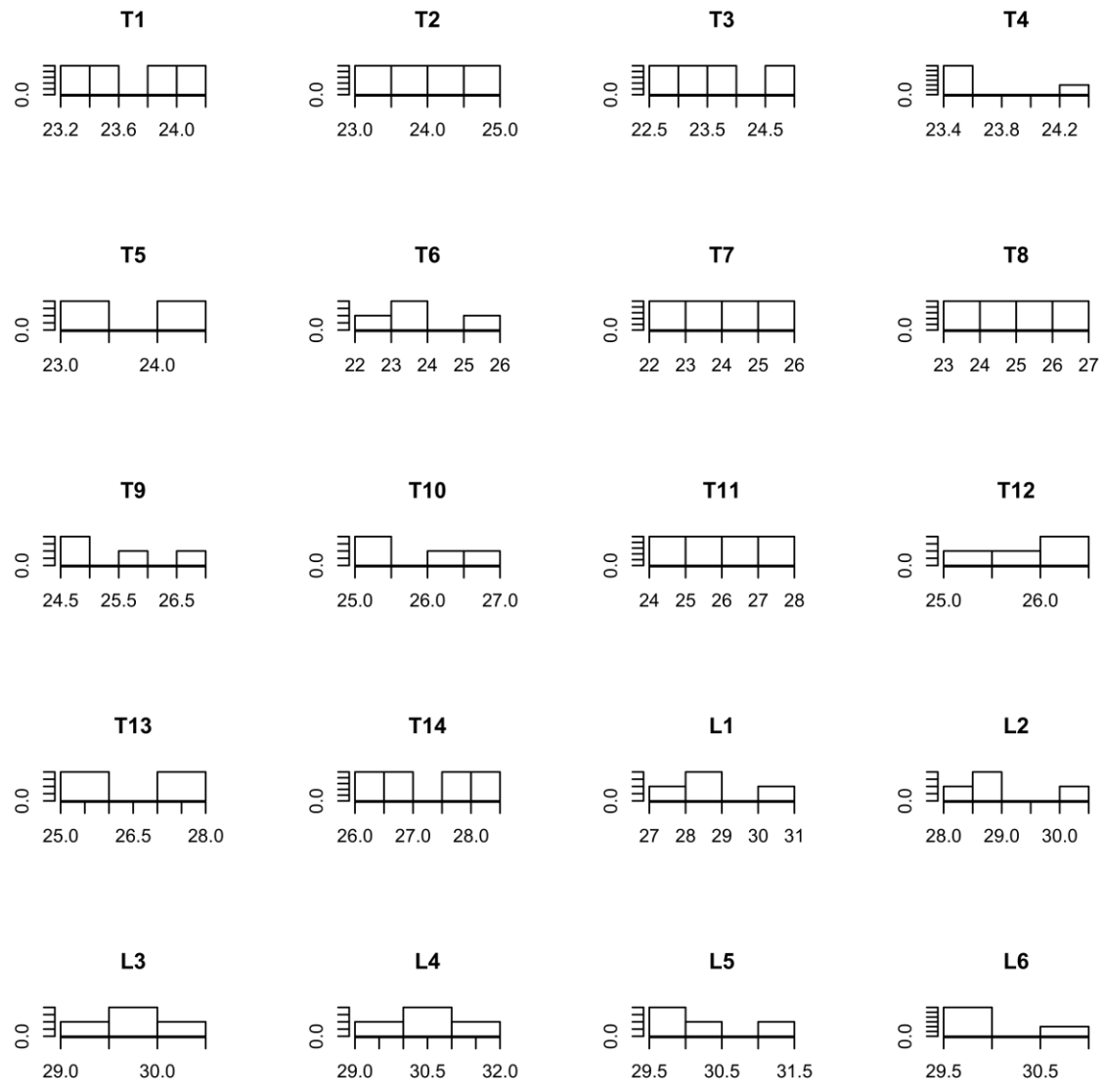
Figure B.2 – Histograms detailing pig vertebral body height data distributions, with measurement size (mm) on the x-axis, and number of specimens on the y-axis
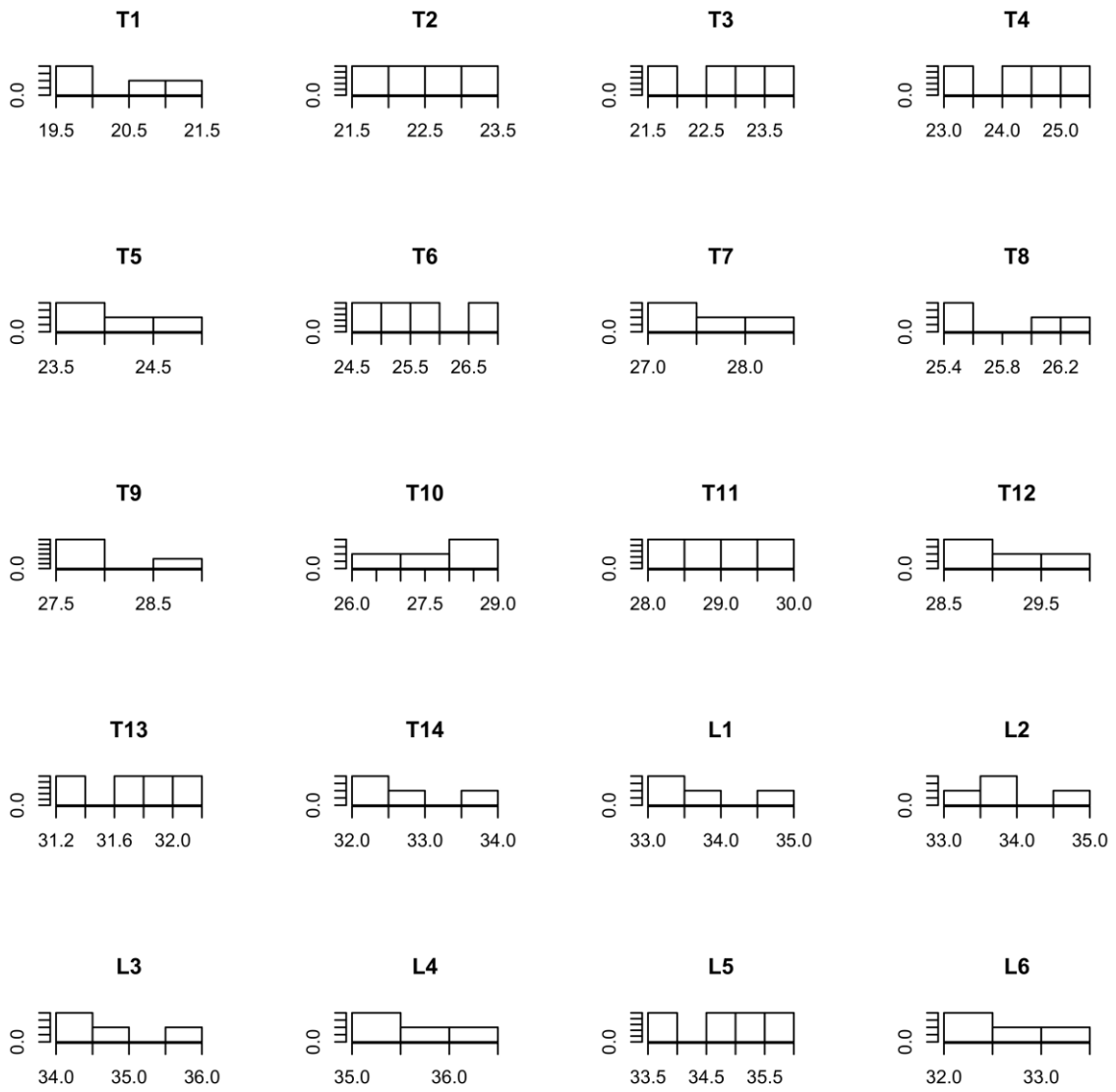
Figure B.3 – Histograms detailing sheep vertebral body height data distributions, with measurement size (mm) on the x-axis, and number of specimens on the y-axis
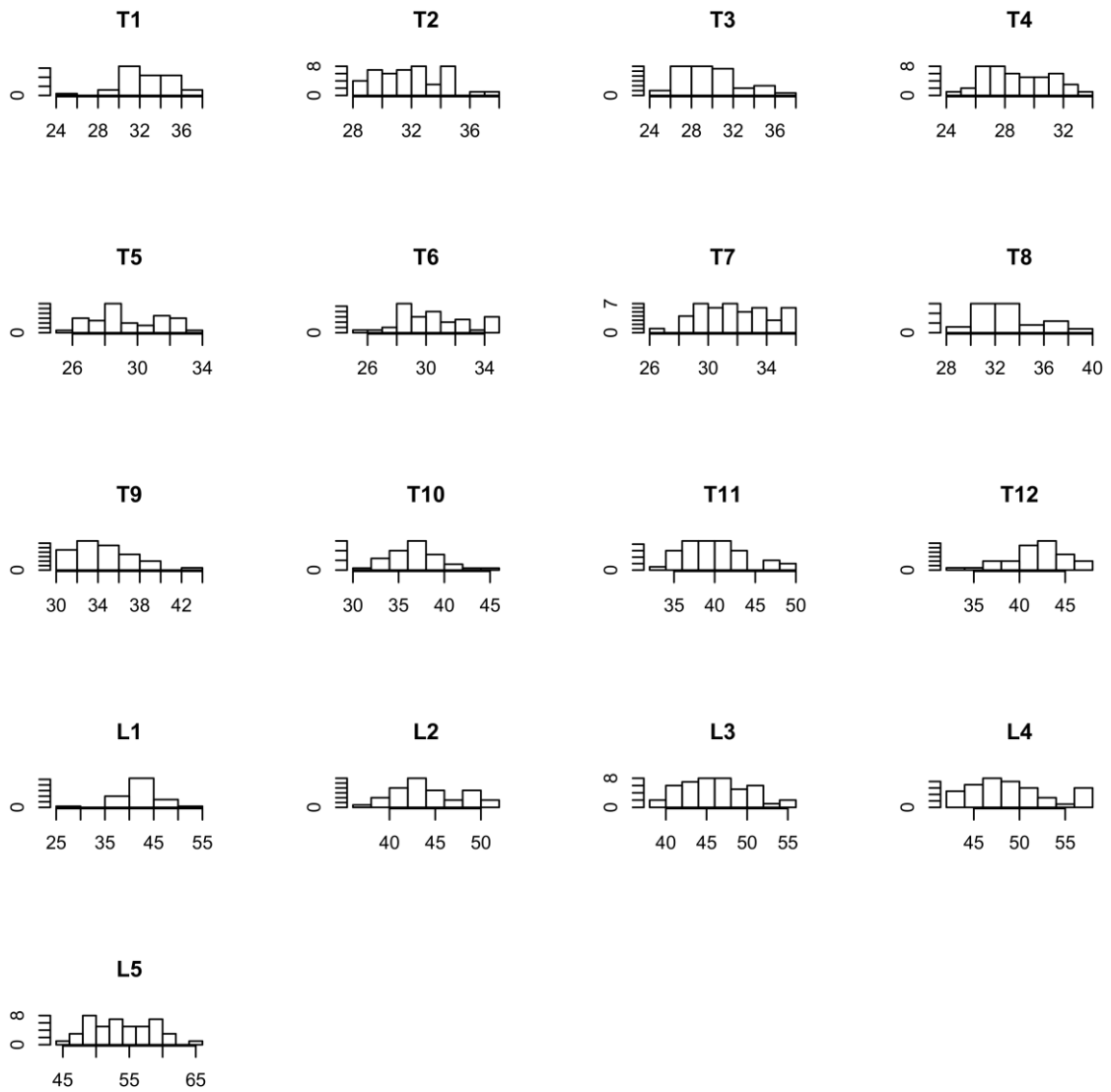
Figure B.4 – Histograms detailing human vertebral body width data distributions, with measurement size (mm) on the x-axis, and number of specimens on the y-axis
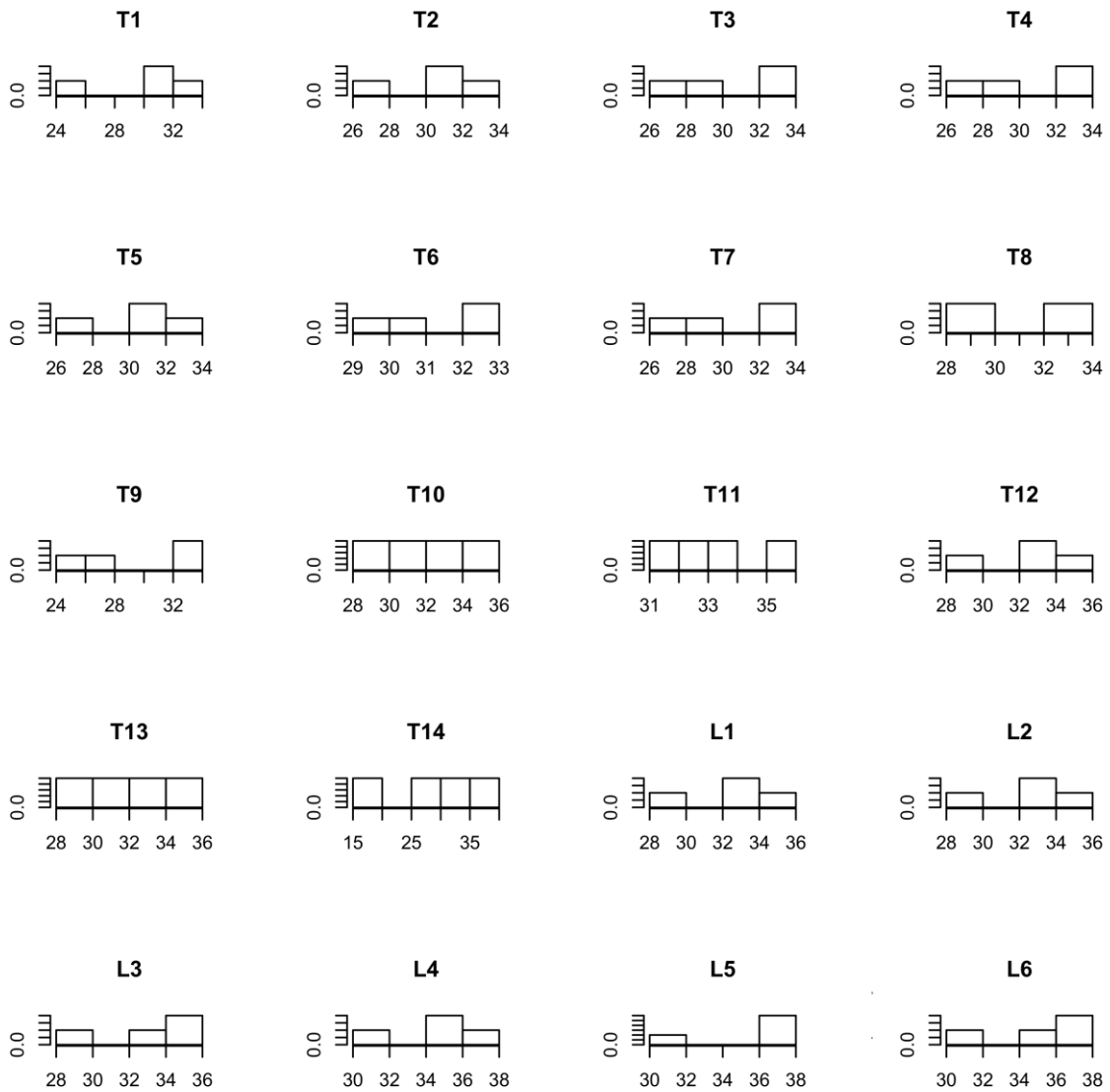
Figure B.5 – Histograms detailing pig vertebral body width data distributions, with measurement size (mm) on the x-axis, and number of specimens on the y-axis
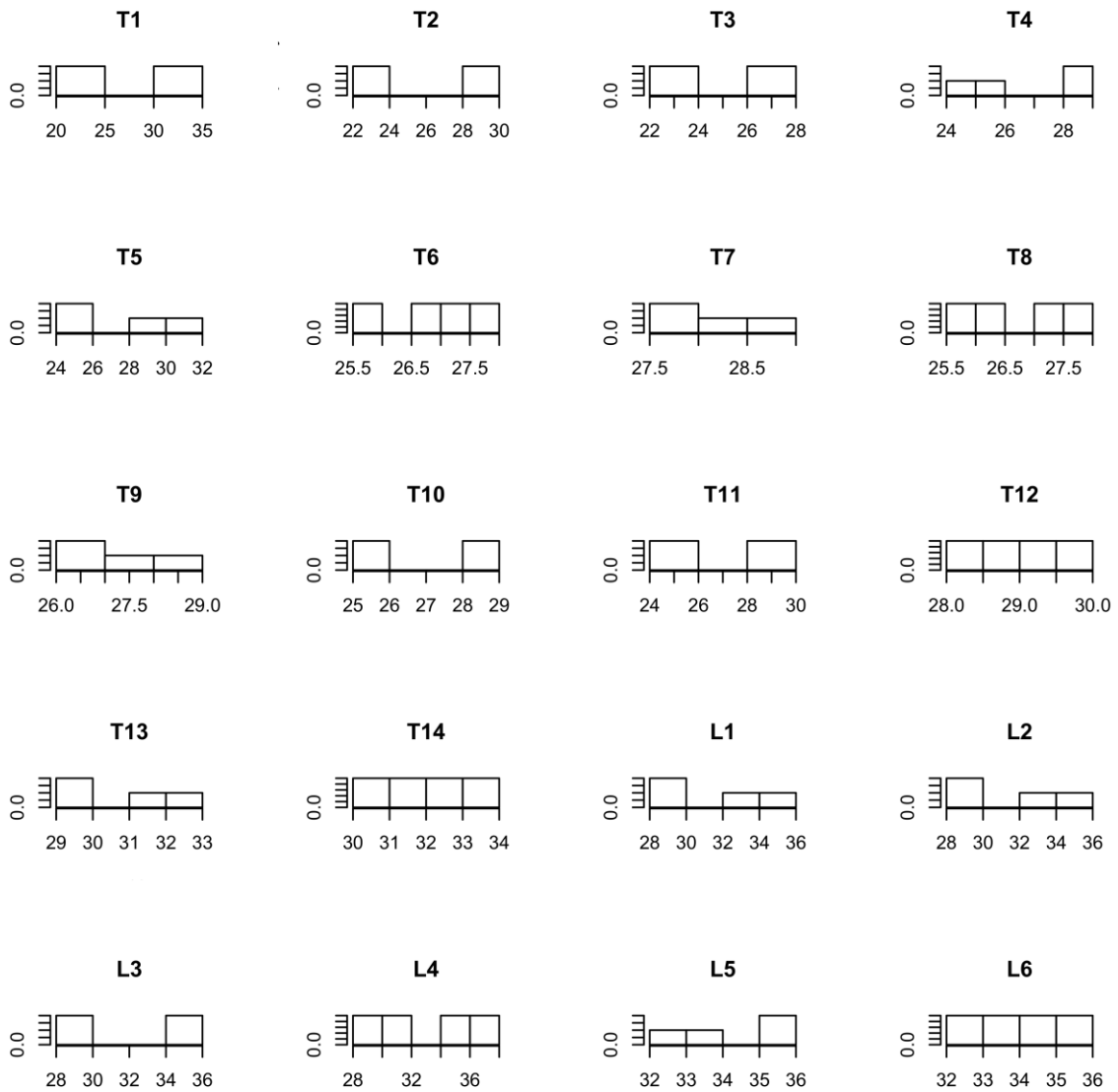
Figure B.6 – Histograms detailing sheep vertebral body width data distributions, with measurement size (mm) on the x-axis, and number of specimens on the y-axis

203
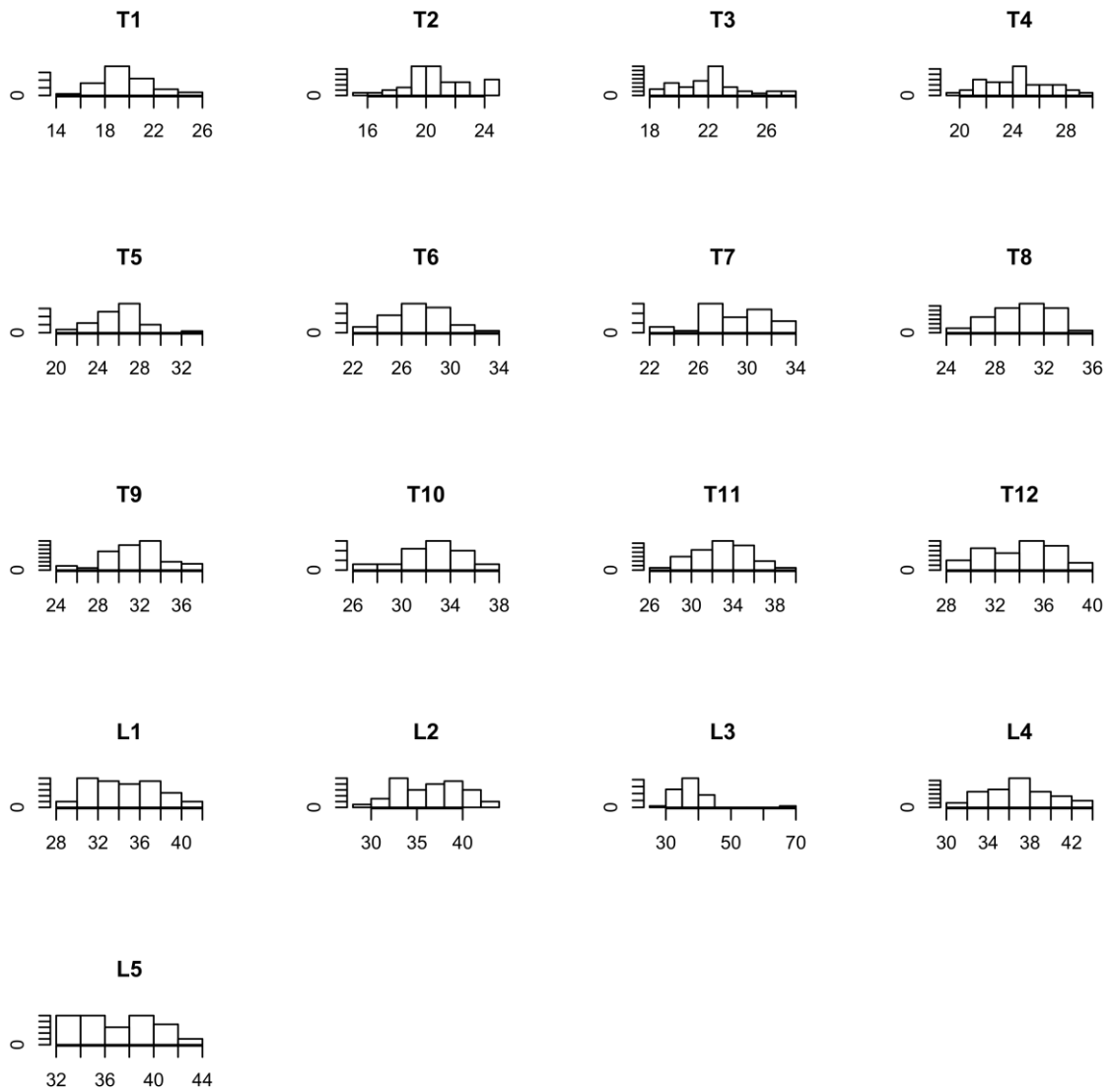
Figure B.7 – Histograms detailing human vertebral body length data distributions, with measurement size (mm) on the x-axis, and number of specimens on the y-axis
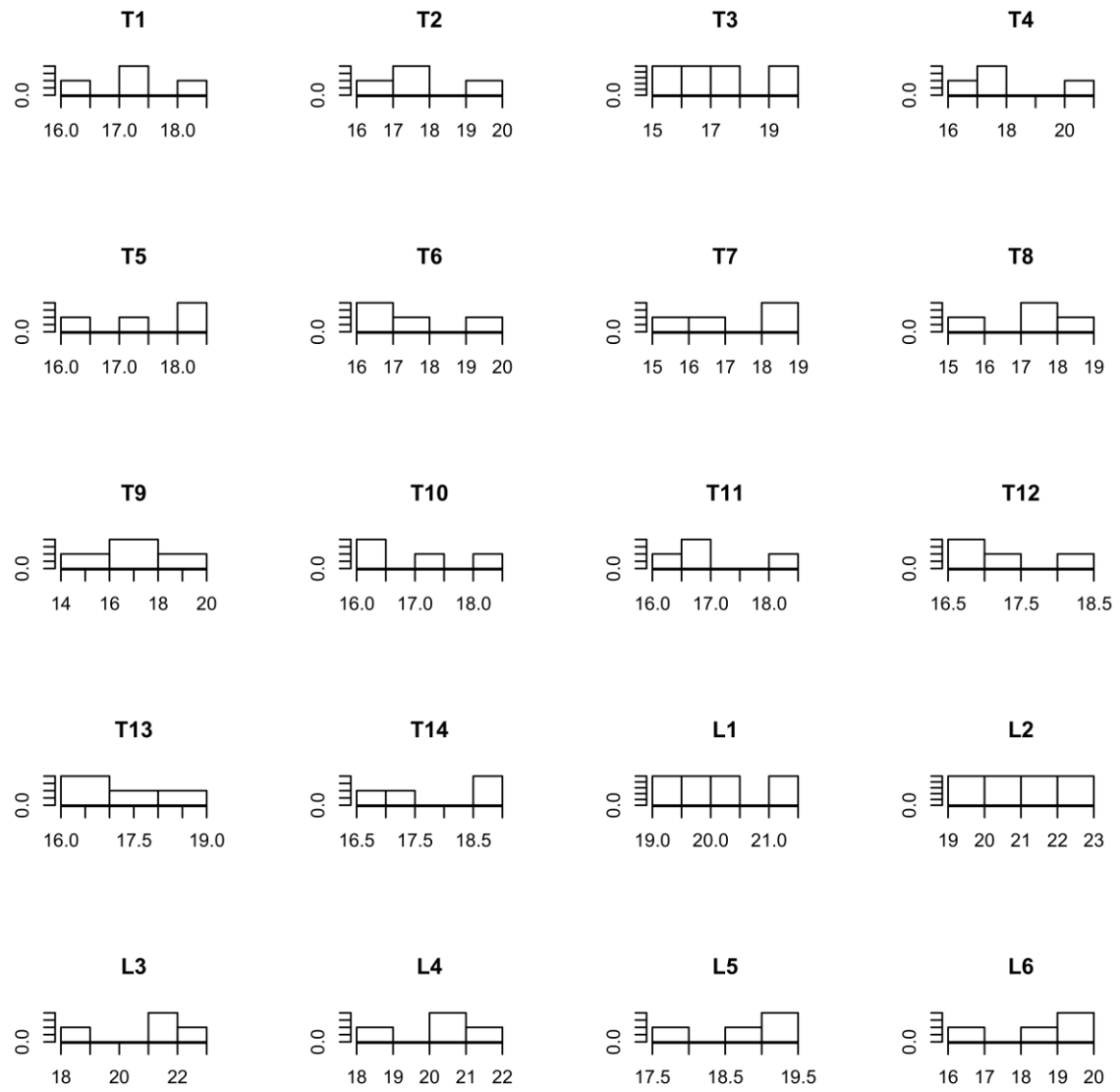
Figure B.8 – Histograms detailing pig vertebral body length data distributions, with measurement size (mm) on the x-axis, and number of specimens on the y-axis
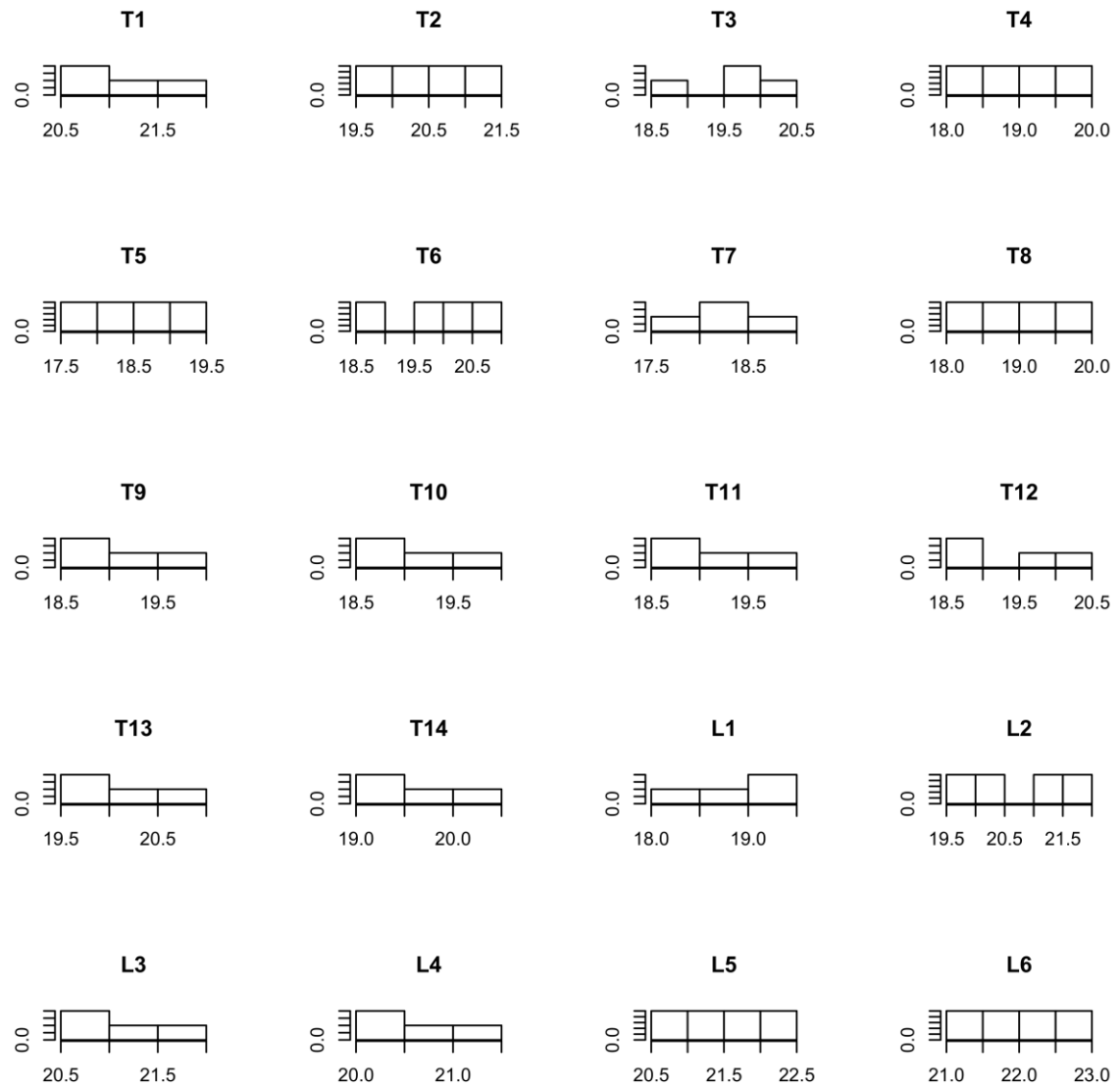
Figure B.9 – Histograms detailing sheep vertebral body length data distributions, with measurement size (mm) on the x-axis, and number of specimens on the y-axis
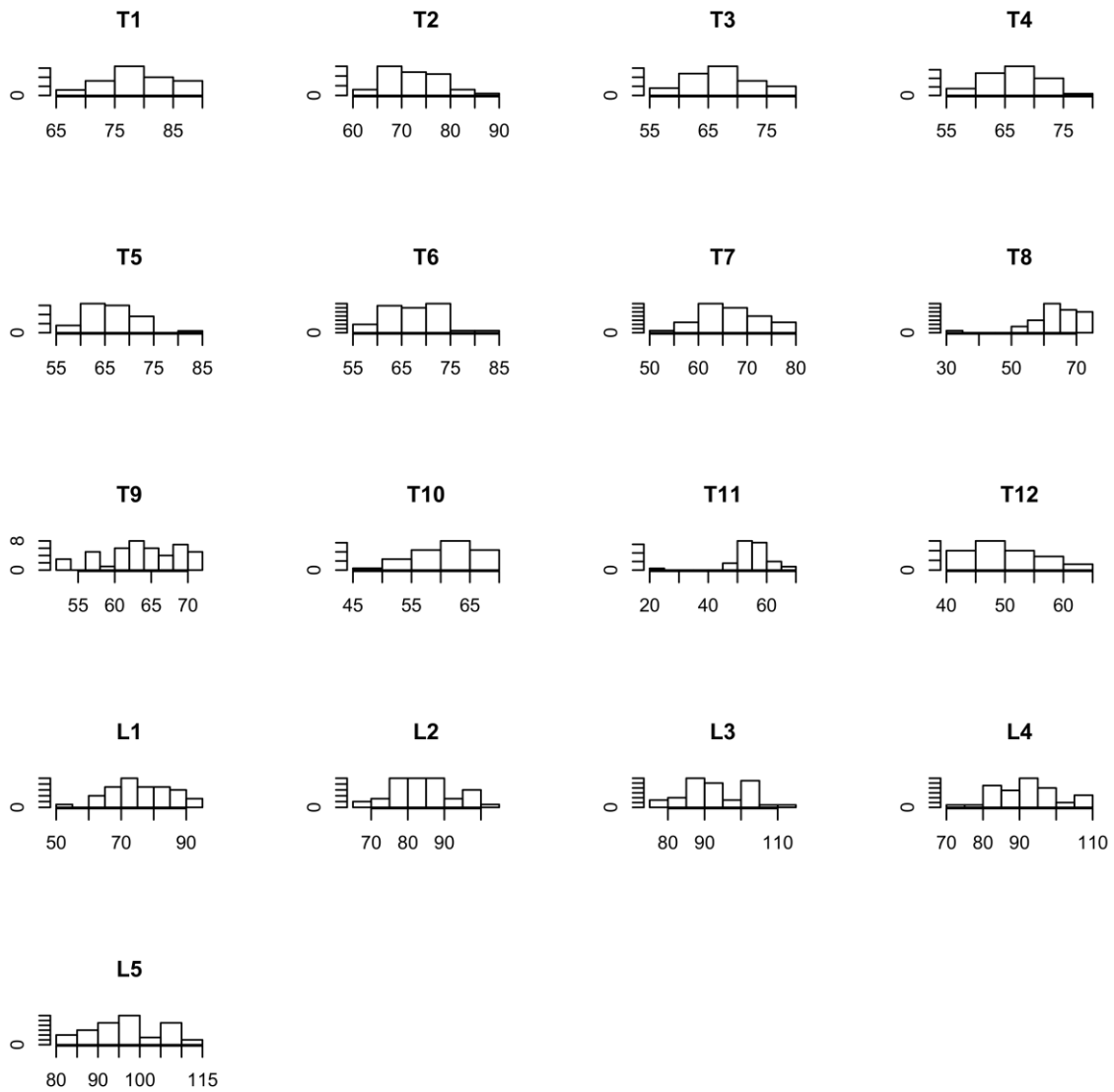
Figure B.10 – Histograms detailing human transverse process width data distributions, with measurement size (mm) on the x-axis, and number of specimens on the y-axis
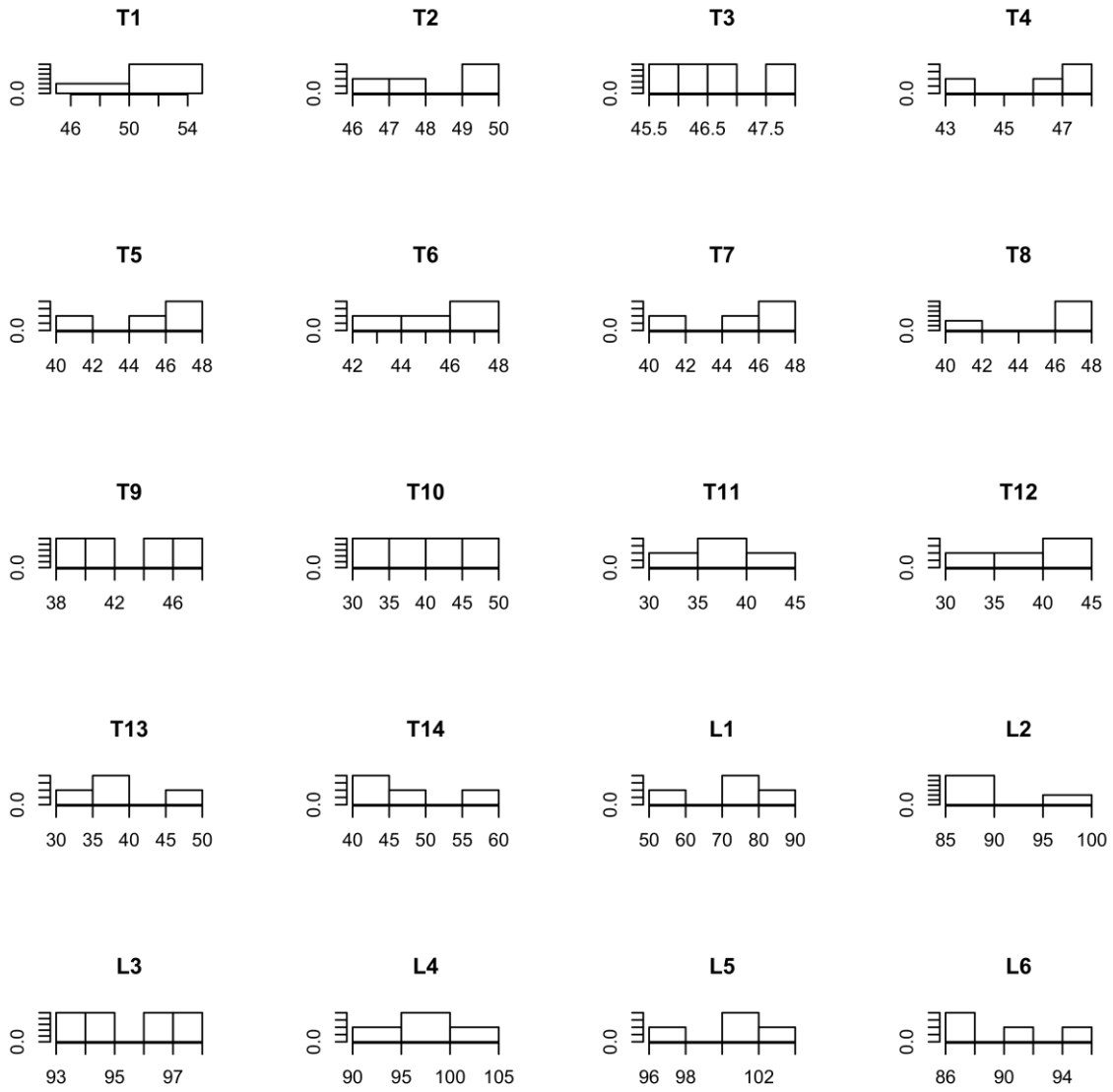
Figure B.11 – Histograms detailing pig transverse process width data distributions, with measurement size (mm) on the x-axis, and number of specimens on the y-axis
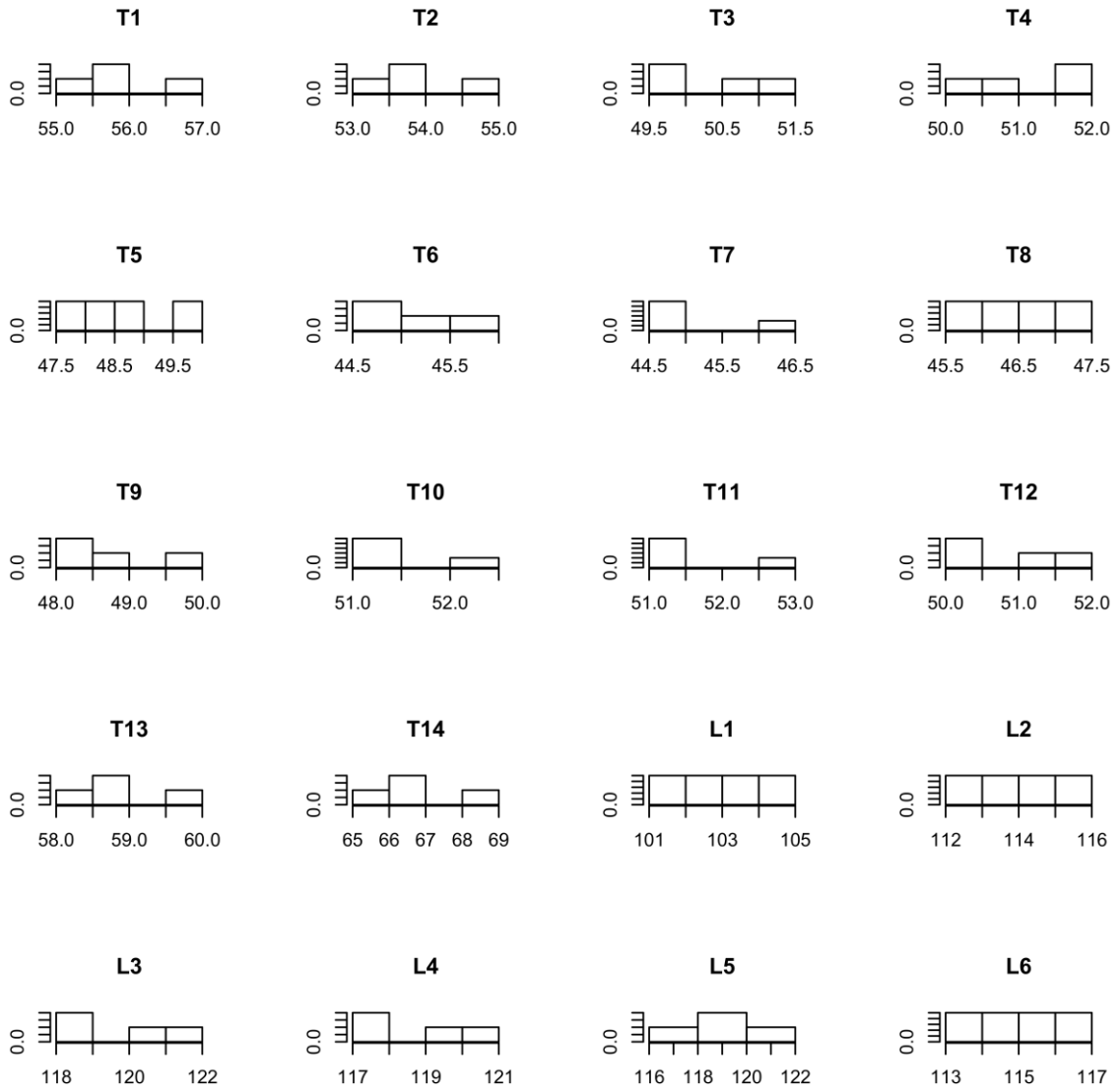
Figure B.12 – Histograms detailing sheep transverse process width data distributions, with measurement size (mm) on the x-axis, and number of specimens on the y-axis
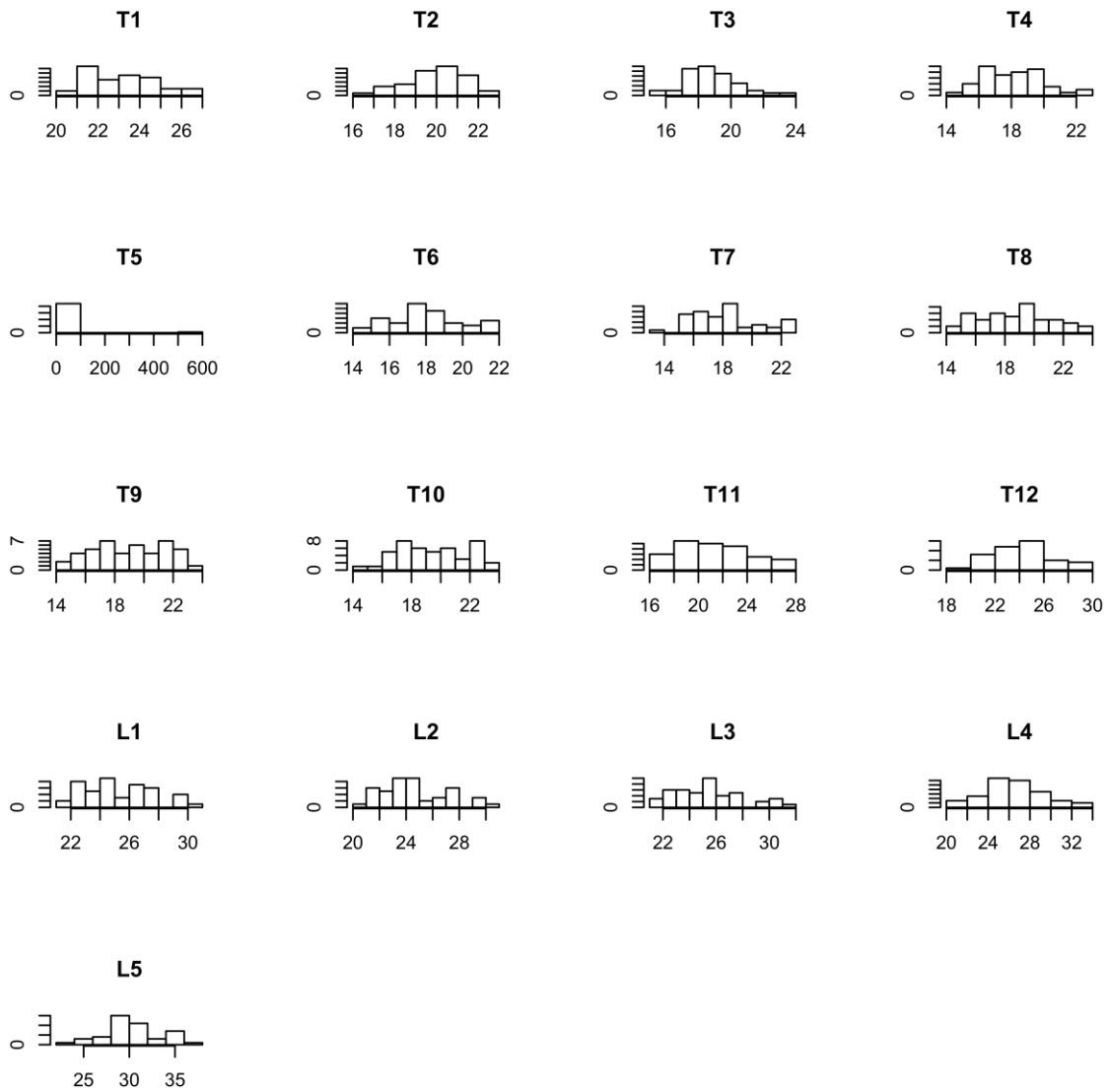
Figure B.13 – Histograms detailing human spinal canal width data distributions, with measurement size (mm) on the x-axis, and number of specimens on the y-axis
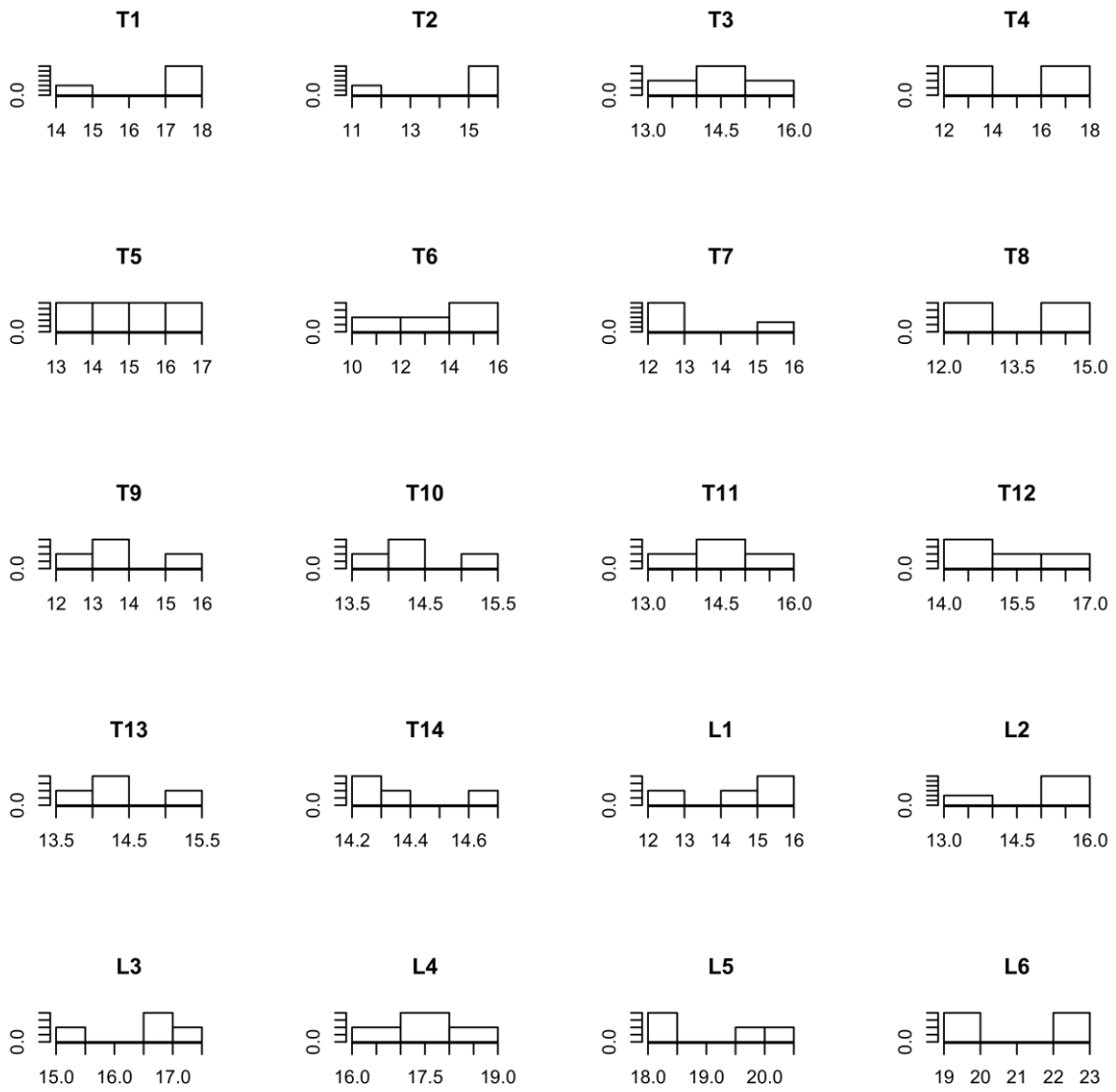
Figure B.14 – Histograms detailing pig spinal canal width data distributions, with measurement size (mm) on the x-axis, and number of specimens on the y-axis
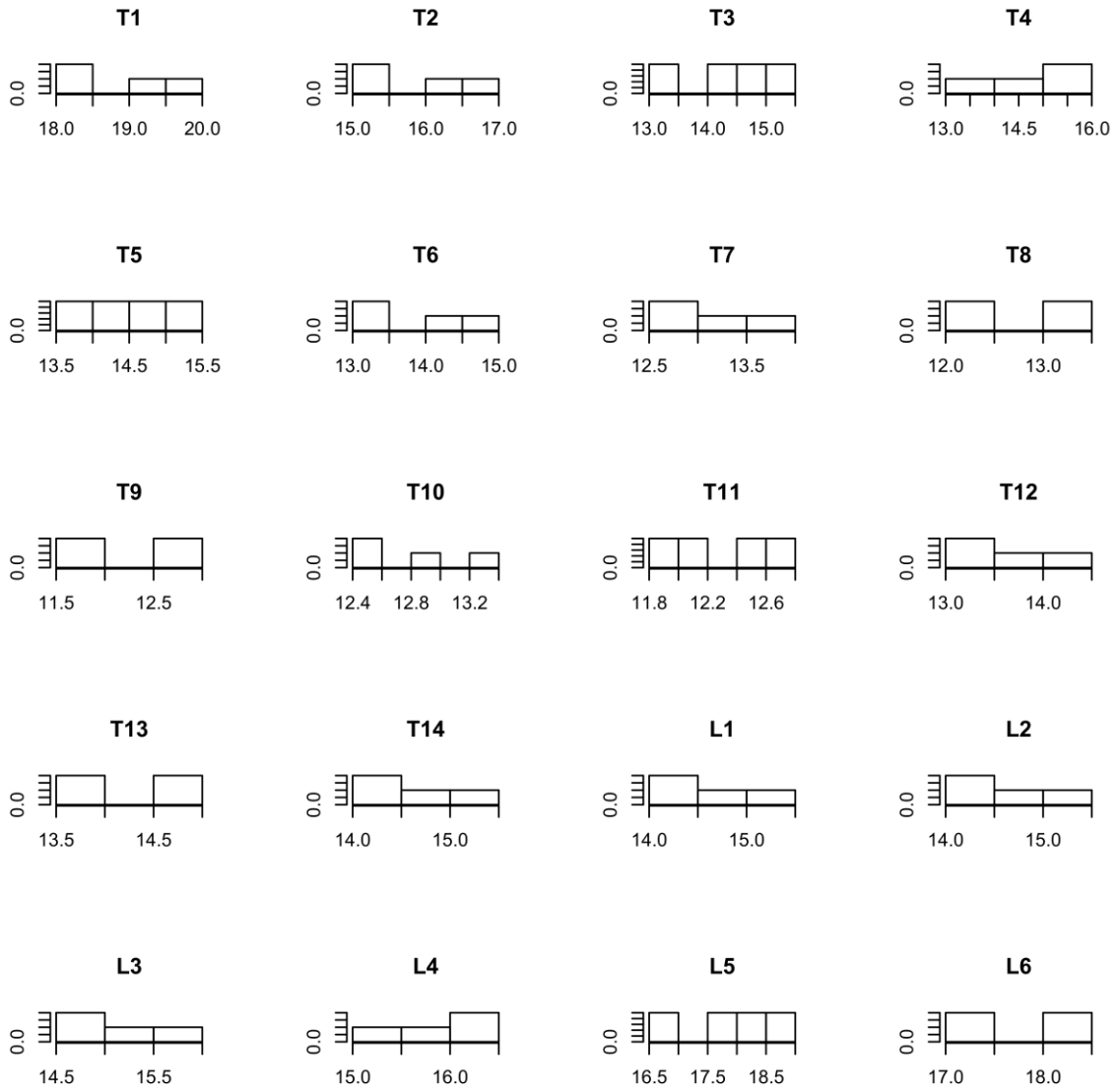
Figure B.15 – Histograms detailing sheep spinal canal width data distributions, with measurement size (mm) on the x-axis, and number of specimens on the y-axis
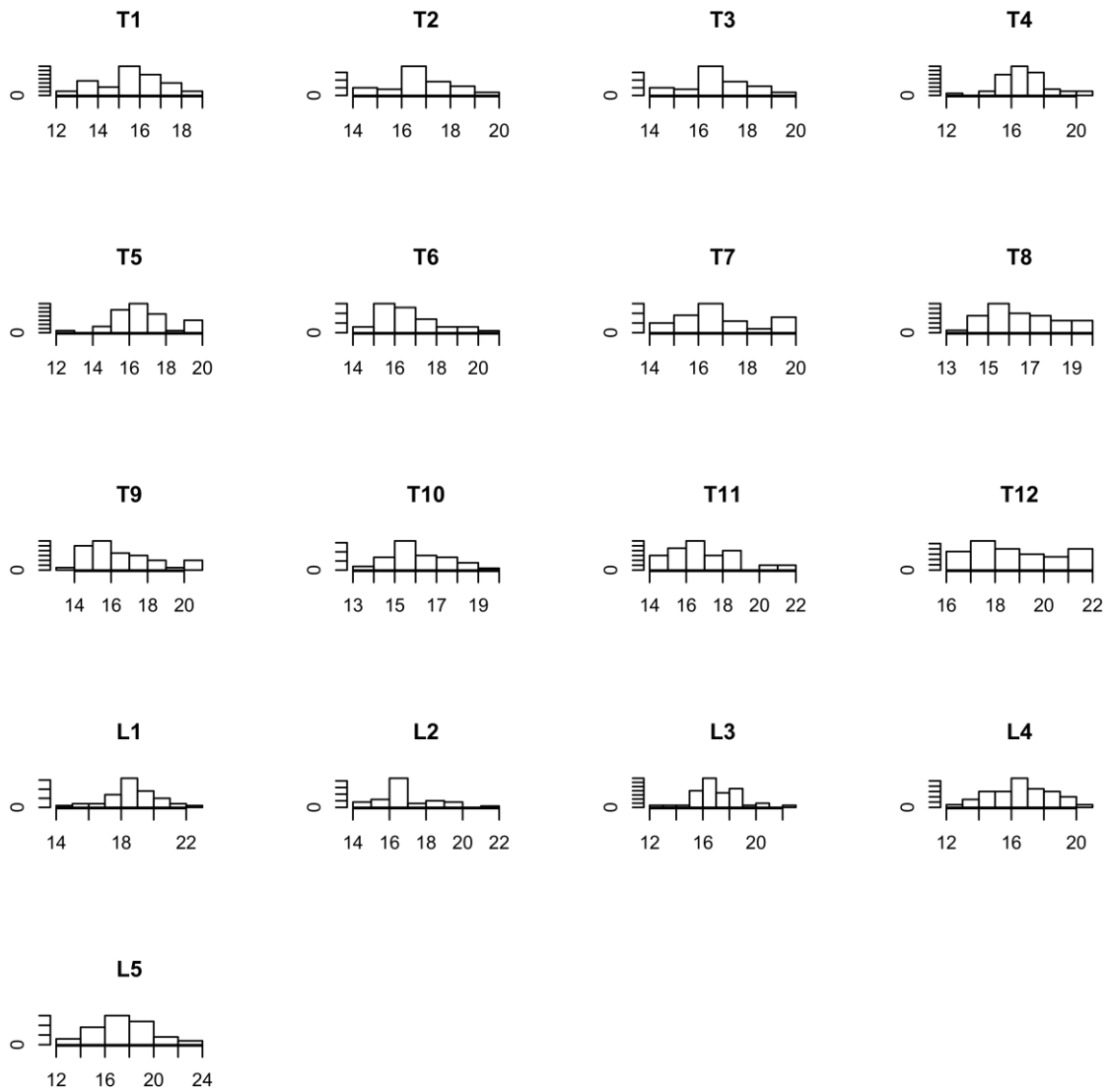
Figure B.16 – Histograms detailing human spinal canal length data distributions, with measurement size (mm) on the x-axis, and number of specimens on the y-axis
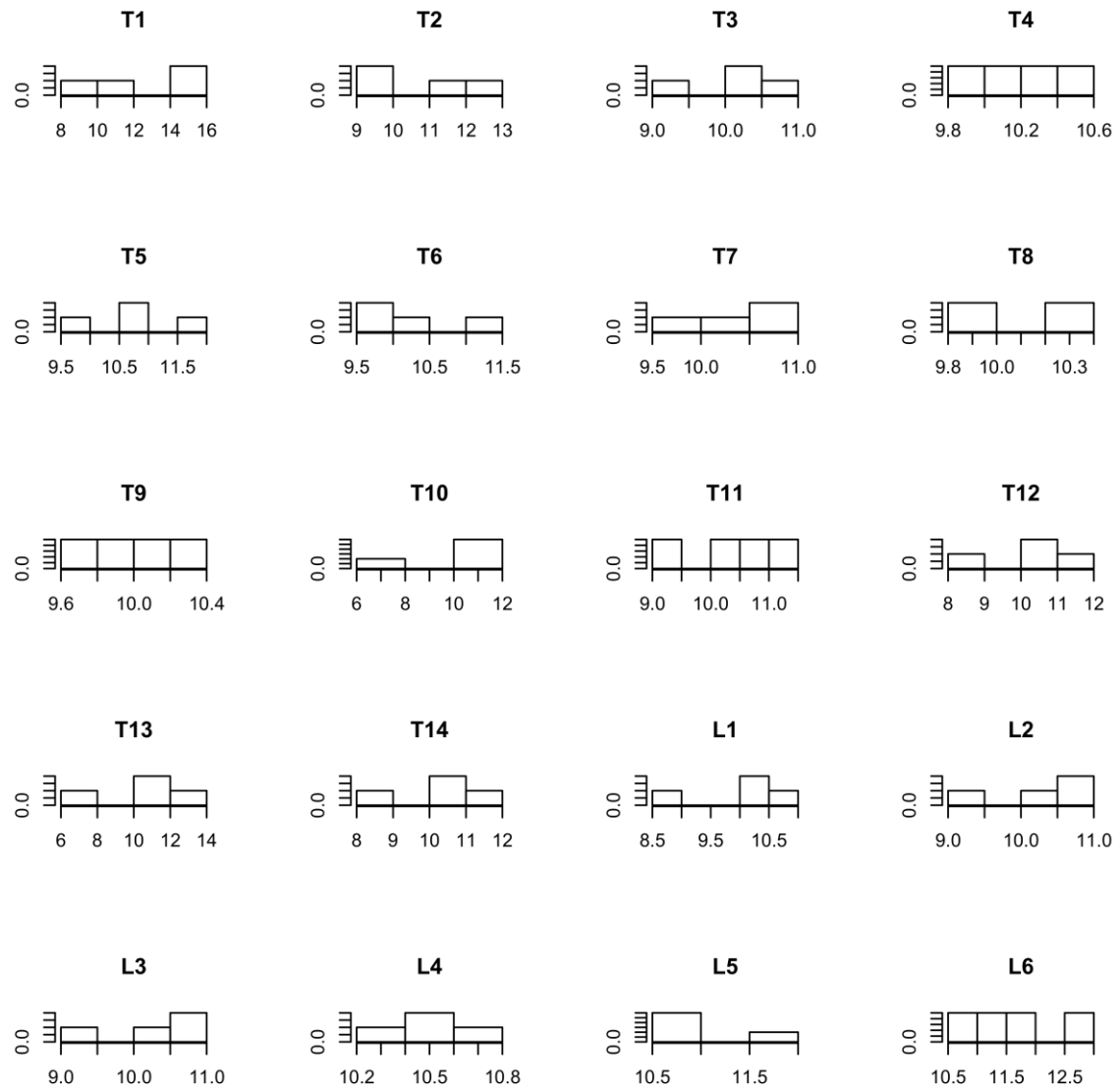
Figure B.17 – Histograms detailing pig spinal canal length data distributions, with measurement size (mm) on the x-axis, and number of specimens on the y-axis

T1

T2

T3

T4

T5

T6

T7

T8

T9

T10

T11

T12

T13

T14

L1

L2

L3

L4

L5

L6
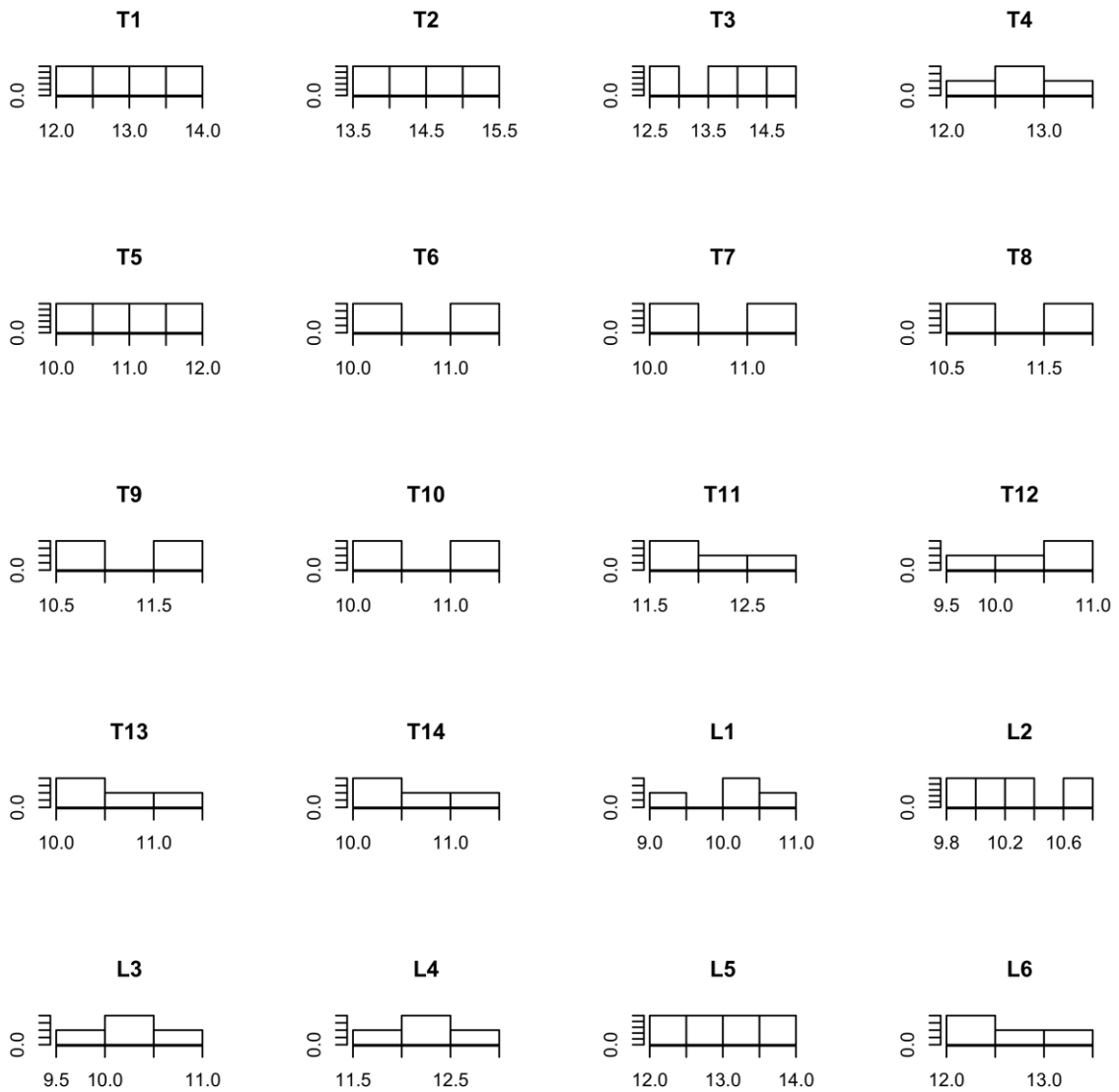
Figure B.18 – Histograms detailing sheep spinal canal length data distributions, with measurement size (mm) on the x-axis, and number of specimens on the y-axis
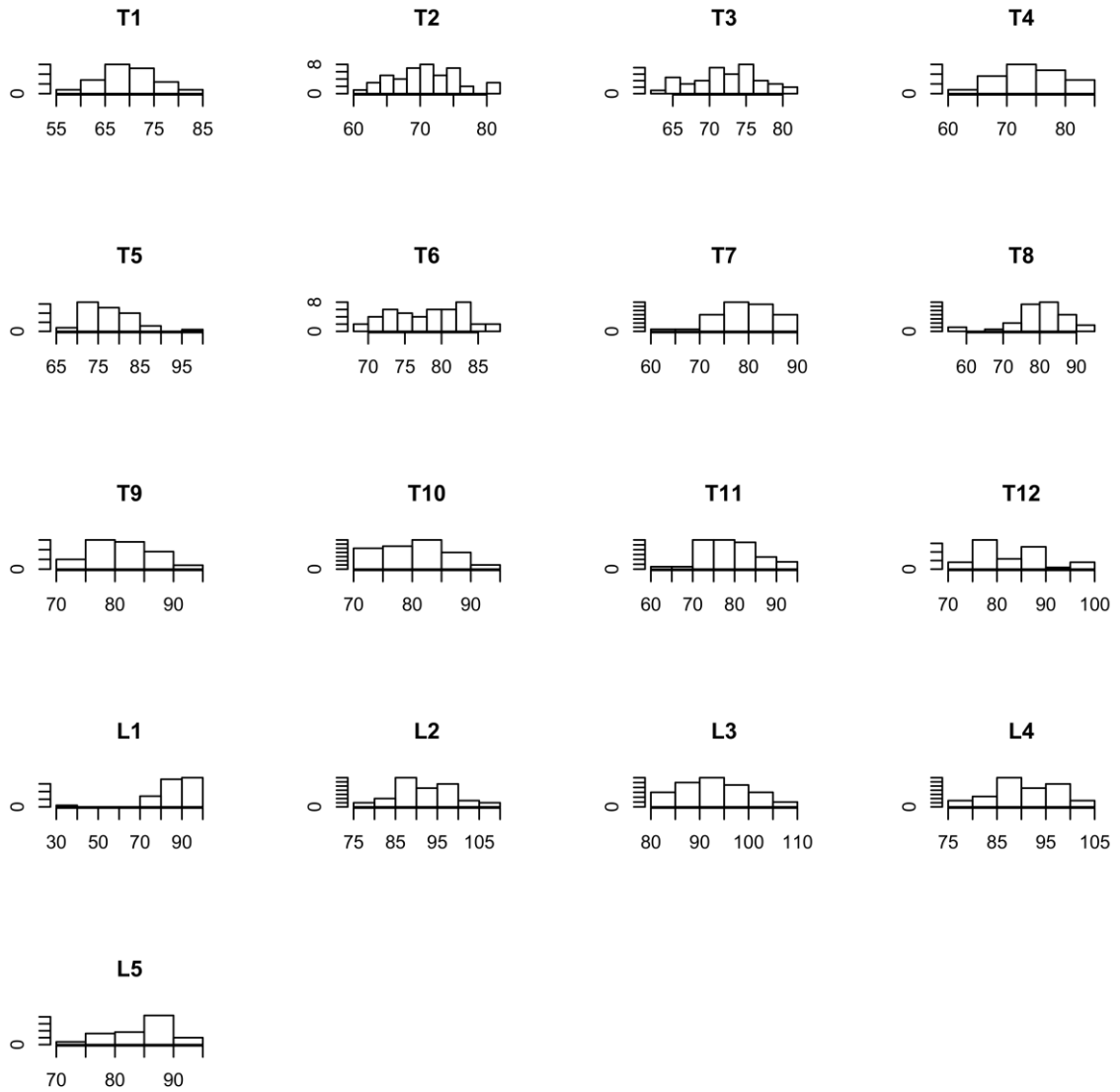
Figure B.19 – Histograms detailing human total anteroposterior length data distributions, with measurement size (mm) on the x-axis, and number of specimens on the y-axis
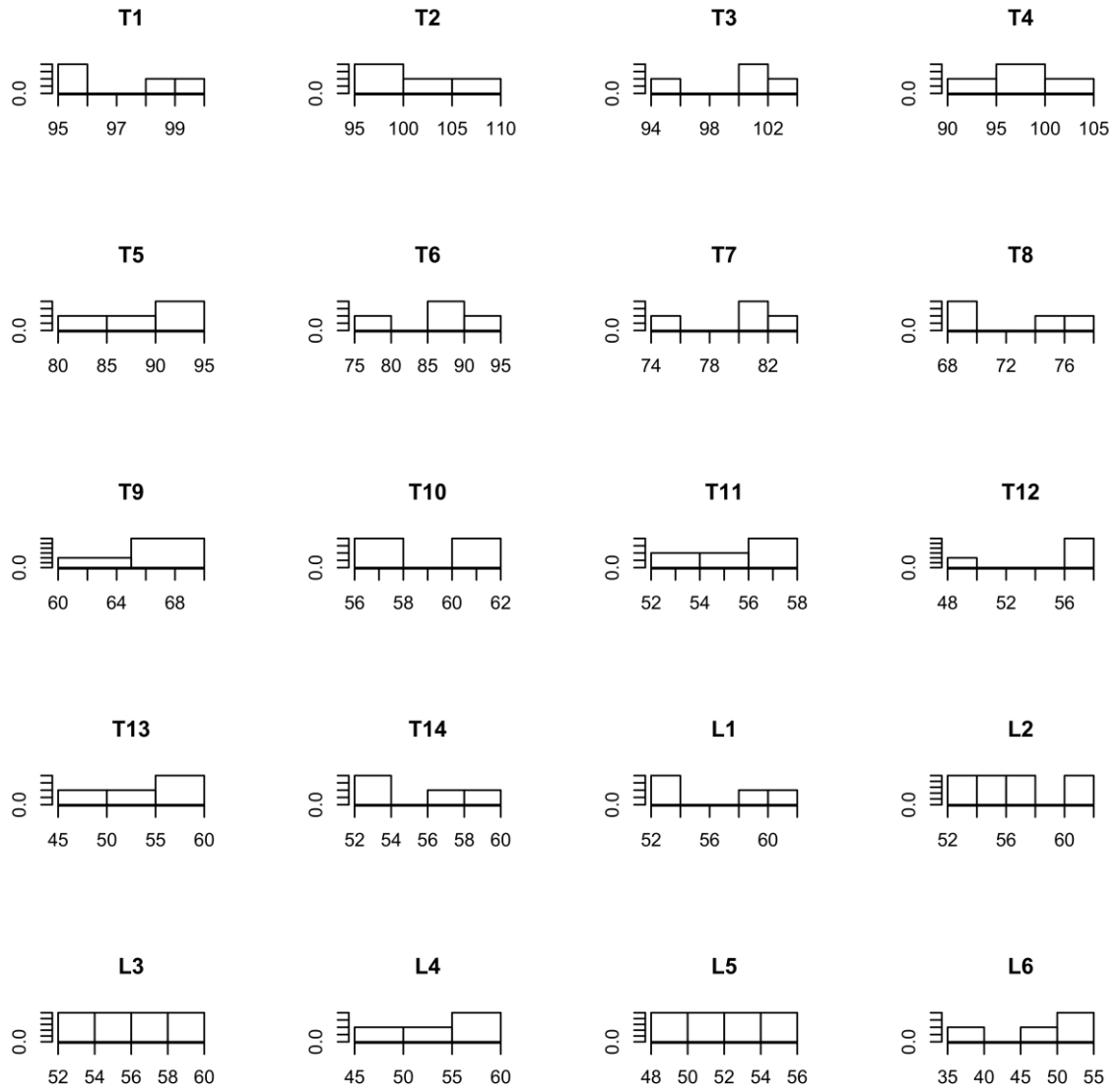
Figure B.20 – Histograms detailing pig total anteroposterior length data distributions, with measurement size (mm) on the x-axis, and number of specimens on the y-axis
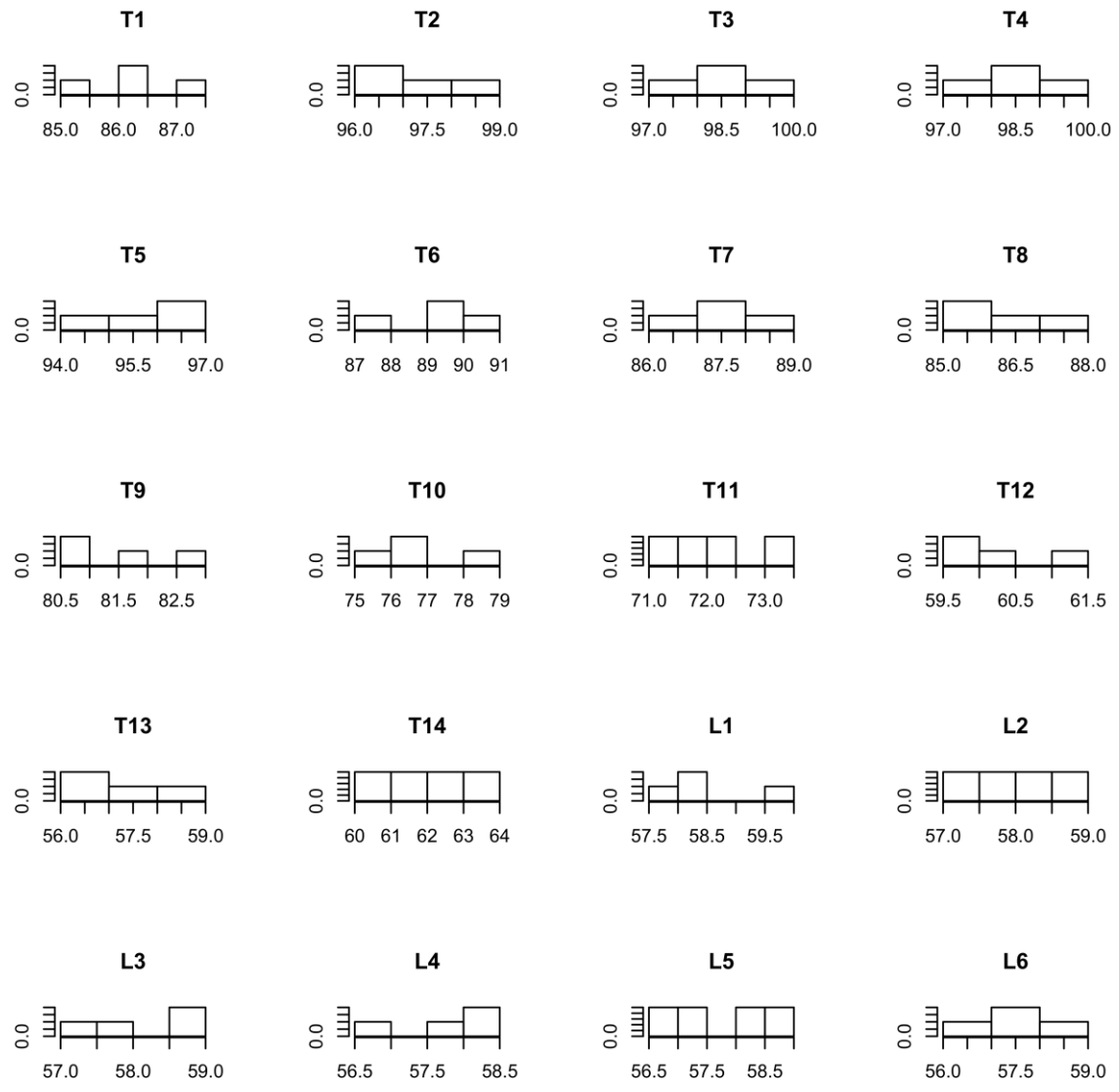
Figure B.21 – Histograms detailing sheep total anteroposterior length data distributions, with measurement size (mm) on the x-axis, and number of specimens on the y-axis
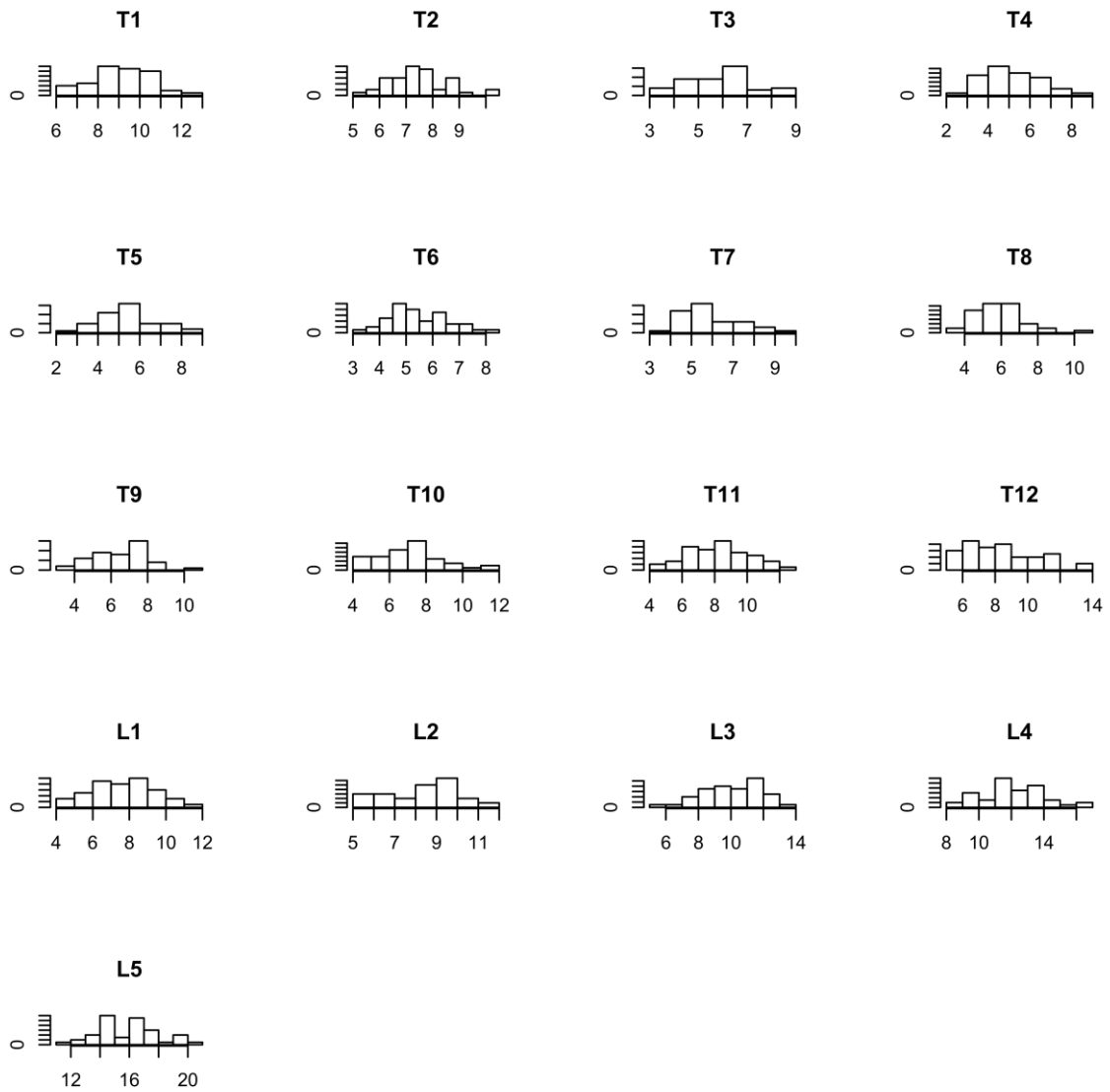
Figure B.22 – Histograms detailing human right pedicle width data distributions, with measurement size (mm) on the x-axis, and number of specimens on the y-axis
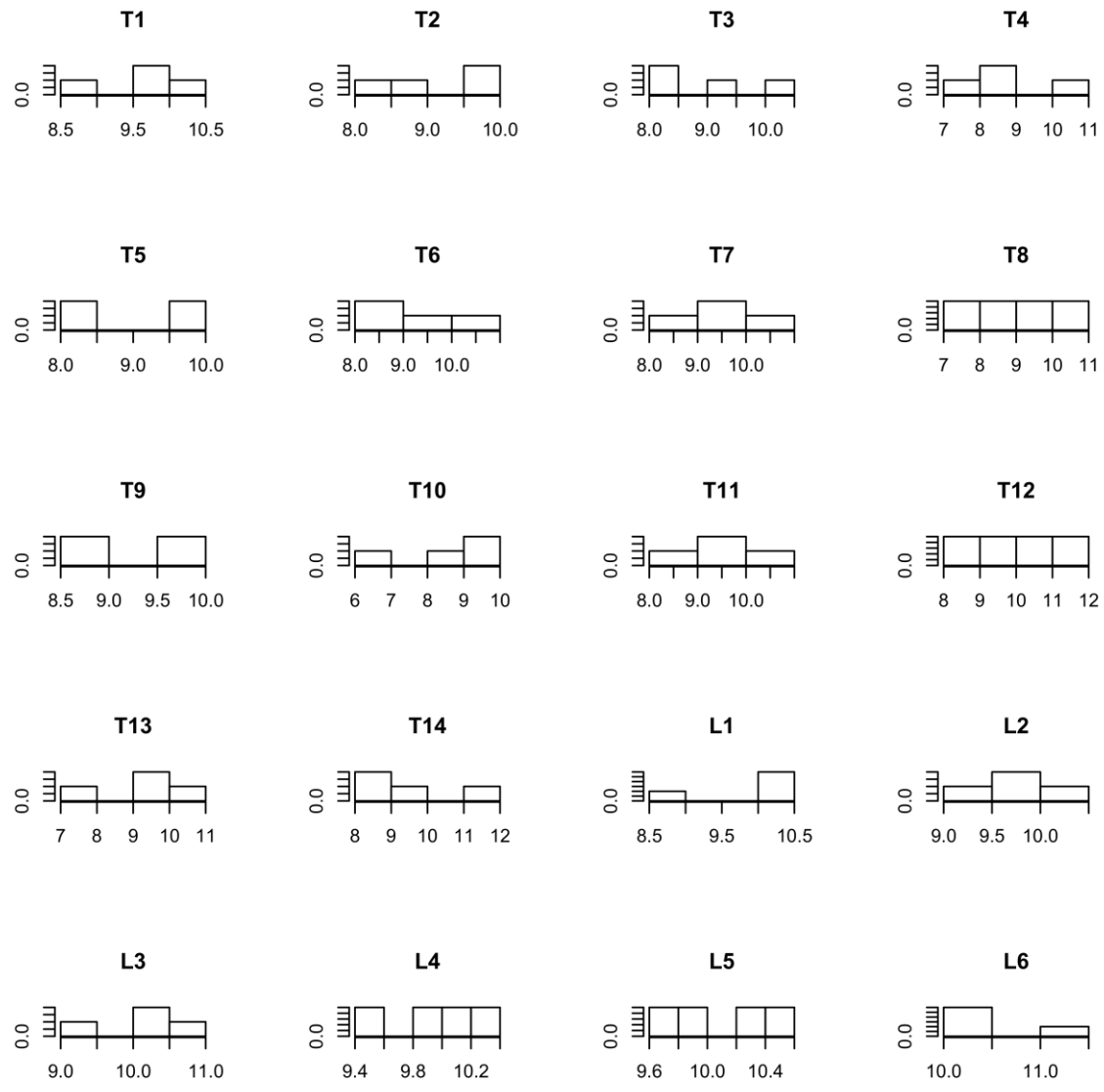
Figure B.23 – Histograms detailing pig right pedicle width data distributions, with measurement size (mm) on the x-axis, and number of specimens on the y-axis
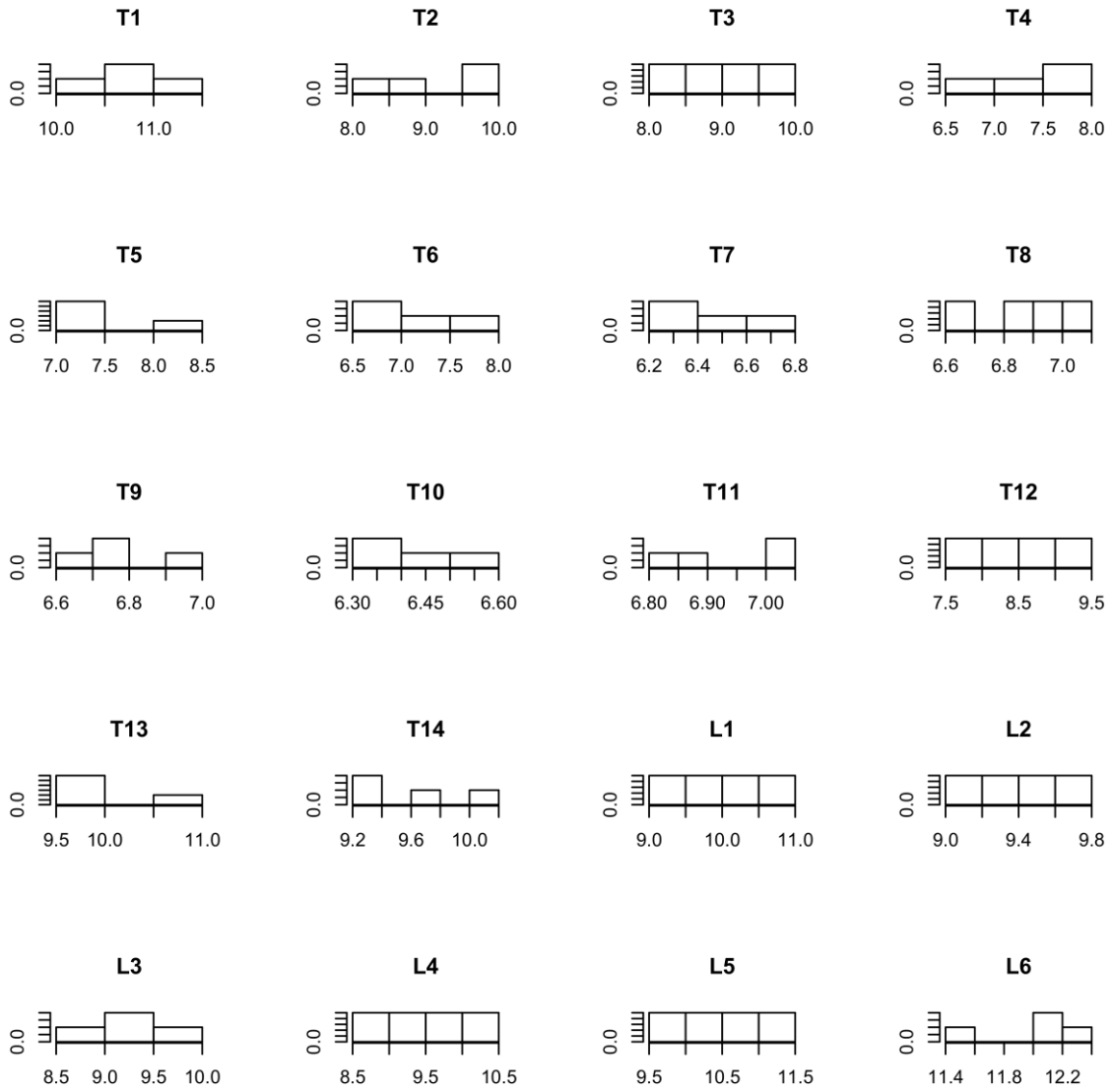
Figure B.24 – Histograms detailing sheep right pedicle width data distributions, with measurement size (mm) on the x-axis, and number of specimens on the y-axis
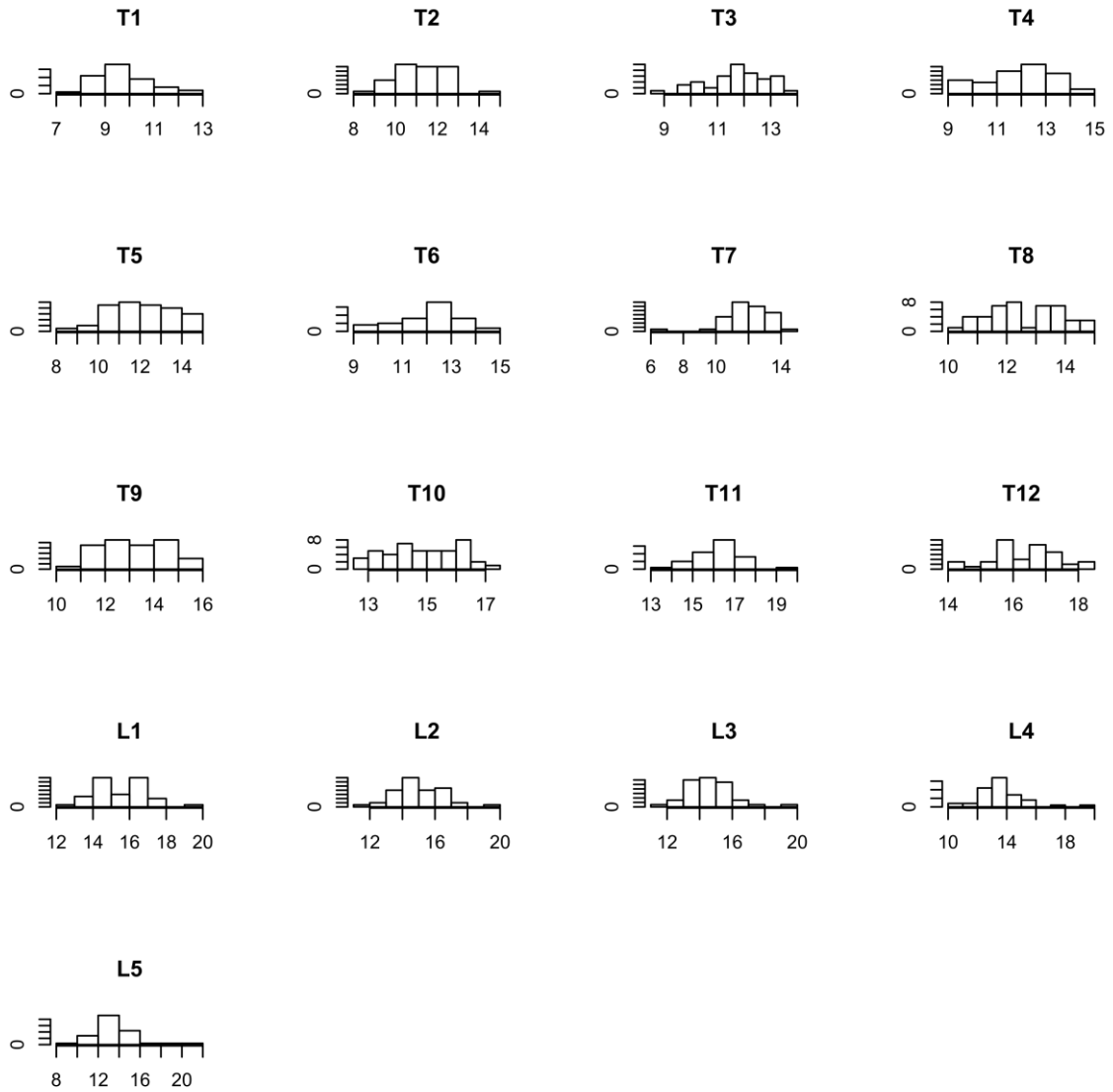
Figure B.25 – Histograms detailing human right pedicle height data distributions, with measurement size (mm) on the x-axis, and number of specimens on the y-axis
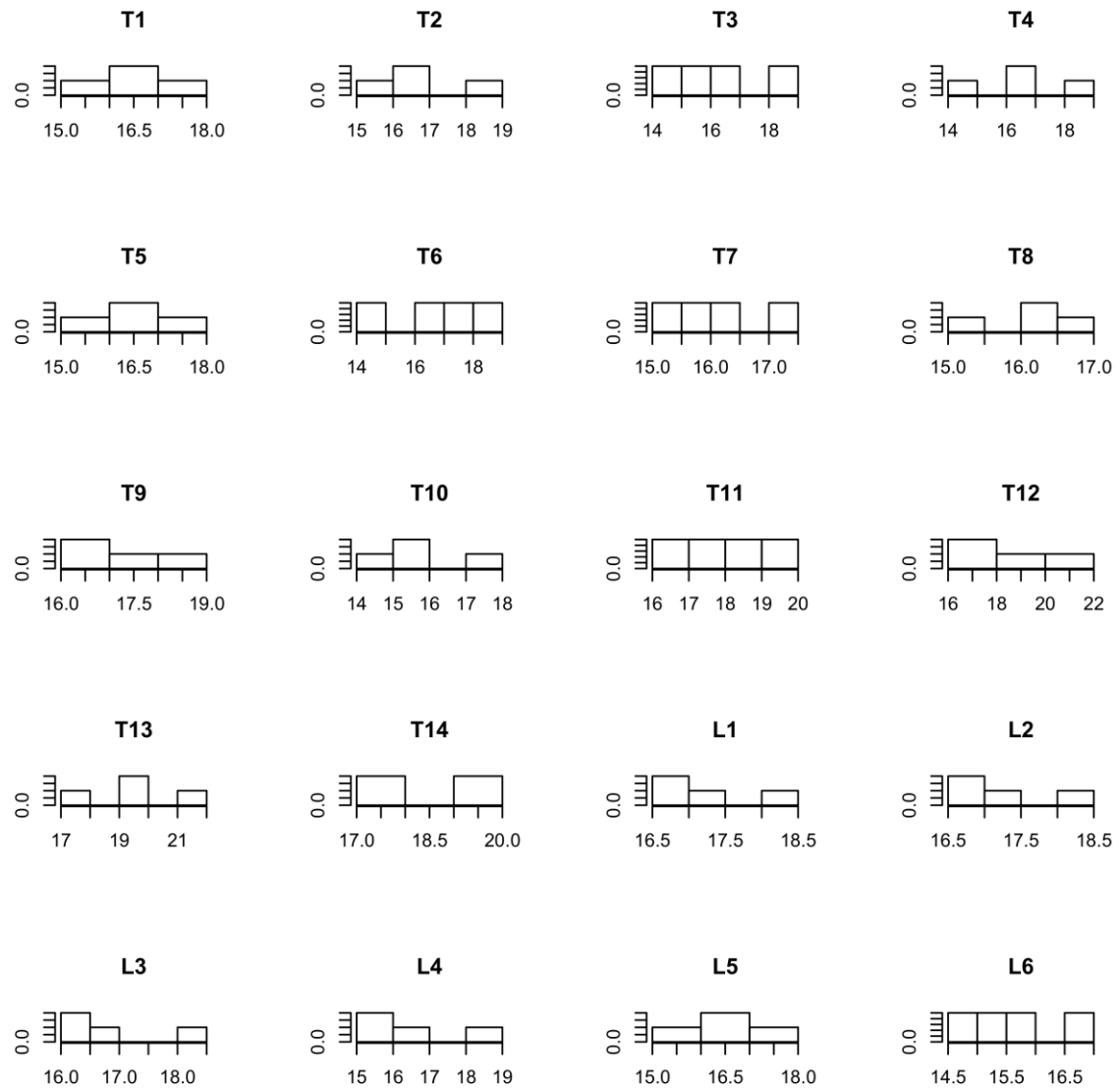
Figure B.26 – Histograms detailing pig right pedicle height data distributions, with measurement size (mm) on the x-axis, and number of specimens on the y-axis
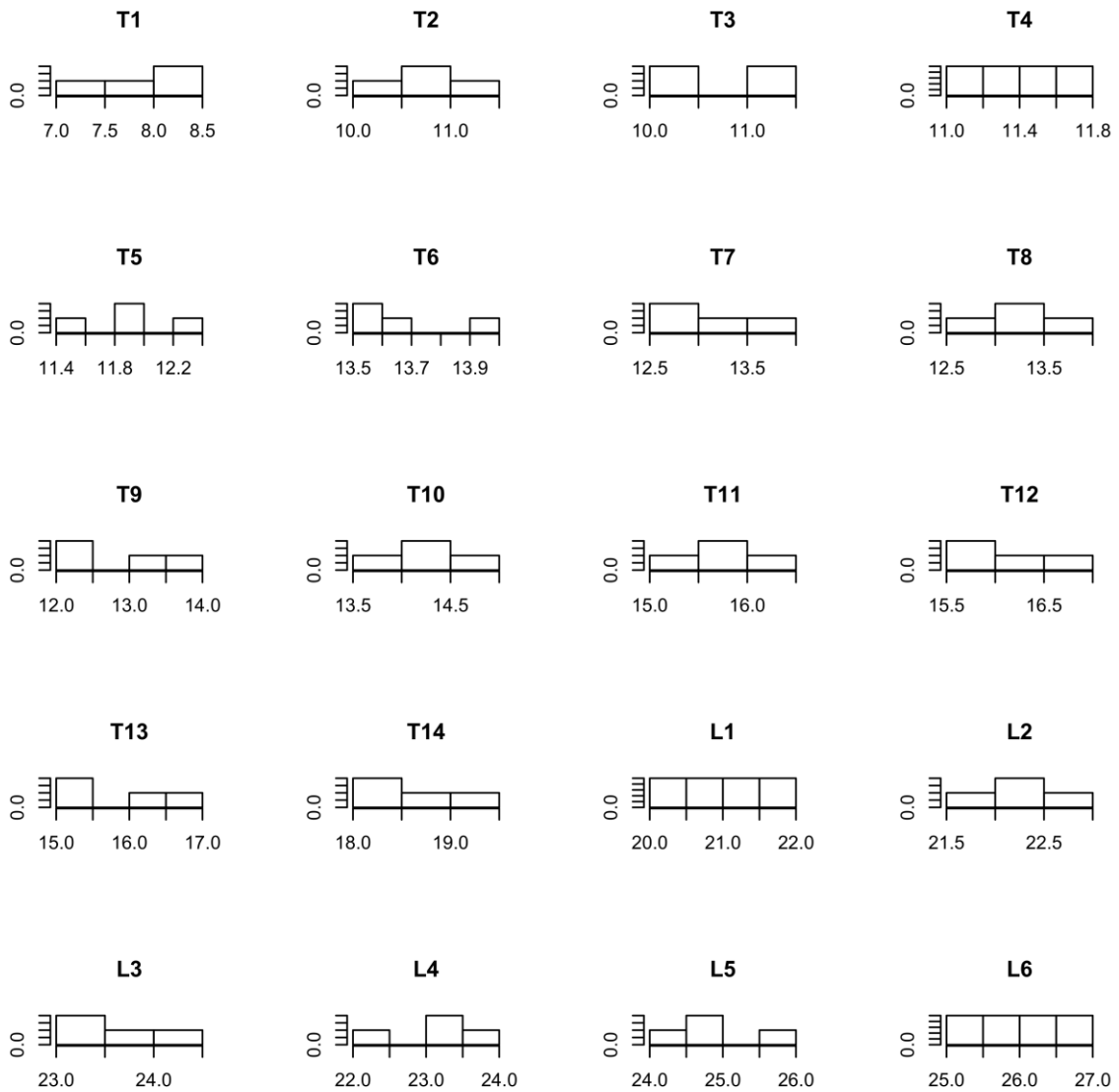
Figure B.27 – Histograms detailing sheep right pedicle height data distributions, with measurement size (mm) on the x-axis, and number of specimens on the y-axis
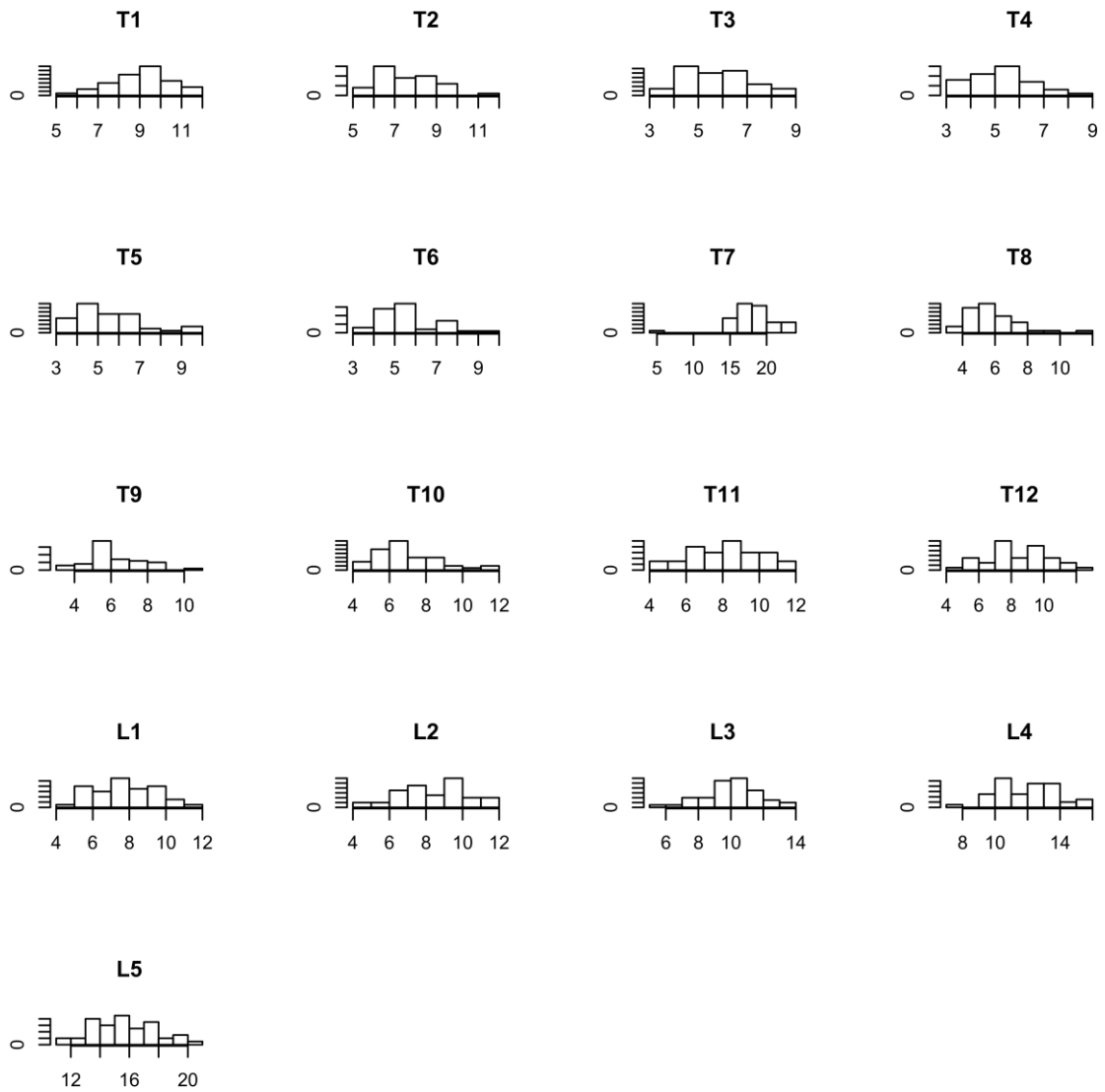
Figure B.28 – Histograms detailing human left pedicle width data distributions, with measurement size (mm) on the x-axis, and number of specimens on the y-axis
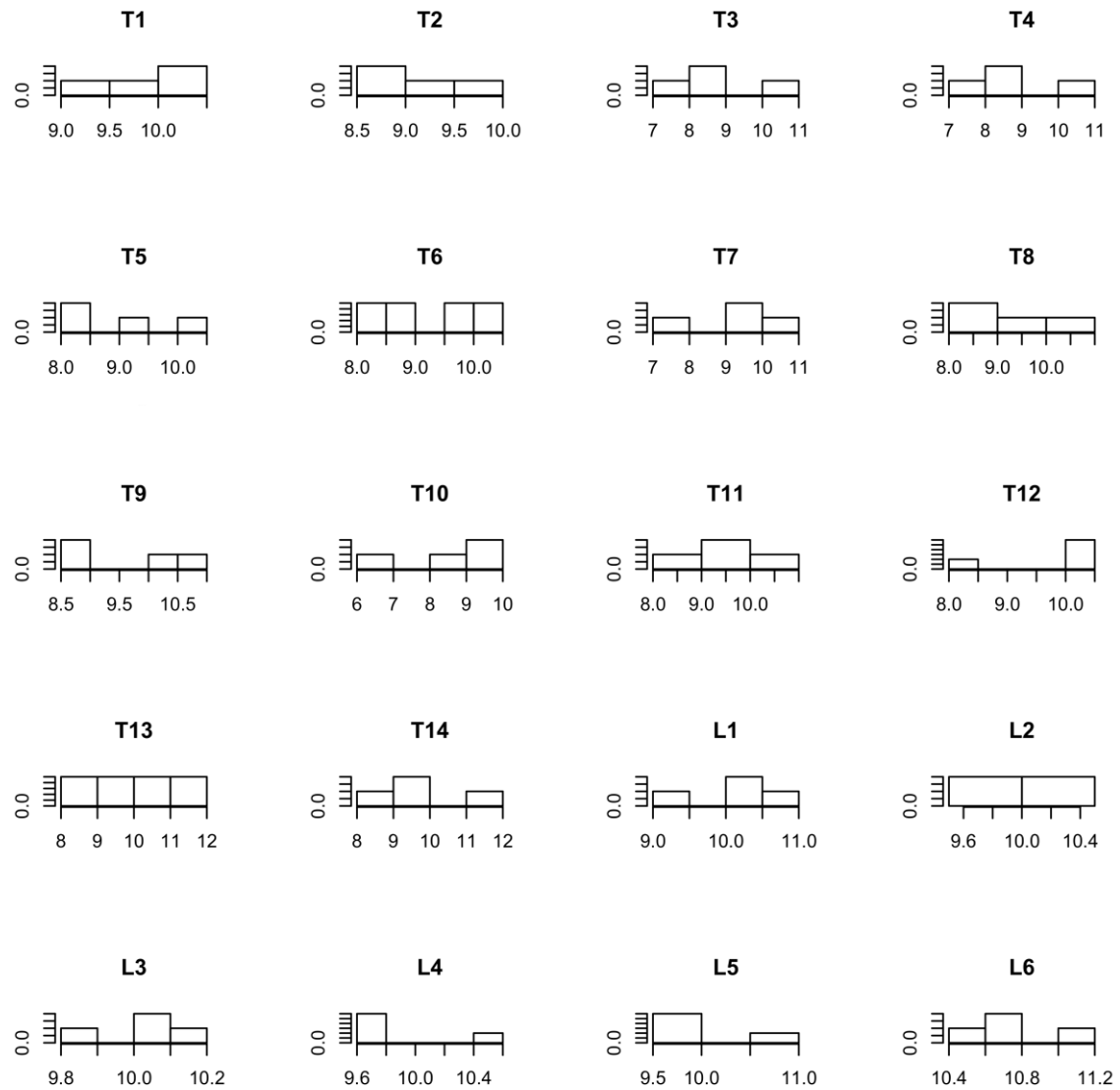
Figure B.29 – Histograms detailing pig left pedicle width data distributions, with measurement size (mm) on the x-axis, and number of specimens on the y-axis
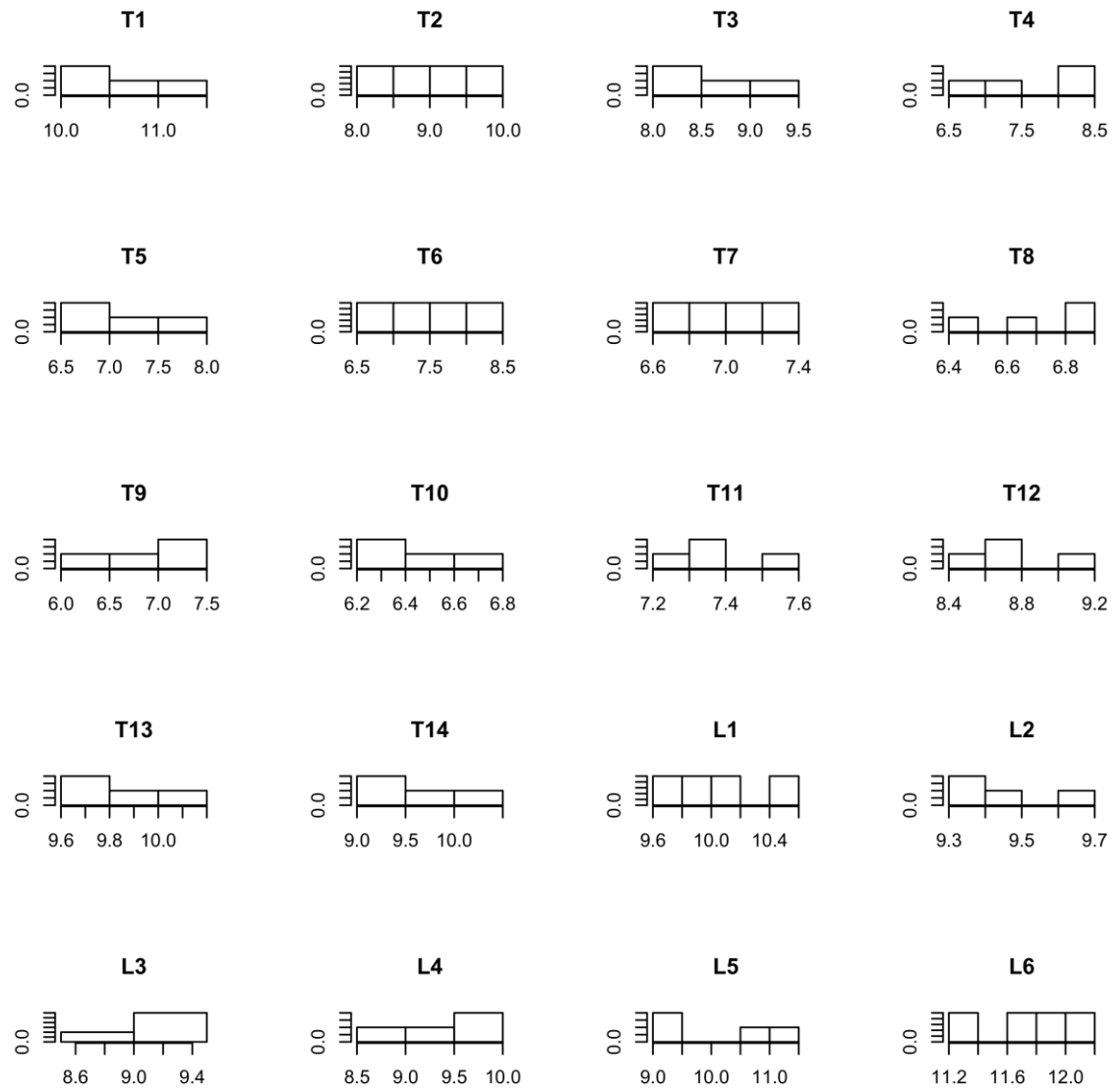
Figure B.30 – Histograms detailing sheep left pedicle width data distributions, with measurement size (mm) on the x-axis, and number of specimens on the y-axis
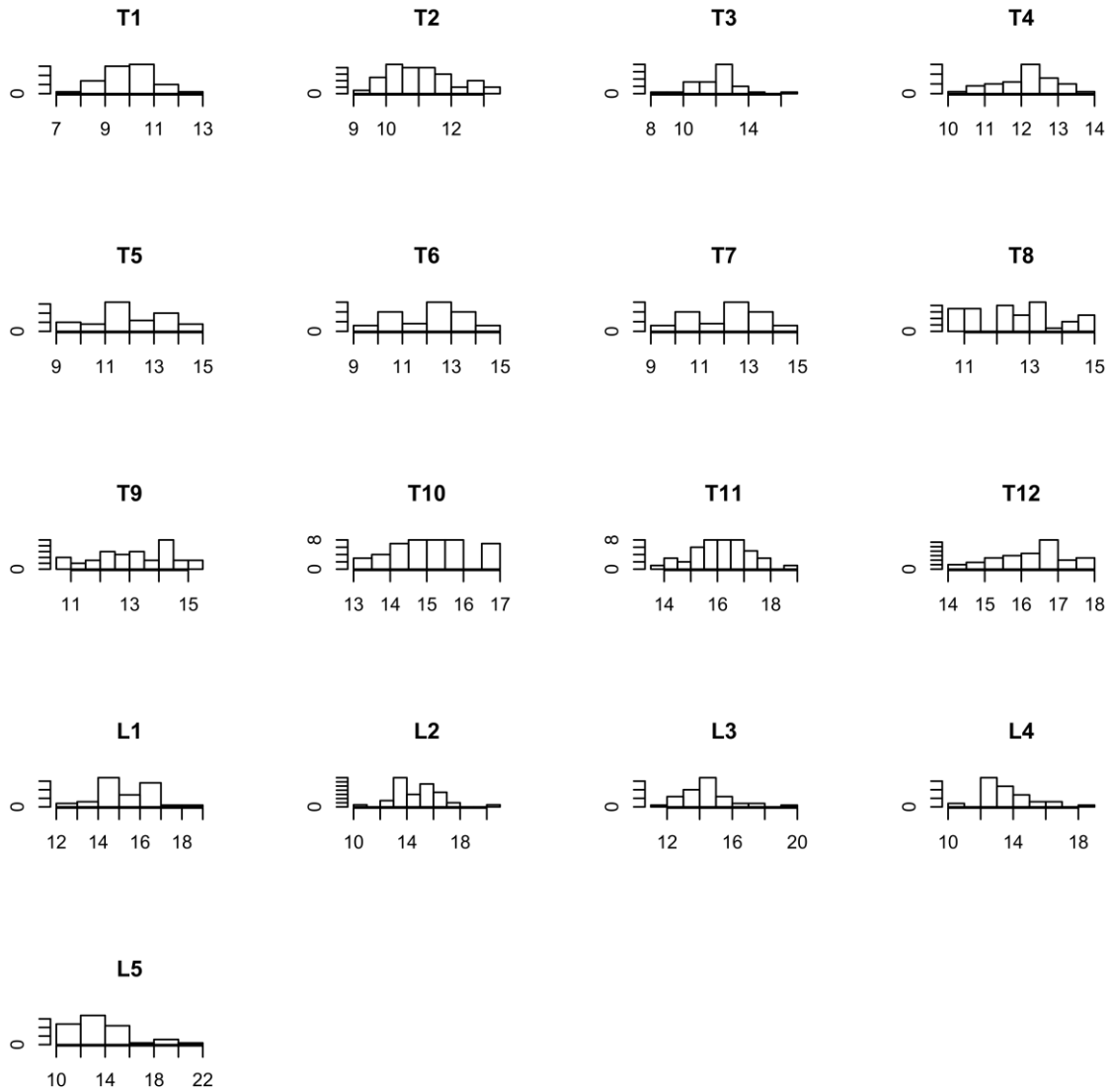
Figure B.31 – Histograms detailing human left pedicle height data distributions, with measurement size (mm) on the x-axis, and number of specimens on the y-axis
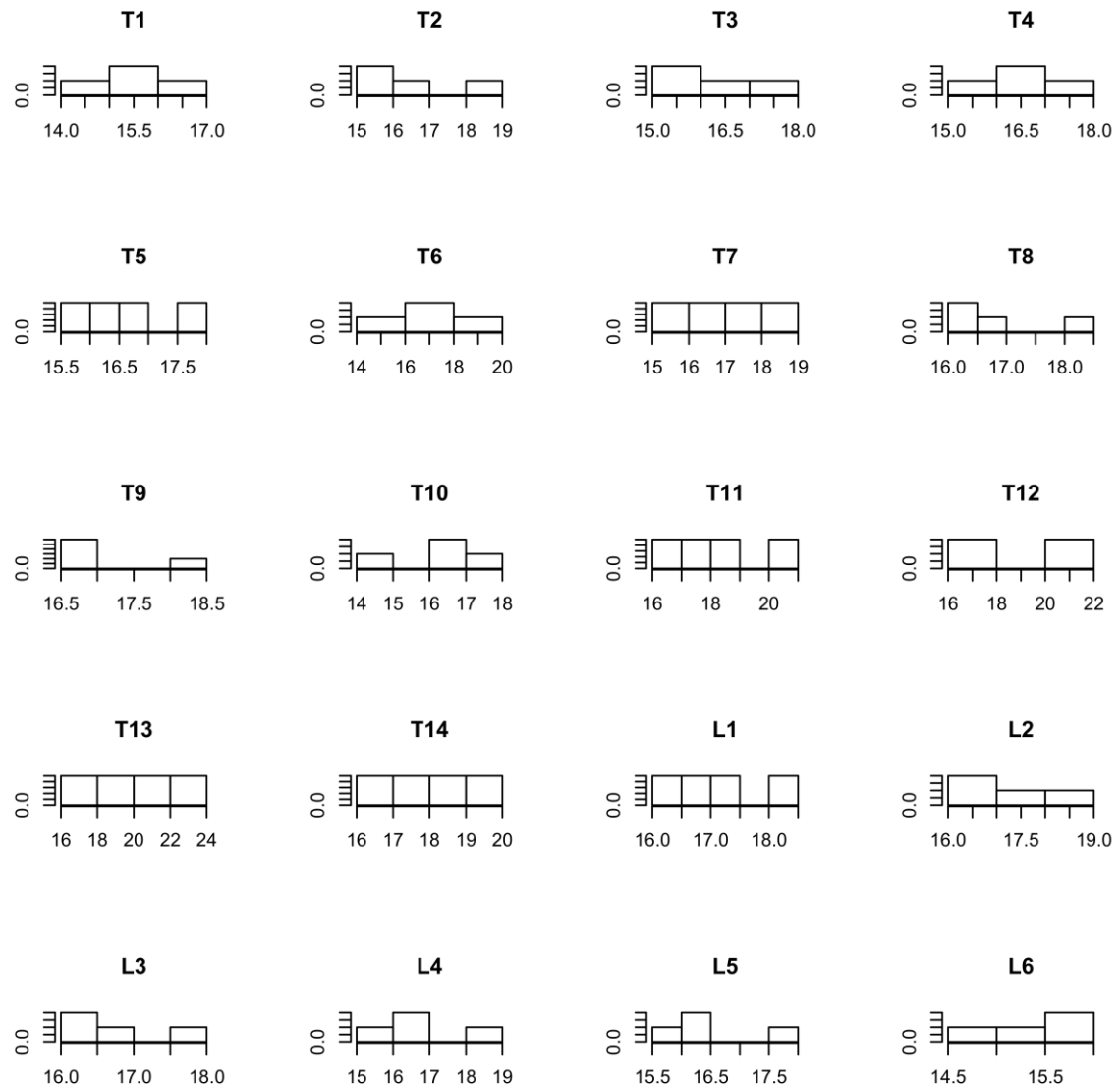
Figure B.32 - Histograms detailing pig left pedicle height data distributions, with measurement size (mm) on the x-axis, and number of specimens on the y-axis
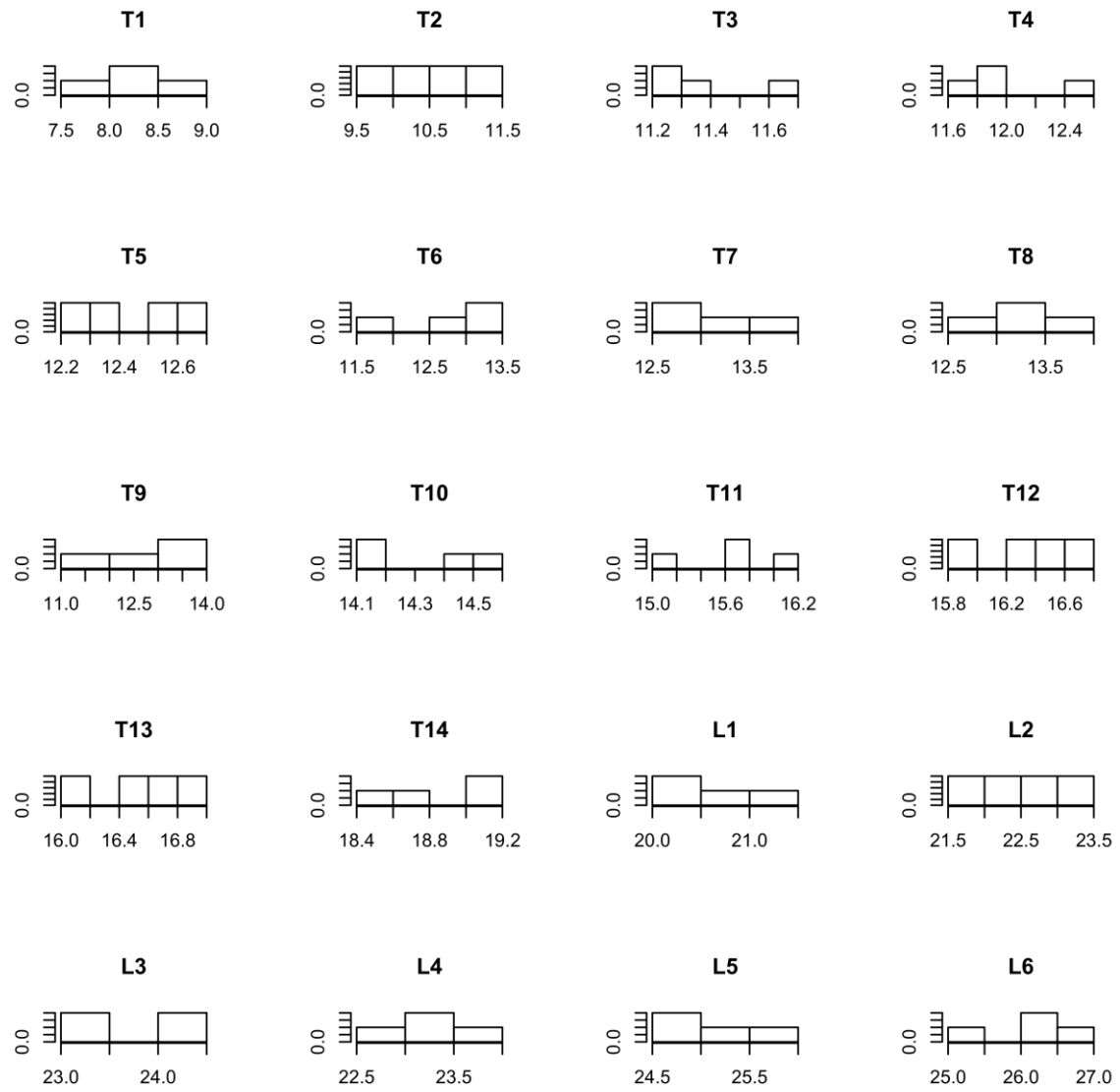
Figure B.33 – Histograms detailing sheep left pedicle height data distributions, with measurement size (mm) on the x-axis, and number of specimens on the y-axis

C – Q-Q PLOTS FOR HUMAN, PIG AND SHEEP MORPHOMETRIC CT MEASUREMENTS
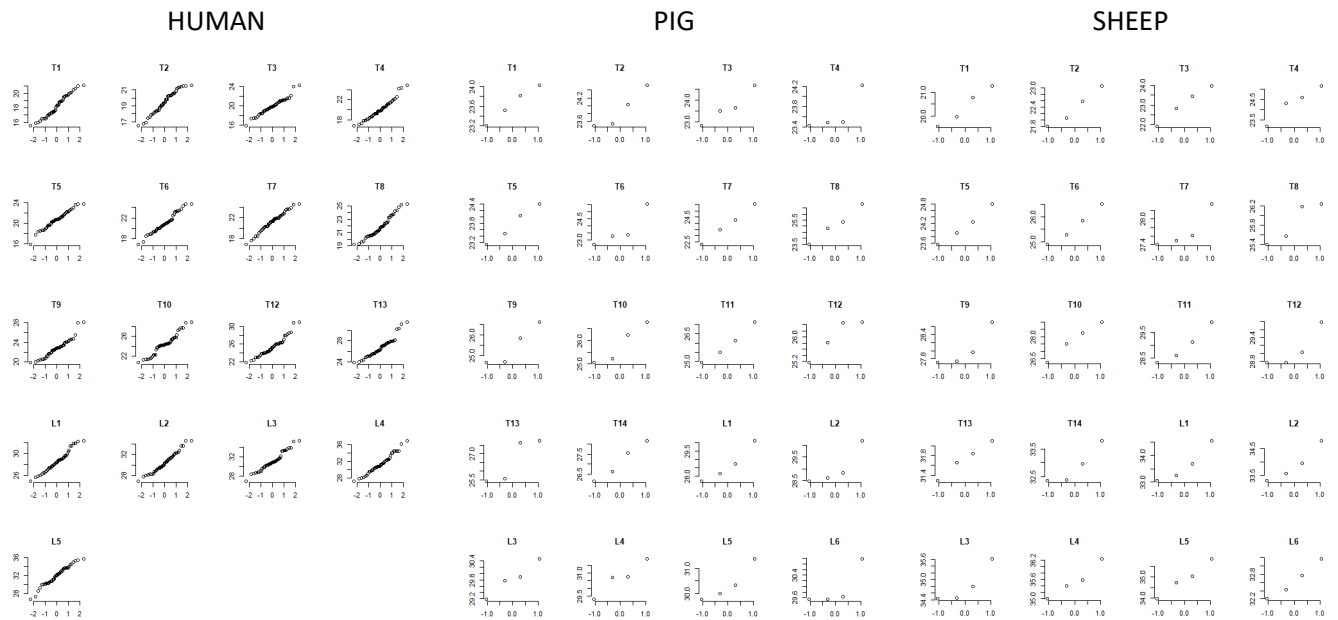
Figure C.1 – Q-Q plots showing vertebral body height data distribution for human, pig, and sheep CT measurements
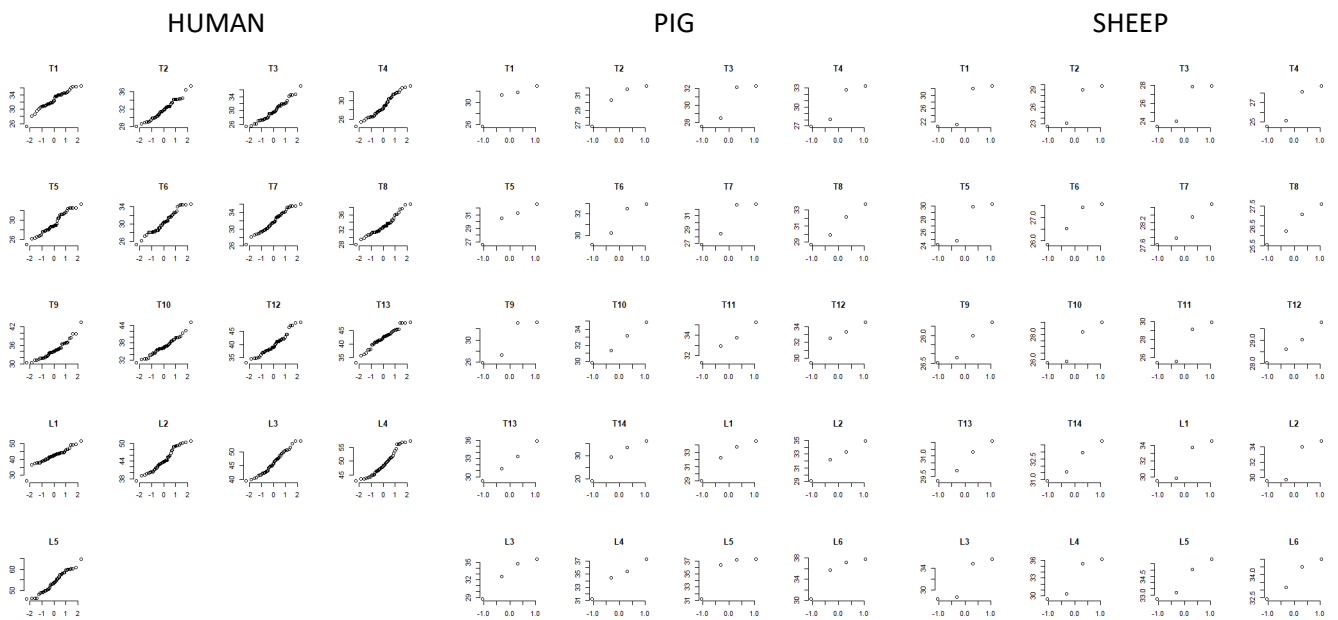
Figure C.2 – Q-Q plots showing vertebral body width data distribution for human, pig, and sheep CT measurements
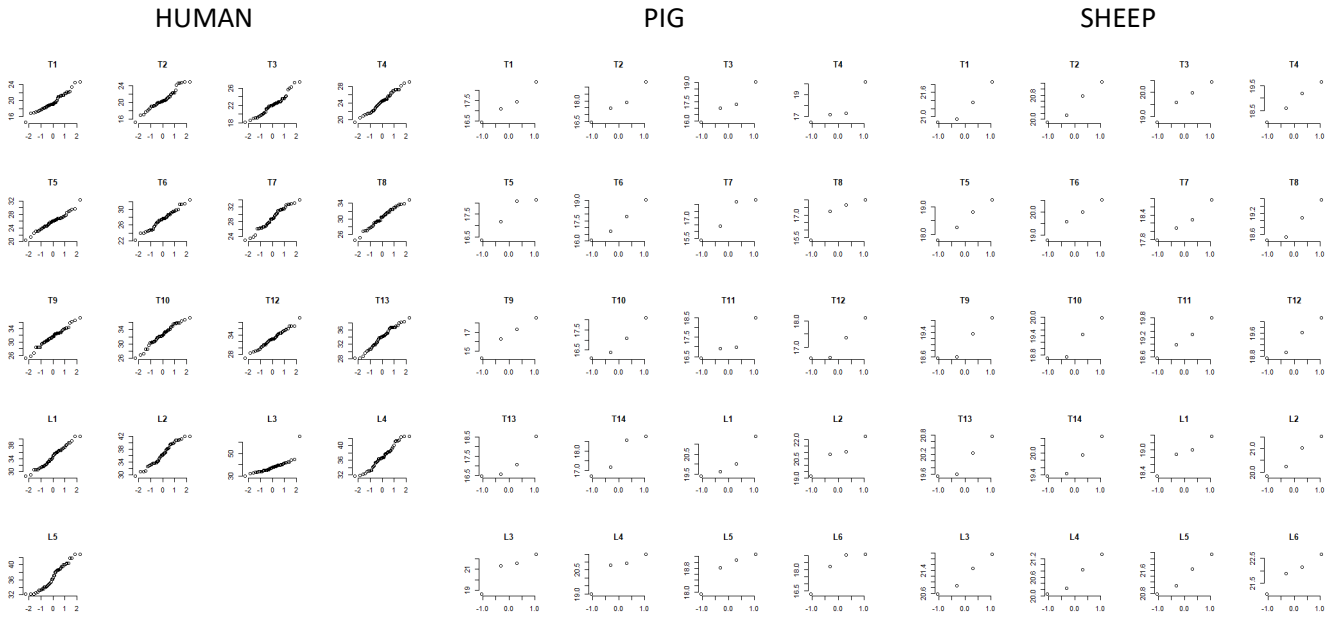
Figure C.3 – Q-Q plots showing vertebral body length data distribution for human, pig, and sheep CT measurements
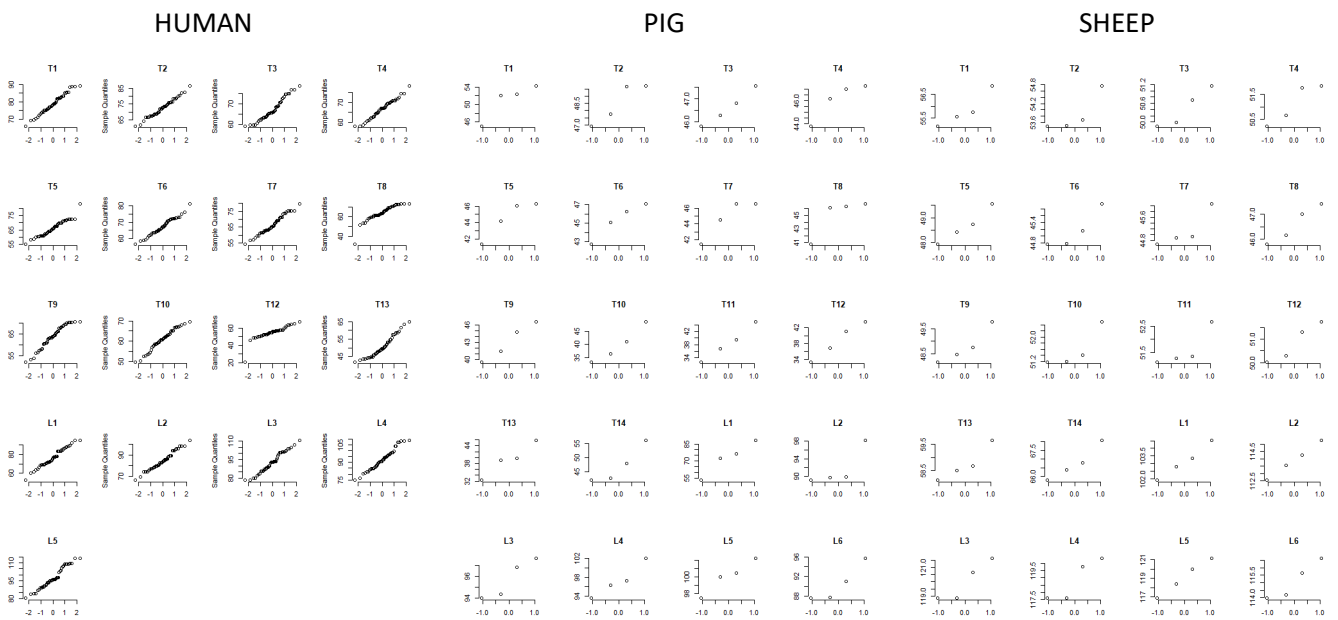
Figure C.4 – Q-Q plots showing transverse process width data distribution for human, pig, and sheep CT measurements
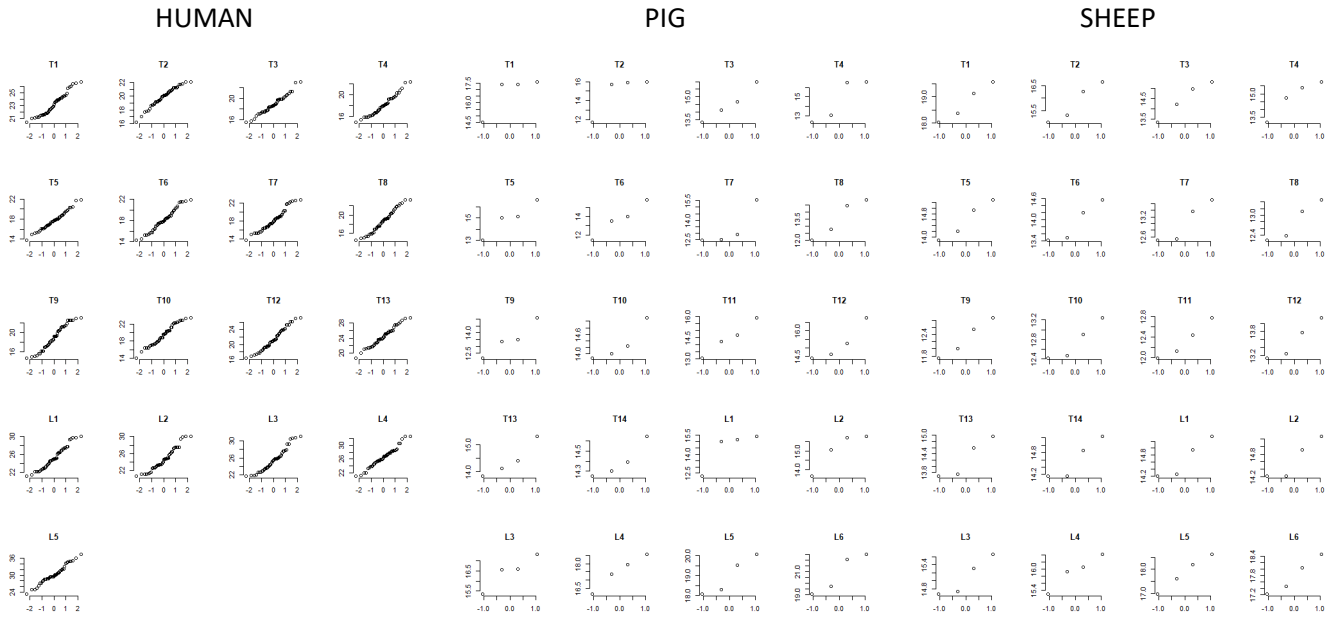
Figure C.5 – Q-Q plots showing spinal canal width data distribution for human, pig, and sheep CT measurements
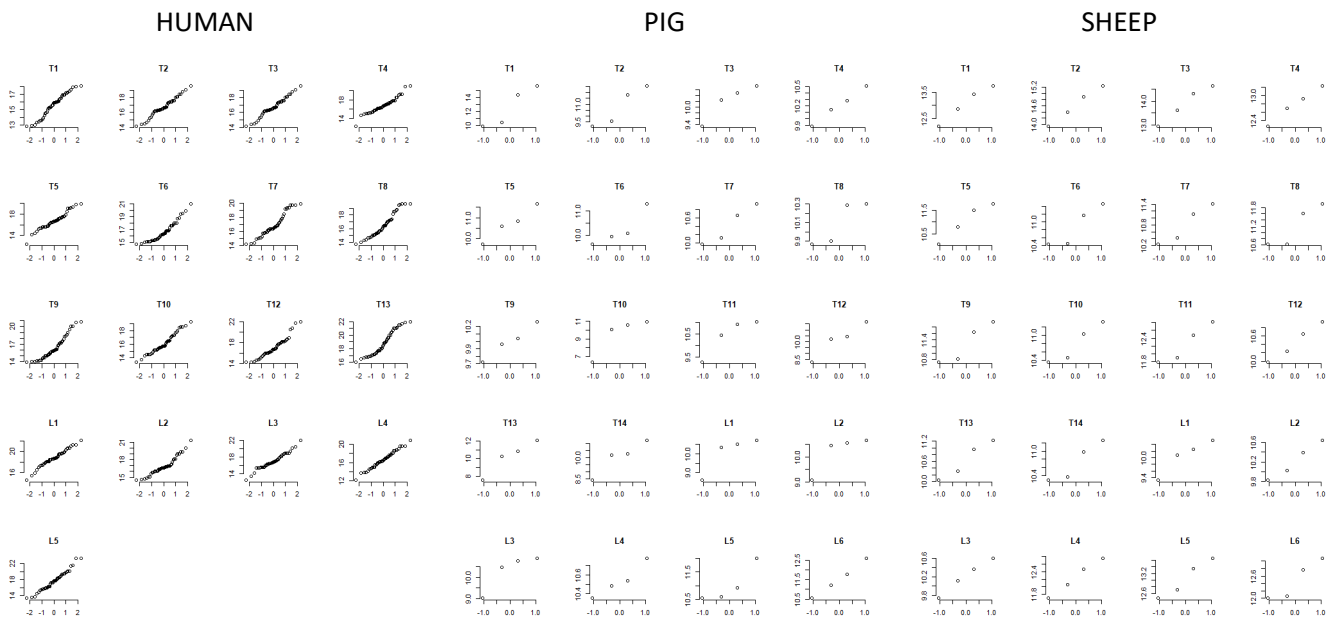
Figure C.6 – Q-Q plots showing spinal canal length data distribution for human, pig, and sheep CT measurements
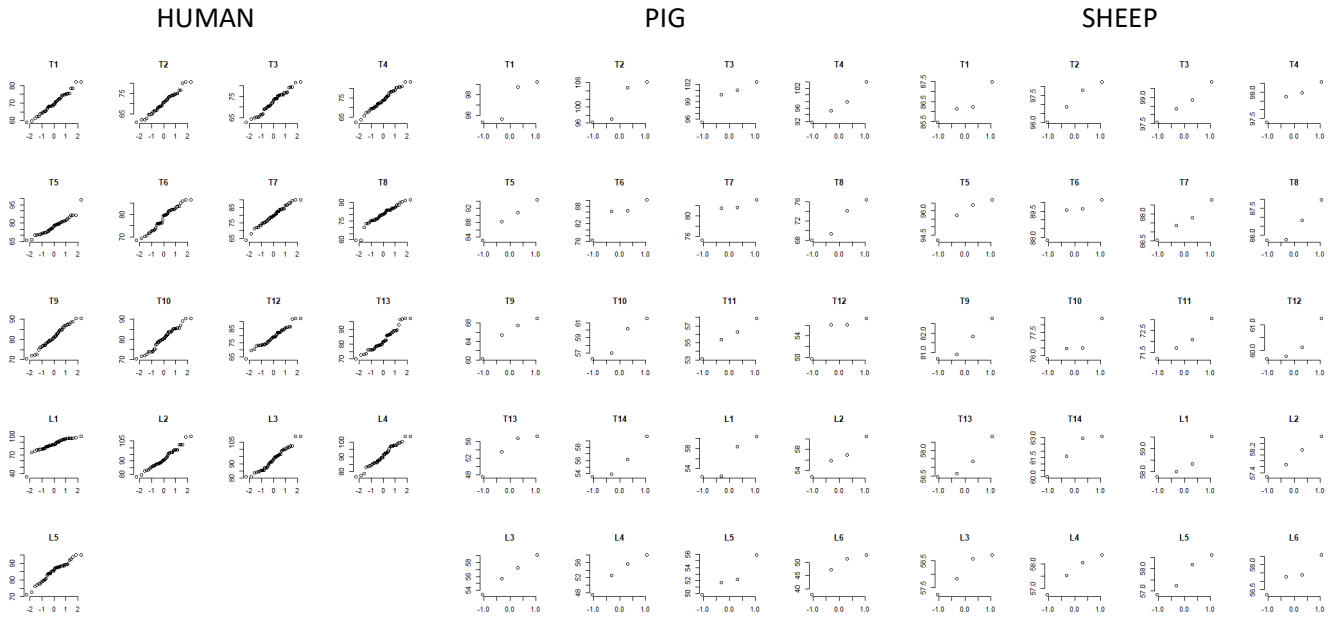
Figure C.7 – Q-Q plots showing total anteroposterior length data distribution for human, pig, and sheep CT measurements
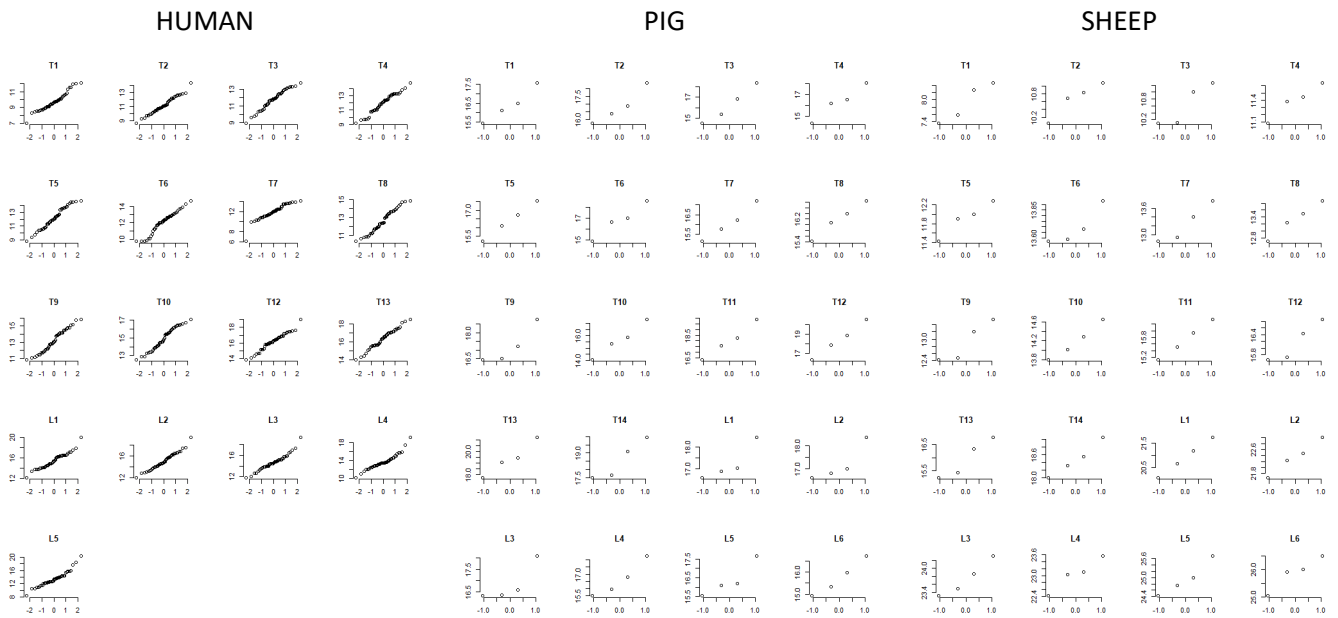
Figure C.8 – Q-Q plots showing right pedicle height data distribution for human, pig, and sheep CT measurements
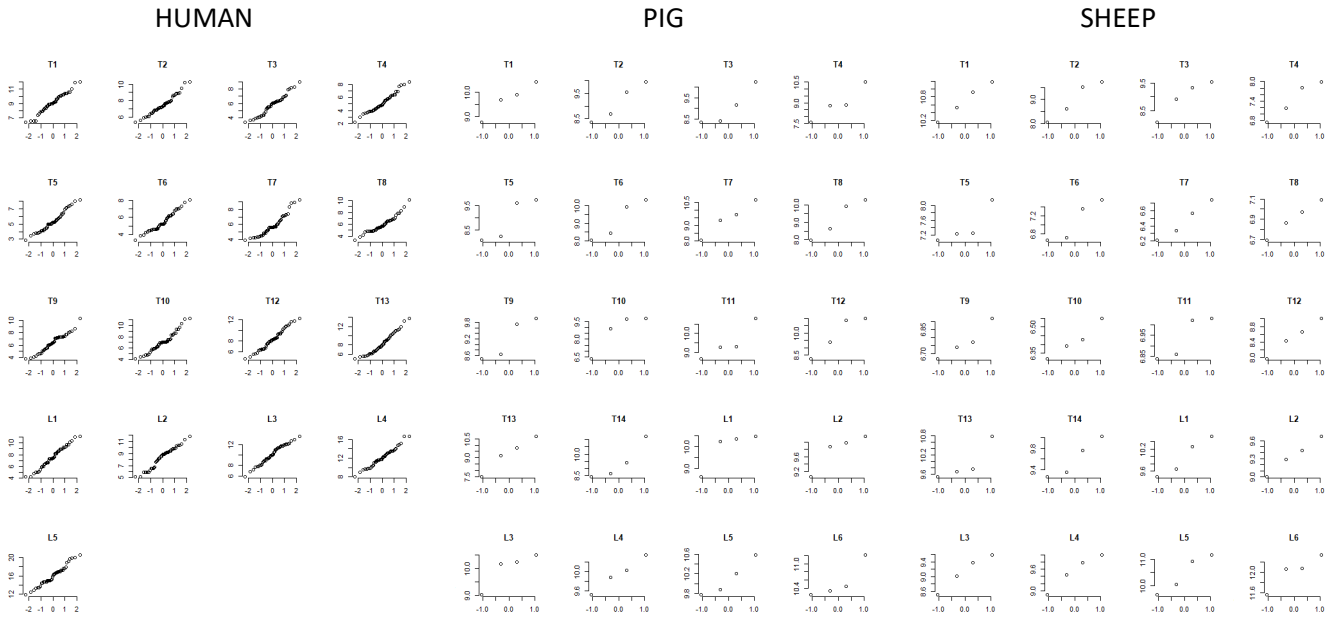
HUMAN PIG SHEEP

Figure C.9 – Q-Q plots showing right pedicle width data distribution for human, pig, and sheep CT measurements
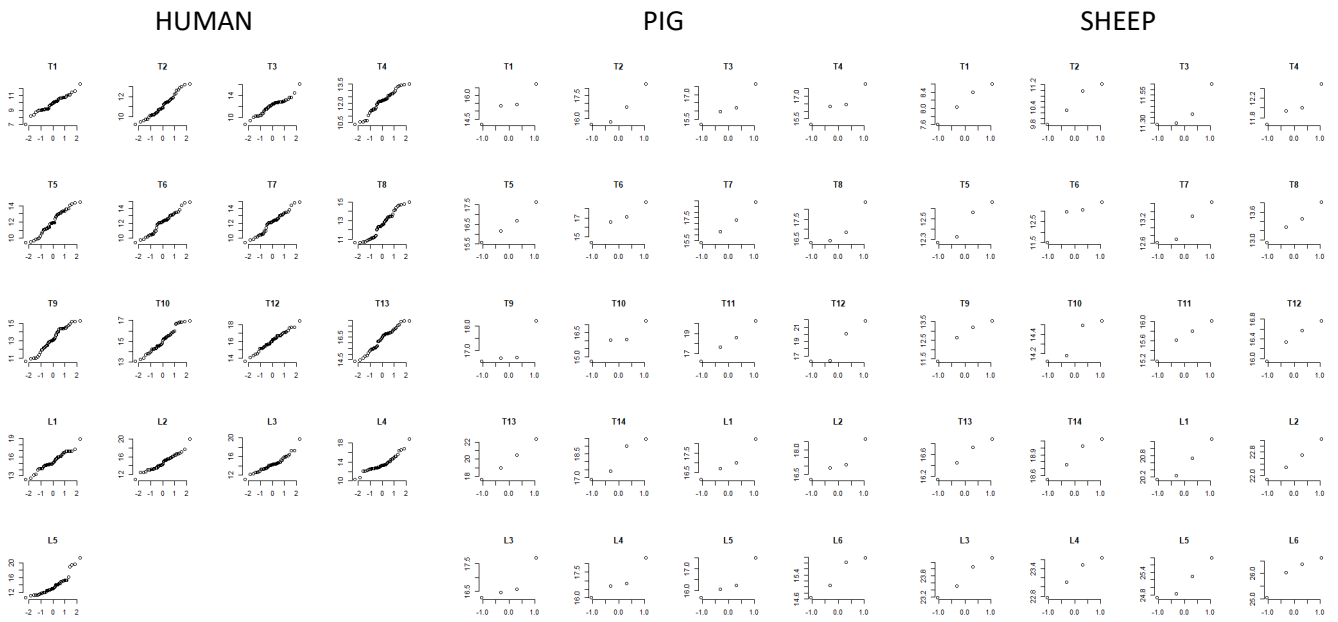
HUMAN PIG SHEEP

Figure C.10 – Q-Q plots showing left pedicle height data distribution for human, pig, and sheep CT measurements
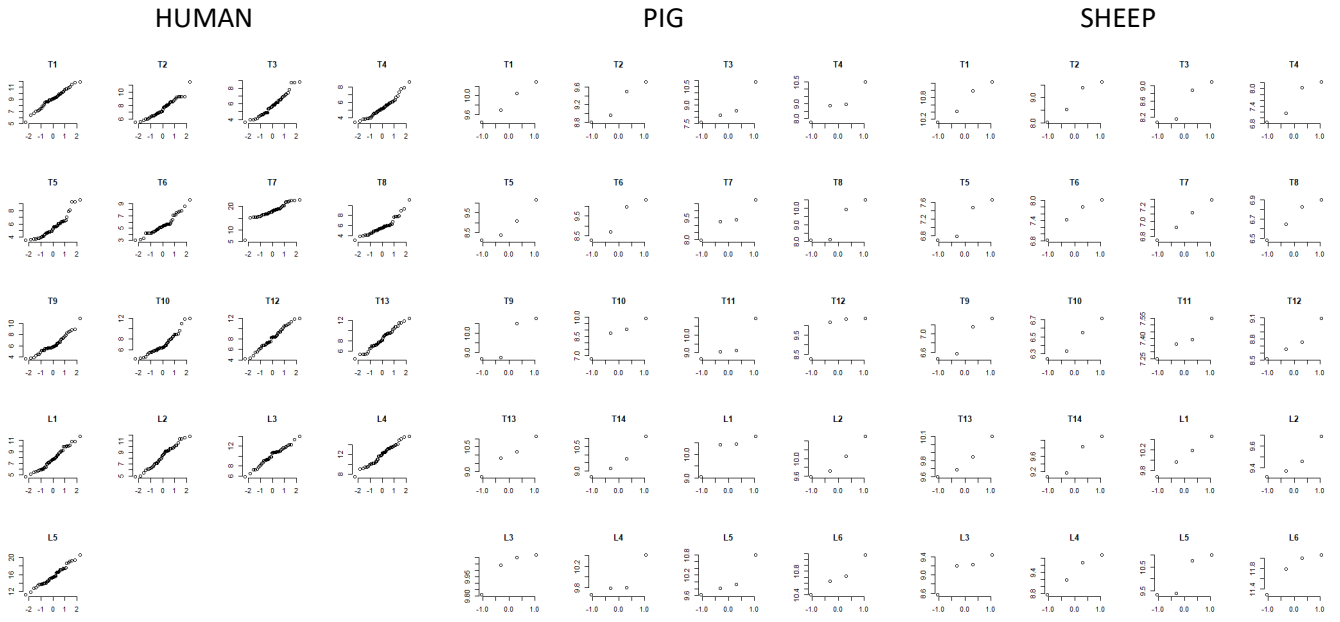
Figure C.11 – Q-Q plots showing left pedicle width data distribution for human, pig, and sheep CT measurements

D – SHAPIRO WILK TEST FOR HUMAN, PIG AND SHEEP CT MEASUREMENTS

T1	Human	Pig	Sheep
VBH	0.20	0.90	0.74
VBW	0.09	0.13	0.90
VBL	0.27	0.91	0.44
TPW	0.74	0.17	0.44
SCW	0.06	0.01	0.74
SCL	0.16	0.32	0.81
TL	0.84	0.15	0.58
RPW	0.54	0.78	0.90
RPH	0.14	0.89	0.43
LPW	0.83	0.86	0.68
LPH	0.53	0.76	0.81

Figure D.1 – Shapiro Wilk test for human, pig and sheep T1 CT measurements

T2	Human	Pig	Sheep
VBH	0.21	0.39	0.81
VBW	0.37	0.28	0.96
VBL	0.14	0.90	0.69
TPW	0.84	0.23	0.23
SCW	0.34	0.01	0.51
SCL	0.27	0.67	0.91
TL	0.57	0.17	0.55
RPW	0.31	0.61	0.54
RPH	0.81	0.68	0.59
LPW	0.07	0.51	0.54
LPH	0.28	0.36	0.71

Figure D.2 – Shapiro Wilk test for human, pig and sheep T2 CT measurements

T3	Human	Pig	Sheep
VBH	0.43	0.77	0.28
VBW	0.21	0.15	0.26
VBL	0.10	0.76	0.26
TPW	0.06	0.93	0.34
SCW	0.50	0.91	0.22
SCL	0.62	0.90	0.21
TL	0.39	0.38	0.58
RPW	0.23	0.19	0.23
RPH	0.44	0.85	0.14
LPW	0.12	0.67	0.13
LPH	0.08	0.66	0.09

Figure D.3 – Shapiro Wilk test for human, pig and sheep T3 CT measurements

T4	Human	Pig	Sheep
VBH	0.17	0.01	0.73
VBW	0.18	0.23	0.99
VBL	0.77	0.12	0.92
TPW	0.78	0.26	0.28
SCW	0.23	0.12	0.48
SCL	0.11	0.96	0.97
TL	0.72	0.90	0.23
RPW	0.37	0.63	0.61
RPH	0.34	0.90	0.83
LPW	0.08	0.56	0.39
LPH	0.13	0.79	0.65

Figure D.4 – Shapiro Wilk test for human, pig and sheep T4 CT measurements

T5	Human	Pig	Sheep
VBH	0.71	0.82	0.94
VBW	0.11	0.44	0.83
VBL	0.71	0.33	0.91
TPW	0.12	0.33	0.79
SCW	<0.01	0.72	0.66
SCL	0.25	0.48	0.69
TL	0.05	0.96	0.89
RPW	0.24	0.51	0.08
RPH	0.32	1.00	0.77
LPW	<0.01	0.41	0.26
LPH	0.16	0.93	0.49

Figure D.5 – Shapiro Wilk test for human, pig and sheep T5 CT measurements

T6	Human	Pig	Sheep
VBH	0.40	0.15	0.87
VBW	0.17	0.41	0.26
VBL	0.76	0.85	0.94
TPW	0.70	0.69	0.43
SCW	0.34	0.91	0.33
SCL	<0.01	0.50	0.22
TL	0.11	0.25	0.55
RPW	0.18	0.63	0.23
RPH	0.12	0.91	0.19
LPW	0.02	0.57	0.69
LPH	0.21	0.88	0.17

Figure D.6 – Shapiro Wilk test for human, pig and sheep T6 CT measurements

T7	Human	Pig	Sheep
VBH	0.88	1.00	0.11
VBW	0.31	0.35	0.75
VBL	0.27	0.19	0.92
TPW	0.52	0.23	0.62
SCW	0.07	0.03	0.23
SCL	0.01	0.50	0.48
TL	<0.01	0.11	0.72
RPW	<0.01	0.08	0.83
RPH	<0.01	0.93	0.51
LPW	<0.01	0.33	0.94
LPH	0.21	0.93	0.45

Figure D.7 – Shapiro Wilk test for human, pig and sheep T7 CT measurements

T8	Human	Pig	Sheep
VBH	0.11	0.97	0.21
VBW	0.10	0.80	0.96
VBL	0.72	0.22	0.45
TPW	0.01	0.01	0.94
SCW	0.29	0.49	0.43
SCL	0.02	0.06	0.15
TL	0.01	0.53	0.93
RPW	0.05	0.81	0.97
RPH	0.23	0.95	0.96
LPW	<0.01	0.16	0.71
LPH	0.03	0.13	1.00

Figure D.8 – Shapiro Wilk test for human, pig and sheep T8 CT measurements

T9	Human	Pig	Sheep
VBH	0.02	0.29	0.12
VBW	0.01	0.13	0.76
VBL	0.74	0.92	0.32
TPW	0.04	0.76	0.69
SCW	0.09	0.74	0.75
SCL	0.01	0.14	0.28
TL	0.59	0.58	0.53
RPW	0.29	0.22	0.65
RPH	0.22	0.19	0.30
LPW	0.03	0.09	0.35
LPH	0.12	0.01	0.54

Figure D.9 – Shapiro Wilk test for human, pig and sheep T9 CT measurements

T10	Human	Pig	Sheep
VBH	0.06	0.45	0.92
VBW	0.53	0.92	0.28
VBL	0.36	0.61	0.32
TPW	0.37	0.79	0.82
SCW	0.22	0.24	0.42
SCL	0.24	0.99	0.47
TL	0.33	0.44	0.45
RPW	0.09	0.43	0.86
RPH	0.15	0.97	0.89
LPW	<0.01	0.35	0.73
LPH	0.16	0.71	0.22

Figure D.10 – Shapiro Wilk test for human, pig and sheep T10 CT measurements

T11	Human	Pig	Sheep
VBH	0.05	0.91	0.70
VBW	0.07	0.99	0.51
VBL	0.99	0.25	0.99
TPW	<0.01	0.98	0.76
SCW	0.29	0.97	0.75
SCL	0.01	0.35	0.47
TL	0.51	0.95	0.30
RPW	0.49	0.29	0.10
RPH	0.50	0.95	0.96
LPW	0.68	0.10	0.83
LPH	0.96	0.99	0.83

Figure D.11 – Shapiro Wilk test for human, pig and sheep T11 CT measurements

T12	Human	Pig	Sheep
VBH	0.01	0.31	0.09
VBW	0.30	0.60	0.81
VBL	0.41	0.32	0.64
TPW	0.03	0.84	0.76
SCW	0.76	0.34	0.51
SCL	0.01	0.16	0.85
TL	0.07	0.06	0.68
RPW	0.09	0.08	0.98
RPH	0.68	0.93	0.35
LPW	0.67	0.06	0.62
LPH	0.17	0.24	0.87

Figure D.12 – Shapiro Wilk test for human, pig and sheep T12 CT measurements

T13	Pig	Sheep
VBH	0.08	0.97
VBW	0.98	0.55
VBL	0.16	0.41
TPW	0.82	0.59
SCW	0.55	0.29
SCL	0.74	0.61
TL	0.26	0.81
RPW	0.96	0.09
RPH	0.88	0.47
LPW	0.95	0.72
LPH	0.96	0.81

Figure D.13 – Shapiro Wilk test for pig and sheep T13 CT measurements

T14	Pig	Sheep
VBH	0.81	0.26
VBW	0.52	0.98
VBL	0.31	0.46
TPW	0.34	0.72
SCW	0.36	0.26
SCL	0.12	0.36
TL	0.36	0.37
RPW	0.28	0.49
RPH	0.40	0.94
LPW	0.70	0.35
LPH	0.46	0.70

Figure D.14 – Shapiro Wilk test for pig and sheep T14 CT measurements

L1	Human	Pig	Sheep
VBH	0.32	0.60	0.49
VBW	0.01	0.54	0.45
VBL	0.56	0.25	0.80
TPW	0.65	0.82	0.51
SCW	0.17	0.04	0.34
SCL	0.79	0.94	0.53
TL	<0.01	0.17	0.81
RPW	0.68	0.02	0.57
RPH	0.20	0.16	0.99
LPW	0.20	0.12	0.99
LPH	0.45	0.69	0.50

Figure D.15 – Shapiro Wilk test for human, pig and sheep L1 CT measurements

L2	Human	Pig	Sheep
VBH	0.36	0.08	0.61
VBW	0.08	0.83	0.62
VBL	0.17	0.77	0.79
TPW	0.67	0.01	0.61
SCW	0.05	0.22	0.24
SCL	0.01	0.27	0.82
TL	0.45	0.96	0.66
RPW	0.12	0.17	0.99
RPH	0.65	0.12	0.98
LPW	0.40	0.64	0.43
LPH	0.25	0.54	0.97

Figure D.16 – Shapiro Wilk test for human, pig and sheep L2 CT measurements

L3	Human	Pig	Sheep
VBH	0.18	0.90	0.17
VBW	0.23	0.49	0.75
VBL	0.77	0.28	0.82
TPW	0.40	0.32	1.00
SCW	0.03	0.60	0.40
SCL	0.45	0.37	0.94
TL	0.28	0.99	0.16
RPW	0.52	0.16	0.80
RPH	0.13	0.03	0.77
LPW	0.62	0.14	0.27
LPH	0.02	0.12	0.74

Figure D.17 – Shapiro Wilk test for human, pig and sheep L3 CT measurements

L4	Human	Pig	Sheep
VBH	0.41	0.68	0.86
VBW	0.02	0.82	0.31
VBL	0.20	0.27	0.64
TPW	0.37	0.74	0.12
SCW	0.54	0.85	0.76
SCL	0.99	0.38	0.92
TL	0.49	0.84	0.12
RPW	0.77	0.98	0.77
RPH	0.01	0.63	0.77
LPW	0.59	0.08	0.78
LPH	<0.01	0.52	0.74

Figure D.18 – Shapiro Wilk test for human, pig and sheep L4 CT measurements

L5	Human	Pig	Sheep
VBH	0.50	0.40	0.98
VBW	0.21	0.03	0.91
VBL	0.03	0.35	0.81
TPW	0.39	0.82	0.38
SCW	0.48	0.45	0.91
SCL	0.47	0.22	0.65
TL	0.14	0.61	0.17
RPW	0.39	0.63	0.54
RPH	0.03	0.36	0.79
LPW	0.66	0.21	0.12
LPH	0.01	0.34	0.54

Figure D.19 – Shapiro Wilk test for human, pig and sheep L5 CT measurements

L6	Pig	Sheep
VBH	0.01	0.86
VBW	0.18	0.89
VBL	0.16	0.88
TPW	0.28	0.17
SCW	0.33	0.74
SCL	0.95	0.30
TL	0.34	0.14
RPW	0.10	0.49
RPH	0.85	0.67
LPW	0.85	0.31
LPH	0.47	0.48

Figure D.20 – Shapiro Wilk test for pig and sheep L6 CT measurements

E – TABLES SHOWING COMPARISONS BETWEEN HUMAN, PIG AND SHEEP

Table E.1 – Comparison of vertebral body height measurements between human, pig, and sheep data.

	Human				Pig						Sheep					
	Mean ± SD		95%CI		Mean ± SD		95%CI		mean diff	p	Mean ± SD		95%CI		mean diff	p
T1	18.23 (1.49)		17.79 —	18.67	23.64 (0.31)		23.33 —	23.95	5.41	<0.01	20.39 (0.66)		19.74 —	21.04	2.16	0.01
T2	19.43 (1.36)		19.03 —	19.83	23.89 (0.42)		23.49 —	24.30	4.46	<0.01	22.37 (0.48)		21.90 —	22.85	2.94	<0.01
T3	19.91 (1.59)		19.44 —	20.38	23.66 (0.67)		23.00 —	24.32	3.76	<0.01	23.04 (0.76)		22.29 —	23.78	3.13	<0.01
T4	20.09 (1.81)		19.55 —	20.62	23.65 (0.33)		23.33 —	23.97	3.56	<0.01	24.31 (0.72)		23.61 —	25.02	4.23	<0.01
T5	20.69 (1.66)		20.19 —	21.18	23.77 (0.48)		23.29 —	24.24	3.08	<0.01	24.13 (0.46)		23.68 —	24.57	3.44	<0.01
T6	20.93 (1.82)		20.39 —	21.47	23.72 (1.09)		22.65 —	24.79	2.79	0.01	25.63 (0.61)		25.03 —	26.23	4.70	<0.01
T7	21.19 (1.77)		20.67 —	21.71	23.91 (1.20)		22.73 —	25.08	2.72	0.01	27.72 (0.37)		27.36 —	28.08	6.53	<0.01
T8	21.83 (1.55)		21.37 —	22.29	25.13 (1.20)		23.95 —	26.30	3.30	<0.01	25.85 (0.37)		25.49 —	26.21	4.02	<0.01
T9	22.82 (1.77)		22.30 —	23.34	25.44 (0.84)		24.61 —	26.26	2.62	0.01	28.03 (0.40)		27.64 —	28.42	5.21	<0.01
T10	24.42 (1.94)		23.84 —	24.99	25.83 (0.71)		25.13 —	26.53	1.41	0.07	27.75 (1.01)		26.76 —	28.73	3.33	<0.01
T11	25.41 (2.03)		24.81 —	26.01	25.92 (0.82)		25.12 —	26.72	0.51	0.36	28.98 (0.58)		28.41 —	29.55	3.57	<0.01
T12	26.72 (1.76)		26.20 —	27.24	25.98 (0.54)		25.44 —	26.51	0.74	0.47	29.09 (0.41)		28.68 —	29.49	2.37	0.01
T13					26.59 (1.10)		25.51 —	27.67	0.13	1.00	31.72 (0.30)		31.43 —	32.01	5.00	<0.01
T14					27.13 (0.77)		26.38 —	27.89	0.41	0.34	32.87 (0.59)		32.29 —	33.45	6.15	<0.01
L1	28.52 (1.82)		27.98 —	29.06	28.66 (0.93)		27.75 —	29.57	0.15	0.87	33.64 (0.59)		33.07 —	34.21	5.12	<0.01
L2	30.44 (1.84)		29.89 —	30.98	29.03 (0.69)		28.36 —	29.70	1.41	0.13	33.91 (0.56)		33.36 —	34.45	3.47	<0.01
L3	31.06 (1.84)		30.52 —	31.60	29.82 (0.45)		29.38 —	30.27	1.24	0.12	34.83 (0.48)		34.36 —	35.30	3.77	<0.01
L4	31.36 (2.13)		30.73 —	31.99	30.66 (0.92)		29.76 —	31.57	0.69	0.56	35.56 (0.45)		35.12 —	36.00	4.20	<0.01
L5	31.95 (2.07)		31.33 —	32.56	30.36 (0.62)		29.75 —	30.96	1.59	0.07	34.90 (0.68)		34.24 —	35.57	2.95	0.01
L6					29.91 (0.61)		29.31 —	30.51	2.03	0.02	32.64 (0.37)		32.28 —	33.01	0.70	0.52

	Human		Pig				Sheep			
	Mean ± SD	95%CI	Mean ± SD	95%CI	mean diff	p	Mean ± SD	95%CI	mean diff	p
T1	32.58 (2.30)	31.90 — 33.26	30.46 (2.80)	27.71 — 33.20	2.12	0.24	22.49 (1.60)	21.12 — 32.35	5.84	0.10
T2	31.86 (2.10)	31.24 — 32.48	30.32 (2.12)	28.24 — 32.40	1.55	0.31	26.11 (3.30)	22.87 — 29.34	5.76	0.00
T3	29.83 (2.66)	29.05 — 30.62	30.12 (2.14)	28.02 — 32.21	-0.28	0.60	25.79 (2.10)	23.73 — 27.85	4.04	0.02
T4	28.88 (2.24)	28.21 — 29.54	30.29 (2.79)	27.56 — 33.01	-1.41	0.32	26.66 (1.81)	24.89 — 28.44	2.21	0.10
T5	29.37 (2.08)	28.76 — 29.99	30.25 (2.20)	28.09 — 32.41	-0.88	0.50	27.29 (2.78)	24.56 — 30.02	2.08	0.22
T6	30.35 (2.36)	29.66 — 31.05	31.20 (1.56)	29.67 — 32.73	-0.85	0.42	26.84 (0.70)	26.15 — 27.52	3.52	<0.01
T7	31.82 (2.34)	31.13 — 32.51	30.17 (2.56)	27.66 — 32.68	1.65	0.22	28.10 (0.43)	27.69 — 28.52	3.71	<0.01
T8	33.07 (2.40)	32.36 — 33.78	31.12 (1.95)	29.20 — 33.03	1.95	0.19	26.62 (0.77)	25.86 — 27.38	6.45	<0.01
T9	34.41 (2.68)	33.61 — 35.20	29.87 (3.28)	26.66 — 33.08	4.53	0.03	27.50 (0.88)	26.65 — 28.36	6.90	<0.01
T10	36.71 (2.84)	35.87 — 37.55	32.29 (1.89)	30.44 — 34.14	4.42	0.01	27.19 (1.44)	25.77 — 28.61	9.52	<0.01
T11	39.84 (3.73)	38.74 — 40.94	33.33 (1.41)	31.95 — 34.71	6.52	<0.01	27.50 (2.01)	25.53 — 29.47	12.34	<0.01
T12	42.13 (3.21)	41.18 — 43.08	32.47 (1.90)	30.61 — 34.33	9.67	<0.01	28.85 (0.64)	28.22 — 29.49	13.28	<0.01
T13			32.47 (2.43)	30.08 — 34.85	9.66	<0.01	30.62 (1.15)	29.50 — 31.75	11.51	<0.01
T14			29.65 (6.47)	23.31 — 35.98	12.49	<0.01	32.31 (1.14)	31.20 — 33.42	9.82	<0.01
L1	42.30 (4.19)	41.06 — 43.54	32.42 (2.14)	30.32 — 34.52	9.88	<0.01	31.90 (2.26)	29.68 — 34.11	10.40	<0.01
L2	44.27 (3.59)	43.21 — 45.33	32.38 (2.13)	30.29 — 34.48	11.89	<0.01	32.04 (2.35)	29.74 — 34.34	12.23	<0.01
L3	46.08 (3.91)	44.93 — 47.24	32.87 (2.64)	30.28 — 35.47	13.21	<0.01	31.89 (3.34)	28.62 — 35.16	14.20	<0.01
L4	49.00 (4.10)	47.79 — 50.21	34.61 (2.26)	32.40 — 36.82	14.39	<0.01	32.83 (3.03)	29.86 — 35.79	16.17	<0.01
L5	53.84 (4.68)	53.22 — 54.45	35.50 (2.55)	33.01 — 38.00	18.33	<0.01	34.20 (1.30)	32.92 — 35.47	19.64	<0.01
L6			35.25 (2.99)	32.32 — 38.18	18.58	<0.01	33.77 (1.03)	32.77 — 34.78	20.06	<0.01

Table E.2 – Comparison of vertebral body width measurements between human, pig, and sheep data.

	Human		Pig				Sheep			
	Mean ± SD	95%CI	Mean ± SD	95%CI	mean diff	p	Mean ± SD	95%CI	mean diff	p
T1	19.68 (2.05)	19.07 – 20.28	17.34 (0.70)	16.66 – 18.03	2.33	0.01	21.26 (0.39)	20.87 – 21.64	1.58	0.10
T2	20.63 (2.19)	19.98 – 21.27	17.80 (1.05)	16.77 – 18.83	2.83	0.01	20.51 (0.53)	19.99 – 21.03	0.12	0.90
T3	22.09 (2.21)	21.44 – 22.74	17.32 (1.13)	16.21 – 18.43	4.77	<0.01	19.68 (0.62)	19.08 – 20.29	2.41	0.03
T4	24.31 (2.31)	23.63 – 25.00	17.80 (1.42)	16.41 – 19.19	6.51	<0.01	18.88 (0.60)	18.29 – 19.46	5.44	<0.01
T5	25.89 (2.23)	25.23 – 26.55	17.43 (0.73)	16.71 – 18.15	8.46	<0.01	18.52 (0.55)	17.98 – 19.06	7.37	<0.01
T6	27.47 (2.27)	26.80 – 28.14	17.42 (1.13)	16.31 – 18.53	10.05	<0.01	19.72 (0.64)	19.10 – 20.35	7.75	<0.01
T7	28.89 (2.73)	28.08 – 29.70	17.06 (1.25)	15.84 – 18.29	11.83	<0.01	18.23 (0.36)	17.88 – 18.58	10.66	<0.01
T8	30.35 (2.35)	29.66 – 31.05	17.07 (1.04)	16.05 – 18.09	13.28	<0.01	18.90 (0.45)	18.46 – 19.34	11.45	<0.01
T9	31.57 (2.61)	30.80 – 32.34	16.59 (1.55)	15.07 – 18.11	14.98	<0.01	19.09 (0.55)	18.55 – 19.63	12.48	<0.01
T10	32.58 (2.64)	31.80 – 33.36	16.91 (0.78)	16.15 – 17.67	15.67	<0.01	19.21 (0.53)	18.69 – 19.74	13.36	<0.01
T11	32.85 (2.62)	32.08 – 33.63	17.20 (0.77)	16.44 – 17.95	15.66	<0.01	19.15 (0.45)	18.71 – 19.60	13.70	<0.01
T12	33.91 (2.82)	33.08 – 34.74	17.17 (0.61)	16.57 – 17.78	16.74	<0.01	19.35 (0.55)	18.81 – 19.88	14.56	<0.01
T13			17.15 (0.85)	16.32 – 17.98	16.76	<0.01	20.04 (0.51)	19.54 – 20.53	13.88	<0.01
T14			17.81 (0.89)	16.94 – 18.68	16.10	<0.01	19.80 (0.44)	19.37 – 20.23	14.11	<0.01
L1	34.59 (3.06)	33.69 – 35.49	20.10 (0.78)	19.33 – 20.87	14.49	<0.01	18.89 (0.39)	18.51 – 19.28	15.70	<0.01
L2	36.48 (3.30)	35.51 – 37.46	20.84 (1.13)	19.73 – 21.95	15.65	<0.01	20.65 (0.66)	20.01 – 21.30	15.83	<0.01
L3	37.94 (5.35)	36.35 – 39.52	20.99 (1.43)	19.58 – 22.39	16.95	<0.01	21.21 (0.54)	20.68 – 21.74	16.72	<0.01
L4	36.85 (3.03)	35.96 – 37.75	20.54 (0.94)	19.62 – 21.46	16.31	<0.01	20.62 (0.51)	20.12 – 21.12	16.23	<0.01
L5	36.76 (3.09)	35.84 – 37.67	18.78 (0.52)	18.27 – 19.29	17.98	<0.01	21.41 (0.53)	20.89 – 21.93	15.34	<0.01
L6			18.16 (1.16)	17.02 – 19.29	18.60	<0.01	21.94 (0.57)	21.38 – 22.50	14.82	<0.01

Table E.3 – Comparison of vertebral body length measurements between human, pig, and sheep data.

	Human			Pig					Sheep				
	Mean ± SD	95%CI		Mean ± SD	95%CI		mean diff	p	Mean ± SD	95%CI		mean diff	p
T1	78.69 (5.56)	77.05 —	80.33	50.96 (3.49)	47.54 —	54.38	27.73	<0.01	55.83 (1.66)	55.21 —	56.45	22.86	<0.01
T2	72.63 (5.51)	71.01 —	74.26	48.51 (1.22)	47.32 —	49.70	24.12	<0.01	53.86 (1.52)	53.35 —	54.37	18.77	<0.01
T3	67.13 (5.18)	65.60 —	68.66	46.62 (0.65)	45.99 —	47.26	20.51	<0.01	50.43 (0.95)	49.92 —	50.95	16.70	<0.01
T4	66.66 (4.59)	65.30 —	68.01	46.07 (1.37)	44.73 —	47.41	20.58	<0.01	51.13 (2.69)	50.45 —	51.81	15.53	<0.01
T5	66.01 (5.19)	64.48 —	67.55	44.46 (1.95)	42.55 —	46.38	21.55	<0.01	48.66 (1.99)	48.08 —	49.24	17.35	<0.01
T6	67.28 (5.20)	65.74 —	68.81	45.30 (1.62)	43.71 —	46.89	21.97	<0.01	45.16 (3.47)	44.69 —	45.62	22.12	<0.01
T7	66.45 (5.83)	64.73 —	68.17	44.77 (2.12)	42.69 —	46.84	21.68	<0.01	45.14 (1.55)	44.60 —	45.67	21.31	<0.01
T8	63.90 (7.41)	61.71 —	66.09	44.98 (2.44)	42.60 —	47.37	18.92	<0.01	46.59 (1.39)	45.96 —	47.21	17.31	<0.01
T9	63.70 (5.03)	62.22 —	65.19	43.06 (2.71)	40.40 —	45.72	20.64	<0.01	48.80 (1.42)	48.22 —	49.38	14.91	<0.01
T10	60.78 (4.89)	59.33 —	62.22	39.76 (6.74)	34.14 —	45.39	21.01	<0.01	51.56 (1.18)	51.03 —	52.10	9.22	<0.01
T11	54.83 (6.92)	52.79 —	56.88	38.45 (4.50)	34.05 —	42.86	16.38	<0.01	51.59 (1.15)	50.98 —	52.20	3.24	0.07
T12	50.62 (5.83)	48.90 —	52.34	38.65 (3.91)	34.82 —	42.48	11.97	<0.01	50.85 (1.04)	50.15 —	51.54	0.23	0.58
T13				39.26 (4.12)	34.54 —	43.99	11.35	<0.01	58.74 (1.02)	58.20 —	59.29	8.13	<0.01
T14				47.23 (3.73)	41.61 —	52.85	3.39	0.22	66.76 (1.86)	65.93 —	67.59	16.14	<0.01
L1	76.28 (9.36)	73.51 —	79.04	72.49 (2.65)	60.10 —	84.89	3.78	0.78	103.14 (1.92)	102.19 —	104.08	26.86	<0.01
L2	84.50 (8.38)	82.03 —	86.98	91.74 (3.78)	88.04 —	95.44	7.24	0.06	113.90 (1.99)	112.92 —	114.87	29.39	<0.01
L3	92.98 (8.03)	90.60 —	95.35	95.71 (1.57)	94.17 —	97.24	2.73	0.35	120.00 (1.61)	118.81 —	121.18	27.02	<0.01
L4	92.17 (8.55)	89.64 —	94.69	97.25 (3.10)	94.22 —	100.29	5.09	0.18	118.83 (1.52)	117.60 —	120.06	26.67	<0.01
L5	97.01 (8.58)	94.47 —	99.54	100.03 (1.72)	98.34 —	101.72	3.02	0.23	119.09 (2.31)	117.49 —	120.69	22.08	<0.01
L6				90.52 (3.30)	87.28 —	93.75	6.49	0.11	115.12 (1.76)	114.05 —	116.19	18.11	<0.01

Table E.4 – Comparison of transverse process width measurements between human, pig, and sheep data.

	Human		Pig				Sheep			
	Mean ± SD	95%CI	Mean ± SD	95%CI	mean diff	p	Mean ± SD	95%CI	mean diff	p
T1	23.21 (1.64)	15.17 — 16.03	16.72 (1.27)	10.16 — 14.95	6.49	0.03	18.78 (0.60)	12.49 — 13.63	4.43	0.01
T2	19.90 (1.37)	16.37 — 17.09	14.84 (1.77)	9.35 — 12.18	5.07	<0.01	15.83 (0.64)	14.14 — 15.10	4.08	<0.01
T3	18.84 (1.66)	16.37 — 17.09	14.53 (0.97)	9.68 — 10.70	4.31	<0.01	14.46 (0.74)	13.24 — 14.53	4.38	<0.01
T4	18.06 (1.75)	16.30 — 17.24	14.62 (1.94)	9.99 — 10.42	3.44	<0.01	14.77 (0.99)	12.44 — 13.13	3.29	<0.01
T5	17.71 (1.74)	16.23 — 17.13	14.94 (1.28)	10.03 — 11.38	2.77	<0.01	14.58 (0.55)	10.40 — 11.66	3.13	<0.01
T6	18.07 (1.97)	16.18 — 17.06	13.70 (1.55)	9.62 — 10.86	4.37	<0.01	13.91 (0.48)	10.44 — 11.33	4.16	<0.01
T7	18.21 (2.25)	16.36 — 17.29	13.37 (1.27)	10.04 — 10.80	4.84	<0.01	13.03 (0.53)	10.32 — 11.27	5.18	<0.01
T8	18.67 (2.37)	16.00 — 16.98	13.54 (1.18)	9.89 — 10.29	5.14	<0.01	12.81 (0.50)	10.63 — 11.76	5.87	<0.01
T9	18.95 (2.44)	15.84 — 16.95	13.53 (1.04)	9.80 — 10.18	5.43	<0.01	12.29 (0.44)	10.76 — 11.80	6.67	<0.01
T10	19.47 (2.33)	15.68 — 16.50	14.31 (0.48)	7.68 — 11.25	5.17	<0.01	12.76 (0.34)	10.41 — 11.17	6.71	<0.01
T11	21.39 (2.86)	16.43 — 17.51	14.46 (1.03)	9.74 — 11.09	6.93	<0.01	12.33 (0.30)	11.83 — 12.65	9.06	<0.01
T12	24.38 (2.49)	18.30 — 19.32	15.26 (0.92)	8.95 — 11.33	9.12	<0.01	13.57 (0.41)	10.09 — 10.81	10.80	<0.01
T13			14.42 (0.56)	8.53 — 11.82	9.96	<0.01	14.25 (0.55)	10.16 — 11.10	10.13	<0.01
T14			14.40 (0.15)	9.03 — 11.05	9.98	<0.01	14.61 (0.47)	10.31 — 11.13	9.77	<0.01
L1	25.22 (2.33)	18.27 — 19.19	14.45 (1.27)	9.21 — 10.84	10.77	<0.01	14.69 (0.49)	9.60 — 10.49	10.54	<0.01
L2	24.64 (2.52)	16.43 — 17.28	15.05 (0.85)	9.54 — 10.83	9.59	<0.01	14.66 (0.46)	9.91 — 10.53	9.98	<0.01
L3	25.46 (2.53)	16.50 — 17.55	16.46 (0.72)	9.55 — 11.00	9.00	<0.01	15.09 (0.42)	9.89 — 10.52	10.37	<0.01
L4	26.43 (2.70)	16.07 — 17.17	17.51 (0.91)	10.38 — 10.69	8.93	<0.01	15.92 (0.41)	11.85 — 12.64	10.51	<0.01
L5	30.23 (3.06)	16.96 — 18.33	18.99 (0.83)	10.43 — 11.59	11.24	<0.01	17.85 (0.64)	12.57 — 13.52	12.38	<0.01
L6			20.83 (1.47)	10.79 — 12.27	9.40	<0.01	17.79 (0.48)	12.02 — 12.93	12.44	<0.01

Table E.5 – Comparison of spinal canal width measurements between human, pig, and sheep data.

	Human		Pig				Sheep			
	Mean ± SD	95%CI	Mean ± SD	95%CI	mean diff	p	Mean ± SD	95%CI	mean diff	p
T1	15.60 (1.45)	15.17 — 16.03	12.56 (2.45)	10.16 — 14.95	3.05	0.03	13.06 (0.58)	12.49 — 13.63	2.54	0.01
T2	16.73 (1.22)	16.37 — 17.09	10.76 (1.44)	9.35 — 12.18	5.96	<0.01	14.62 (0.49)	14.14 — 15.10	2.11	<0.01
T3	16.73 (1.22)	16.37 — 17.09	10.19 (0.52)	9.68 — 10.70	6.54	<0.01	13.88 (0.66)	13.24 — 14.53	2.85	<0.01
T4	16.77 (1.58)	16.30 — 17.24	10.21 (0.22)	9.99 — 10.42	6.56	<0.01	12.78 (0.35)	12.44 — 13.13	3.99	<0.01
T5	16.68 (1.53)	16.23 — 17.13	10.70 (0.69)	10.03 — 11.38	5.98	<0.01	11.03 (0.65)	10.40 — 11.66	5.65	<0.01
T6	16.62 (1.48)	16.18 — 17.06	10.24 (0.63)	9.62 — 10.86	6.38	<0.01	10.88 (0.45)	10.44 — 11.33	5.74	<0.01
T7	16.82 (1.57)	16.36 — 17.29	10.42 (0.39)	10.04 — 10.80	6.40	<0.01	10.79 (0.48)	10.32 — 11.27	6.03	<0.01
T8	16.49 (1.66)	16.00 — 16.98	10.09 (0.21)	9.89 — 10.29	6.40	<0.01	11.19 (0.58)	10.63 — 11.76	5.29	<0.01
T9	16.40 (1.88)	15.84 — 16.95	9.99 (0.19)	9.80 — 10.18	6.41	<0.01	11.28 (0.53)	10.76 — 11.80	5.12	<0.01
T10	16.09 (1.38)	15.68 — 16.50	9.46 (1.82)	7.68 — 11.25	6.63	<0.01	10.79 (0.39)	10.41 — 11.17	5.30	<0.01
T11	16.97 (1.82)	16.43 — 17.51	10.41 (0.69)	9.74 — 11.09	6.55	<0.01	12.24 (0.42)	11.83 — 12.65	4.73	<0.01
T12	18.81 (1.72)	18.30 — 19.32	10.14 (1.21)	8.95 — 11.33	8.67	<0.01	10.45 (0.37)	10.09 — 10.81	8.36	<0.01
T13			10.18 (1.68)	8.53 — 11.82	8.63	<0.01	10.63 (0.48)	10.16 — 11.10	8.18	<0.01
T14			10.04 (1.03)	9.03 — 11.05	8.77	<0.01	10.72 (0.42)	10.31 — 11.13	8.09	<0.01
L1	18.73 (1.55)	18.27 — 19.19	10.03 (0.83)	9.21 — 10.84	8.70	<0.01	10.05 (0.45)	9.60 — 10.49	8.68	<0.01
L2	16.86 (1.44)	16.43 — 17.28	10.18 (0.66)	9.54 — 10.83	6.67	<0.01	10.22 (0.32)	9.91 — 10.53	6.63	<0.01
L3	17.02 (1.79)	16.50 — 17.55	10.28 (0.74)	9.55 — 11.00	6.75	<0.01	10.20 (0.32)	9.89 — 10.52	6.82	<0.01
L4	16.62 (1.86)	16.07 — 17.17	10.54 (0.16)	10.38 — 10.69	6.08	<0.01	12.24 (0.40)	11.85 — 12.64	4.38	<0.01
L5	17.64 (2.32)	16.96 — 18.33	11.01 (0.59)	10.43 — 11.59	6.63	<0.01	13.04 (0.49)	12.57 — 13.52	4.60	<0.01
L6			11.53 (0.76)	10.79 — 12.27	6.11	<0.01	12.48 (0.46)	12.02 — 12.93	5.17	<0.01

Table E.6 – Comparison of spinal canal length measurements between human, pig, and sheep data.

	Human		Pig				Sheep			
	Mean ± SD	95%CI	Mean ± SD	95%CI	mean diff	p	Mean ± SD	95%CI	mean diff	p
T1	69.88 (5.41)	68.28 — 71.47	97.20 (1.76)	95.47 — 98.93	27.32	<0.01	86.33 (0.72)	85.63 — 87.04	16.45	<0.01
T2	70.54 (4.83)	69.12 — 71.97	101.09 (4.45)	96.73 — 105.46	30.55	<0.01	97.22 (0.86)	96.38 — 98.06	26.68	<0.01
T3	72.43 (4.76)	71.03 — 73.84	99.79 (2.66)	97.18 — 102.39	27.35	<0.01	98.66 (0.83)	97.85 — 99.47	26.23	<0.01
T4	74.03 (5.11)	72.52 — 75.54	97.23 (4.47)	92.85 — 101.61	23.20	<0.01	98.64 (0.83)	97.83 — 99.45	24.61	<0.01
T5	77.34 (6.10)	75.54 — 79.14	89.06 (4.06)	85.09 — 93.04	11.72	<0.01	95.72 (0.97)	94.78 — 96.67	18.38	<0.01
T6	78.10 (4.87)	76.66 — 79.54	84.85 (5.12)	79.84 — 89.87	6.76	0.01	89.30 (0.86)	88.45 — 90.14	11.20	<0.01
T7	79.74 (5.88)	78.00 — 81.48	80.31 (3.00)	77.37 — 83.25	0.57	0.87	87.62 (0.81)	86.83 — 88.42	7.88	<0.01
T8	80.13 (6.79)	78.12 — 82.14	71.99 (3.42)	68.65 — 75.34	8.14	0.01	86.57 (0.91)	85.67 — 87.47	6.44	0.02
T9	81.35 (5.03)	79.87 — 82.84	65.57 (3.30)	62.33 — 68.80	15.79	<0.01	81.53 (0.83)	80.72 — 82.35	0.18	0.93
T10	80.43 (5.14)	78.92 — 81.95	58.74 (2.23)	56.55 — 60.93	21.69	<0.01	76.81 (0.98)	75.84 — 77.77	3.62	0.11
T11	79.24 (6.00)	77.47 — 81.01	55.67 (1.71)	54.00 — 57.35	23.57	<0.01	72.02 (0.68)	71.35 — 72.68	7.22	0.01
T12	82.71 (6.76)	80.72 — 84.71	54.81 (2.91)	51.96 — 57.66	27.90	<0.01	60.22 (0.62)	59.61 — 60.83	22.50	<0.01
T13			53.81 (3.86)	50.03 — 57.60	28.90	<0.01	57.32 (0.93)	56.40 — 58.23	25.40	<0.01
T14			55.79 (2.46)	53.38 — 58.20	26.92	<0.01	61.91 (1.25)	60.68 — 63.13	20.81	<0.01
L1	86.59 (10.27)	83.56 — 89.63	55.90 (3.55)	52.42 — 59.38	30.69	<0.01	58.41 (0.66)	57.76 — 59.07	28.18	<0.01
L2	91.86 (6.83)	89.84 — 93.88	56.49 (2.72)	53.82 — 59.15	35.38	<0.01	57.94 (0.52)	57.43 — 58.45	33.92	<0.01
L3	92.89 (6.92)	90.85 — 94.94	56.35 (2.12)	54.27 — 58.43	36.54	<0.01	58.09 (0.60)	57.50 — 58.67	34.81	<0.01
L4	90.92 (6.57)	88.97 — 92.86	53.44 (3.98)	49.54 — 57.34	37.48	<0.01	57.67 (0.63)	57.05 — 58.29	33.25	<0.01
L5	84.92 (5.45)	83.31 — 86.53	52.42 (2.24)	50.22 — 54.61	32.50	<0.01	57.72 (0.71)	57.02 — 58.41	27.21	<0.01
L6			47.32 (5.98)	41.46 — 53.17	37.60	<0.01	57.36 (0.86)	56.51 — 58.20	27.56	<0.01

Table E.7 – Comparison of total anteroposterior length measurements between human, pig, and sheep data.

	Human		Pig				Sheep			
	Mean ± SD	95%CI	Mean ± SD	95%CI	mean diff	p	Mean ± SD	95%CI	mean diff	p
T1	9.73 (1.06)	9.41 – 10.04	16.41 (0.77)	15.65 – 17.16	6.68	<0.01	7.91 (0.47)	7.46 – 8.37	1.81	<0.01
T2	11.23 (1.15)	10.89 – 11.57	16.83 (0.98)	15.88 – 17.79	5.60	<0.01	10.66 (0.38)	10.29 – 11.03	0.57	0.26
T3	11.77 (1.13)	11.43 – 12.10	16.27 (1.47)	14.83 – 17.72	4.51	<0.01	10.62 (0.52)	10.11 – 11.14	1.14	0.04
T4	11.94 (1.30)	11.56 – 12.33	16.29 (1.32)	15.00 – 17.58	4.35	<0.01	11.39 (0.20)	11.19 – 11.58	0.56	0.33
T5	12.12 (1.51)	11.68 – 12.57	16.38 (0.86)	15.54 – 17.23	4.26	<0.01	11.90 (0.30)	11.60 – 12.20	0.22	0.76
T6	12.10 (1.24)	11.73 – 12.47	16.78 (1.31)	15.49 – 18.06	4.68	<0.01	13.69 (0.14)	13.56 – 13.83	1.60	0.01
T7	11.92 (1.45)	11.49 – 12.35	16.08 (0.75)	15.35 – 16.81	4.16	<0.01	13.24 (0.36)	12.89 – 13.60	1.32	0.06
T8	12.63 (1.23)	12.27 – 12.99	16.18 (0.51)	15.68 – 16.68	3.55	<0.01	13.32 (0.42)	12.91 – 13.74	0.69	0.25
T9	13.20 (1.33)	12.81 – 13.59	17.24 (0.93)	16.33 – 18.15	4.04	<0.01	12.91 (0.48)	12.45 – 13.38	0.29	0.72
T10	14.89 (1.19)	14.54 – 15.24	15.66 (1.16)	14.52 – 16.80	0.77	0.36	14.19 (0.32)	13.87 – 14.50	0.70	0.26
T11	16.20 (1.03)	15.89 – 16.50	18.02 (1.27)	16.77 – 19.26	1.82	0.02	15.73 (0.45)	15.29 – 16.17	0.47	0.23
T12	16.34 (1.02)	16.04 – 16.64	18.41 (1.55)	16.90 – 19.93	2.07	0.02	16.17 (0.50)	15.68 – 16.66	0.17	0.73
T13			19.35 (1.25)	18.13 – 20.58	3.01	<0.01	15.95 (0.63)	15.33 – 16.56	0.40	0.30
T14			18.54 (1.02)	17.54 – 19.54	2.20	<0.01	18.47 (0.38)	18.10 – 18.84	2.13	<0.01
L1	15.42 (1.42)	15.01 – 15.84	17.23 (0.70)	16.54 – 17.92	1.80	0.01	20.91 (0.61)	20.31 – 21.51	20.91	<0.01
L2	14.99 (1.46)	14.56 – 15.42	17.20 (0.68)	16.54 – 17.87	2.21	<0.01	22.34 (0.48)	21.87 – 22.81	22.34	<0.01
L3	14.67 (1.37)	14.27 – 15.08	16.83 (0.74)	16.11 – 17.56	2.16	0.01	23.75 (0.38)	23.37 – 24.12	8.32	<0.01
L4	13.60 (1.55)	13.14 – 14.06	16.62 (1.08)	15.56 – 17.68	3.02	<0.01	23.03 (0.41)	22.63 – 23.44	8.04	<0.01
L5	13.40 (2.14)	12.77 – 14.04	16.38 (0.79)	15.60 – 17.15	2.97	0.01	24.97 (0.46)	24.51 – 25.42	10.29	<0.01
L6			15.74 (0.68)	15.07 – 16.41	2.34	0.01	25.87 (0.54)	25.34 – 26.40	12.46	<0.01

Table E.8 – Comparison of right pedicular height measurements between human, pig, and sheep data.

	Human		Pig				Sheep			
	Mean ± SD	95%CI	Mean ± SD	95%CI	mean diff	p	Mean ± SD	95%CI	mean diff	p
T1	9.11 (1.31)	8.72 — 9.50	9.69 (0.60)	9.10 — 10.27	0.57	0.36	10.69 (0.39)	10.32 — 11.07	1.58	0.01
T2	7.48 (1.11)	7.15 — 7.80	9.14 (0.64)	8.51 — 9.77	1.66	0.01	8.98 (0.68)	8.31 — 9.64	1.50	0.02
T3	5.80 (1.32)	5.41 — 6.19	9.04 (0.75)	8.31 — 9.78	3.24	<0.01	8.96 (0.56)	8.42 — 9.50	3.16	<0.01
T4	5.16 (1.36)	4.76 — 5.56	8.93 (1.04)	7.92 — 9.95	3.77	<0.01	7.43 (0.50)	6.94 — 7.92	2.27	0.01
T5	5.36 (1.27)	4.99 — 5.74	8.92 (0.76)	8.17 — 9.66	3.55	<0.01	7.42 (0.42)	7.01 — 7.83	2.06	0.01
T6	5.46 (1.10)	5.14 — 5.79	9.18 (0.96)	8.23 — 10.12	3.72	<0.01	7.07 (0.39)	6.69 — 7.45	1.61	0.01
T7	5.84 (1.31)	5.46 — 6.23	9.44 (0.94)	8.52 — 10.36	3.60	<0.01	6.46 (0.20)	6.26 — 6.66	0.62	0.13
T8	5.95 (1.30)	5.56 — 6.33	9.19 (0.93)	8.28 — 10.11	3.25	<0.01	6.90 (0.15)	6.76 — 7.05	0.96	0.03
T9	6.39 (1.40)	5.97 — 6.80	9.20 (0.64)	8.58 — 9.83	2.81	<0.01	6.78 (0.09)	6.69 — 6.87	0.39	0.73
T10	7.05 (1.65)	6.57 — 7.54	8.67 (1.38)	7.32 — 10.03	1.62	0.08	6.42 (0.08)	6.34 — 6.50	0.63	0.36
T11	8.25 (1.91)	7.68 — 8.81	9.51 (0.79)	8.74 — 10.28	1.26	0.14	6.94 (0.09)	6.85 — 7.02	1.31	0.20
T12	8.32 (2.17)	7.68 — 8.96	9.89 (1.13)	8.78 — 11.00	1.56	0.12	8.52 (0.37)	8.16 — 8.89	0.20	0.67
T13			9.28 (1.15)	8.15 — 10.41	0.96	0.28	9.94 (0.49)	9.45 — 10.42	1.61	0.10
T14			9.42 (1.10)	8.34 — 10.50	1.09	0.25	9.60 (0.31)	9.30 — 9.90	1.28	0.15
L1	7.60 (1.74)	7.08 — 8.11	9.91 (0.76)	9.17 — 10.65	2.31	0.01	9.98 (0.44)	9.54 — 10.41	2.38	0.01
L2	8.39 (1.64)	7.90 — 8.87	9.76 (0.42)	9.35 — 10.18	1.38	0.05	9.35 (0.24)	9.11 — 9.59	0.96	0.19
L3	10.09 (1.77)	9.56 — 10.61	9.99 (0.58)	9.42 — 10.55	0.10	0.90	9.12 (0.41)	8.72 — 9.52	0.97	0.25
L4	12.13 (1.88)	11.57 — 12.68	9.95 (0.30)	9.65 — 10.24	2.18	0.03	9.53 (0.42)	9.11 — 9.94	2.60	<0.01
L5	15.98 (2.09)	15.36 — 16.60	10.11 (0.32)	9.80 — 10.42	5.87	<0.01	10.44 (0.62)	9.83 — 11.05	5.54	<0.01
L6			10.56 (0.39)	10.18 — 10.94	5.42	<0.01	12.01 (0.28)	11.73 — 12.28	3.97	<0.01

Table E.9 – Comparison of right pedicular width measurements between human, pig, and sheep data.

	Human			Pig				Sheep			
	Mean ± SD	95%CI		Mean ± SD	95%CI	mean diff	p	Mean ± SD	95%CI	mean diff	p
T1	9.90 (1.02)	9.59 — 10.20		15.43 (0.92)	14.53 — 16.34	5.53	<0.01	8.16 (0.38)	7.79 — 8.53	1.74	<0.01
T2	11.11 (1.01)	10.81 — 11.41		16.61 (1.05)	15.59 — 17.64	5.50	<0.01	10.57 (0.57)	10.01 — 11.13	0.54	0.32
T3	12.10 (1.34)	11.70 — 12.50		16.24 (0.89)	15.36 — 17.11	4.14	<0.01	11.40 (0.14)	11.26 — 11.54	0.70	0.14
T4	12.11 (0.82)	11.87 — 12.35		16.42 (0.94)	15.50 — 17.34	4.31	<0.01	12.02 (0.30)	11.73 — 12.31	0.09	0.62
T5	12.03 (1.37)	11.62 — 12.43		16.50 (0.75)	15.76 — 17.24	4.48	<0.01	12.45 (0.16)	12.30 — 12.61	0.43	0.66
T6	12.08 (1.36)	11.68 — 12.48		16.68 (1.54)	15.18 — 18.19	4.61	<0.01	12.73 (0.73)	12.02 — 13.45	0.66	0.32
T7	12.08 (1.36)	11.68 — 12.48		16.93 (1.31)	15.65 — 18.22	4.86	<0.01	13.06 (0.42)	12.65 — 13.47	0.98	0.07
T8	12.56 (1.30)	12.18 — 12.94		16.96 (0.84)	16.15 — 17.78	4.40	<0.01	13.37 (0.31)	13.06 — 13.68	0.81	0.16
T9	13.19 (1.29)	12.81 — 13.57		17.05 (0.67)	16.39 — 17.71	3.86	<0.01	12.70 (0.82)	11.89 — 13.50	0.49	0.50
T10	15.05 (1.05)	14.74 — 15.36		16.02 (0.89)	15.15 — 16.89	0.96	0.07	14.33 (0.18)	14.15 — 14.51	0.72	0.10
T11	16.09 (1.04)	15.78 — 16.40		18.18 (1.48)	16.72 — 19.63	2.09	0.02	15.65 (0.31)	15.35 — 15.95	0.44	0.28
T12	16.31 (0.95)	16.03 — 16.59		18.64 (2.41)	16.28 — 21.00	2.34	0.15	16.41 (0.30)	16.11 — 16.71	0.10	0.90
T13				19.87 (1.76)	18.15 — 21.59	3.57	<0.01	16.55 (0.29)	16.27 — 16.83	0.24	0.78
T14				18.18 (1.07)	17.13 — 19.24	1.88	0.01	18.87 (0.23)	18.64 — 19.09	2.56	<0.01
L1	15.34 (1.28)	14.96 — 15.72		17.03 (0.77)	16.28 — 17.78	1.69	0.01	20.58 (0.45)	20.14 — 21.02	5.24	<0.01
L2	14.72 (1.69)	14.22 — 15.23		17.20 (0.90)	16.32 — 18.08	2.47	0.01	22.52 (0.51)	22.01 — 23.02	7.79	<0.01
L3	14.36 (1.51)	13.92 — 14.81		16.75 (0.58)	16.18 — 17.31	2.39	<0.01	23.76 (0.45)	23.32 — 24.21	9.40	<0.01
L4	13.59 (1.55)	13.13 — 14.05		16.97 (0.88)	16.11 — 17.83	3.38	<0.01	23.25 (0.34)	22.91 — 23.59	9.66	<0.01
L5	13.71 (2.40)	13.01 — 14.42		16.38 (0.69)	15.70 — 17.06	2.67	0.01	25.16 (0.43)	24.74 — 25.58	11.45	<0.01
L6				15.38 (0.55)	14.84 — 15.92	1.66	0.03	26.01 (0.60)	25.42 — 26.60	12.30	<0.01

Table E.10 – Comparison of left pedicular height measurements between human, pig, and sheep data.

	Human		Pig				Sheep			
	Mean ± SD	95%CI	Mean ± SD	95%CI	mean diff	p	Mean ± SD	95%CI	mean diff	p
T1	9.08 (1.42)	8.66 — 9.50	9.86 (0.33)	9.54 — 10.19	0.78	0.16	10.68 (0.44)	10.25 — 11.12	1.60	0.02
T2	7.56 (1.26)	7.18 — 7.93	9.24 (0.38)	8.87 — 9.61	1.69	0.01	8.89 (0.64)	8.26 — 9.52	1.34	0.03
T3	5.81 (1.30)	5.42 — 6.19	8.82 (1.24)	7.60 — 10.04	3.01	<0.01	8.55 (0.45)	8.10 — 8.99	2.74	<0.01
T4	5.31 (1.18)	4.96 — 5.65	9.02 (0.96)	8.08 — 9.97	3.72	<0.01	7.57 (0.58)	7.00 — 8.14	2.26	<0.01
T5	5.50 (1.50)	5.05 — 5.94	8.92 (0.79)	8.15 — 9.70	3.43	<0.01	7.15 (0.42)	6.74 — 7.57	1.66	0.01
T6	5.49 (1.39)	5.08 — 5.90	9.31 (0.84)	8.49 — 10.14	3.83	<0.01	7.51 (0.46)	7.07 — 7.96	2.02	0.01
T7	5.84 (0.85)	5.59 — 6.09	9.33 (1.01)	8.34 — 10.32	3.49	<0.01	7.02 (0.20)	6.82 — 7.22	1.18	<0.01
T8	5.70 (1.33)	5.36 — 6.27	9.15 (1.07)	8.10 — 10.19	3.44	<0.01	6.71 (0.16)	6.55 — 6.87	1.01	0.04
T9	6.15 (1.39)	5.75 — 6.64	9.67 (0.96)	8.73 — 10.62	3.52	<0.01	6.88 (0.37)	6.51 — 7.24	0.73	0.16
T10	6.96 (1.77)	6.45 — 7.52	8.62 (1.14)	7.50 — 9.74	1.66	0.04	6.46 (0.19)	6.28 — 6.64	0.50	0.97
T11	8.18 (1.94)	7.61 — 8.75	9.44 (0.89)	8.57 — 10.32	1.26	0.14	7.39 (0.11)	7.28 — 7.49	0.79	0.45
T12	8.40 (1.89)	7.84 — 8.96	9.79 (0.86)	8.94 — 10.63	1.38	0.11	8.75 (0.21)	8.55 — 8.96	0.35	0.81
T13			9.97 (0.87)	9.12 — 10.82	1.57	0.09	9.81 (0.19)	9.62 — 10.00	1.41	0.07
T14			9.67 (0.92)	8.77 — 10.58	1.27	0.17	9.55 (0.43)	9.12 — 9.97	1.14	0.21
L1	7.80 (1.69)	7.30 — 8.29	10.17 (0.66)	9.52 — 10.81	2.37	0.01	10.07 (0.29)	9.79 — 10.35	2.27	0.01
L2	8.38 (1.80)	7.85 — 8.91	9.97 (0.35)	9.62 — 10.31	1.59	0.05	9.46 (0.14)	9.32 — 9.60	1.08	0.19
L3	10.08 (1.74)	9.57 — 10.59	10.02 (0.12)	9.90 — 10.14	0.06	0.84	9.11 (0.33)	8.79 — 9.43	0.97	0.17
L4	11.94 (1.87)	11.39 — 12.49	9.92 (0.30)	9.63 — 10.21	2.02	0.03	9.37 (0.45)	8.93 — 9.81	2.57	0.01
L5	15.63 (2.09)	15.02 — 16.25	10.04 (0.45)	9.60 — 10.49	5.59	<0.01	10.12 (0.77)	9.37 — 10.87	5.51	<0.01
L6			10.71 (0.25)	10.47 — 10.95	4.93	<0.01	11.78 (0.31)	11.48 — 12.09	3.85	<0.01

Table E.11 – Comparison of left pedicular width measurements between human, pig, and sheep data.

	Male				Female				Mean Difference (p)		
	Mean (SD)		95%CI		Mean (SD)		95%CI				
T1	18.99 (1.27)		18.52 – 19.45		16.83 (0.74)		16.45 – 17.21		2.16 (0.00)		
T2	20.17 (1.02)		19.79 – 20.54		18.09 (0.84)		17.67 – 18.52		2.08 (0.00)		
T3	20.60 (1.36)		20.10 – 21.09		18.67 (1.29)		18.02 – 19.32		1.93 (0.00)		
T4	20.71 (1.79)		20.06 – 21.36		18.90 (1.33)		18.23 – 19.57		1.82 (0.00)		
T5	21.52 (1.26)		21.06 – 21.98		19.09 (1.25)		18.46 – 19.73		2.43 (0.00)		
T6	21.76 (1.61)		21.17 – 22.34		19.35 (1.15)		18.77 – 19.93		2.40 (0.00)		
T7	22.01 (1.33)		21.53 – 22.50		19.82 (1.54)		19.03 – 20.60		2.20 (0.00)		
T8	22.45 (1.54)		21.89 – 23.01		20.69 (0.86)		20.25 – 21.13		1.76 (0.00)		
T9	23.40 (1.79)		22.75 – 24.05		21.77 (1.31)		21.11 – 22.43		1.63 (0.00)		
T10	24.94 (2.11)		24.17 – 25.70		23.43 (1.26)		22.79 – 24.07		1.50 (0.01)		
T11	26.11 (2.14)		25.33 – 26.89		23.98 (0.87)		23.54 – 24.42		2.13 (0.00)		
T12	27.33 (1.81)		26.67 – 27.99		25.59 (1.10)		25.03 – 26.14		1.74 (0.00)		
L1	28.96 (1.92)		28.26 – 29.66		27.69 (1.46)		26.95 – 28.43		1.27 (0.02)		
L2	30.88 (1.90)		30.18 – 31.57		29.70 (1.57)		28.90 – 30.49		1.18 (0.03)		
L3	31.49 (1.83)		30.82 – 32.15		30.19 (1.72)		29.32 – 31.06		1.29 (0.03)		
L4	31.82 (2.08)		31.06 – 32.57		30.42 (2.14)		29.34 – 31.50		1.39 (0.05)		
L5	32.51 (1.96)		31.80 – 33.23		30.85 (2.05)		29.82 – 31.89		1.66 (0.02)		

Table F.1 – Comparison of vertebral body height measurements between human male and female vertebrae, showing male and female mean measurements with standard deviations (SD), and 95% confidence intervals, and the mean difference between male and female vertebral body height

	Male			Female			Mean Difference (p)	
	Mean (SD)		95%CI	Mean (SD)		95%CI		
T1	33.30 (1.99)	32.57 – 34.02		31.58 (2.62)	30.25 – 32.90		1.72 (0.04)	
T2	32.75 (1.98)	32.03 – 33.47		30.23 (1.31)	29.57 – 30.89		2.52 (0.00)	
T3	31.03 (2.53)	30.11 – 31.95		27.56 (1.18)	26.96 – 28.16		3.47 (0.00)	
T4	29.76 (2.15)	28.97 – 30.54		27.34 (1.52)	26.57 – 28.11		2.42 (0.00)	
T5	30.24 (2.01)	29.51 – 30.97		27.79 (1.21)	27.18 – 28.40		2.45 (0.00)	
T6	31.50 (2.06)	30.76 – 32.25		28.21 (1.28)	27.56 – 28.86		3.29 (0.00)	
T7	32.78 (2.10)	32.01 – 33.55		30.07 (1.83)	29.15 – 30.99		2.71 (0.00)	
T8	33.76 (2.55)	32.83 – 34.69		31.85 (1.66)	31.01 – 32.70		1.91 (0.00)	
T9	35.28 (2.89)	34.23 – 36.33		32.89 (1.38)	32.20 – 33.59		2.38 (0.00)	
T10	37.58 (3.01)	36.49 – 38.68		35.32 (1.68)	34.47 – 36.17		2.26 (0.00)	
T11	40.94 (4.00)	39.48 – 42.39		38.08 (2.22)	36.96 – 39.20		2.86 (0.00)	
T12	43.10 (3.00)	42.01 – 44.19		40.85 (2.43)	39.63 – 42.08		2.24 (0.01)	
L1	43.81 (3.43)	42.56 – 45.06		39.61 (4.41)	37.37 – 41.84		4.21 (0.00)	
L2	45.65 (3.35)	44.43 – 46.87		41.87 (2.77)	40.47 – 43.27		3.78 (0.00)	
L3	47.68 (3.82)	46.29 – 49.07		43.38 (2.19)	42.27 – 44.49		4.30 (0.00)	
L4	50.48 (4.26)	48.93 – 52.03		46.45 (2.12)	45.38 – 47.53		4.03 (0.00)	
L5	55.81 (4.53)	54.16 – 57.46		50.55 (2.27)	49.40 – 51.71		5.26 (0.00)	

Table F.2 – Comparison of vertebral body width measurements between human male and female vertebrae, showing male and female mean measurements with standard deviations (SD), and 95% confidence intervals, and the mean difference between male and female vertebral body width

	Male						Female						Mean Difference (p)		
	Mean (SD)			95%CI			Mean (SD)			95%CI					
T1	20.47	(	1.94	)	19.77	–	21.17	18.47	(	1.17	)	17.88	–	19.07	2.00	(	0.00	)
T2	21.60	(	1.96	)	20.89	–	22.31	19.48	(	3.24	)	17.84	–	21.12	2.12	(	0.03	)
T3	23.02	(	2.02	)	22.29	–	23.75	21.16	(	3.18	)	19.55	–	22.77	1.86	(	0.05	)
T4	25.25	(	1.87	)	24.57	–	25.93	22.60	(	2.25	)	21.46	–	23.74	2.64	(	0.00	)
T5	26.84	(	1.91	)	26.14	–	27.53	24.12	(	1.84	)	23.19	–	25.05	2.71	(	0.00	)
T6	28.39	(	1.83	)	27.72	–	29.05	25.78	(	2.21	)	24.66	–	26.90	2.61	(	0.00	)
T7	30.06	(	2.53	)	29.14	–	30.98	26.72	(	1.80	)	25.81	–	27.63	3.34	(	0.00	)
T8	31.47	(	1.93	)	30.77	–	32.18	28.31	(	1.72	)	27.44	–	29.17	3.17	(	0.00	)
T9	32.77	(	2.02	)	32.03	–	33.50	29.34	(	2.30	)	28.18	–	30.50	3.43	(	0.00	)
T10	33.83	(	1.91	)	33.14	–	34.53	30.23	(	2.42	)	29.00	–	31.45	3.61	(	0.00	)
T11	34.11	(	2.00	)	33.39	–	34.84	30.67	(	2.15	)	29.58	–	31.75	3.45	(	0.00	)
T12	35.11	(	2.23	)	34.30	–	35.92	31.79	(	2.67	)	30.44	–	33.14	3.32	(	0.00	)
L1	36.15	(	2.51	)	35.23	–	37.06	31.79	(	1.82	)	30.87	–	32.70	4.36	(	0.00	)
L2	38.09	(	2.76	)	37.09	–	39.10	33.52	(	2.13	)	32.44	–	34.60	4.57	(	0.00	)
L3	38.81	(	2.93	)	37.75	–	39.88	34.39	(	2.20	)	33.28	–	35.51	4.42	(	0.00	)
L4	38.25	(	2.69	)	37.27	–	39.23	34.24	(	1.87	)	33.30	–	35.19	4.01	(	0.00	)
L5	37.52	(	2.80	)	36.50	–	38.54	34.09	(	1.88	)	33.14	–	35.04	3.43	(	0.00	)

Table F.3 – Comparison of vertebral length length measurements between human male and female vertebrae, showing male and female mean measurements with standard deviations (SD), and 95% confidence intervals, and the mean difference between male and female vertebral body length

	Male					Female					Mean Difference (p)		
	Mean (SD)			95%CI			Mean (SD)			95%CI				
T1	81.18	(	4.74	)	79.45	–	82.91	73.67	(	3.70	)	71.80	–	75.54	7.51 (0.00)
T2	75.38	(	4.56	)	73.72	–	77.04	67.29	(	3.11	)	65.71	–	68.86	8.09 (0.00)
T3	69.19	(	5.09	)	67.34	–	71.04	63.06	(	2.79	)	61.65	–	64.47	6.13 (0.00)
T4	67.38	(	5.34	)	65.44	–	69.32	61.35	(	2.18	)	60.25	–	62.45	6.03 (0.00)
T5	67.81	(	5.48	)	65.82	–	69.81	62.45	(	2.49	)	61.19	–	63.71	5.36 (0.00)
T6	69.53	(	4.61	)	67.86	–	71.21	62.59	(	2.95	)	61.10	–	64.08	6.94 (0.00)
T7	68.13	(	5.33	)	66.19	–	70.07	62.90	(	5.61	)	60.06	–	65.74	5.23 (0.01)
T8	66.90	(	5.26	)	64.98	–	68.81	57.85	(	7.89	)	53.85	–	61.84	9.05 (0.00)
T9	65.62	(	4.41	)	64.02	–	67.23	59.68	(	3.97	)	57.67	–	61.69	5.95 (0.00)
T10	62.59	(	4.14	)	61.08	–	64.09	56.88	(	4.10	)	54.80	–	58.95	5.71 (0.00)
T11	57.33	(	4.30	)	55.76	–	58.90	49.88	(	8.80	)	45.43	–	54.34	7.45 (0.01)
T12	52.23	(	6.19	)	49.98	–	54.49	47.67	(	4.14	)	45.58	–	49.77	4.56 (0.01)
L1	79.47	(	9.75	)	75.92	–	83.02	70.37	(	5.63	)	67.52	–	73.22	9.11 (0.00)
L2	88.09	(	7.50	)	85.36	–	90.82	77.85	(	6.16	)	74.73	–	80.97	10.24 (0.00)
L3	96.10	(	7.36	)	93.42	–	98.78	86.95	(	6.33	)	83.75	–	90.15	9.15 (0.00)
L4	95.01	(	8.87	)	91.78	–	98.24	86.85	(	5.46	)	84.09	–	89.62	8.15 (0.00)
L5	100.35	(	8.37	)	97.31	–	103.40	91.07	(	5.53	)	88.27	–	93.87	9.28 (0.00)

Table F.4 – Comparison of transverse process width measurements between human male and female vertebrae, showing male and female mean measurements with standard deviations (SD), and 95% confidence intervals, and the mean difference between male and female transverse process width.

	Male					Female					Mean Difference (p)		
	Mean (SD)			95%CI		Mean (SD)			95%CI					
T1	23.63	(	1.68	)	23.01 – 24.24	22.44	(	1.39	)	21.74 – 23.15	1.18	(	0.02	)
T2	20.34	(	1.29	)	19.87 – 20.81	19.10	(	1.24	)	18.47 – 19.73	1.23	(	0.00	)
T3	19.34	(	1.65	)	18.74 – 19.94	17.97	(	1.39	)	17.26 – 18.67	1.37	(	0.01	)
T4	18.37	(	1.86	)	17.70 – 19.05	17.58	(	1.48	)	16.83 – 18.32	0.80	(	0.13	)
T5	18.00	(	1.73	)	17.37 – 18.63	17.33	(	1.72	)	16.46 – 18.20	0.68	(	0.23	)
T6	18.43	(	1.91	)	17.74 – 19.13	17.53	(	2.05	)	16.49 – 18.56	0.91	(	0.17	)
T7	18.62	(	2.33	)	17.77 – 19.47	17.61	(	2.00	)	16.60 – 18.62	1.01	(	0.14	)
T8	18.96	(	2.49	)	18.05 – 19.87	18.28	(	2.19	)	17.17 – 19.39	0.68	(	0.36	)
T9	19.30	(	2.68	)	18.33 – 20.28	18.46	(	1.92	)	17.49 – 19.43	0.84	(	0.24	)
T10	19.80	(	2.53	)	18.88 – 20.72	18.99	(	1.98	)	17.99 – 19.99	0.80	(	0.25	)
T11	21.89	(	3.12	)	20.75 – 23.02	20.71	(	2.15	)	19.62 – 21.80	1.18	(	0.15	)
T12	24.91	(	2.73	)	23.92 – 25.91	23.56	(	1.68	)	22.71 – 24.41	1.35	(	0.05	)
L1	25.56	(	2.56	)	24.63 – 26.49	24.78	(	1.81	)	23.86 – 25.70	0.78	(	0.25	)
L2	25.09	(	2.86	)	24.05 – 26.13	24.00	(	1.52	)	23.23 – 24.77	1.09	(	0.10	)
L3	26.17	(	2.70	)	25.18 – 27.15	24.20	(	1.76	)	23.31 – 25.10	1.96	(	0.01	)
L4	26.97	(	2.83	)	25.94 – 28.00	25.61	(	2.32	)	24.44 – 26.78	1.36	(	0.10	)
L5	30.53	(	3.17	)	29.38 – 31.68	29.98	(	2.85	)	28.54 – 31.42	0.55	(	0.56	)

Table F.5 – Comparison of spinal canal width measurements between human male and female vertebrae, showing male and female mean measurements with standard deviations (SD), and 95% confidence intervals, and the mean difference between male and female spinal canal width.

	Male						Female						Mean Difference (p)		
	Mean (SD)				95%CI		Mean (SD)				95%CI					
T1	15.97	(	1.24	)	15.52	–	16.42	14.78	(	1.58	)	13.98	–	15.58	1.19	(	0.02	)
T2	16.49	(	1.38	)	15.98	–	16.99	15.89	(	1.18	)	15.29	–	16.49	0.59	(	0.15	)
T3	16.76	(	1.29	)	16.29	–	17.23	16.71	(	1.19	)	16.10	–	17.31	0.05	(	0.90	)
T4	16.93	(	1.79	)	16.28	–	17.58	16.53	(	1.21	)	15.91	–	17.14	0.41	(	0.38	)
T5	16.59	(	1.58	)	16.02	–	17.17	16.84	(	1.57	)	16.04	–	17.63	0.24	(	0.63	)
T6	16.61	(	1.39	)	16.10	–	17.12	16.62	(	1.79	)	15.72	–	17.53	0.01	(	0.99	)
T7	17.04	(	1.70	)	16.42	–	17.66	16.52	(	1.33	)	15.85	–	17.19	0.52	(	0.27	)
T8	16.56	(	1.83	)	15.89	–	17.22	16.37	(	1.44	)	15.64	–	17.10	0.19	(	0.71	)
T9	16.57	(	2.15	)	15.79	–	17.35	16.16	(	1.39	)	15.45	–	16.86	0.41	(	0.44	)
T10	16.06	(	1.49	)	15.51	–	16.60	16.18	(	1.30	)	15.53	–	16.84	0.13	(	0.77	)
T11	17.31	(	2.06	)	16.56	–	18.06	16.37	(	1.19	)	15.77	–	16.97	0.93	(	0.06	)
T12	19.28	(	1.78	)	18.63	–	19.93	17.80	(	1.20	)	17.19	–	18.40	1.48	(	0.00	)
L1	18.92	(	1.47	)	18.39	–	19.46	18.19	(	1.59	)	17.38	–	18.99	0.73	(	0.15	)
L2	16.95	(	1.43	)	16.43	–	17.47	16.75	(	1.58	)	15.95	–	17.55	0.20	(	0.69	)
L3	17.02	(	1.76	)	16.38	–	17.66	17.08	(	2.01	)	16.06	–	18.10	0.06	(	0.92	)
L4	16.54	(	1.87	)	15.86	–	17.23	16.68	(	1.99	)	15.67	–	17.69	0.14	(	0.83	)
L5	17.74	(	2.15	)	16.95	–	18.52	17.45	(	2.83	)	16.02	–	18.88	0.28	(	0.74	)

Table F.6 – Comparison of spinal canal length measurements between human male and female vertebrae, showing male and female mean measurements with standard deviations (SD), and 95% confidence intervals, and the mean difference between male and female spinal canal length.

	Male						Female						Mean Difference (p)		
	Mean (SD)			95%CI			Mean (SD)			95%CI					
T1	72.42	(	4.46	)	70.80	–	74.04	63.33	(	4.47	)	61.07	–	65.59	9.09	(	0.00	)
T2	73.20	(	3.60	)	71.89	–	74.51	65.66	(	2.84	)	64.22	–	67.10	7.54	(	0.00	)
T3	75.09	(	3.31	)	73.89	–	76.30	67.52	(	3.09	)	65.96	–	69.08	7.57	(	0.00	)
T4	76.54	(	4.07	)	75.06	–	78.02	69.31	(	3.69	)	67.44	–	71.18	7.23	(	0.00	)
T5	79.24	(	4.44	)	77.63	–	80.86	73.83	(	7.68	)	69.95	–	77.72	5.41	(	0.02	)
T6	80.87	(	3.33	)	79.66	–	82.09	73.00	(	3.04	)	71.47	–	74.54	7.87	(	0.00	)
T7	82.60	(	4.52	)	80.96	–	84.25	74.53	(	4.76	)	72.12	–	76.94	8.08	(	0.00	)
T8	82.18	(	7.44	)	79.47	–	84.89	76.40	(	3.63	)	74.56	–	78.23	5.78	(	0.00	)
T9	83.84	(	3.94	)	82.41	–	85.28	76.69	(	3.72	)	74.81	–	78.57	7.16	(	0.00	)
T10	82.70	(	4.26	)	81.15	–	84.25	76.24	(	4.30	)	74.06	–	78.41	6.46	(	0.00	)
T11	81.65	(	5.39	)	79.69	–	83.61	74.91	(	4.86	)	72.45	–	77.37	6.74	(	0.00	)
T12	85.77	(	6.16	)	83.53	–	88.01	77.25	(	4.05	)	75.20	–	79.30	8.51	(	0.00	)
L1	90.71	(	5.98	)	88.54	–	92.89	81.10	(	4.64	)	78.76	–	83.45	9.61	(	0.00	)
L2	94.81	(	6.46	)	92.46	–	97.16	86.46	(	4.03	)	84.42	–	88.49	8.35	(	0.00	)
L3	95.49	(	6.38	)	93.17	–	97.81	87.85	(	5.59	)	85.02	–	90.68	7.64	(	0.00	)
L4	93.27	(	5.72	)	91.19	–	95.35	86.22	(	6.16	)	83.10	–	89.34	7.05	(	0.00	)
L5	86.49	(	4.56	)	84.83	–	88.15	81.58	(	5.95	)	78.57	–	84.59	4.91	(	0.01	)

Table F.7 – Comparison of vertebral total anteroposterior length measurements between human male and female vertebrae, showing male and female mean measurements with standard deviations (SD), and 95% confidence intervals, and the mean difference between male and female total anteroposterior length.

	Male						Female						Mean Difference (p)		
	Mean (SD)			95%CI			Mean (SD)			95%CI						
T1	9.51	(	1.13	)	9.10	–	9.92	8.56	(	1.43	)	7.84	–	9.29	0.95	(	0.04	)
T2	7.76	(	1.05	)	7.38	–	8.14	6.83	(	0.88	)	6.39	–	7.28	0.93	(	0.00	)
T3	6.12	(	1.37	)	5.62	–	6.62	5.16	(	1.08	)	4.61	–	5.70	0.97	(	0.02	)
T4	6.20	(	1.03	)	5.83	–	6.58	4.73	(	1.15	)	4.15	–	5.32	1.47	(	0.00	)
T5	5.61	(	1.38	)	5.10	–	6.11	4.77	(	0.79	)	4.37	–	5.17	0.84	(	0.01	)
T6	5.72	(	1.16	)	5.30	–	6.14	5.00	(	0.90	)	4.54	–	5.45	0.73	(	0.03	)
T7	6.59	(	2.24	)	5.77	–	7.41	5.39	(	0.76	)	5.01	–	5.78	1.20	(	0.01	)
T8	6.22	(	1.45	)	5.70	–	6.75	5.45	(	0.91	)	4.99	–	5.91	0.78	(	0.04	)
T9	6.85	(	1.20	)	6.41	–	7.28	5.97	(	1.19	)	5.37	–	6.57	0.88	(	0.03	)
T10	7.81	(	1.43	)	7.28	–	8.33	6.77	(	1.52	)	6.00	–	7.54	1.04	(	0.04	)
T11	8.93	(	1.58	)	8.36	–	9.51	7.87	(	1.20	)	7.26	–	8.48	1.06	(	0.02	)
T12	8.88	(	2.11	)	8.11	–	9.64	7.46	(	1.29	)	6.80	–	8.11	1.42	(	0.01	)
L1	8.51	(	1.47	)	7.98	–	9.05	7.09	(	1.16	)	6.51	–	7.68	1.42	(	0.00	)
L2	8.92	(	1.54	)	8.36	–	9.48	7.72	(	1.39	)	7.02	–	8.43	1.20	(	0.01	)
L3	10.70	(	1.44	)	10.18	–	11.22	9.52	(	1.69	)	8.66	–	10.37	1.18	(	0.03	)
L4	12.71	(	1.95	)	12.00	–	13.42	11.28	(	1.08	)	10.73	–	11.83	1.43	(	0.00	)
L5	16.71	(	2.17	)	15.92	–	17.50	14.63	(	1.22	)	14.01	–	15.25	2.08	(	0.00	)

Table F.8 – Comparison of right pedicle width measurements between human male and female vertebrae, showing male and female mean measurements with standard deviations (SD), and 95% confidence intervals, and the mean difference between male and female right pedicle width.

	Male						Female						Mean Difference (p)		
	Mean (SD)				95%CI		Mean (SD)				95%CI				
T1	10.10	(	1.04	)	9.72	–	10.48	8.99	(	1.10	)	8.44	–	9.55	1.10	(	0.00	)
T2	11.73	(	0.99	)	11.37	–	12.09	10.34	(	0.91	)	9.88	–	10.80	1.39	(	0.00	)
T3	12.32	(	0.81	)	12.02	–	12.61	10.74	(	1.00	)	10.23	–	11.25	1.58	(	0.00	)
T4	12.50	(	1.16	)	12.08	–	12.92	10.89	(	0.97	)	10.40	–	11.38	1.60	(	0.00	)
T5	12.85	(	1.26	)	12.39	–	13.30	10.75	(	1.02	)	10.24	–	11.27	2.09	(	0.00	)
T6	12.65	(	1.00	)	12.29	–	13.01	11.04	(	1.07	)	10.50	–	11.58	1.61	(	0.00	)
T7	12.37	(	1.57	)	11.80	–	12.95	11.03	(	0.71	)	10.67	–	11.39	1.34	(	0.00	)
T8	13.11	(	1.10	)	12.71	–	13.51	11.73	(	1.05	)	11.20	–	12.26	1.38	(	0.00	)
T9	13.66	(	1.32	)	13.18	–	14.14	12.38	(	0.97	)	11.89	–	12.87	1.28	(	0.00	)
T10	15.35	(	1.17	)	14.92	–	15.77	14.09	(	0.78	)	13.70	–	14.49	1.26	(	0.00	)
T11	16.62	(	0.86	)	16.30	–	16.93	15.51	(	0.91	)	15.05	–	15.97	1.11	(	0.00	)
T12	16.81	(	0.82	)	16.51	–	17.11	15.49	(	0.86	)	15.05	–	15.93	1.32	(	0.00	)
L1	15.88	(	1.42	)	15.37	–	16.40	14.53	(	1.07	)	13.99	–	15.07	1.35	(	0.00	)
L2	15.47	(	1.46	)	14.94	–	16.00	14.05	(	1.06	)	13.51	–	14.59	1.42	(	0.00	)
L3	15.11	(	1.37	)	14.61	–	15.61	13.93	(	1.07	)	13.39	–	14.47	1.18	(	0.00	)
L4	14.01	(	1.63	)	13.42	–	14.61	12.81	(	1.17	)	12.22	–	13.40	1.20	(	0.01	)
L5	14.00	(	2.39	)	13.13	–	14.88	12.43	(	0.99	)	11.94	–	12.93	1.57	(	0.00	)

Table F.9 – Comparison of right pedicle height measurements between human male and female vertebrae, showing male and female mean measurements with standard deviations (SD), and 95% confidence intervals, and the mean difference between male and female right pedicle height.

	Male						Female						Mean Difference (p)		
	Mean (SD)			95%CI			Mean (SD)			95%CI					
T1	9.54	(	1.23	)	9.09	–	9.98	8.26	(	1.49	)	7.50	–	9.01	1.28	(	0.01	)
T2	7.90	(	1.32	)	7.42	–	8.38	6.93	(	0.97	)	6.44	–	7.43	0.97	(	0.01	)
T3	6.04	(	1.42	)	5.53	–	6.56	5.31	(	0.99	)	4.80	–	5.81	0.74	(	0.05	)
T4	5.52	(	1.25	)	5.07	–	5.98	4.85	(	0.99	)	4.35	–	5.35	0.67	(	0.06	)
T5	5.76	(	1.76	)	5.12	–	6.39	4.96	(	0.80	)	4.55	–	5.36	0.80	(	0.05	)
T6	5.67	(	1.60	)	5.09	–	6.25	5.14	(	0.93	)	4.67	–	5.61	0.53	(	0.17	)
T7	6.35	(	2.07	)	5.60	–	7.10	5.35	(	0.93	)	4.88	–	5.82	0.99	(	0.03	)
T8	6.18	(	1.79	)	5.53	–	6.83	5.16	(	0.70	)	4.81	–	5.52	1.02	(	0.01	)
T9	6.49	(	1.74	)	5.86	–	7.13	5.60	(	0.81	)	5.19	–	6.01	0.90	(	0.02	)
T10	7.37	(	1.93	)	6.66	–	8.07	6.27	(	1.47	)	5.53	–	7.02	1.09	(	0.04	)
T11	8.21	(	2.13	)	7.43	–	8.98	8.10	(	1.71	)	7.24	–	8.97	0.10	(	0.86	)
T12	8.60	(	1.83	)	7.94	–	9.27	8.14	(	2.09	)	7.08	–	9.20	0.46	(	0.47	)
L1	8.24	(	1.86	)	7.56	–	8.92	7.06	(	0.97	)	6.57	–	7.55	1.18	(	0.01	)
L2	8.83	(	1.84	)	8.16	–	9.50	7.74	(	1.38	)	7.04	–	8.44	1.09	(	0.03	)
L3	10.53	(	1.77	)	9.89	–	11.18	9.45	(	1.30	)	8.79	–	10.11	1.09	(	0.03	)
L4	12.47	(	1.82	)	11.81	–	13.14	11.20	(	1.41	)	10.48	–	11.91	1.28	(	0.01	)
L5	16.23	(	2.09	)	15.47	–	17.00	14.59	(	1.77	)	13.69	–	15.48	1.65	(	0.01	)

Table F.10 – Comparison of left pedicle width measurements between human male and female vertebrae, showing male and female mean measurements with standard deviations (SD), and 95% confidence intervals, and the mean difference between male and female left pedicle width.

	Male						Female						Mean Difference (p)		
	Mean (SD)			95%CI			Mean (SD)			95%CI					
T1	10.22	(	0.91	)	9.89	–	10.55	9.28	(	1.21	)	8.67	–	9.90	0.94	(	0.01	)
T2	11.96	(	0.89	)	11.64	–	12.28	10.43	(	0.91	)	9.97	–	10.89	1.53	(	0.00	)
T3	12.77	(	0.97	)	12.42	–	13.13	10.81	(	1.07	)	10.27	–	11.35	1.96	(	0.00	)
T4	12.46	(	0.66	)	12.22	–	12.70	10.94	(	1.19	)	10.34	–	11.54	1.52	(	0.00	)
T5	12.65	(	1.12	)	12.24	–	13.05	10.84	(	1.12	)	10.27	–	11.40	1.81	(	0.00	)
T6	12.75	(	1.02	)	12.38	–	13.12	10.78	(	1.06	)	10.24	–	11.32	1.97	(	0.00	)
T7	12.46	(	1.78	)	11.81	–	13.10	11.09	(	1.04	)	10.56	–	11.61	1.37	(	0.00	)
T8	13.06	(	1.20	)	12.62	–	13.50	11.61	(	1.02	)	11.09	–	12.13	1.45	(	0.00	)
T9	13.68	(	1.19	)	13.24	–	14.11	12.31	(	1.06	)	11.77	–	12.85	1.36	(	0.00	)
T10	15.47	(	0.98	)	15.12	–	15.83	14.37	(	0.68	)	14.03	–	14.72	1.10	(	0.00	)
T11	16.48	(	0.93	)	16.14	–	16.82	15.44	(	0.91	)	14.98	–	15.89	1.05	(	0.00	)
T12	16.75	(	0.73	)	16.48	–	17.01	15.50	(	0.84	)	15.08	–	15.92	1.25	(	0.00	)
L1	15.93	(	1.04	)	15.55	–	16.31	14.25	(	1.05	)	13.72	–	14.78	1.68	(	0.00	)
L2	15.38	(	1.57	)	14.81	–	15.95	13.43	(	1.27	)	12.79	–	14.07	1.95	(	0.00	)
L3	14.79	(	1.52	)	14.24	–	15.35	13.67	(	1.21	)	13.06	–	14.29	1.12	(	0.01	)
L4	13.93	(	1.74	)	13.29	–	14.56	12.93	(	0.97	)	12.44	–	13.42	1.00	(	0.02	)
L5	14.10	(	2.34	)	13.25	–	14.95	13.15	(	2.52	)	11.88	–	14.42	0.95	(	0.23	)

Table F.11 – Comparison of left pedicle height measurements between human male and female vertebrae, showing male and female mean measurements with standard deviations (SD), and 95% confidence intervals, and the mean difference between male and female left pedicle height.

G – TABLES SHOWING COMPARISONS BETWEEN HUMAN OLD AND YOUNG CT VERTEBRAL MEASUREMENTS

	<57						≥57						Mean Difference (p)		
	Mean (SD)			95%CI			Mean (SD)			95%CI					
T1	18.29	(	1.65	)	17.58	–	19.00	18.22	(	1.42	)	17.64	–	18.80	0.07	(	0.89	)
T2	19.63	(	1.67	)	18.92	–	20.35	19.30	(	1.06	)	18.87	–	19.74	0.33	(	0.94	)
T3	20.23	(	1.78	)	19.47	–	20.99	19.67	(	1.43	)	19.09	–	20.26	0.56	(	0.80	)
T4	20.27	(	1.97	)	19.43	–	21.12	19.93	(	1.76	)	19.21	–	20.65	0.34	(	0.51	)
T5	20.86	(	1.88	)	20.06	–	21.67	20.54	(	1.55	)	19.90	–	21.17	0.33	(	0.71	)
T6	21.15	(	1.96	)	20.31	–	21.99	20.74	(	1.78	)	20.01	–	21.46	0.42	(	0.81	)
T7	21.44	(	2.08	)	20.55	–	22.33	21.10	(	1.40	)	20.53	–	21.67	0.34	(	0.54	)
T8	22.16	(	1.76	)	21.40	–	22.91	21.57	(	1.37	)	21.00	–	22.13	0.59	(	0.46	)
T9	23.25	(	1.75	)	22.50	–	24.00	22.47	(	1.81	)	21.73	–	23.21	0.78	(	0.76	)
T10	25.05	(	1.66	)	24.34	–	25.76	23.85	(	2.12	)	22.98	–	24.71	1.21	(	0.62	)
T11	25.89	(	2.03	)	25.02	–	26.76	24.93	(	2.04	)	24.09	–	25.76	0.96	(	0.66	)
T12	27.14	(	1.73	)	26.40	–	27.88	26.37	(	1.82	)	25.63	–	27.11	0.77	(	0.48	)
L1	28.70	(	1.82	)	27.92	–	29.48	27.94	(	1.60	)	27.28	–	28.59	0.77	(	0.09	)
L2	30.81	(	2.08	)	29.92	–	31.70	30.17	(	1.62	)	29.51	–	30.83	0.64	(	0.62	)
L3	31.28	(	2.20	)	30.34	–	32.22	30.84	(	1.55	)	30.20	–	31.47	0.44	(	0.78	)
L4	31.60	(	2.28	)	30.62	–	32.57	31.11	(	2.11	)	30.25	–	31.97	0.48	(	0.99	)
L5	32.13	(	2.11	)	31.23	–	33.04	31.78	(	2.16	)	30.90	–	32.66	0.35	(	0.97	)

Figure G.1 - Comparison of vertebral body height measurements between human old and young vertebrae, showing old and young mean measurements with standard deviations (SD), and 95% confidence intervals, and the mean difference between old and young vertebral body height

	<57						≥57						Mean Difference (p)		
	Mean (SD)			95%CI			Mean (SD)			95%CI					
T1	32.36	(	2.68	)	31.21	–	33.51	32.82	(	2.05	)	31.98	–	33.65	0.46	(	0.94	)
T2	32.35	(	2.45	)	31.30	–	33.40	31.47	(	1.75	)	30.75	–	32.19	0.88	(	0.68	)
T3	30.16	(	2.93	)	28.91	–	31.41	29.56	(	2.55	)	28.52	–	30.61	0.59	(	0.59	)
T4	28.99	(	2.34	)	27.99	–	29.99	28.88	(	2.24	)	27.97	–	29.79	0.11	(	0.45	)
T5	29.61	(	2.09	)	28.71	–	30.50	29.22	(	2.17	)	28.33	–	30.11	0.38	(	0.31	)
T6	30.64	(	2.16	)	29.71	–	31.56	30.15	(	2.63	)	29.07	–	31.23	0.49	(	0.26	)
T7	32.02	(	2.11	)	31.12	–	32.93	31.71	(	2.64	)	30.63	–	32.78	0.32	(	0.52	)
T8	33.22	(	2.27	)	32.25	–	34.19	32.66	(	2.19	)	31.76	–	33.55	0.56	(	0.06	)
T9	34.82	(	2.87	)	33.60	–	36.05	34.14	(	2.58	)	33.08	–	35.20	0.68	(	0.20	)
T10	37.10	(	2.99	)	35.81	–	38.38	36.55	(	2.71	)	35.45	–	37.66	0.54	(	0.09	)
T11	39.84	(	3.11	)	38.50	–	41.17	40.08	(	4.28	)	38.33	–	41.83	0.25	(	0.58	)
T12	42.38	(	2.71	)	41.22	–	43.54	42.29	(	3.28	)	40.95	–	43.63	0.09	(	0.65	)
L1	42.45	(	5.06	)	40.28	–	44.61	42.31	(	3.47	)	40.90	–	43.73	0.13	(	0.32	)
L2	44.53	(	3.11	)	43.20	–	45.86	43.72	(	3.79	)	42.17	–	45.27	0.81	(	0.07	)
L3	46.53	(	4.23	)	44.72	–	48.34	45.92	(	3.66	)	44.43	–	47.42	0.60	(	0.29	)
L4	49.35	(	4.52	)	47.42	–	51.28	48.89	(	3.82	)	47.32	–	50.45	0.46	(	0.66	)
L5	53.75	(	4.53	)	51.81	–	55.68	54.27	(	4.79	)	52.31	–	56.23	0.52	(	0.65	)

Figure G.2 - Comparison of vertebral body width measurements between human old and young vertebrae, showing old and young mean measurements with standard deviations (SD), and 95% confidence intervals, and the mean difference between old and young vertebral body width.

	<57						≥57						Mean Difference (p)		
	Mean (SD)			95%CI			Mean (SD)			95%CI					
T1	19.88	(	2.06	)	19.00	–	20.76	19.71	(	1.89	)	18.93	–	20.48	0.17	(	0.93	)
T2	20.77	(	2.14	)	19.86	–	21.68	20.97	(	3.06	)	19.72	–	22.23	0.20	(	0.86	)
T3	22.45	(	2.98	)	21.18	–	23.73	22.33	(	2.25	)	21.41	–	23.25	0.13	(	0.28	)
T4	24.44	(	2.31	)	23.45	–	25.42	24.26	(	2.44	)	23.27	–	25.26	0.17	(	0.79	)
T5	25.64	(	2.08	)	24.75	–	26.53	26.16	(	2.46	)	25.16	–	27.16	0.52	(	0.85	)
T6	27.15	(	2.09	)	26.25	–	28.04	27.82	(	2.50	)	26.80	–	28.84	0.67	(	0.59	)
T7	28.54	(	2.79	)	27.35	–	29.73	29.27	(	2.80	)	28.12	–	30.41	0.73	(	0.53	)
T8	29.93	(	2.66	)	28.79	–	31.07	30.82	(	2.07	)	29.97	–	31.67	0.89	(	0.66	)
T9	30.99	(	2.56	)	29.89	–	32.08	32.16	(	2.68	)	31.07	–	33.26	1.18	(	0.56	)
T10	32.19	(	2.97	)	30.92	–	33.46	32.99	(	2.42	)	32.00	–	33.98	0.80	(	0.38	)
T11	32.79	(	2.99	)	31.51	–	34.06	33.08	(	2.28	)	32.15	–	34.01	0.29	(	0.95	)
T12	33.87	(	3.11	)	32.54	–	35.20	34.07	(	2.65	)	32.99	–	35.16	0.20	(	0.83	)
L1	34.66	(	3.40	)	33.21	–	36.12	34.66	(	2.85	)	33.49	–	35.83	0.00	(	0.95	)
L2	36.17	(	3.51	)	34.67	–	37.67	36.86	(	3.25	)	35.54	–	38.19	0.69	(	0.39	)
L3	37.30	(	3.54	)	35.78	–	38.81	37.31	(	3.38	)	35.93	–	38.69	0.02	(	0.77	)
L4	36.65	(	2.96	)	35.38	–	37.91	37.10	(	3.26	)	35.77	–	38.43	0.45	(	0.79	)
L5	36.97	(	3.41	)	35.51	–	38.43	36.57	(	2.98	)	35.36	–	37.79	0.40	(	0.78	)

Figure G.3 - Comparison of vertebral body length measurements between human old and young vertebrae, showing old and young mean measurements with standard deviations (SD), and 95% confidence intervals, and the mean difference between old and young vertebral body length.

	<57						≥57						Mean Difference (p)		
	Mean (SD)			95%CI			Mean (SD)			95%CI					
T1	79.28	(	5.88	)	76.77	−	81.79	78.02	(	5.52	)	75.76	−	80.27	1.26	(	0.38	)
T2	73.83	(	6.07	)	71.24	−	76.43	71.51	(	5.09	)	69.44	−	73.59	2.32	(	0.29	)
T3	67.83	(	5.47	)	65.50	−	70.17	66.43	(	5.16	)	64.32	−	68.54	1.41	(	0.35	)
T4	66.29	(	5.36	)	64.00	−	68.59	64.44	(	5.27	)	62.29	−	66.59	1.85	(	0.27	)
T5	66.96	(	5.64	)	64.55	−	69.38	65.09	(	4.94	)	63.07	−	67.11	1.87	(	0.12	)
T6	67.56	(	4.39	)	65.69	−	69.44	65.93	(	5.17	)	63.82	−	68.05	1.63	(	0.07	)
T7	66.75	(	5.22	)	64.52	−	68.98	65.97	(	6.59	)	63.28	−	68.66	0.78	(	0.11	)
T8	65.27	(	5.44	)	62.95	−	67.60	62.48	(	8.99	)	58.80	−	66.15	2.80	(	0.15	)
T9	63.90	(	5.43	)	61.58	−	66.22	63.32	(	4.87	)	61.33	−	65.31	0.58	(	0.43	)
T10	61.62	(	4.93	)	59.51	−	63.73	59.74	(	4.83	)	57.77	−	61.72	1.88	(	0.09	)
T11	55.18	(	9.17	)	51.26	−	59.10	54.44	(	4.59	)	52.56	−	56.31	0.74	(	0.40	)
T12	50.92	(	6.04	)	48.34	−	53.50	50.46	(	5.99	)	48.01	−	52.91	0.46	(	0.38	)
L1	77.80	(	10.84	)	73.16	−	82.44	75.06	(	8.24	)	71.70	−	78.43	2.74	(	0.79	)
L2	86.36	(	10.19	)	82.00	−	90.72	82.99	(	6.54	)	80.32	−	85.66	3.37	(	0.56	)
L3	93.73	(	8.71	)	90.01	−	97.46	92.29	(	7.87	)	89.08	−	95.51	1.44	(	0.39	)
L4	92.61	(	9.01	)	88.75	−	96.46	91.88	(	8.66	)	88.34	−	95.42	0.73	(	0.48	)
L5	96.77	(	8.63	)	93.08	−	100.46	97.57	(	8.91	)	93.93	−	101.21	0.80	(	0.89	)

Figure G.4 - Comparison of transverse process width measurements between human old and young vertebrae, showing old and young mean measurements with standard deviations (SD), and 95% confidence intervals, and the mean difference between old and young transverse process width.

	<57						≥57						Mean Difference (p)		
	Mean (SD)			95%CI			Mean (SD)			95%CI					
T1	23.27	(	1.59	)	22.59	–	23.95	23.18	(	1.78	)	22.46	–	23.91	0.08	(	0.98	)
T2	20.21	(	1.21	)	19.70	–	20.73	19.65	(	1.53	)	19.02	–	20.27	0.56	(	0.75	)
T3	19.37	(	1.48	)	18.74	–	20.01	18.42	(	1.77	)	17.69	–	19.14	0.96	(	0.19	)
T4	18.78	(	1.61	)	18.09	–	19.47	17.48	(	1.69	)	16.79	–	18.18	1.30	(	0.19	)
T5	18.40	(	1.62	)	17.71	–	19.09	17.20	(	1.67	)	16.51	–	17.88	1.20	(	0.23	)
T6	18.90	(	1.89	)	18.10	–	19.71	17.41	(	1.82	)	16.67	–	18.16	1.49	(	0.23	)
T7	18.87	(	2.34	)	17.87	–	19.87	17.74	(	2.06	)	16.89	–	18.58	1.13	(	0.50	)
T8	19.46	(	2.25	)	18.50	–	20.43	18.06	(	2.36	)	17.10	–	19.03	1.40	(	0.21	)
T9	19.79	(	2.48	)	18.73	–	20.85	18.31	(	2.25	)	17.38	–	19.23	1.49	(	0.17	)
T10	20.12	(	2.41	)	19.09	–	21.15	18.98	(	2.23	)	18.07	–	19.89	1.14	(	0.22	)
T11	22.16	(	3.02	)	20.87	–	23.45	20.87	(	2.61	)	19.80	–	21.94	1.30	(	0.27	)
T12	24.62	(	2.37	)	23.60	–	25.63	24.30	(	2.64	)	23.22	–	25.38	0.32	(	0.86	)
L1	24.99	(	2.43	)	23.95	–	26.03	25.57	(	2.27	)	24.64	–	26.50	0.58	(	0.13	)
L2	24.71	(	2.66	)	23.57	–	25.85	24.73	(	2.44	)	23.73	–	25.73	0.02	(	0.76	)
L3	25.34	(	2.35	)	24.34	–	26.35	25.64	(	2.81	)	24.49	–	26.79	0.30	(	0.69	)
L4	26.41	(	2.82	)	25.20	–	27.62	26.60	(	2.68	)	25.50	–	27.69	0.19	(	0.74	)
L5	30.72	(	3.59	)	29.19	–	32.26	29.99	(	2.48	)	28.98	–	31.01	0.73	(	0.24	)

Figure G.5 - Comparison of spinal canal width measurements between human old and young vertebrae, showing old and young mean measurements with standard deviations (SD), and 95% confidence intervals, and the mean difference between old and young spinal canal width.

	<57						≥57						Mean Difference (p)		
	Mean (SD)			95%CI			Mean (SD)			95%CI					
T1	15.76	(	1.37	)	15.17	–	16.35	15.39	(	1.55	)	14.76	–	16.02	0.37	(	0.83	)
T2	16.11	(	1.45	)	15.49	–	16.73	16.45	(	1.24	)	15.94	–	16.95	0.34	(	0.74	)
T3	16.66	(	1.42	)	16.05	–	17.27	16.81	(	1.08	)	16.37	–	17.25	0.15	(	0.66	)
T4	17.03	(	1.71	)	16.30	–	17.76	16.58	(	1.52	)	15.96	–	17.20	0.45	(	0.39	)
T5	17.05	(	1.84	)	16.26	–	17.83	16.34	(	1.21	)	15.85	–	16.83	0.71	(	0.23	)
T6	17.05	(	1.79	)	16.29	–	17.82	16.21	(	1.12	)	15.75	–	16.67	0.84	(	0.57	)
T7	17.39	(	1.69	)	16.66	–	18.11	16.38	(	1.34	)	15.83	–	16.93	1.01	(	0.49	)
T8	16.99	(	1.72	)	16.26	–	17.73	16.04	(	1.57	)	15.39	–	16.68	0.96	(	0.58	)
T9	16.84	(	1.87	)	16.04	–	17.64	16.06	(	1.92	)	15.27	–	16.84	0.78	(	0.74	)
T10	16.52	(	1.49	)	15.88	–	17.16	15.72	(	1.25	)	15.20	–	16.23	0.80	(	0.63	)
T11	16.84	(	2.88	)	15.61	–	18.08	16.42	(	1.53	)	15.80	–	17.05	0.42	(	0.30	)
T12	18.97	(	1.74	)	18.23	–	19.72	18.59	(	1.76	)	17.87	–	19.31	0.38	(	0.29	)
L1	18.51	(	1.49	)	17.88	–	19.15	18.81	(	1.60	)	18.16	–	19.46	0.30	(	0.54	)
L2	17.03	(	1.66	)	16.32	–	17.74	16.75	(	1.28	)	16.22	–	17.27	0.28	(	0.78	)
L3	17.29	(	2.11	)	16.39	–	18.19	16.81	(	1.53	)	16.19	–	17.44	0.48	(	0.58	)
L4	16.93	(	1.96	)	16.10	–	17.77	16.28	(	1.81	)	15.54	–	17.02	0.65	(	0.84	)
L5	18.15	(	2.38	)	17.13	–	19.17	17.18	(	2.33	)	16.23	–	18.13	0.97	(	0.73	)

Figure G.6 - Comparison of spinal canal length measurements between human old and young vertebrae, showing old and young mean measurements with standard deviations (SD), and 95% confidence intervals, and the mean difference between old and young spinal canal length.

	<57						≥57						Mean Difference (p)			
	Mean (SD)			95%CI			Mean (SD)			95%CI						
T1	69.96	(	5.92	)	67.43	–	72.49	66.57	(	12.07	)	61.63	–	71.50	3.39	(	0.38	)
T2	70.76	(	4.92	)	68.66	–	72.87	70.51	(	5.01	)	68.46	–	72.55	0.25	(	0.89	)
T3	73.14	(	4.87	)	71.06	–	75.23	71.93	(	4.84	)	69.95	–	73.91	1.21	(	0.67	)
T4	75.09	(	5.04	)	72.93	–	77.25	73.14	(	5.31	)	70.97	–	75.31	1.94	(	0.87	)
T5	78.68	(	7.17	)	75.61	–	81.75	76.23	(	5.10	)	74.15	–	78.32	2.44	(	0.68	)
T6	78.98	(	5.27	)	76.72	–	81.23	77.47	(	4.63	)	75.58	–	79.37	1.50	(	0.41	)
T7	81.13	(	6.26	)	78.45	–	83.80	78.68	(	5.58	)	76.40	–	80.96	2.45	(	0.17	)
T8	79.51	(	8.60	)	75.83	–	83.19	80.84	(	5.07	)	78.77	–	82.91	1.33	(	0.97	)
T9	81.86	(	5.77	)	79.39	–	84.33	80.99	(	4.58	)	79.12	–	82.86	0.87	(	0.32	)
T10	80.81	(	5.96	)	78.26	–	83.36	80.21	(	4.60	)	78.33	–	82.09	0.60	(	0.42	)
T11	79.80	(	7.17	)	76.73	–	82.86	78.95	(	5.03	)	76.89	–	81.00	0.85	(	0.34	)
T12	83.58	(	7.50	)	80.37	–	86.79	82.21	(	6.27	)	79.65	–	84.77	1.37	(	0.37	)
L1	87.98	(	7.91	)	84.60	–	91.37	85.63	(	12.40	)	80.57	–	90.70	2.35	(	0.24	)
L2	91.49	(	7.76	)	88.17	–	94.81	92.39	(	6.29	)	89.82	–	94.96	0.90	(	0.73	)
L3	92.77	(	7.69	)	89.48	–	96.05	92.99	(	6.64	)	90.28	–	95.71	0.23	(	0.84	)
L4	90.25	(	7.06	)	87.23	–	93.27	91.44	(	6.49	)	88.78	–	94.09	1.19	(	0.58	)
L5	84.46	(	6.24	)	81.79	–	87.13	85.15	(	4.91	)	83.14	–	87.16	0.69	(	0.36	)

Figure G.7 - Comparison of total anteroposterior vertebral length measurements between human old and young vertebrae, showing old and young mean measurements with standard deviations (SD), and 95% confidence intervals, and the mean difference between old and young total anteroposterior vertebral length.

	<57						≥57						Mean Difference (p)		
	Mean (SD)			95%CI			Mean (SD)			95%CI						
T1	8.99	(	1.17	)	8.49	−	9.49	9.23	(	1.50	)	8.62	−	9.85	0.25	(	0.60	)
T2	7.70	(	1.29	)	7.15	−	8.25	7.34	(	1.03	)	6.92	−	7.77	0.35	(	0.37	)
T3	5.84	(	1.39	)	5.24	−	6.43	5.75	(	1.34	)	5.20	−	6.30	0.09	(	0.55	)
T4	5.04	(	1.43	)	4.43	−	5.65	5.27	(	1.37	)	4.71	−	5.83	0.23	(	0.69	)
T5	5.40	(	1.22	)	4.88	−	5.92	5.25	(	1.34	)	4.70	−	5.80	0.15	(	0.62	)
T6	5.62	(	1.27	)	5.08	−	6.16	5.34	(	0.97	)	4.94	−	5.74	0.28	(	0.11	)
T7	6.21	(	2.01	)	5.35	−	7.08	6.15	(	1.93	)	5.36	−	6.94	0.06	(	0.93	)
T8	6.05	(	1.58	)	5.38	−	6.73	5.87	(	1.09	)	5.43	−	6.32	0.18	(	0.19	)
T9	6.47	(	1.63	)	5.77	−	7.17	6.33	(	1.26	)	5.82	−	6.85	0.14	(	0.37	)
T10	6.96	(	1.31	)	6.40	−	7.52	7.16	(	2.00	)	6.34	−	7.98	0.20	(	0.79	)
T11	8.24	(	1.58	)	7.56	−	8.91	8.31	(	2.26	)	7.38	−	9.23	0.07	(	0.39	)
T12	8.59	(	2.25	)	7.62	−	9.55	8.05	(	1.88	)	7.28	−	8.82	0.54	(	0.05	)
L1	7.27	(	1.15	)	6.77	−	7.76	7.40	(	1.82	)	6.66	−	8.15	0.14	(	0.08	)
L2	8.60	(	1.81	)	7.82	−	9.37	8.30	(	1.48	)	7.70	−	8.91	0.30	(	0.11	)
L3	10.27	(	1.96	)	9.43	−	11.11	10.06	(	1.56	)	9.43	−	10.70	0.20	(	0.14	)
L4	12.24	(	2.03	)	11.37	−	13.11	12.20	(	1.65	)	11.53	−	12.88	0.04	(	0.69	)
L5	16.04	(	2.15	)	15.12	−	16.96	15.97	(	2.16	)	15.09	−	16.85	0.07	(	0.29	)

Figure G.8 - Comparison of right pedicle width measurements between human old and young vertebrae, showing old and young mean measurements with standard deviations (SD), and 95% confidence intervals, and the mean difference between old and young right pedicle width.

	<57						≥57						Mean Difference (p)		
	Mean (SD)			95%CI			Mean (SD)			95%CI					
T1	9.55	(	1.28	)	9.00	–	10.10	9.88	(	1.07	)	9.44	–	10.31	0.33	(	0.29	)
T2	11.35	(	1.24	)	10.82	–	11.88	11.17	(	1.12	)	10.72	–	11.63	0.18	(	0.92	)
T3	11.87	(	1.25	)	11.34	–	12.41	11.70	(	1.07	)	11.26	–	12.14	0.17	(	0.47	)
T4	12.13	(	1.43	)	11.51	–	12.74	11.79	(	1.23	)	11.29	–	12.29	0.34	(	0.22	)
T5	12.18	(	1.62	)	11.49	–	12.88	12.09	(	1.50	)	11.47	–	12.70	0.10	(	0.77	)
T6	12.14	(	1.40	)	11.54	–	12.74	12.06	(	1.17	)	11.59	–	12.54	0.08	(	0.90	)
T7	11.84	(	1.82	)	11.07	–	12.62	11.98	(	1.13	)	11.52	–	12.44	0.14	(	0.88	)
T8	12.62	(	1.27	)	12.08	–	13.17	12.65	(	1.27	)	12.13	–	13.17	0.03	(	0.40	)
T9	13.19	(	1.32	)	12.62	–	13.75	13.26	(	1.40	)	12.68	–	13.83	0.07	(	0.47	)
T10	15.09	(	1.25	)	14.56	–	15.63	14.76	(	1.17	)	14.28	–	15.24	0.33	(	0.87	)
T11	16.37	(	1.17	)	15.87	–	16.87	16.12	(	0.86	)	15.77	–	16.47	0.25	(	0.77	)
T12	16.52	(	0.97	)	16.11	–	16.94	16.21	(	1.10	)	15.76	–	16.66	0.31	(	0.65	)
L1	15.76	(	1.47	)	15.13	–	16.39	15.12	(	1.39	)	14.55	–	15.68	0.64	(	0.61	)
L2	15.45	(	1.60	)	14.77	–	16.14	14.56	(	1.27	)	14.04	–	15.07	0.90	(	0.12	)
L3	14.20	(	1.93	)	13.37	–	15.02	14.21	(	1.01	)	13.80	–	14.63	0.02	(	0.78	)
L4	12.94	(	1.58	)	12.26	–	13.61	12.99	(	1.24	)	12.49	–	13.50	0.05	(	0.35	)
L5	13.66	(	1.84	)	12.87	–	14.45	12.86	(	1.92	)	12.07	–	13.64	0.80	(	0.23	)

Figure G.9 - Comparison of right pedicle height measurements between human old and young vertebrae, showing old and young mean measurements with standard deviations (SD), and 95% confidence intervals, and the mean difference between old and young right pedicle height.

	<57						>55						Mean Difference (p)		
	Mean (SD)			95%CI			Mean (SD)			95%CI					
T1	9.01	(	1.49	)	8.37	–	9.65	9.18	(	1.43	)	8.60	–	9.76	0.17	(	0.58	)
T2	7.75	(	1.44	)	7.14	–	8.37	7.40	(	1.14	)	6.94	–	7.87	0.35	(	0.72	)
T3	5.72	(	1.30	)	5.17	–	6.28	5.86	(	1.38	)	5.29	–	6.42	0.14	(	0.82	)
T4	5.25	(	1.28	)	4.70	–	5.79	5.33	(	1.15	)	4.86	–	5.80	0.08	(	0.71	)
T5	5.41	(	1.53	)	4.76	–	6.07	5.55	(	1.57	)	4.91	–	6.19	0.14	(	0.87	)
T6	5.37	(	1.48	)	4.73	–	6.00	5.60	(	1.39	)	5.03	–	6.17	0.23	(	0.60	)
T7	6.05	(	1.88	)	5.24	–	6.85	5.97	(	1.79	)	5.24	–	6.70	0.08	(	1.00	)
T8	5.88	(	1.90	)	5.07	–	6.69	5.79	(	1.26	)	5.28	–	6.31	0.09	(	0.22	)
T9	6.08	(	1.63	)	5.39	–	6.78	6.28	(	1.49	)	5.68	–	6.89	0.20	(	0.51	)
T10	6.81	(	1.60	)	6.12	–	7.49	7.16	(	2.07	)	6.32	–	8.01	0.36	(	0.78	)
T11	8.25	(	1.81	)	7.47	–	9.03	8.10	(	2.16	)	7.22	–	8.98	0.15	(	0.32	)
T12	8.64	(	1.86	)	7.85	–	9.44	8.27	(	1.98	)	7.46	–	9.08	0.37	(	0.21	)
L1	8.11	(	1.68	)	7.39	–	8.83	7.59	(	1.72	)	6.89	–	8.29	0.52	(	0.06	)
L2	8.56	(	1.93	)	7.73	–	9.38	8.37	(	1.63	)	7.71	–	9.04	0.19	(	0.09	)
L3	10.02	(	1.64	)	9.32	–	10.72	9.94	(	1.50	)	9.33	–	10.56	0.08	(	0.08	)
L4	11.98	(	1.99	)	11.13	–	12.83	12.09	(	1.62	)	11.43	–	12.75	0.11	(	0.68	)
L5	15.73	(	2.35	)	14.72	–	16.73	15.62	(	1.94	)	14.83	–	16.42	0.11	(	0.43	)

Figure G.10 - Comparison of left pedicle width measurements between human old and young vertebrae, showing old and young mean measurements with standard deviations (SD), and 95% confidence intervals, and the mean difference between old and young left pedicle width.

	<57						>55						Mean Difference (p)		
	Mean (SD)			95%CI			Mean (SD)			95%CI						
T1	9.86	(	1.29	)	9.31	–	10.41	9.94	(	0.93	)	9.56	–	10.32	0.08	(	0.36	)
T2	11.54	(	1.17	)	11.04	–	12.04	11.34	(	1.15	)	10.87	–	11.81	0.20	(	0.75	)
T3	12.13	(	1.40	)	11.53	–	12.73	12.08	(	1.37	)	11.52	–	12.64	0.05	(	0.37	)
T4	12.03	(	1.21	)	11.52	–	12.55	11.86	(	1.07	)	11.42	–	12.29	0.18	(	0.44	)
T5	12.05	(	1.31	)	11.49	–	12.62	12.01	(	1.51	)	11.39	–	12.63	0.05	(	0.62	)
T6	12.06	(	1.34	)	11.49	–	12.63	12.09	(	1.47	)	11.49	–	12.69	0.03	(	0.88	)
T7	11.72	(	2.11	)	10.81	–	12.62	12.24	(	1.18	)	11.75	–	12.72	0.52	(	0.43	)
T8	12.36	(	1.27	)	11.82	–	12.91	12.75	(	1.38	)	12.18	–	13.31	0.38	(	0.39	)
T9	13.16	(	1.33	)	12.59	–	13.73	13.25	(	1.33	)	12.71	–	13.80	0.09	(	0.51	)
T10	15.06	(	1.20	)	14.54	–	15.57	15.14	(	0.86	)	14.78	–	15.49	0.08	(	0.38	)
T11	16.39	(	1.16	)	15.90	–	16.89	15.88	(	0.86	)	15.52	–	16.23	0.52	(	0.45	)
T12	16.58	(	0.98	)	16.17	–	17.00	16.08	(	0.91	)	15.71	–	16.45	0.50	(	0.15	)
L1	15.74	(	1.20	)	15.23	–	16.26	15.00	(	1.33	)	14.46	–	15.55	0.74	(	0.23	)
L2	14.90	(	1.81	)	14.12	–	15.67	14.11	(	1.47	)	13.51	–	14.71	0.79	(	0.12	)
L3	13.62	(	2.35	)	12.62	–	14.63	13.79	(	1.13	)	13.32	–	14.25	0.16	(	0.63	)
L4	13.35	(	1.86	)	12.56	–	14.15	12.93	(	1.19	)	12.45	–	13.42	0.42	(	0.20	)
L5	13.68	(	2.57	)	12.58	–	14.78	13.00	(	1.80	)	12.26	–	13.74	0.68	(	0.44	)

Figure G.11 - Comparison of left pedicle height measurements between human old and young vertebrae, showing old and young mean measurements with standard deviations (SD), and 95% confidence intervals, and the mean difference between old and young left pedicle height.

REFERENCES

1.   Patlak M. Bone builders: the discoveries behind preventing and treating osteoporosis. FASEB J. 2001;15(10):1677E-E.

2.   Evans CH. John Hunter and the origins of modern orthopaedic research. J Orthop Res. 2007;25(4):556-60.

3.   Wolff J. The Law of Bone Remodelling. Berlin. Verlag von August Hirschwald. 1892.

4.   Albright F, Smith PH, Richardson AM. POSTMENOPAUSAL OSTEOPOROSIS: ITS CLINICAL FEATURES. JAMA. 1941;116(22):2465-74.

5.   Manring MM, Calhoun JH. Biographical Sketch: Fuller Albright, MD 1900–1969. Clin Orthop Relat Res. 2011;469(8):2092-5.

6.   Manolagas SC. From Estrogen-Centric to Aging and Oxidative Stress: A Revised Perspective of the Pathogenesis of Osteoporosis. Endocr Rev. 2010;31(3):266-300.

7.   Nordin BEC. The definition and diagnosis of osteoporosis. Calcified Tissue International. 1987;40(2):57-8.

8.   Osteoporosis | Harrison's Principles of Internal Medicine, 19e | AccessPharmacy | McGraw-Hill Medical.

9.   Kanis JA, Melton LJ, Christiansen C, Johnston CC, Khaltaev N. The diagnosis of osteoporosis. J Bone Miner Res. 1994;9(8):1137-41.

10.   Hernlund E, Svedbom A, Ivergård M, Compston J, Cooper C, Stenmark J, et al. Osteoporosis in the European Union: medical management, epidemiology and economic burden. Arch Osteoporos. 2013;8(1-2).

11.   Clarke B. Normal Bone Anatomy and Physiology. CJASN. 2008;3(Supplement 3):S131-S9.

12.   Cowin SC, Hegedus DH. Bone remodeling I: theory of adaptive elasticity. J Elasticity. 1976;6(3):313-26.

13.   Rho J-Y, Kuhn-Spearing L, Zioupos P. Mechanical properties and the hierarchical structure of bone. Medical Engineering & Physics. 1998;20(2):92-102.

14.   Koch JC. The laws of bone architecture. Am J Anat. 1917;21(2):177-298.

15.   Rho JY, Ashman RB, Turner CH. Young's modulus of trabecular and cortical bone material: Ultrasonic and microtensile measurements. Journal of biomechanics. 1993;26(2):111-9.

16.   Pittenger MF, Mackay AM, Beck SC, Jaiswal RK, Douglas R, Mosca JD, et al. Multilineage Potential of Adult Human Mesenchymal Stem Cells. Science. 1999;284(5411):143-7.

17.   Maeda K, Kobayashi Y, Udagawa N, Uehara S, Ishihara A, Mizoguchi T, et al. Wnt5a-Ror2 signaling between osteoblast-lineage cells and osteoclast precursors enhances osteoclastogenesis. Nat Med. 2012;18(3):405-12.

18.   Anderson HC. Matrix vesicles and calcification. Curr Rheumatol Rep. 2003;5(3):222-6.

19.   Boyle WJ, Simonet WS, Lacey DL. Osteoclast differentiation and activation. Nature. 2003;423(6937):337-42.

20.   Inaoka T, Bilbe G Fau - Ishibashi O, Ishibashi O Fau - Tezuka K, Tezuka K Fau - Kumegawa M, Kumegawa M Fau - Kokubo T, Kokubo T. Molecular cloning of human cDNA for cathepsin K: novel cysteine proteinase predominantly expressed in bone. (0006-291X (Print)).

21.   Henriksen K, Bollerslev J Fau - Everts V, Everts V Fau - Karsdal MA, Karsdal MA. Osteoclast activity and subtypes as a function of physiology and pathology--implications for future treatments of osteoporosis. (1945-7189 (Electronic)).

22.   Cherian PP, Cheng B, Gu S, Sprague E, Bonewald LF, Jiang JX. Effects of Mechanical Strain on the Function of Gap Junctions in Osteocytes Are Mediated through the Prostaglandin EP2 Receptor. J Biol Chem. 2003;278(44):43146-56.

23.   Burr DB. Targeted and nontargeted remodeling. Bone. 2002;30(1):2-4.

24.   Plotkin LI, Aguirre JI, Kousteni S, Manolagas SC, Bellido T. Bisphosphonates and Estrogens Inhibit Osteocyte Apoptosis via Distinct Molecular Mechanisms Downstream of Extracellular Signal-regulated Kinase Activation. J Biol Chem. 2005;280(8):7317-25.

25.   Plotkin LI, Weinstein RS, Parfitt AM, Roberson PK, Manolagas SC, Bellido T. Prevention of osteocyte and osteoblast apoptosis by bisphosphonates and calcitonin. J Clin Invest. 1999;104(10):1363-74.

26.   Roodman GD. Cell biology of the osteoclast. Exp Hematol. 1999;27(8):1229-41.

27.   Raggatt LJ, Partridge NC. Cellular and Molecular Mechanisms of Bone Remodeling. J Biol Chem. 2010;285(33):25103-8.

28.   Baht GS, Vi L, Alman BA. The Role of the Immune Cells in Fracture Healing. 2018(1544-2241 (Electronic)).

29.   Raisz LG. Pathogenesis of osteoporosis: concepts, conflicts, and prospects. J Clin Invest. 2005;115(12):3318-25.

30.   Lindsay R, Hart DM, Aitken JM, MacDonald EB, Anderson JB, Clarke AC. Long-term prevention of postmenopausal osteoporosis by oestrogen. Evidence for an increased bone mass after delayed onset of oestrogen treatment. Lancet. 1976;1(7968):1038-41.

31.   Lindsay R, Hart DM, Forrest C, Baird C. PREVENTION OF SPINAL OSTEOPOROSIS IN OOPHORECTOMISED WOMEN. The Lancet. 1980;316(8205):1151-4.

32.   Aitken JM, Hart DM, Lindsay R. Oestrogen Replacement Therapy for Prevention of Osteoporosis after Oophorectomy. Br Med J. 1973;3(5879):515-8.

33.   Christiansen C, Sanvig Christensen M, Transbl I. BONE MASS IN POSTMENOPAUSAL WOMEN AFTER WITHDRAWAL OF OESTROGEN/GESTAGEN REPLACEMENT THERAPY. The Lancet. 1981;317(8218):459-61.

34.   Riggs BL, Melton LJ. Involutional osteoporosis. N Engl J Med. 1986;314(26):1676-86.

35.   Rodan GA. Bone mass homeostasis and bisphosphonate action. Bone. 1997;20(1):1-4.

36.   Francis. The effects of testosterone on osteoporosis in men. Clin Endocrinol (Oxf). 1999;50(4):411-4.

37.   Fink HA, Ewing SK, Ensrud KE, Barrett-Connor E, Taylor BC, Cauley JA, et al. Association of Testosterone and Estradiol Deficiency with Osteoporosis and Rapid Bone Loss in Older Men. J Clin Endocrinol Metab. 2006;91(10):3908-15.

38.   Eriksen EF, Colvard DS, Berg NJ, Graham ML, Mann KG, Spelsberg TC, et al. Evidence of estrogen receptors in normal human osteoblast-like cells. Science. 1988;241(4861):84-6.

39.   Nakamura T, Imai Y, Matsumoto T, Sato S, Takeuchi K, Igarashi K, et al. Estrogen Prevents Bone Loss via Estrogen Receptor α and Induction of Fas Ligand in Osteoclasts. Cell. 2007;130(5):811-23.

40.   Rudman D, Drinka PJ, Wilson CR, Mattson DE, Scherman F, Cuisinier MC, et al. Relations of endogenous anabolic hormones and physical activity to bone mineral density and lean body mass in elderly men. Clin Endocrinol (Oxf). 1994;40(5):653-61.

41.   Drinka PJ, Olson J, Bauwens S, Voeks SK, Carlson I, Wilson M. Lack of association between free testosterone and bone density separate from age in elderly males. Calcified Tissue International. 1993;52(1):67-9.

42.   Carlsen CG, Soerensen TH, Eriksen EF. Prevalence of low serum estradiol levels in male osteoporosis. Osteoporosis international: a journal established as result of cooperation between the European Foundation for Osteoporosis and the National Osteoporosis Foundation of the USA. 2000;11(8):697-701.

43.   Tuck SP, Scane AC, Fraser WD, Diver MJ, Eastell R, Francis RM. Sex steroids and bone turnover markers in men with symptomatic vertebral fractures. Bone. 2008;43(6):999-1005.

44.   Looker AC, Wahner HW, Dunn WL, Calvo MS, Harris TB, Heyse SP, et al. Updated data on proximal femur bone mineral levels of US adults. Osteoporosis international: a journal established as result of cooperation between the European Foundation for Osteoporosis and the National Osteoporosis Foundation of the USA. 1998;8(5):468-89.

45.   Riggs BL, Melton LJ, Robb RA, Camp JJ, Atkinson EJ, McDaniel L, et al. A population-based assessment of rates of bone loss at multiple skeletal sites: evidence for substantial trabecular bone loss in young adult women and men. J Bone Miner Res. 2008;23(2):205-14.

46.   Frost HM. On Our Age-Related Bone Loss: Insights from a New Paradigm. Journal of Bone and Mineral Research. 1997;12(10):1539-46.

47.   Basu S, Michaëlsson K, Olofsson H, Johansson S, Melhus H. Association between Oxidative Stress and Bone Mineral Density. Biochemical and Biophysical Research Communications. 2001;288(1):275-9.

48.   Baek KH, Oh KW, Lee WY, Lee SS, Kim MK, Kwon HS, et al. Association of Oxidative Stress with Postmenopausal Osteoporosis and the Effects of Hydrogen Peroxide on Osteoclast Formation in Human Bone Marrow Cell Cultures. Calcified Tissue International. 2010;87(3):226-35.

49.   Bailey AJ, Knott L. Molecular changes in bone collagen in osteoporosis and osteoarthritis in the elderly. Exp Gerontol. 1999;34(3):337-51.

50.   Riggs BL, Khosla S, Melton LJ. Sex steroids and the construction and conservation of the adult skeleton. Endocr Rev. 2002;23(3):279-302.

51.   Dempster D, Lindsay R, Dempster, Lindsay. Pathogenesis of osteoporosis. The Lancet. 1993;341(8848):797-801.

52.   Saltman PD, Strause LG. The role of trace minerals in osteoporosis. Journal of the American College of Nutrition. 1993;12(4):384-9.

53.   Tranquilli AL, Lucino E, Garzetti GG, Romanini C. Calcium, phosphorus and magnesium intakes correlate with bone mineral content in postmenopausal women. Gynecological Endocrinology. 1994;8(1):55-8.

54.   Gür A, Çolpan L, Nas K, Çevik R, Saraç J, Erdoğan F, et al. The role of trace minerals in the pathogenesis of postmenopausal osteoporosis and a new effect of calcitonin. J Bone Miner Metab. 2002;20(1):39-43.

55.   Arikan DC, Coskun A, Ozer A, Kilinc M, Atalay F, Arikan T. Plasma Selenium, Zinc, Copper and Lipid Levels in Postmenopausal Turkish Women and Their Relation with Osteoporosis. Biol Trace Elem Res. 2011;144(1-3):407-17.

56.   Slemenda CW, Turner CH, Peacock M, Christian JC, Sorbel J, Hui SL, et al. The genetics of proximal femur geometry, distribution of bone mass and bone mineral density. Osteoporosis Int. 1996;6(2):178-82.

57.   Slemenda CW, Christian JC, Williams CJ, Norton JA, Johnston CC. Genetic determinants of bone mass in adult women: a reevaluation of the twin model and the potential importance of gene interaction on heritability estimates. J Bone Miner Res. 1991;6(6):561-7.

58.	Guéguen R, Jouanny P, Guillemin F, Kuntz C, Pourel J, Siest G. Segregation analysis and variance components analysis of bone mineral density in healthy families. J Bone Miner Res. 1995;10(12):2017-22.

59.	Makovey J, Nguyen TV, Naganathan V, Wark JD, Sambrook PN. Genetic effects on bone loss in peri- and postmenopausal women: a longitudinal twin study. J Bone Miner Res. 2007;22(11):1773-80.

60.	Shaffer JR, Kammerer CM, Bruder JM, Cole SA, Dyer TD, Almasy L, et al. Genetic influences on bone loss in the San Antonio Family Osteoporosis Study. Osteoporosis international : a journal established as result of cooperation between the European Foundation for Osteoporosis and the National Osteoporosis Foundation of the USA. 2008;19(12):1759-67.

61.	Kelly PJ, Nguyen T, Hopper J, Pocock N, Sambrook P, Eisman J. Changes in axial bone density with age: a twin study. J Bone Miner Res. 1993;8(1):11-7.

62.	Rivadeneira F, Styrkársdottir U, Estrada K, Halldórsson BV, Hsu Y-H, Richards JB, et al. Twenty bone-mineral-density loci identified by large-scale meta-analysis of genome-wide association studies. Nat Genet. 2009;41(11):1199-206.

63.	Becherini L, Gennari L, Masi L, Mansani R, Massart F, Morelli A, et al. Evidence of a linkage disequilibrium between polymorphisms in the human estrogen receptor alpha gene and their relationship to bone mass variation in postmenopausal Italian women. Hum Mol Genet. 2000;9(13):2043-50.

64.	Lohmueller KE, Pearce CL, Pike M, Lander ES, Hirschhorn JN. Meta-analysis of genetic association studies supports a contribution of common variants to susceptibility to common disease. Nat Genet. 2003;33(2):177-82.

65.	Efstathiadou Z, Tsatsoulis A, Ioannidis JPA. Association of Collagen Iα 1 Sp1 Polymorphism with the Risk of Prevalent Fractures: A Meta-Analysis. Journal of Bone and Mineral Research. 2001;16(9):1586-92.

66.	Dalle Carbonare L, Bertoldo F, Valenti MT, Zenari S, Zanatta M, Sella S, et al. Histomorphometric analysis of glucocorticoid-induced osteoporosis. Micron. 2005;36(7-8):645-52.

67.	O'Brien CA, Jia D, Plotkin LI, Bellido T, Powers CC, Stewart SA, et al. Glucocorticoids act directly on osteoblasts and osteocytes to induce their apoptosis and reduce bone formation and strength. Endocrinology. 2004;145(4):1835-41.

68.	Weinstein RS, Chen J-R, Powers CC, Stewart SA, Landes RD, Bellido T, et al. Promotion of osteoclast survival and antagonism of bisphosphonate-induced osteoclast apoptosis by glucocorticoids. J Clin Invest. 2002;109(8):1041-8.

69.   Ton FN, Gunawardene SC, Lee H, Neer RM. Effects of low-dose prednisone on bone metabolism. J Bone Miner Res. 2005;20(3):464-70.

70.   Paz-Pacheco E, Fuleihan GE, LeBoff MS. Intact parathyroid hormone levels are not elevated in glucocorticoid-treated subjects. J Bone Miner Res. 1995;10(11):1713-8.

71.   Lee SY, Jung SH, Lee SU, Ha YC, Lim JY. Can Bisphosphonates Prevent Recurrent Fragility Fractures? A Systematic Review and Meta-Analysis of Randomized Controlled Trials. 2018(1538-9375 (Electronic)).

72.   Vaccaro AR, Oner C Fau - Kepler CK, Kepler Ck Fau - Dvorak M, Dvorak M Fau - Schnake K, Schnake K Fau - Bellabarba C, Bellabarba C Fau - Reinhold M, et al. AOSpine thoracolumbar spine injury classification system: fracture description, neurological status, and key modifiers. 2013(1528-1159 (Electronic)).

73.   Parreira PCS, Maher CG, Megale RZ, March L, Ferreira ML. An overview of clinical guidelines for the management of vertebral compression fracture: a systematic review. The Spine Journal. 2017;17(12):1932-8.

74.   Ensrud KE, Schousboe JT. Vertebral Fractures. New England Journal of Medicine. 2011;364(17):1634-42.

75.   Blattert TR, Schnake KJ, Gonschorek O, Gercek E, Hartmann F, Katscher S, et al. Nonsurgical and Surgical Management of Osteoporotic Vertebral Body Fractures: Recommendations of the Spine Section of the German Society for Orthopaedics and Trauma (DGOU). Global Spine J. 2018;8(2 Suppl):50S-5S.

76.   McPherson K, Steel CM, Dixon JM. Breast cancer—epidemiology, risk factors, and genetics. BMJ. 2000;321(7261):624-8.

77.   Garg PP, Kerlikowske K, Subak L, Grady D. Hormone replacement therapy and the risk of epithelial ovarian carcinoma: a meta-analysis. Obstetrics & Gynecology. 1998;92(3):472-9.

78.   Beresford SAA, Weiss NS, Voigt LF, McKnight B. Risk of endometrial cancer in relation to use of oestrogen combined with cyclic progestagen therapy in postmenopausal women. The Lancet. 1997;349(9050):458-61.

79.   Høibraaten E, Qvigstad E, Arnesen H, Larsen S, Wickstrøm E, Sandset PM. Increased Risk of Recurrent Venous Thromboembolism during Hormone Replacement Therapy Results of the Randomized, Double-blind, Placebo-controlled Estrogen in Venous Thromboembolism Trial (EVTET). Thromb Haemost. 2000;84(6):961-7.

80.   Galibert P, Deramond H, Rosat P, Le Gars D. [Preliminary note on the treatment of vertebral angioma by percutaneous acrylic vertebroplasty]. Neuro-Chirurgie. 1987;33(2):166-8.

81.   Bascoulergue YD JL, R; Mottolese, C; Lapras, C. . Percutaneous injection of methyl methacrylate in the vertebral body for the treatment of various diseases: percutaneous vertebroplasty. Radiology 1988(169):372.

82.   Jensen ME, Evans AJ, Mathis JM, Kallmes DF, Cloft HJ, Dion JE. Percutaneous polymethylmethacrylate vertebroplasty in the treatment of osteoporotic vertebral body compression fractures: technical aspects. AJNR Am J Neuroradiol. 1997;18(10):1897-904.

83.   Mathis JM, Petri M, Naff N. Percutaneous vertebroplasty treatment of steroid-induced osteoporotic compression fractures. Arthritis and rheumatism. 1998;41(1):171-5.

84.   Debussche-Depriester C, Deramond H, Fardellone P, Heleg A, Sebert JL, Cartz L, et al., editors. Percutaneous vertebroplasty with acrylic cement in the treatment of osteoporotic vertebral crush fracture syndrome1991; Berlin, Heidelberg: Springer Berlin Heidelberg.

85.   Weill A, Chiras J, Simon JM, Rose M, Sola-Martinez T, Enkaoua E. Spinal metastases: indications for and results of percutaneous injection of acrylic surgical cement. Radiology. 1996;199(1):241-7.

86.   Kobayashi N, Numaguchi Y, Fuwa S, Uemura A, Matsusako M, Okajima Y, et al. Prophylactic Vertebroplasty: Cement Injection into Non-fractured Vertebral Bodies During Percutaneous Vertebroplasty. Academic Radiology. 2009;16(2):136-43.

87.   Chiang CK, Wang YH, Yang CY, Yang BD, Wang JL. Prophylactic vertebroplasty may reduce the risk of adjacent intact vertebra from fatigue injury: an ex vivo biomechanical study. Spine (Phila Pa 1976). 2009;34(4):356-64.

88.   Buchbinder R, Kallmes DF, Jarvik JG, Deyo RA. Conduct and reporting of a vertebroplasty trial warrants critical examination. Evidence Based Medicine. 2017;22(3):106-7.

89.   Buchbinder R, Osborne RH, Ebeling PR, Wark JD, Mitchell P, Wriedt C, et al. A Randomized Trial of Vertebroplasty for Painful Osteoporotic Vertebral Fractures. New England Journal of Medicine. 2009;361(6):557-68.

90.   Firanescu C, Lohle Pn Fau - de Vries J, de Vries J Fau - Klazen CA, Klazen Ca Fau - Juttmann JR, Juttmann Jr Fau - Clark W, Clark W Fau - van Rooij WJ, et al. A randomised sham controlled trial of vertebroplasty for painful acute osteoporotic vertebral fractures (VERTOS IV). 2018(1745-6215 (Electronic)).

91.   Kallmes DF, Comstock BA, Heagerty PJ, Turner JA, Wilson DJ, Diamond TH, et al. A Randomized Trial of Vertebroplasty for Osteoporotic Spinal Fractures. New England Journal of Medicine. 2009;361(6):569-79.

92.	Klazen CA, Lohle PN, de Vries J, Jansen FH, Tielbeek AV, Blonk MC, et al. Vertebroplasty versus conservative treatment in acute osteoporotic vertebral compression fractures (Vertos II): an open-label randomised trial. Lancet. 2010;376(9746):1085-92.

93.	Clark W, Bird P, Gonski P, Diamond TH, Smerdely P, McNeil HP, et al. Safety and efficacy of vertebroplasty for acute painful osteoporotic fractures (VAPOUR): a multicentre, randomised, double-blind, placebo-controlled trial. Lancet. 2016;388(10052):1408-16.

94.	Gangi A, Kastler BA, Dietemann JL. Percutaneous vertebroplasty guided by a combination of CT and fluoroscopy. American Journal of Neuroradiology. 1994;15(1):83-6.

95.	Gangi A, Guth S, Imbert JP, Marin H, Dietemann JL. Percutaneous vertebroplasty: indications, technique, and results. Radiographics. 2003;23(2):e10.

96.	Weber CH, Krotz M, Hoffmann RT, Euler E, Heining S, Pfeifer KJ, et al. [CT-guided vertebroplasty and kyphoplasty: comparing technical success rate and complications in 101 cases]. Rofo. 2006;178(6):610-7.

97.	Pitton MB, Herber S, Koch U, Oberholzer K, Drees P, Duber C. CT-guided vertebroplasty: analysis of technical results, extraosseous cement leakages, and complications in 500 procedures. Eur Radiol. 2008;18(11):2568-78.

98.	Schmidt R, Cakir B, Mattes T, Wegener M, Puhl W, Richter M. Cement leakage during vertebroplasty: an underestimated problem? European spine journal : official publication of the European Spine Society, the European Spinal Deformity Society, and the European Section of the Cervical Spine Research Society. 2005;14(5):466-73.

99.	Mathis JM, Barr JD, Belkoff SM, Barr MS, Jensen ME, Deramond H. Percutaneous vertebroplasty: a developing standard of care for vertebral compression fractures. AJNR Am J Neuroradiol. 2001;22(2):373-81.

100.	Kim DJ, Kim TW, Park KH, Chi MP, Kim JO. The Proper Volume and Distribution of Cement Augmentation on Percutaneous Vertebroplasty. Journal of Korean Neurosurgical Society. 2010;48(2):125-8.

101.	Nieuwenhuijse MJ, Bollen L, van Erkel AR, Dijkstra PD. Optimal intravertebral cement volume in percutaneous vertebroplasty for painful osteoporotic vertebral compression fractures. Spine (Phila Pa 1976). 2012;37(20):1747-55.

102.	Jang JS, Lee SH, Jung SK. Pulmonary embolism of polymethylmethacrylate after percutaneous vertebroplasty: a report of three cases. Spine (Phila Pa 1976). 2002;27(19):E416-8.

103.	Hodler J, Peck D, Gilula LA. Midterm outcome after vertebroplasty: predictive value of technical and patient-related factors. Radiology. 2003;227(3):662-8.

104.   Sidhu GS, Kepler CK, Savage KE, Eachus B, Albert TJ, Vaccaro AR. Neurological deficit due to cement extravasation following a vertebral augmentation procedure. J Neurosurg Spine. 2013;19(1):61-70.

105.   Jensen ME, Evans AJ, Mathis JM, Kallmes DF, Cloft HJ, Dion JE. Percutaneous polymethylmethacrylate vertebroplasty in the treatment of osteoporotic vertebral body compression fractures: technical aspects. American Journal of Neuroradiology. 1997;18(10):1897-904.

106.   Cortet B, Cotten A, Boutry N, Flipo RM, Duquesnoy B, Chastanet P, et al. Percutaneous vertebroplasty in the treatment of osteoporotic vertebral compression fractures: an open prospective study. The Journal of rheumatology. 1999;26(10):2222-8.

107.   Cyteval C, Sarrabere MP, Roux JO, Thomas E, Jorgensen C, Blotman F, et al. Acute osteoporotic vertebral collapse: open study on percutaneous injection of acrylic surgical cement in 20 patients. AJR American journal of roentgenology. 1999;173(6):1685-90.

108.   Barr JD, Barr MS, Lemley TJ, McCann RM. Percutaneous Vertebroplasty for Pain Relief and Spinal Stabilization. Spine. 2000;25(8):923-8.

109.   Grados F, Depriester C, Cayrolle G, Hardy N, Deramond H, Fardellone P. Long-term observations of vertebral osteoporotic fractures treated by percutaneous vertebroplasty. Rheumatology (Oxford, England). 2000;39(12):1410-4.

110.   McGraw JK, Lippert JA, Minkus KD, Rami PM, Davis TM, Budzik RF. Prospective evaluation of pain relief in 100 patients undergoing percutaneous vertebroplasty: results and follow-up. Journal of vascular and interventional radiology : JVIR. 2002;13(9 Pt 1):883-6.

111.   Perez-Higueras A, Alvarez L, Rossi RE, Quinones D, Al-Assir I. Percutaneous vertebroplasty: long-term clinical and radiological outcome. Neuroradiology. 2002;44(11):950-4.

112.   McKiernan F, Faciszewski T, Jensen R. Quality of life following vertebroplasty. The Journal of bone and joint surgery American volume. 2004;86-a(12):2600-6.

113.   Kobayashi K, Shimoyama K, Nakamura K, Murata K. Percutaneous vertebroplasty immediately relieves pain of osteoporotic vertebral compression fractures and prevents prolonged immobilization of patients. European Radiology. 2005;15(2):360-7.

114.   Voormolen MH, Mali WP, Lohle PN, Fransen H, Lampmann LE, van der Graaf Y, et al. Percutaneous vertebroplasty compared with optimal pain medication treatment: short-term clinical outcome of patients with subacute or chronic painful osteoporotic vertebral compression fractures. The VERTOS study. AJNR Am J Neuroradiol. 2007;28(3):555-60.

115.   Clark W, Bird P, Gonski P, Diamond TH, Smerdely P, McNeil HP, et al. Safety and efficacy of vertebroplasty for acute painful osteoporotic fractures (VAPOUR): a multicentre, randomised, double-blind, placebo-controlled trial. The Lancet. 2016;388(10052):1408-16.

116.   Cyteval C, Sarrabère MP, Roux JO, Thomas E, Jorgensen C, Blotman F, et al. Acute osteoporotic vertebral collapse: open study on percutaneous injection of acrylic surgical cement in 20 patients. American Journal of Roentgenology. 1999;173(6):1685-90.

117.   Barr JD, Barr MS, Lemley TJ, McCann RM. Percutaneous vertebroplasty for pain relief and spinal stabilization. Spine (Phila Pa 1976). 2000;25(8):923-8.

118.   Kobayashi K, Shimoyama K, Nakamura K, Murata K. Percutaneous vertebroplasty immediately relieves pain of osteoporotic vertebral compression fractures and prevents prolonged immobilization of patients. Eur Radiol. 2005;15(2):360-7.

119.   Buchbinder R, Osborne RH, Ebeling PR, Wark JD, Mitchell P, Wriedt C, et al. A Randomized Trial of Vertebroplasty for Painful Osteoporotic Vertebral Fractures. New England Journal of Medicine. 2009;361(6):557-68.

120.   Kallmes DF, Comstock BA, Heagerty PJ, Turner JA, Wilson DJ, Diamond TH, et al. A Randomized Trial of Vertebroplasty for Osteoporotic Spinal Fractures. New England Journal of Medicine. 2009;361(6):569-79.

121.   Bono CM, Heggeness M, Mick C, Resnick D, Watters WC, 3rd. North American Spine Society: Newly released vertebroplasty randomized controlled trials: a tale of two trials. The spine journal : official journal of the North American Spine Society. 2010;10(3):238-40.

122.   Baerlocher MO, Munk PL, Liu DM, Tomlinson G, Badii M, Kee ST, et al. Clinical Utility of Vertebroplasty: Need for Better Evidence. Radiology. 2010;255(3):669-74.

123.   Buchbinder R, Kallmes DF. Vertebroplasty: when randomized placebo-controlled trial results clash with common belief. The spine journal : official journal of the North American Spine Society. 2010;10(3):241-3.

124.   Ross PD, Ettinger B, Davis JW, Melton LJ, 3rd, Wasnich RD. Evaluation of adverse health outcomes associated with vertebral fractures. Osteoporosis international : a journal established as result of cooperation between the European Foundation for Osteoporosis and the National Osteoporosis Foundation of the USA. 1991;1(3):134-40.

125.   Pham T, Azulay-Parrado J, Champsaur P, Chagnaud C, Legre V, Lafforgue P. "Occult" osteoporotic vertebral fractures: vertebral body fractures without radiologic collapse. Spine (Phila Pa 1976). 2005;30(21):2430-5.

126.   Mink JH, Deutsch AL. Occult cartilage and bone injuries of the knee: detection, classification, and assessment with MR imaging. Radiology. 1989;170(3 Pt 1):823-9.

127.   Vellet AD, Marks PH, Fowler PJ, Munro TG. Occult posttraumatic osteochondral lesions of the knee: prevalence, classification, and short-term sequelae evaluated with MR imaging. Radiology. 1991;178(1):271-6.

128.   Miller MD, Osborne JR, Gordon WT, Hinkin DT, Brinker MR. The natural history of bone bruises. A prospective study of magnetic resonance imaging-detected trabecular microfractures in patients with isolated medial collateral ligament injuries. The American journal of sports medicine. 1998;26(1):15-9.

129.   Buchbinder R, Kallmes DF, Jarvik JG, Deyo RA. Conduct and reporting of a vertebroplasty trial warrants critical examination. Evid Based Med. 2017;22(3):106-7.

130.   Firanescu CE, de Vries J, Lodder P, Venmans A, Schoemaker MC, Smeet AJ, et al. Vertebroplasty versus sham procedure for painful acute osteoporotic vertebral compression fractures (VERTOS IV): randomised sham controlled clinical trial. BMJ. 2018;361:k1551.

131.   Buchbinder R, Johnston RV, Rischin KJ, Homik J, Jones CA, Golmohammadi K, et al. Percutaneous vertebroplasty for osteoporotic vertebral compression fracture. Cochrane Database of Systematic Reviews. 2018(11).

132.   Bae H, Shen M, Maurer P, Peppelman W, Beutler W, Linovitz R, et al. Clinical Experience Using Cortoss for Treating Vertebral Compression Fractures With Vertebroplasty and Kyphoplasty: Twenty Four-Month Follow-up. Spine. 2010;35(20):E1030-E6.

133.   Zhang L, Liu Z, Wang J, Feng X, Yang J, Tao Y, et al. Unipedicular versus bipedicular percutaneous vertebroplasty for osteoporotic vertebral compression fractures: a prospective randomized study. 2015(1471-2474 (Electronic)).

134.   Cornwall J, Stringer MD. The wider importance of cadavers: educational and research diversity from a body bequest program. Anat Sci Educ. 2009;2(5):234-7.

135.   Crandall Jr, Bose D, Forman J, Untaroiu Cd, Arregui-Dalmases C, Shaw Cg, et al. Human surrogates for injury biomechanics research. Clin Anat. 2011;24(3):362-71.

136.   Begeman PC, King AI, Levine RS, Viano DC. Biodynamic Response of the Musculoskeletal System to Impact Acceleration. SAE Transactions. 1980;89:3992-4007.

137.   Goel VK, Panjabi MM, Patwardhan AG, Dooris AP, Serhan H, American Society for T, et al. Test protocols for evaluation of spinal implants. The Journal of bone and joint surgery American volume. 2006;88 Suppl 2:103-9.

138.   Patwardhan AG, Havey RM, Meade KP, Lee B, Dunlap B. A follower load increases the load-carrying capacity of the lumbar spine in compression. Spine (Phila Pa 1976). 1999;24(10):1003-9.

139.   Krogh A. The Progress of Physiology. American Journal of Physiology. 1929;90:243–51.

140.   Auer JA, Goodship A, Arnoczky S, Pearce S, Price J, Claes L, et al. Refining animal models in fracture research: seeking consensus in optimising both animal welfare and scientific validity for appropriate biomedical use. BMC Musculoskelet Disord. 2007;8:72.

141.   Smit TH. The use of a quadruped as an in vivo model for the study of the spine – biomechanical considerations. European Spine Journal. 2002;11(2):137-44.

142.   Busscher I, Ploegmakers JJ, Verkerke GJ, Veldhuizen AG. Comparative anatomical dimensions of the complete human and porcine spine. Eur Spine J. 2010;19(7):1104-14.

143.   Parfitt AM, Drezner MK, Glorieux FH, Kanis JA, Malluche H, Meunier PJ, et al. Bone histomorphometry: standardization of nomenclature, symbols, and units. Report of the ASBMR Histomorphometry Nomenclature Committee. J Bone Miner Res. 1987;2(6):595-610.

144.   Mann KA, Miller MA, Cleary RJ, Janssen D, Verdonschot N. Experimental micromechanics of the cement-bone interface. J Orthop Res. 2008;26(6):872-9.

145.   Zhang QH, Tozzi G, Tong J. Micro-mechanical damage of trabecular bone-cement interface under selected loading conditions: a finite element study. Comput Methods Biomech Biomed Engin. 2014;17(3):230-8.

146.   Zhang QH, Cossey A, Tong J. Stress shielding in bone of a bone-cement interface. Med Eng Phys. 2016;38(4):423-6.

147.   Rockoff SD, Scandrett J, Zacher R. Quantitation of Relevant Image Information: Automated Radiographic Bone Trabecular Characterization. Radiology. 1971;101(2):435-9.

148.   Haralick RM, Shanmugam K, Dinstein I. Textural Features for Image Classification. IEEE Transactions on Systems, Man, and Cybernetics. 1973;SMC-3(6):610-21.

149.   Ito M, Ohki M, Hayashi K, Yamada M, Uetani M, Nakamura T. Trabecular texture analysis of CT images in the relationship with spinal fracture. Radiology. 1995;194(1):55-9.

150.   Haralick RM. Statistical and structural approaches to texture. Proceedings of the IEEE. 1979;67(5):786-804.

151.   Galloway M. Texture analysis using gray level run lengths1974. 172-99 p.

152.   Thomsen JS, Laib A, Koller B, Prohaska S, Mosekilde L, Gowin W. Stereological measures of trabecular bone structure: comparison of 3D micro computed tomography with 2D histological sections in human proximal tibial bone biopsies. J Microsc. 2005;218(Pt 2):171-9.

153.   du Plessis A, Broeckhoven C, Guelpa A, le Roux SG. Laboratory x-ray micro-computed tomography: a user guideline for biological samples. Gigascience. 2017;6(6):1-11.

154.   Link TM, Majumdar S, Lin JC, Augat P, Gould RG, Newitt D, et al. Assessment of trabecular structure using high resolution CT images and texture analysis. J Comput Assist Tomogr. 1998;22(1):15-24.

155.   Dryden I.L. MKV. Statistical Shape Analysis: With Applications in R. 2nd edn ed: Wiley; 2016.

156.   Kendall DG. The diffusion of shape. Advances in Applied Probability. 1977;9(3):428-30.

157.   Gunz P, Mitteroecker P. Semilandmarks: a method for quantifying curves and surfaces. Hystrix, the Italian Journal of Mammalogy. 2013;24(1):103-9.

158.   Bookstein FL. The Measurement of Biological Shape and Shape Change. Lecture Notes in Biomathematics Vol. 24. Biometrical Journal. 1979;21(3):298-.

159.   G. G. Discorsi e dimostrazioni matematiche, informo a due nuoue scienze attenti alla mecanica i movimenti locali: appresso gli Elsevirii; Opere VIII. ; 1638.

160.   Rao CR. Tests of Significance in Multivariate Analysis. Biometrika. 1948;35(1/2):58-79.

161.   Reyment R.A. BRECNA. Multivariate Morphometrics, 2nd ed. 2nd edn ed: Cambridge University Press; 1986. 186- p.

162.   Pearson K. On the Coefficient of Racial Likeness. Biometrika. 1926;18(1/2):105-17.

163.   Thompson DAW. On Growth and Form. Cambridge: Cambridge University Press; 1992.

164.   Bookstein FL. Can biometrical shape be a homologous character? . In: Hall BK, editor. Homology: The Hierarchical Basis of Comparative Biology Academic Press; 1994.

165.   Kass M, Witkin A, Terzopoulos D. Snakes: Active contour models. International Journal of Computer Vision. 1988;1(4):321-31.

166.   Cootes TF, Taylor CJ, Cooper DH, Graham J, editors. Training Models of Shape from Sets of Examples1992; London: Springer London.

167.   Cootes TF, Taylor CJ, Cooper DH, Graham J. Active Shape Models-Their Training and Application. Computer Vision and Image Understanding. 1995;61(1):38-59.

168.   Gunz P. MP, Bookstein F.L. Semilandmarks in Three Dimensions. In: Slice DE, editor. Modern Morphometrics in Physical Anthropology Developments in Primatology: Progress and Prospects. Boston, MA: Springer; 2005. p. 73-98.

169.   Leondes CT. Medical Imaging Systems Technology - Volume 3: Methods In General Anatomy: World Scientific Publishing Co Pte Ltd; 2005.

170.   Boas F. THE HORIZONTAL PLANE OF THE SKULL AND THE GENERAL PROBLEM OF THE COMPARISON OF VARIABLE FORMS. Science. 1905;21(544):862-3.

171.   Hurley JR, Cattell RB. The procrustes program: Producing direct rotation to test a hypothesized factor structure. Behavioral Science. 1962;7(2):258-62.

172.   Kent JT. New directions in shape analysis. In: Mardia KV, editor. The Art of Statistical Science Wiley; 1992.

173.   Pearson K. On Lines and Planes of Closest Fit to Points in Space1900. 559-72 p.

174.   Hotelling H. Analysis of a complex of statistical variables into principal components. Journal of Educational Psychology. 1933;24(6):417-41.

175.   Hotelling H. Relations Between Two Sets of Variates. Biometrika. 1936;28(3/4):321-77.

176.   Kent JT. The Complex Bingham Distribution and Shape Analysis. Journal of the Royal Statistical Society Series B (Methodological). 1994;56(2):285-99.

177.   Chow LC, Takagi S. A Natural Bone Cement—A Laboratory Novelty Led to the Development of Revolutionary New Biomaterials. Journal of Research of the National Institute of Standards and Technology. 2001;106(6):1029-33.

178.   Carrodeguas RG, V´zquez B, del Barrio JSR, de la Cal AM. Barium titanate-filled bone cements. I. Chemical, physical, and mechanical characterization. International Journal of Polymeric Materials and Polymeric Biomaterials. 2002;51(7):591-605.

179.   Hecht BP, Fischgrund JS, Herkowitz HN, Penman L, Toth JM, Shirkhoda A. The Use of Recombinant Human Bone Morphogenetic Protein 2 (rhBMP-2) to Promote Spinal Fusion in a Nonhuman Primate Anterior Interbody Fusion Model. Spine. 1999;24(7):629-36.

180.   Ahlgren BDMD, Vasavada AMS, Brower RSMD, Lydon CBS, Herkowitz HNMD, Panjabi MMPD. Anular Incision Technique on the Strength and Multidirectional Flexibility of the Healing Intervertebral Disc. [Miscellaneous]. Spine April 15, 1994;19(8):948-954.

181.   Allan DG, Russell GG, Moreau MJ, Raso VJ, Budney D. Vertebral end-plate failure in porcine- and bovine models of spinal fracture instrumentation. Journal of Orthopaedic Research. 1990;8(1):154-6.

182.   Gurwitz GSMD, Dawson JMP, McNamara MJMD, Federspiel CFP, Spengler DMMD. Biomechanical Analysis of Three Surgical Approaches for Lumbar Burst Fractures Using Short-Segment Instrumentation. Spine. 1993;18(8):977-82.

183.   Sheng S-R, Wang X-Y, Xu H-Z, Zhu G-Q, Zhou Y-F. Anatomy of large animal spines and its comparison to the human spine: a systematic review. European Spine Journal. 2010;19(1):46-56.

184.   Cotterill PC, Kostuik JP, D'Angelo G, Fernie GR, Maki BE. An anatomical comparison of the human and bovine thoracolumbar spine. Journal of Orthopaedic Research. 1986;4(3):298-303.

185.   Yingling VR, Callaghan JP, McGill SM. The porcine cervical spine as a model of the human lumbar spine: An anatomical, geometric, and functional comparison. Journal of Spinal Disorders. 1999;12(5):415-23.

186.   Bozkus H, Crawford NR, Chamberlain RH, Valenzuela TD, Espinoza A, Yüksel Z, et al. Comparative anatomy of the porcine and human thoracic spines with reference to thoracoscopic surgical techniques. Surgical Endoscopy And Other Interventional Techniques. 2005;19(12):1652-65.

187.   Dath R, Ebinesan AD, Porter KM, Miles AW. Anatomical measurements of porcine lumbar vertebrae. Clinical Biomechanics. 2007;22(5):607-13.

188.   Wilke HJ, Kettler A, Wenger KH, Claes LE. Anatomy of the sheep spine and its comparison to the human spine. Anatomical Record. 1997;247(4):542-55.

189.   Mageed M, Berner D, Jülke H, Hohaus C, Brehm W, Gerlach K. Is sheep lumbar spine a suitable alternative model for human spinal researches? Morphometrical comparison study. Laboratory Animal Research. 2013;29(4):183-9.

190.   Kumar N, Kukreti S, Ishaque M, Mulholland R. Anatomy of deer spine and its comparison to the human spine. Anat Rec. 2000;260(2):189-203.

191.   F. McLain R, Yerby SA, Moseley TA. Comparative Morphometry of L4 Vertebrae: Comparison of Large Animal Models for the Human Lumbar Spine. Spine. 2002;27(8):E200-E6.

192.   Panjabi MM, Takata K, Goel V, Federico D, Oxland T, Duranceau J, et al. Thoracic human vertebrae: Quantitative three-dimensional anatomy. Spine. 1991;16(8):888-901.

193.   Panjabi MM, Goel V, Oxland T, Takata K, Duranceau J, Krag M, et al. Human lumbar vertebrae: Quantitative three-dimensional anatomy. Spine. 1992;17(3):299-306.

194.   Nissan M, Gilad I. Dimensions of human lumbar vertebrae in the sagittal plane. Journal of biomechanics. 1986;19(9):753-8.

195.   White AAIP, M. M. Physical properties and functional biomechanics of the spine: Philadelphia, JB Lippincott; 1990 1990.

196.   Berry JL, Moran JM, Berg WS, Steffee AD. A morphometric study of human lumbar and selected thoracic vertebrae. Spine (Phila Pa 1976). 1987;12(4):362-7.

197.   Mageed M, Berner D, Jülke H, Hohaus C, Brehm W, Gerlach K. Morphometrical dimensions of the sheep thoracolumbar vertebrae as seen on digitised CT images. Lab Anim Res. 2013;29(3):138-47.

198.   Perry A, Mahar A, Massie J, Arrieta N, Garfin S, Kim C. Biomechanical evaluation of kyphoplasty with calcium sulfate cement in a cadaveric osteoporotic vertebral compression fracture model. The Spine Journal. 2005;5(5):489-93.

199.   Kayanja MM, Evans K, Milks R, Lieberman IH. Adjacent level load transfer following vertebral augmentation in the cadaveric spine. Spine. 2006;31(21):E790-7.

200.   Wilke H-J, Mehnert U, Claes LE, Bierschneider MM, Jaksche H, Boszczyk BM. Biomechanical evaluation of vertebroplasty and kyphoplasty with polymethyl methacrylate or calcium phosphate cement under cyclic loading. Spine. 2006;31(25):2934-41.

201.   Oakland RJ, Furtado NR, Wilcox RK, Timothy J, Hall RM. The biomechanical effectiveness of prophylactic vertebroplasty: a dynamic cadaveric study. Journal of Neurosurgery: Spine. 2008;8(5):442-9.

202.   Hauerstock D. RR, Steffen T. , editor Telemetric measurement of compressive loads in the sheep lumbar spine. Transactions of the 47th Annual Meeting of the Orthopaedic Research Society; 2001.

203.   Reitmaier S, Schmidt H, Ihler R, Kocak T, Graf N, Ignatius A, et al. Preliminary investigations on intradiscal pressures during daily activities: an in vivo study using the merino sheep. PLoS One. 2013;8(7):e69610.

204.   Ebbesen EN, Thomsen Js Fau - Beck-Nielsen H, Beck-Nielsen H Fau - Nepper-Rasmussen HJ, Nepper-Rasmussen Hj Fau - Mosekilde L, Mosekilde L. Age- and gender-related differences in vertebral bone mass, density, and strength. 1999(0884-0431 (Print)).

205.   Twomey LT, Taylor JR. Age changes in lumbar vertebrae and intervertebral discs. 1987(0009-921X (Print)).

206.   Eng J. Sample size estimation: how many individuals should be studied? Radiology. 2003;227(2):309-13.

207.   Bland JM, Altman DG. Statistics Notes: Measurement error. BMJ. 1996;313(7059):744.

208.   Team RC. R: A language and environment for statistical computing. R Foundation for Statistical Computing, Vienna, Austria.URL https://www.R-project.org/. 2019.

209.   Schieber MH. Chapter 2 Comparative anatomy and physiology of the corticospinal system. Handb Clin Neurol. 2007;82:15-37.

210.   Fields AJ, Keaveny TM. Trabecular Architecture and Vertebral Fragility in Osteoporosis. Current Osteoporosis Reports. 2012;10(2):132-40.

211.   Schindelin J, Arganda-Carreras I, Frise E, Kaynig V, Longair M, Pietzsch T, et al. Fiji: an open-source platform for biological-image analysis. Nat Methods. 2012;9(7):676-82.

212.   Doube M, Klosowski MM, Arganda-Carreras I, Cordelieres FP, Dougherty RP, Jackson JS, et al. BoneJ: Free and extensible bone image analysis in ImageJ. Bone. 2010;47(6):1076-9.

213.   Hildebrand T, Rüegsegger P. A new method for the model-independent assessment of thickness in three-dimensional images. Journal of Microscopy. 1997;185(1):67-75.

214.   Dougherty R, Kunzelmann K-H. Computing Local Thickness of 3D Structures with ImageJ2007.

215.   Inui A, Itamoto K, Takuma T, Tsutsumi H, Tanigawa M, Hayasaki M, et al. Age-related changes of bone mineral density and microarchitecture in miniature pigs. J Vet Med Sci. 2004;66(6):599-609.

216. Wang Y, Liu G, Li T, Xiao Y, Han Q, Xu R, et al. Morphometric comparison of the lumbar cancellous bone of sheep, deer, and humans. Comp Med. 2010;60(5):374-9.

217. Beddoe AH. A quantitative study of the structure of trabecular bone in man, rhesus monkey, beagle and miniature pig. Calcified Tissue Research. 1978;25(1):273-81.

218. Aerssens J, Boonen S, Lowet G, Dequeker J. Interspecies differences in bone composition, density, and quality: potential implications for in vivo bone research. Endocrinology. 1998;139(2):663-70.

219. Tumer N, Blankevoort L, van de Giessen M, Terra MP, de Jong PA, Weinans H, et al. Bone shape difference between control and osteochondral defect groups of the ankle joint. Osteoarthritis Cartilage. 2016;24(12):2108-15.

220. Pedoia V, Lansdown DA, Zaid M, McCulloch CE, Souza R, Ma CB, et al. Three-dimensional MRI-based statistical shape model and application to a cohort of knees with acute ACL injury. Osteoarthritis and cartilage. 2015;23(10):1695-703.

221. Treece G, Prager R, Gee A. Stradwin [Available from: http://mi.eng.cam.ac.uk/~rwp/stradwin/.

222. Treece GM, Prager R, Gee AH. Regularized marching tetrahedra: Improved iso-surface extraction1999. 583-98 p.

223. Gee A. BC, Helmy A. . wxRegSurf http://mi.eng.cam.ac.uk/~ahg/wxRegSurf/.

224. Horn JL. A rationale and test for the number of factors in factor analysis. Psychometrika. 1965;30(2):179-85.

225. Inc TM. MATLAB 2018a. Natick, Massachusets: The MathWorks Inc; 2018a.

226. Merckaert S, Pierzchala K, Kulik G, Schizas C. Influence of anatomical variations on lumbar foraminal stenosis pathogenesis. Eur Spine J. 2015;24(2):313-8.